

Towards the Development of a Biocatalytic Cascade for the Synthesis of Iminosugars

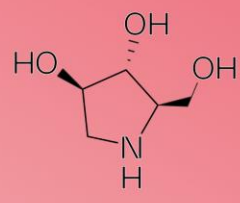
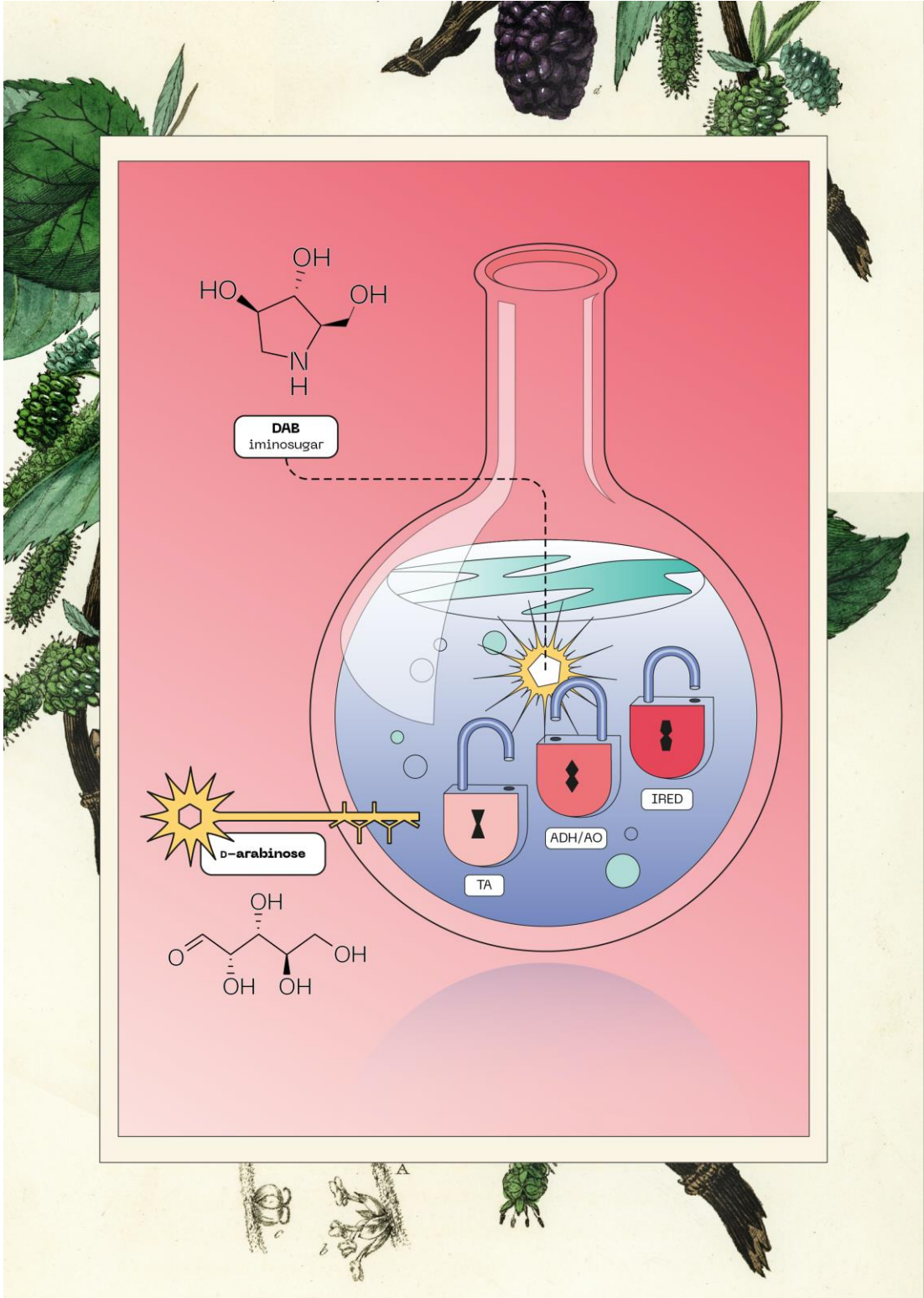
Doctor of Philosophy (PhD)

Justyna Kuska

Thesis to be submitted to the University of Nottingham in partial fulfilment of requirements for the degree of PhD

University of Nottingham, School of Chemistry, University Park,
Nottingham, NG7 2RD

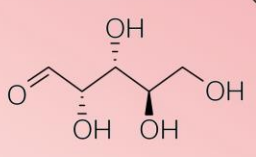
January 2021



DAB
iminosugar



D-arabinose



*For my beloved two sets of parents: Mama Olga, Tato Jan, Ciocia Helena and Wujek
Czeslaw for their ongoing support and faith in me.*

Acknowledgement

First and foremost, I would like to express my enormous gratitude to Dr Elaine O'Reilly, who supported me throughout my PhD journey. Elaine is an excellent supervisor, great leader and brilliant scientist. If I had to describe Elaine in two words, it would be: ELAINE CARES. Thank you so much, Elaine, for teaching me how to be a better scientist, celebrating with me smaller and bigger successes, for your invaluable feedback and words of advice (not only on the science matter) and of course the encouragement during the 'darker days'.

The O'Reilly hub has been a great source of knowledge and a source of friendships. I would like to thank James for teaching me all the tricks and tips in Organic Synthesis. I still remember my excitement during our first synthesis and the excitement of running my first column chromatography. Thank you, James, for your lessons on NMR analysis and Organic Chemistry, and the enormous contribution you made in this project. Special thanks to Chris who I can always count on. Chris, I am so grateful for all the knowledge and lab tips you shared and keep sharing with me. I enjoyed so much being your 'bench neighbour', and all the laughter with you compensated for the many unsuccessful syntheses. Freya, thank you so much for your help, especially on NMR analysis. You are a great teacher. It has been such a lovely year with you, finally working in a clean and organised laboratory. From the Biology side, I would like to thank Ryan and Stelios, who were always willing to discuss and troubleshoot problems with me. Thank you for being faithful pub buddies on Fridays, and I am sorry for abandoning you and moving to the 'filthy' chemistry corner.

This work would not have been possible without the incredible support from Adam. Adam, thank you so much for your wise conversations, encouragements, and always having faith in me. Thank you for reminding me about 'the big picture' during the hard times. However, you have also benefited from my PhD by listening and learning about Biocatalysis, NMR, cloning, DNA, small molecules. I know it has been a great journey for you too!

My family's support has been of great help, particularly my mum, dad and auntie. My little sisters but also my friends Julia and Łucja have been incredible listeners. Thank you so much for answering my calls, understanding and making me laugh. Olga, thank you so much for designing and executing so beautifully the graphic picture for my thesis.

My dear friends Justyna and Laura... Justyna, thank you so much for your support, random calls, for your down to earth beautiful spirit. Our trips during my PhD were definitely the highlight of that time! Laura, thank you so much for being always there for me, for your laughter, words of wisdom, and shared experience.

From Mitchell's corner, Andrea and Salwa, thank you for being good friends over the last year. Especially Andrea, thank you so much for the chemistry discussions, and being always so helpful.

Finally, I would like to thank the DTP in Biotechnological and Biological Sciences for the unique training program, offering academic freedom, and generous funding.

Table of Contents

Acknowledgement	iii
Abbreviations	1
Abstract	5
1 Thesis Overview	7
1.1 Iminosugars	8
1.1.1 Iminosugars: classification, structure and natural occurrence	9
1.1.2 Iminosugars as glycosidase inhibitors	10
1.1.3 Clinical relevance.....	16
1.1.4 Chemical synthesis of iminosugars.....	21
1.1.5 Application of biocatalysis in iminosugars synthesis.....	23
1.2 Biocatalytic cascades for the synthesis of organic molecules	28
1.2.1 Transaminases	35
1.2.2 Alcohol dehydrogenases and alcohol oxidases	42
1.2.3 Imine reductases	52
1.2.4 Monoamine oxidases	56
2 Aims and Objectives and Key Challenges	60
3 General Biological Methods and Materials	62
3.1 Materials	62
3.2 Sterilisation	62
3.3 Stock solutions	62
3.4 Microbiological media preparation	63
3.5 Bacteria culturing	64
3.6 Agarose gel electrophoresis	64
3.7 Cloning of I Pip2CR/Pyr2CR from <i>Pseudomonas putida</i>	65
3.8 Plasmid isolation	66
3.9 Preparation of <i>E. coli</i> chemically competent cells	66
3.10 Transformation of chemically competent cells	67

3.11	Heterologous protein expression	67
3.12	SDS-PAGE.....	68
4	<i>Chemical synthesis of protected amino alcohols for oxidation with <i>G. oxydans</i></i>	70
	Aims and objectives	70
4.1	Synthesis of protected amino alcohol substrates.....	70
4.1.1	Benzyl amino alcohols 191-195 : synthesis and biotransformation with <i>G. oxydans</i> ...	71
4.1.2	Formation of amino alcohols 199-205	74
4.1.3	Derivatisation of the amine group with a suitable protecting group in amino alcohols 206-212	75
4.2	Conclusions.....	79
4.3	Experimental	79
4.4	Disclosure	88
5	<i>Biocatalytic oxidations of amino alcohols</i>	89
	Aims and objectives	89
5.1	Introduction.....	90
5.2	Evaluation of the regioselective oxidation of amino alcohols.....	91
5.3	Reaction optimisation and product quantification.....	101
5.4	Preparative scale biotransformations	102
5.5	Regioselective oxidation of simple alcohols with <i>G. oxydans</i>	105
5.6	Summary and conclusions	108
5.7	Experimental	109
5.8	Disclosure	112
6	<i>Reduction of oxidised alcohols</i>.....	113
	Aims and objectives	113
6.1	Introduction.....	114
6.2	IREN enzyme selection	115
6.2.1	IRENs cloning, expression and activity test	117

6.3	Biotransformations of cyclic polar imines with IREDs	120
6.4	Chemical reduction of polyhydroxylated cyclic imines	123
6.5	Biotransformations of iminosugars with monoamine oxidises	127
6.6	Summary and conclusions	131
6.7	Experimental	132
6.8	Disclosure	141
7	<i>Chemo-enzymatic route for the synthesis of iminosugars</i>	142
	Aims and objectives	142
7.1	Step 1 and 2: transamination of aldoses and Cbz-protection.....	143
7.2	Step 3 and 4: microbial oxidation with <i>G. oxydans</i> and chemical reduction ...	145
7.3	Summary and conclusions	146
7.4	Experimental	147
7.5	Disclosure	148
7.6	Final conclusions and future work	148
8	<i>Appendix</i>	153
	<i>Bibliography</i>	155

Abbreviations

ADH	alcohol dehydrogenase
AcK	acetate kinase
ACVS	(L- α -aminoadipyl)- L-cysteine-D-valine synthetase
AO	alcohol oxidise
APS	ammonium persulfate
ASSC	active-site-specific chaperone
AT	isopenicillin N acyltransferase
ATA	amine transferase
Boc	<i>tert</i> -butyl carbamates
CAR	carboxylic acid reductase
Cbz-	benzyloxycarbonyl
Cbz-Cl	benzyl chloroformate
Cbz-OSu	<i>N</i> -(benzyloxycarbonyloxy)succinimide
^{13}C NMR	carbon nuclear magnetic resonance
DAB	1,4-dideoxy-1,4-imino-D-arabinitol
DERA	deoxyribose-phosphate aldolase
DGJ	1,5-dideoxy-1,5-imino-D-galactitol
DHA	dihydroxyacetone
DHAP	dihydroxyacetone phosphate
DHFR	dihydrofolate reductase
DMAP	<i>p</i> -dimethylaminopyridine
DMDP	2,5-dideoxy-2,5-imino-D-mannitol

DMF	dimethylformamide
DMP	2,2-dimethoxypropane
DMSO	dimethyl sulfoxide
DNJ	1-deoxynojirimycin
DOPAL	3,4-dihydroxyphenylacetaldehyde
ESI	Electron Spray Ionisation
ERAD	endoplasmic-reticulum-associated protein degradation
ER	endoplasmic reticulum
FAD	flavin adenine dinucleotide
FDP	fructose 1,6-diphosphate aldolase
Fmoc	fluorenylmethoxycarbonyl
FSA	D-fructose-6-phosphate aldolase
FucA	L-fuculose phosphate aldolase
GO	galactose oxidase
GSI	gamma secretase inhibitor
HA	hydroxyacetone
HCV	hepatitis C virus
HIV	human immunodeficiency viruses
HLADH	horse liver alcohol dehydrogenase
¹ H NMR	proton nuclear magnetic resonance
HPLC	High Performance Liquid Chromatography
IPA	isopropylamine
IPNS	isopenicillin N synthase

IPTG	isopropyl β -D-1-thiogalactopyranoside
IRED	imine reductase
KP _i	potassium phosphate buffer
NaP _i	sodium phosphate buffer
LB	Luria-Bertani
LDH	lactose dehydrogenase (LDH)
LSDs	lysosomal storage disorders
MAO	monoamine oxidase
MDH	mannitol dehydrogenase
2-MPN	2-methyl-1-pyrroline
<i>Mv</i> -TA	transaminase from <i>Mycobacterium vanbaalenii</i>
NAD ⁺	nicotinamide adenine dinucleotide
NAD(P) ⁺	nicotinamide adenine dinucleotide phosphate
NJ	nojirimycin
NOESY	Nuclear Overhauser Effect Spectroscopy
NoX	NAD(P)H oxidase enzyme
OD ₆₀₀	optical density at 600 nm
PanK	pantothenate kinase
PB	phosphate buffer
PCR	polymerase chain reaction
PLP	pyridoxal 5' phosphate (PLP)
PMP	pyridoxamine 5'-phosphate (PMP)
PNP	purine nucleoside phosphorylase

PPM	phosphopentomutase
PQQ	pyrroloquinoline quinone
Pyr/Pip2CR	Δ^1 -pyrroline/piperidine -2-carboxylate reductase
RedAm	reductive aminase
RhuA	L-rhamnulose-1-phosphate aldolase
SDS	sodium dodecyl sulfate
Sfp	4'-phosphopantetheinyl transferase
(S)-MBA	(S)-methylbenzylamine
SU	sucrose phosphorylase
TA	transaminases
TEMED	tetramethylethylenediamine
TS	transition state
UV-Vis	Ultraviolet Visible Spectroscopy

Abstract

Long and inefficient synthetic routes for the preparation of iminosugars impede the commercialisation and development of iminosugar based therapeutics. The excellent selectivity of enzymes makes them adapted to perform highly efficient cascade reactions. This project aimed to simplify the iminosugar synthesis and develop a one-pot enzymatic biocascade, which recruits transaminase, alcohol oxidase/alcohol dehydrogenase and imine reductase starting from aldose. Specifically, this work focused on the biocatalytic oxidation and reduction steps, with the particular attention paid to the first one.

Chapter 5 explored regioselective oxidation of amino alcohols mediated by resting cells of *Gluconobacter oxydans* DSM 2003, which required Cbz protection of amine functionality. The biocatalyst was very efficient by transforming protected amino alcohols in the preparative-scale reactions in nearly quantitative conversions, generating four intermediates suitable for the synthesis of iminosugars. However, the requirement for amine protection impacted the initial cascade design, which was modified by adding two chemical steps: protection and deprotection.

Chapter 6 investigated biocatalytic imine reduction of five-membered polyhydroxylated imines, which were the oxidation products with *G. oxydans*. Five known imine reductases were tested on these polar imine substrates to no avail. Chemical reduction and Cbz deprotection involving catalytic hydrogenation with Pd/C led to the final iminosugar products. This process resulted in two optically pure iminosugar compounds and two diastereoisomeric mixtures. The racemic mixtures were attempted to be deracemised with engineered variants of monoamine oxidases from *Aspergillus niger*; however, either of the enzymes accepted these highly polar substrates.

Chapter 7 combined the established biocatalytic and chemical steps in the chemo-enzymatic route, which led to the synthesis of three iminosugar products starting from 2-deoxy-D-ribose, D-arabinose and D-ribose. The biocatalytic steps recruited a commercially available transaminase ATA-256 and *Gluconobacter oxydans* DSM 2003, while chemical steps involved Cbz-protection and reduction with Pd/C. The

overall synthesis required fewer steps than the reported sequences used for the same or similar targets, which also utilised carbohydrate-based starting materials.

1 Thesis Overview

Iminosugars are a class of sugar mimetics that are extremely promising drug candidates for a wide range of diseases. They have attracted enormous interest in the pharmaceutical industry due to their inhibitory properties towards a diverse array of carbohydrate processing enzymes. These small organic molecules are widely present in nature and exhibit a number of biological and chemical properties that make them ideal drug candidates.

Common approaches for the preparation of iminosugars rely on multistep syntheses, made more challenging by the stereochemical complexity and polyfunctionalised nature of the targets and often involving, low-yielding synthetic sequences. The application of chemo-, regio-, and stereoselective biocatalytic methods could simplify and shorten the synthetic routes and improve the commercial potential of iminosugars. Additionally, access to a greater variety of derivatives using biocatalytic approaches could uncover novel activities and iminosugars with better pharmacokinetic properties.

Due to the extraordinary selectivity, enzymes are perfectly suitable to perform cascade reactions, where the product of one biocatalytic step becomes the substrate for the next reaction. The use of biocatalytic cascades in organic synthesis is highly beneficial, as it eliminates the need for purification of intermediates, reduces operating time, costs and waste and can lead to improved yields and atom economy.

This project aims to simplify the preparation of iminosugars through the construction of a one-pot artificial biocatalytic cascade, which exploits readily available aldoses as building blocks. The cascade recruits three enzymes, namely transaminase (TA), alcohol dehydrogenase (ADH)/oxidase (AO) and imine reductase (IRED), and this PhD project investigates the biocatalytic oxidation and reduction.

The following introductory chapter provides background information on iminosugars, including structures, natural occurrence, mechanism of biological activity, therapeutic opportunities, and discusses the commonly used synthetic approaches for their preparation. The second part of the introduction explores

various enzymes that could be used in our proposed cascade and focuses on the enzymes employed in this study.

1.1 Iminosugars

Iminosugars, also known as polyhydroxylated alkaloids or azasugars, are sugar mimics in which the endocyclic oxygen is replaced with a nitrogen atom (**Figure 1**). These compounds are widely produced in nature by plants and microorganisms [1].

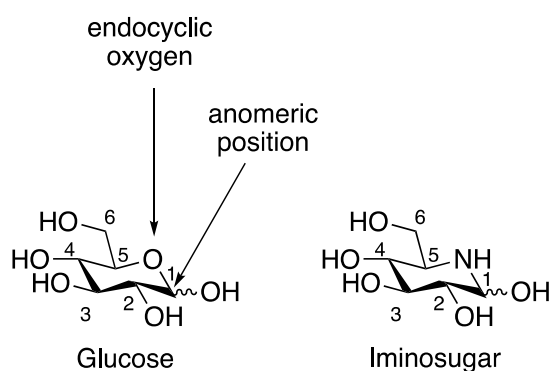


Figure 1. Basic structure of an iminosugar, using D-glucose as an example.

Interest in iminosugars initially arose due to their ability to inhibit glucosidases [2] and later, their inhibitory properties towards additional carbohydrate processing enzymes, such as glycotransferases [3,4], glycogen phosphorylases [5–7] nucleoside-processing enzymes [8,9], sugar mutases [10,11] and metalloproteinases [12] were uncovered. These enzymes are associated with a number of disorders including Gaucher [13], Pompe [14] and Fabry disease [15]; all of which have been successfully treated with iminosugar-based therapeutics [16]. Synthesis of iminosugars is challenging due to their high polarity, stereochemical complexity and absence of a chromophore. Predominant methods for iminosugars production are based on multistep chemical synthesis, starting from simple carbohydrate precursors or non-carbohydrate-based substrates (e.g. cyclic compounds that already contain a nitrogen atom) as starting materials [17]. Iminosugars have also been synthesised in good yield and excellent selectivity using chemo-enzymatic methods that involve whole cells [18] and isolated enzymes [19]. The sections below present an overview of iminosugar structures, natural occurrence, biological activity, therapeutic applications and their syntheses.

1.1.1 Iminosugars: classification, structure and natural occurrence

Natural iminosugars are divided into five main structural categories: the five membered pyrrolidines, six membered piperidines, bicyclic pyrrolizidines, indolizidines and nortropanes [20] (**Figure 2**). They are widely produced by plants and microorganisms and have been isolated from bulbs, leaves, bark, roots, seeds and from *Streptomyces* and *Bacillus* fermentation broths [1,21,22].

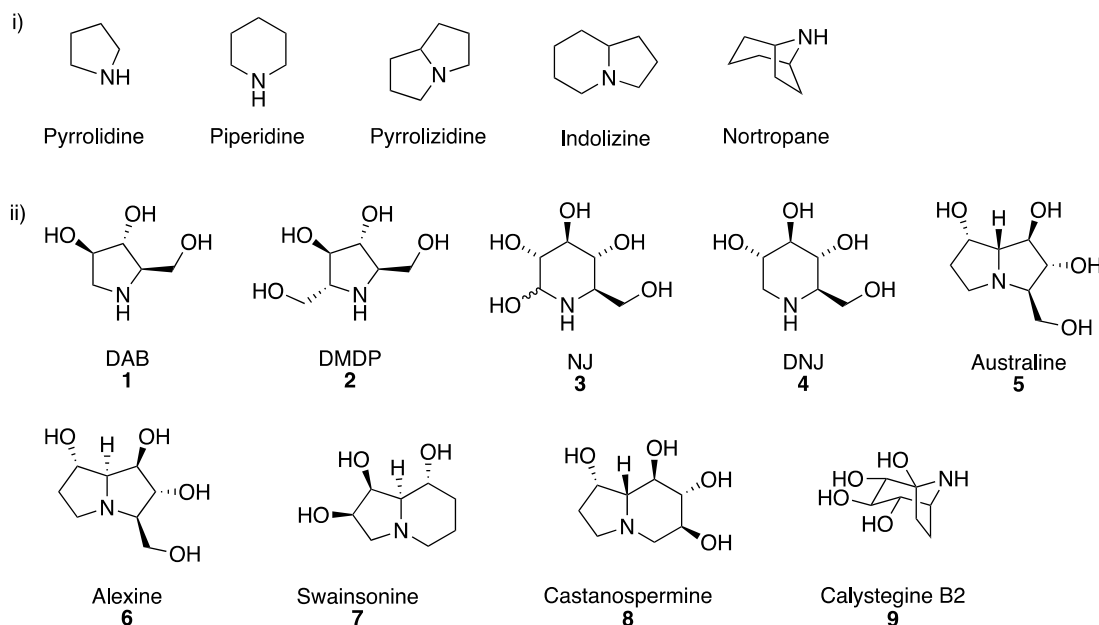


Figure 2. Generic motifs of natural iminosugars i) with the corresponding examples of selected naturally occurring iminosugars ii). Pyrrolidine: 1,4-dideoxy-1,4-imino-D-arabinitol (DAB) (**1**), 2,5-dideoxy-2,5-imino-D-mannitol (DMMP) (**2**), piperidine: nojirimycin (NJ) (**3**), 1-deoxynojirimycin (DNJ) (**4**), pyrrolizidine: australine (**5**), alexine (**6**), indolizine: swainsonine (**7**) and castanospermine (**8**), nortropane: calystegine (**9**).

Nojirimycin (NJ) (**3**) was the first reported iminosugar isolated from *Streptomyces nojiriensis* in 1966 [21]. However, this alkaloid appeared to be fairly unstable under physiological conditions due to the presence of the highly acid labile hemiaminal moiety [21]. Soon after, its stable derivative of 1-deoxynojirimycin (DNJ) (**4**) was synthesized [23], and later isolated from the mulberry tree in 1976 [24]. Some of the first pyrrolidine iminosugars discovered were 1,4-dideoxy-1,4-imino-D-arabinitol (DAB) (**1**) and 2,5-dideoxy-2,5-imino-D-mannitol (DMMP) (**2**), both isolated from legume genera [25,26]. The indolizine iminosugars including swainsonine (**7**) and castanospermine (**8**) were first isolated from *Swainsona canescens* and *Castanospermum australe*, respectively [27,28]. Interestingly, plants rich in these

alkaloids especially, in swainsonine, appeared to be poisonous to the livestock causing so called 'pea struck', which led to their discovery [1]. The pyrrolizidines such as alexine (**6**) and australine (**7**) were isolated from *Alexa* spp. [29] and *Castanospermum australe* plants [30], respectively, and later found in many different *Leguminosae* [1]. Finally, the nortropane iminosugars were first reported at the beginning of 1990 and isolated from a variety of plants including (sweet) potatoes, and aubergine [1,31,32].

It is not fully understood why plants and microorganisms produce iminosugars. Plants likely generate them to protect their carbohydrates products produced *via* photosynthesis. Another hypothesis states that iminosugars are produced as a defence strategy against insects [40,304]. It is thought that microorganisms produce iminosugars to decrease competition from other microorganisms through inhibiting their glycosidases. Iminosugars may also help in regulations of endogenous glycosidase activity. However, many of the natural iminosugars, which were isolated in recent years, were active towards many other carbohydrate processing enzymes besides glycosidases. This suggests that these molecules can play other functions in nature, such as recently discovered chaperoning activity and modulation of the immune response of mammals [305].

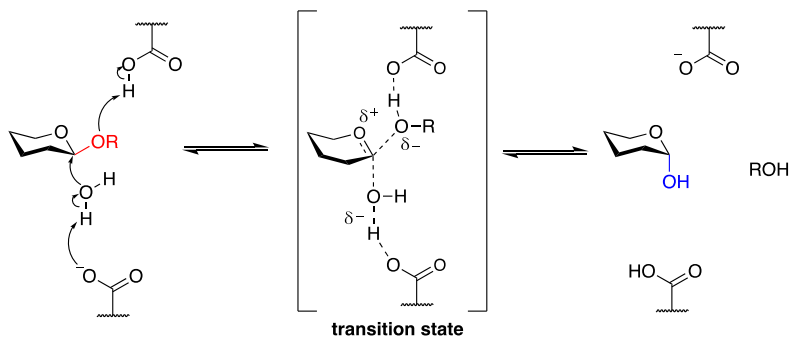
The inhibitory properties of these natural iminosugars towards glycosidases evoked enormous interest in their therapeutic applications. To date, more than 100 structurally and functionally distinct iminosugar compounds have been isolated from natural sources [1].

1.1.2 Iminosugars as glycosidase inhibitors

The therapeutic properties of iminosugars stems from their ability to reversibly inhibit glycosidases. These enzymes are ubiquitous through all kingdoms of life and catalyse the hydrolysis of α - and β -glycosidic bonds in di-, oligo- and polysaccharides, as well as glycoconjugates. Depending on the mode of action, glycosidases employ inverting or retaining mechanisms, which were first suggested by Koshland in 1953 (**Figure 3**) [33,34]. Commonly (although there are exceptions), glycosidases contain two conserved carboxylic acid residues in the active site derived from aspartate or

glutamate, which act as an acid and a base during the hydrolysis [35,36]. The inversion mechanism proceeds through a single displacement, which allows water and substrate to be bound simultaneously. One of the carboxylate residues protonates the glycosidic oxygen atom, while the other deprotonates the water molecule, which then carries on the nucleophilic attack that results in the hydrolysis of the glycosidic bond and departure of the leaving group. The resulting product displays the opposite conformation at the anomeric carbon to the substrate [37,38]. The retention mechanism occurs through a double displacement and involves a two-step glycosylation and deglycosylation. During the first step, one of the catalytic carboxylates acts as a general acid and donates a proton to the glycosidic oxygen. The second deprotonated carboxylate acts as a nucleophile and attacks the anomeric carbon at the oxocarbenium ion transition state. This leads to the formation of the covalently bound glycosyl-enzyme intermediate, and displacement of the aglycon moiety (ROH). During the second deglycosylation step, the glycosyl enzyme complex is hydrolysed by water with the other carboxylate now acting as a base and abstracting the proton from the incoming water molecule, which performs the nucleophilic attack on the carbohydrate enzyme linkage and displaces the product with a retained configuration at the anomeric centre. Regardless of which enzymatic mechanism, each reaction step occurs *via* a transition state (TS) with substantial oxocarbenium ion character [36,37].

Inverting mechanism of β -glycosidases



Retaining mechanism of β -glycosidases

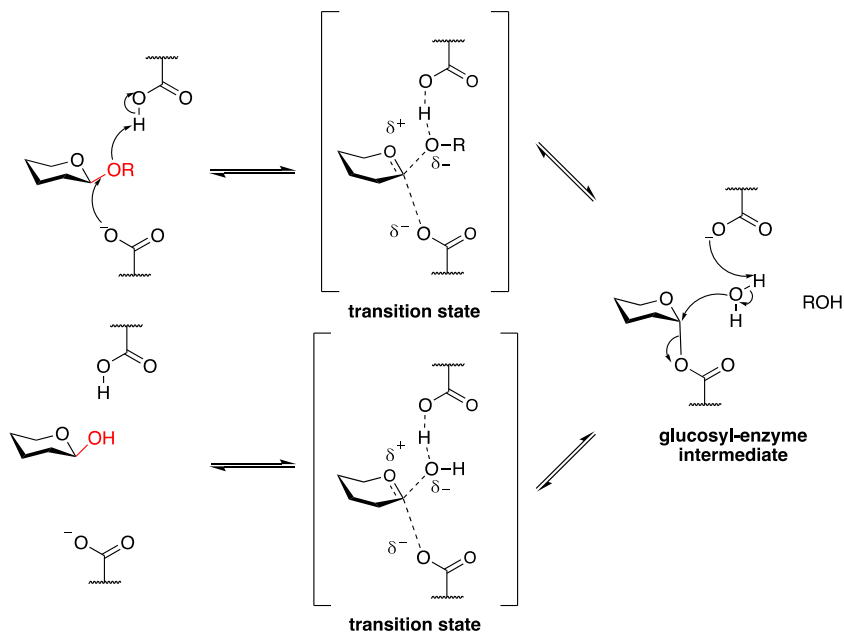


Figure 3. General mechanism of retaining and inverting β -glycosidases, which typically involves two carboxylate residues in the active site acting as a general base and general acid. The inverting mechanism is achieved through a single displacement allowing water and substrate to be bound simultaneously. It proceeds *via* one oxocarbenium-ion-like transition state and generates a hemiacetal product having the opposite stereochemistry at the anomeric centre as depicted above. The retaining mechanism is achieved *via* double displacement and proceeds through two oxocarbenium-ion-like transition states. The first step (glycosylation) results in the formation of the glycosyl-enzyme intermediate, which in the second step (deglycosylation) is hydrolysed by a water molecule to the corresponding product with retained configuration at the anomeric carbon. Modified from [34].

Iminosugars are transition state mimics, as they are protonated at physiological pH, resulting in a species that resembles the oxocarbenium character of the hydrolysis transition states [39] (**Figure 4**). In general, the following factors impact the potency of iminosugar inhibition: the position of the basic (cationic) centre, geometry and charge distribution, basicity, hydroxylation pattern, ring size and flexibility, interactions with the aglycon binding site and hydrogen bonding formation with the

catalytic acid [40]. The charge distribution of the oxocarbenium character differs in the transition states of α - and β -retaining glycosidases, and studies by Bols and co-workers [41–43] as well as those by Ichikawa and co-workers [44–46] demonstrate that it affects the potency of inhibition by iminosugars. In the α -glucosidases, the nucleophilic residue is positioned to favour a build-up of positive charge at the endocyclic oxygen, while the anomeric group is ejected resulting in a transition state with oxocarbenium character. In case of the β -glucosidases, the nucleophile carboxyl oxygens are positioned to interact with the anomeric centre and the adjacent hydroxyl group, which favours the formation of a carbocation at the anomeric position in the transition state (**Figure 5**) [37]. Common examples of strong iminosugar inhibitors for α - and β -glycosidases that display these features include isofagomine and DNJ (**4**), respectively [41,47].

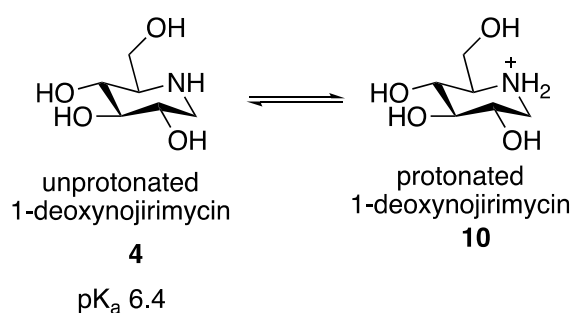


Figure 4. Structure of DNJ in the protonated and unprotonated form; the latter one mimics the oxocarbenium ion in the hydrolysis transition state.

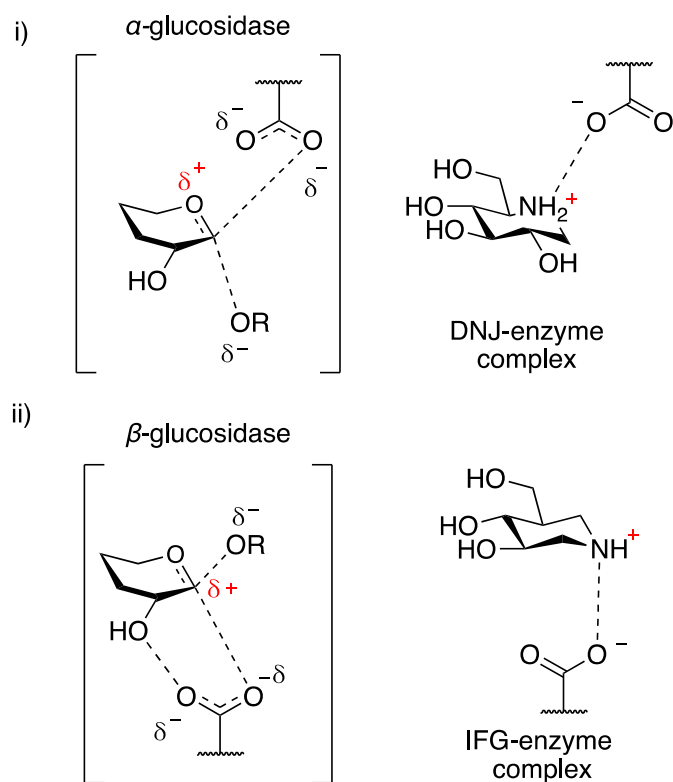


Figure 5. Comparison of the charge distribution in the transition state for α - (i) and β -glucosidases (ii), and the corresponding potent transition analogue inhibitor DNJ and IFG respectively. In α -glucosidases the positive charge is positioned at endocyclic oxygen, while in the β -glucosidases the formation of carbocation occurs at the anomeric centre. Modified from [34].

The selectivity of iminosugars towards glycosidases is also determined by the configuration of the hydroxyl groups that are involved in binding in the active site [48]. A piperidine iminosugar with the identical or closely related arrangement of hydroxyls to the natural sugar is frequently but not always an inhibitor of the processing enzyme associated with this sugar (Figure 6) [20]. For example, the *gluco* configuration in DNJ (**4**) mimics D-glucose (**11**), and it is a strong inhibitor of sucrase, maltase and isomaltase [49]. Similarly, the *galacto* configured 1,5-dideoxy-1,5-imino-D-galactitol (DGJ) (**13**) mimics D-galactose (**12**), and it is a potent inhibitor of α -galactosidase [50].

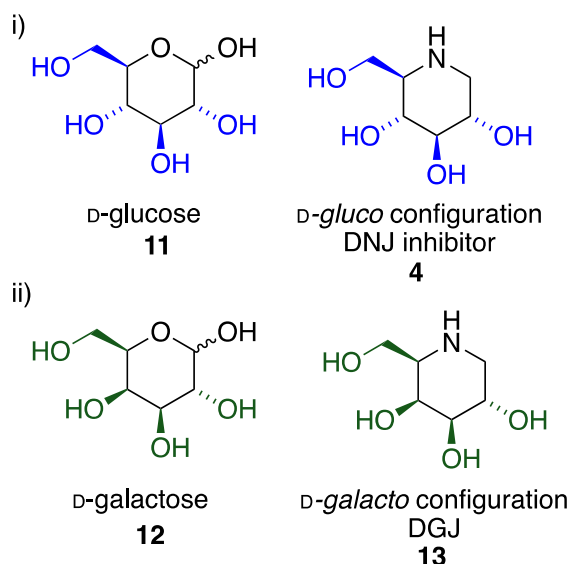


Figure 6. Representation of the resemblance of the hydroxyl group arrangement in piperidine iminosugars (DNJ and DGJ) to the corresponding natural sugars (D-glucose and D-galactose). These iminosugars are frequently inhibitors of the processing enzymes associated with these sugars [20].

Pyrrolidine iminosugars often make more potent inhibitors than their six-membered counterparts [51], which is rationalised by the better resemblance of the half-chair furanose structures in the transition state (**Figure 7**) [52,53]. In addition, bicyclic iminosugars represent another degree of structural complexity, and differ from monocyclic analogues mainly by the restriction of conformational flexibility of the polyhydroxylated ring by a four (swainsonine **7**) three (castanospermine **8**), or two (calystegine B2 **9**) carbon bridge (**Figure 2**). Studies demonstrated that in many cases, the bicyclic iminosugars are stronger in comparison to their monocyclic equivalents due to their rigid structure and the resemblance of the hydroxyl group arrangement of the transition state intermediate of the corresponding natural sugar (**Figure 8**) [20,39,54].

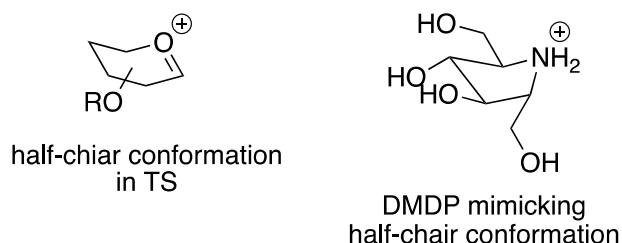


Figure 7. A five membered DMDP iminosugar mimicking a half-chaired conformation in TS of glucosyl hydrolases.

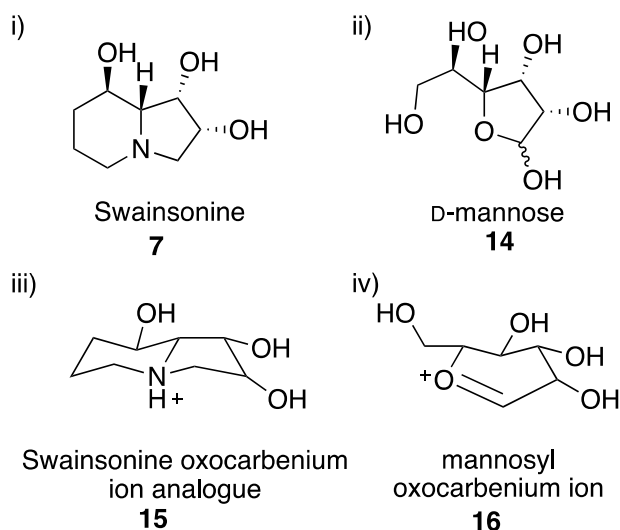


Figure 8. A representation of the structural resemblance of swainsonine (i) and D-mannose in the furanose form (ii), and the similar arrangement of the hydroxyl groups in swainsonine oxocarbenium ion analogue (iii) to mannosyl oxocarbenium ion (iv), which rationalises its inhibitory potency towards D-mannosidase [20].

1.1.3 Clinical relevance

The therapeutic use of iminosugars can be traced back to the traditional Chinese phytomedicines. In China, traditional practitioners recommended the white mulberry rootbark (*sang bai pi*) for the treatment of respiratory congestion, urinary symptoms and lowering blood pressure. In Western medicine, the extract from the mulberry tree was found in cosmetics for skin whitening and in drugs as laxative vermifuges. In the 17th century, Herman Boerhaave, a Dutch botanist and chemist, developed and commercialised a medicinal product known as Haarlem Oil, containing extract from mulberry leaves for weight loss, skin whitening and the treatment of diabetes. Haarlem Oil is still produced today and is licensed as a dietary supplement. However, the scientific history of iminosugars began in the early 1960s, with the isolation of NJ (**3**) from *Streptomyces* species [21], and the synthesis of its stable derivative DNJ (**4**) [23]. Their initial therapeutic applications were related to their ability to inhibit glycosidases [40,55–57]. With more discoveries, the iminosugar inhibitory activities have been further extended towards glycotransferases [3,4], glycogen phosphorylases [5–7], nucleoside-processing enzymes [8,9], a sugar mutase [10,11] and metalloproteinases [12]. These enzymes take part in various fundamental biological processes and this provides an opportunity for the development of the novel iminosugars based drugs

for a wide range of diseases [58,59]. The therapeutic applications of iminosugars are broad, including diabetes type II [60], cancer treatment [61,62], infectious diseases [63–65] and lysosomal storage disorders [66,67]. Besides their biological activity, iminosugars possess additional positive features as potential drug candidates, such as excellent water solubility and absorption, chemical and metabolic stability [68]. Several iminosugar-based therapeutics are on the market and a number of them have resulted in clinical trials (**Figure 9**). It is outside the scope of this thesis to discuss all the iminosugar-based therapies, and only a select few examples will be introduced in this section.

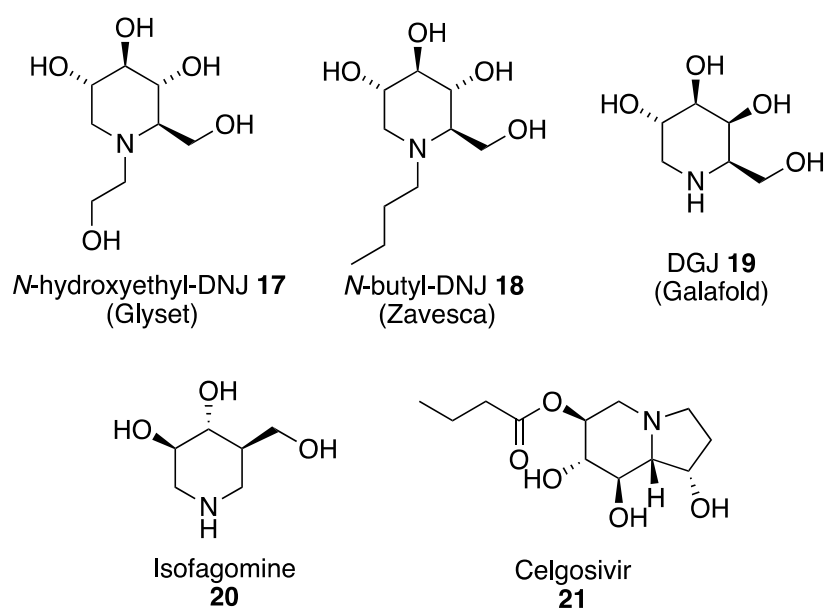


Figure 9. Structures of licensed drugs (trade name in the brackets) and selected iminosugar clinical candidates. These include Glyset (**17**) for diabetes type II, Zavesca (**18**) for type I Gaucher disease, Galafold (**19**) for Fabry disease, Isofagomine (**20**) and Celgosivir (**21**) were candidates in the second phase of clinical trials for Gaucher disease and anti-HIV therapy, respectively [68].

Diabetes II

Diabetes type II is a metabolic condition characterised by insulin resistance. The fundamental function of insulin is to stimulate the uptake of circulating glucose into muscle and adipose tissue [69]. In type II diabetes sufferers, insulin-stimulated glucose transport is impaired, which leads to hyperinsulinemia and hyperglycaemia. The long term effect of this disease often results in heart attack, blindness, strokes and kidney failure [70].

The therapeutic application of iminosugars towards type II diabetes relies on the inhibition of intestinal α -glucosidase enzymes, which delays the absorption of ingested carbohydrates and reduces the postprandial insulin and glucose peaks [70]. Since 1996, the iminosugar based therapeutic for the management of type II diabetes, *N*-hydroxyethyl-DNJ (**17**) also known as Miglitol, has been available on the market under the name Glyset (**Figure 9**).

Antiviral agents

The high mutability rate and adaptability of viruses is one of the key challenges when designing effective antiviral drugs. One approach to overcome this problem is targeting the cellular process of the host. The therapeutic application of iminosugars towards viruses targets the biosynthesis of the viral glycoproteins, which takes place in the host endoplasmic reticulum (ER). The glycoproteins are an integral part of the membrane surface in all enveloped viruses, and their primary role is to recognise and bind a receptor on the host cell surface, which allows the viral capsid to enter and infect the host. During the virus maturation, the glycan portion of glycoproteins undergo modifications by the host ER α -glucosidases I and II before they transit to the Golgi apparatus for further remodelling [71]. The *N*-butyl-DNJ (**18**) and Celgosivir (**21**) iminosugars (**Figure 9**) were found to be effective inhibitors of the ER α -glucosidases; preventing the full development of the viral HIV [64,72,73] and Hepatitis C (HCV) [65] envelope, respectively. The produced viral particles were shown to be non-infectious because of the altered conformation of the envelope that could not correctly bind to the respective receptor. However, the *in vivo* study showed that the inhibition with *N*-butyl-DNJ was only achieved with a very high extracellular concentration of the iminosugar, due to the location of the glucosidases in the lumen of the ER [74]. Celgosisir progressed to the second phase of clinical trials but suffered from a moderate potency and lack of the glycosidase specificity [68].

Lysosomal storage disorders (LSDs)

Lysosomes are membrane-enclosed organelles containing close to 50 digestive enzymes that break down biological polymers – proteins, nucleic acids,

carbohydrates, and lipids [75]. Lysosomal enzymes are synthesised in the ER, where they undergo folding and self-assembly in a thermodynamic fashion with the help of molecular chaperones. The correctly folded proteins are sent to the Golgi apparatus, while those incorrectly folded are retained in the ER and eventually sent to the cytosol for degradation. Mutations in the genes that encode for the lysosomal proteins cause lysosomal dysfunctions commonly known as lysosomal storage disorders (LSDs), which result from the abnormal metabolism of macro substances such as glycosphingolipids, glycogen, mucopolysaccharides and glycoproteins [76]. In some LSDs, the mutated enzymes are sent for degradation due to their incorrect fold, despite exhibiting residual activity. Active-site-specific chaperone therapy (ASSC) utilises iminosugars for the treatment of LSDs (**Figure 10**). The small molecules of iminosugars act as competitive inhibitors and induce a correct fold of the mutated enzyme towards the native-like conformation. This inhibition prevents the premature degradation of the mutant protein, which can be secreted out of the ER and sent to lysosomes. In lysosomes, the competitive iminosugar inhibitor dissociates from the complex in a presence of highly concentrated substrate to allow the function of the enzyme [77]. A DGJ (**19**) (Migalastat) iminosugar therapeutic is applied for the treatment of Fabry disease, which is caused by a mutation of the lysosomal enzyme α -galactosidase A (α -Gal A) [15]. Acting as an ASSC, DGJ was shown to induce the correct structure of the mutant enzyme enabling its trafficking to the lysosome [78]. In 2018, the DGJ medication for the treatment for Fabry disease was approved by the U.S. Food and Drug Administration and marketed under name Galafold (**19**) [79]. In addition, iminosugar based ASSCs, including *isofagomine* (**20**) and DNJ (**4**) were tested in the clinical trials for the treatment of Gaucher and Pompe disease, which are characterised by mutations in β -glucocerebrosidase (GBA) and α -1,4-glucosidase (GAA), respectively [76,77].

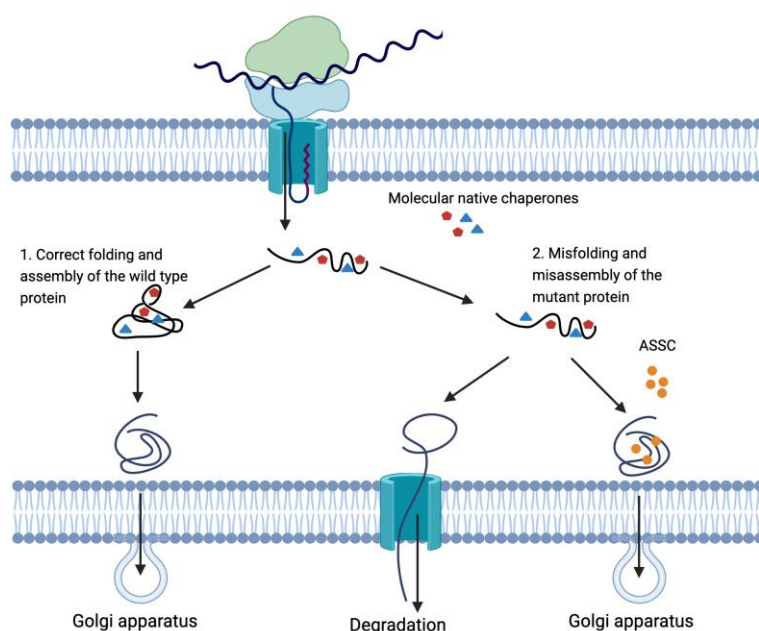


Figure 10. The endoplasmic reticulum (ER) quality control system and application of active-site-specific chaperone (ASSC) therapy. 1) The newly synthesised protein is correctly folded with the assistance of molecular chaperones (white ovals and blue pentagons), and subsequently transported out of the ER to the Golgi apparatus; 2) misfolded and unfolded mutant protein is retained in ER and further degraded *via* endoplasmic-reticulum-associated protein degradation (ERAD) pathway. The application of ASSC therapy (red triangles) can prevent the ER degradation by binding to the active site of the mutated enzyme and stabilise the proper fold, which is subsequently transported to the Golgi apparatus.

The application of iminosugars is also used in substrate reduction therapy (SRT) for the treatment of LSDs. This strategy aims to reduce the accumulation of substrates in a biosynthetic pathway by inhibiting a key enzyme with an iminosugar drug. It results in the reduced number of molecules, which is required for catabolism, thus contributing to the balance of the rate of synthesis with the impaired rate of catabolism [66,80] The licensed iminosugar drug, *N*-butyl-DNJ, marketed under the name Zavesca (Miglustat) **(18)** (**Figure 9**) is used for the treatment of type I Gaucher's. This disease leads to the accumulation of intracellular β -glucosylceramide due to impaired activity of glucocerebrosidase. The inhibition of glucosylceramide synthase (the enzyme responsible for the syntheses of glucosylceramide) leads to the lower build-up of the substrate and mitigates some symptoms of the disease [16].

1.1.4 Chemical synthesis of iminosugars

The chemical synthesis of iminosugars is challenging due to a combination of the polar polyhydroxylated structures, their stereochemical complexities and the lack of a chromophore, which can complicate reaction monitoring and purification. Synthetic methods for accessing iminosugars typically utilise chiral catalysts or chiral auxiliaries to create new asymmetric centres and control the stereochemical conformation [81,82]. Another more common approach takes advantage of chiral pool reagents; predominantly carbohydrates [11,55,83], and less often amino acids [84,85]. Both strategies rely heavily on protecting group manipulations to mask reactive groups. In the section below, only the synthetic examples from the chiral pool starting materials are discussed.

A classic example starting from carbohydrate-derived materials is the synthesis of DNJ. In the study of Behling *et al.* [86], L-sorbose undergoes selective protection (**22**), followed by introduction of an azide group (**23**). The azide is then reduced to the corresponding amine (**24**) and the acetal protecting group cleaved, which results in cyclisation. The final step is the imine reduction with H₂ and Pd/C, which affords the DNJ product (**Figure 11**).

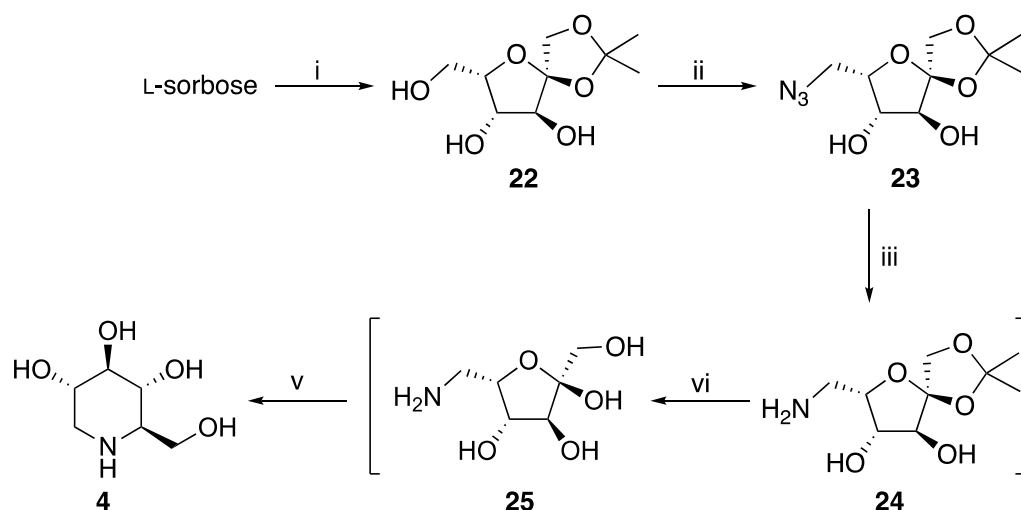


Figure 11. A five-step preparation method of DNJ from L-sorbose. Reaction conditions- i) DMP, H₂O, H⁺, ii) TIBSCl and NaN₃, iii) Ph₃PO, H₂O, iv) Dowex resins, H₂O, v) H₂, Pd/C. The intermediates (in parentheses) were not isolated and absorbed on the Dowex acidic support, which resulted in the deprotection followed by the direct reduction with molecular hydrogen and Pd/C.

Readily available alditols have been extensively used in the preparation of iminosugars [87–89]. The study of McCaig *et al.*, employs a six-step strategy that converts xylitol and D- or L-arabinitol to six membered iminosugars, represented by the example in **Figure 12**. In the first step, the primary alcohols of the alditols undergo protection to provide ditrityl derivatives (**26**), followed by the protection of the secondary alcohols as benzyl ethers (**27**), and finally detritylation, which affords the diols (**28**). The diols are then converted into the ditosylates and are reacted with a primary amine, which after deprotection of the benzyl ethers, provides the iminosugars (**31**).

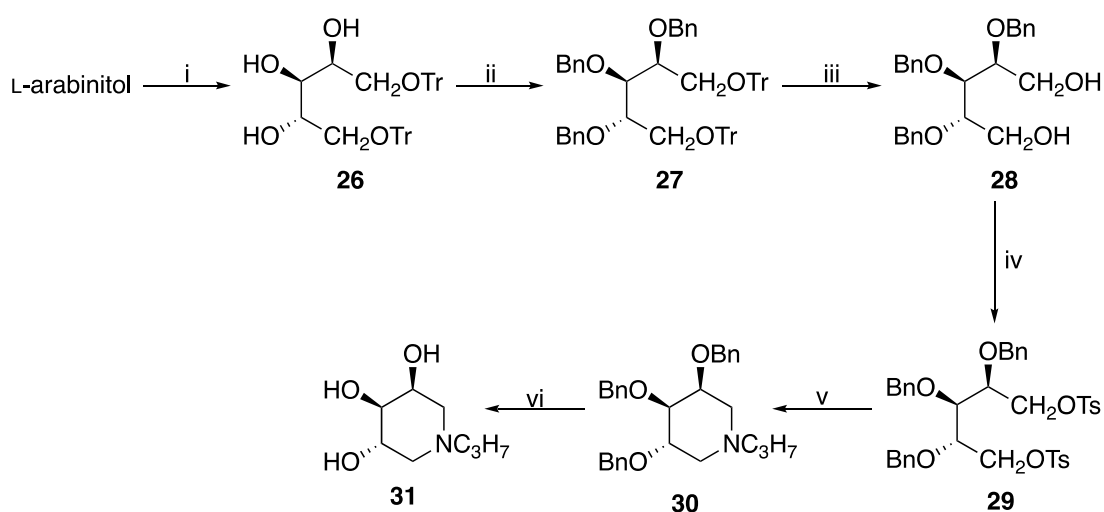


Figure 12. A six-step preparation of a piperidine iminosugar (**31**) from L-arabinitol. Reaction conditions- i) TrCl, DMAP, Et₃N, DMF, ii) NaH, BnBr, DMF, iii) diluted HCl, dioxane, iv) TsCl, C₅H₅N, CH₂Cl₂, v) C₃H₇NH₂, 40 °C, vi) H₂, Pd/C, AcOH.

Gluconolactones have also been applied for the preparation of iminosugars [90,91]. Lactones readily react with amines to form the corresponding amides, which cyclise to form lactams and are eventually reduced to amines. This approach was used in the study of Meng and Hesse (**Figure 13**) where a commercially available 2,3,5-tri-O-benzyl-D-arabinolactone (**32**) was converted into an amide (**33**) using benzylamine. The formation of the iminosugar (**35**) proceeds through mesylation of the free hydroxyl group and subsequent amide reduction with borane.

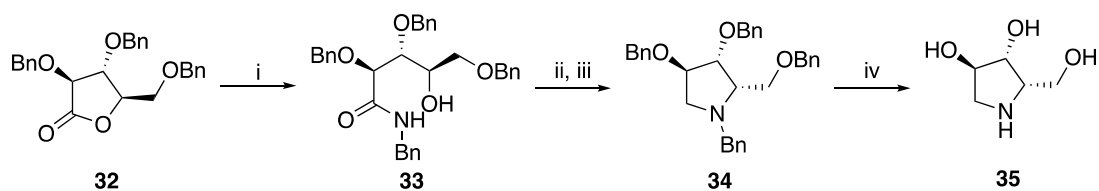


Figure 13. Preparation of iminosugar (**35**) starting from benzyl-protected gluconolactone. Reaction conditions: i) BnNH_2 , NaBH_3CN , MeOH ii) MsCl , Et_3N , iii) BH_3SMe_2 , iv) 2N HCl, EtOH, Pd/C.

Although, traditional synthetic chemistry approaches allow access to a wide range of structures, these routes are often hampered by long synthetic sequences. The extensive protecting group manipulations and inconvenient activation reactions often result in limited overall yields. Consequently, application of these synthetic routes on an industrial scale often represents a major problem. Thus, an important objective in the field of iminosugars is to simplify the synthetic route in order to improve their commercial potential. One possible approach would be the application of more regio- and stereo methods, including biocatalysis, to avoid protecting group manipulations and shorten the synthetic route.

1.1.5 Application of biocatalysis in iminosugars synthesis

Biocatalysis is the use of enzymes or microorganisms as catalysts for chemical transformations. As a result of their highly complex three-dimensional structure, enzymes catalyse chemical reactions with high chemo-, regio- and enantio/diastereoselectivity. In addition to the exceptional selectivity achievable, enzymatic reactions are mostly performed in the aqueous environment, under mild conditions (ambient temperatures and pressures), often without the need for functional group protection and with need for only minimal purification. This affords shorter routes and generates less waste compared to conventional organic synthesis, rendering them both environmentally attractive and cost-effective [92,93]. Despite all the benefits offered, very few examples of the application of biocatalytic steps in the syntheses of iminosugars have been reported in the literature.

Aldolases were predominantly used in the chemo-enzymatic route for preparation of the iminosugar libraries. These enzymes mediate the formation of carbon-carbon bonds in a stereoselective manner by catalysing an aldol reaction between a donor

ketone substrate (the nucleophile) and an acceptor aldehyde (the electrophile) (**Figure 14**) [18,94–96]. Several different aldolases, such as fructose 1,6-diphosphate aldolase (FDP), L-rhamnulose-1-phosphate aldolase (RhuA), L-fuculose phosphate aldolase (FucA), D-fructose-6-phosphate aldolase (FSA) and deoxyribose-phosphate aldolase (DERA) have been applied for the synthesis of the piperidine, pyrrolidine and bicyclic iminosugars, which typically proceeds through three steps: biocatalytic aldol addition, removal of the phosphate group and reduction under molecular hydrogen with Pd/C [18,97,98], (**Figure 15**). These aldolases accept a wide range of aldehyde acceptors, including azido aldehydes and *N*-Cbz amino aldehydes (**Figure 16**). However, their drawback relates to the minimal variation possible with the donor substrates that they tolerate, and FDP, FucA and RhuA are exclusively dihydroxyacetone phosphate (DHAP) (**37**) dependent [18]. The DHAP compound is expensive, relatively unstable, and the phosphate group is not required in the final product. The exceptions are the FSA aldolase, which accepts the non-phosphorylated donors, dihydroxyacetone (DHA) and hydroxyacetone (HA) and the DERA aldolase, which can accept ethanal and propanone. These enzymes were used in the preparative-scale synthesis of several iminosugars of five and six-membered heterocycles and bicyclic structures [99,100].

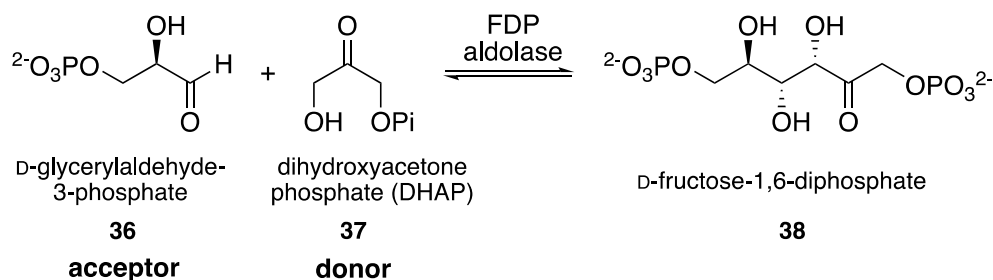


Figure 14. An example of the *in vivo* reaction catalysed by FDP aldolase, which involves DHAP as a nucleophile (donor) and D-glyceraldehyde-3-phosphate as an electrophile (acceptor) and results in the synthesis of a metabolic sugar D-fructose-1,6-diphosphate.

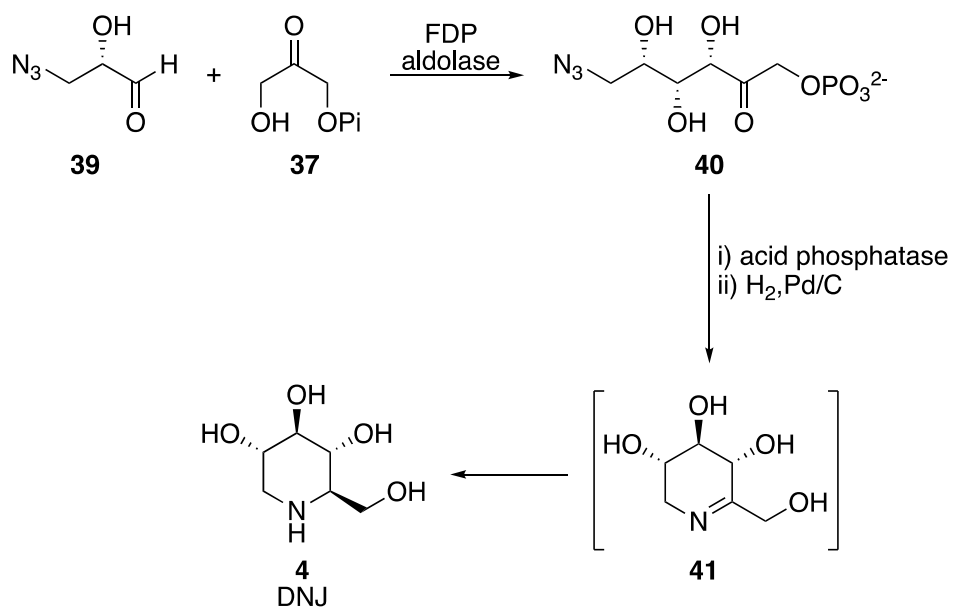


Figure 15. An example of the application of the DHAP dependent fructose-1,6-diphosphate aldolase (FDP) in the synthesis of DNJ (**4**). The transformation proceeds through the biocatalytic aldol addition between the azido aldehyde (**39**) and DHAP (**37**), followed by the phosphate group removal by acid phosphatase and direct reduction of an imine intermediate (**41**) to DNJ.

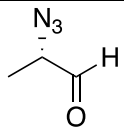
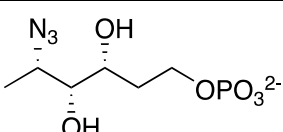
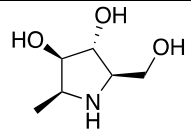
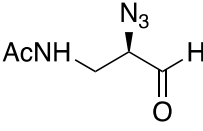
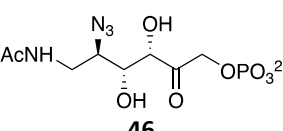
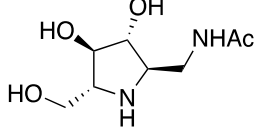
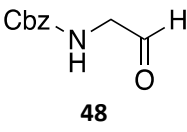
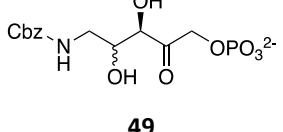
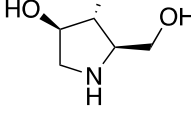
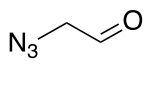
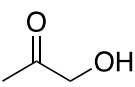
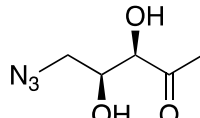
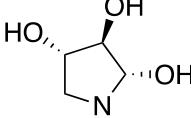
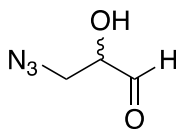
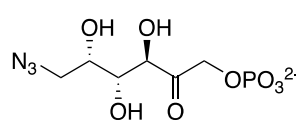
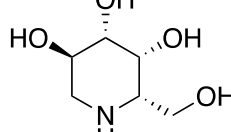
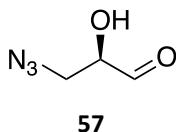
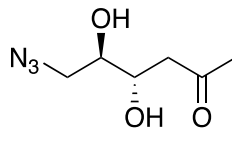
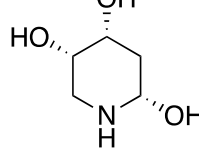
Aldolase	Acceptor	Donor	Product	Iminosugar
FDP	 42	DHAP	 43	 44
FDP	 45	DHAP	 46	 47
FDP	 48	DHAP	 49	 1
FSA	 50	 51	 52	 53
FucA	 54	DHAP	 55	 56
DERA	 57	 58	 59	 60

Figure 16. Selected examples of the synthesis of five and six-membered iminosugars using aldolases. References: **44, 47, 56-** [101], **1-** [18], **53-** [99], **60-** [102].

A whole-cell biocatalytic transformation with *Gluconobacter oxydans* (*G. oxydans*) DSM 2003 was used for the production of several iminosugars. This microorganism possesses a number of different membrane-bound dehydrogenases capable of oxidising secondary alcohols of polyols, including aminopolyols, in a chemo-, regio- and stereoselective manner [103,104]. However, in the case of the amino polyol substrates, the oxidation only occurs when the amine functionality is protected with

Cbz or formyl group [19]. In 1981, Kinast and Schedel developed a chemo-enzymatic route employing *G. oxydans* DSM 2003 for the production of DNJ starting from D-glucose (**Figure 17**). The reaction proceeds *via* the reductive amination of D-glucose, subsequent protection of the amine group with benzyloxycarbonyl (Cbz), selective oxidation of a secondary alcohol group with resting cells of *G. oxydans*, and finally deprotection and reduction of the spontaneously formed imine using molecular hydrogen and Pd/C [105]. In their later study, the microbial oxidation was performed on an industrial scale with a substrate concentration of 250 kg/m³ (1.2 M) and a 2.5 kg/m³ loading of the lyophilised cells, resulting in quantitative oxidation within 16 h. One of the critical steps to achieving high conversion with *G. oxydans* was the external supply of oxygen to the reactor and maintaining the stability of the biocatalyst [19]. The same approach was used for the production of two other iminosugars DAB (**1**) and a six membered galactonojirimycin from D-arabinose and D-galactose, respectively. Here, the sugar derived amino alcohols were protected with a formyl group [106,107]. In the study of Landis et al., *G. oxydans* DSM 2003 was shown to also tolerate a butyl group and oxidise *N*-butylglucamine in the synthesis of *N*-butyl-DNJ known as Miglustat (**18**).

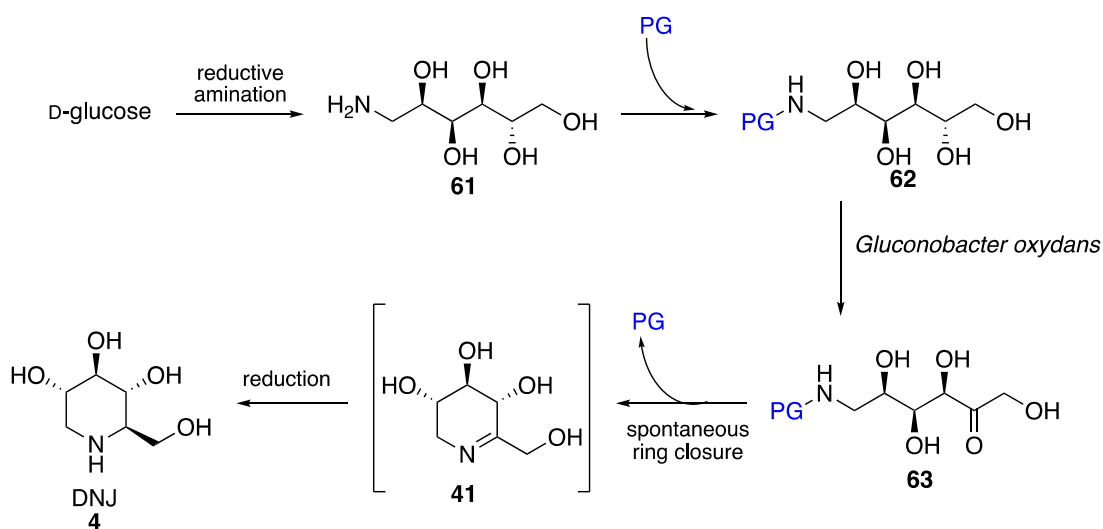


Figure 17. The chemo-enzymatic approach of DNJ (**4**) synthesis with *G. oxydans* starts from D-glucose. The reaction commences with reductive amination of D-glucose, affording the corresponding amino alcohol (**61**). Chemical protection of the resulting amine group (Cbz or formyl) followed by microbiological oxidation with *G. oxydans* and removal of the protecting group leads to spontaneous intramolecular cyclisation (**41**). The resulting cyclic imine intermediate is finally reduced to DNJ with hydrogen and Pd/C [19].

1.2 Biocatalytic cascades for the synthesis of organic molecules

Traditional organic synthesis commonly utilises a step-by-step approach to convert a starting material into the desired product and often requires isolation and purification of intermediates along the synthetic route. This often results in low overall yields, can be time intensive and generates considerable waste [108]. One of the goals in green chemistry is the integration of catalytic steps into a one-pot system, without isolation of intermediates [109]. Enzymatic reactions in living organisms essentially function as a one-pot-system, being assembled in a highly efficient network of cascades, where the product of one biocatalytic step becomes a substrate for the next transformation, (**Figure 18**). These natural cascades utilise a relatively simple set of starting materials to construct complex products. Commonly in nature, enzymatic reactions operate at low concentration of reactants to facilitate high selectivity and avoid by-product formation, and without the separation of intermediates [110]. The efficiency of biosynthetic pathways has been an inspiration for organic chemists for decades, and in 1984, the first artificial *in vitro* cascade was developed, which employed lactate and alanine dehydrogenase for the transformation of lactic acid to L-alanine *via* pyruvate in flow [111,112]. The application of biocatalytic cascades in organic synthesis brings numerous benefits, including no requirement for purification of intermediates, reduced operating time, costs and waste, which leads to overall higher yields and improved atom economy. Moreover, biocatalytic processes, generally operate under similar conditions in aqueous buffers, ambient temperature and atmospheric pressure, which facilitates their integration into cascades [93,110,112]. However, to achieve a successful, cascade, several key features must be considered and incorporated into the design, and these include: the overall thermodynamic parameters of the cascade must be favourable ($\Delta G_{\text{cascade}} < 0$); the selected enzymes must catalyse the reactions with high specificity to avoid undesired reactivity with different substrates; the kinetic parameters (for example substrate concentration and temperature) and pH of the individual reactions must be tuned to facilitate product formation and prevent enzyme deactivation [113,114].

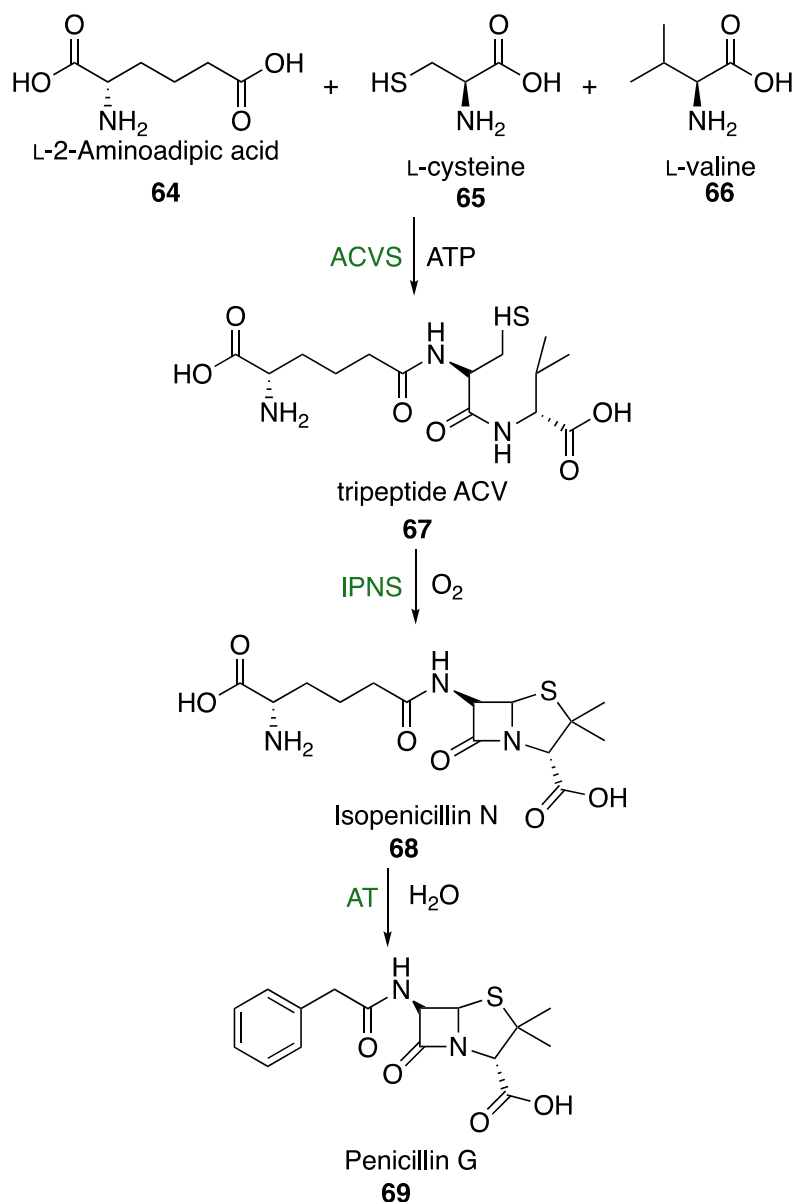


Figure 18. Penicillin biosynthesis in microorganisms, which involves three enzymatic steps. It begins with the condensation of L- α -aminoadipic acid (**64**), L-cysteine (**65**) and L-valine (**66**) into a tripeptide (**67**) catalysed by δ -(L- α -aminoadipyl)-L-cysteine-D-valine synthetase (ACVS), followed by the oxidation with Isopenicillin N synthase (IPNS) to Isopenicillin N (**68**). The final step involves the side-chain exchange catalysed by isopenicillin N acyltransferase (AT) to afford Penicillin G. (**69**). Adapted from [115,116].

The most commonly applied biocatalytic cascades adopt *in vitro* (i) and *in vivo* (ii) designs, both offering enormous flexibility (**Figure 19**) [117]. The construction of the *in vivo* biocatalytic cascade typically recruit a tandem of heterologously expressed enzymes within a single host to form an artificial pathway. This system eliminates the need for expensive and time-intensive protein purification and benefits from the natural supply of cofactors produced by a host organism. However, it presents

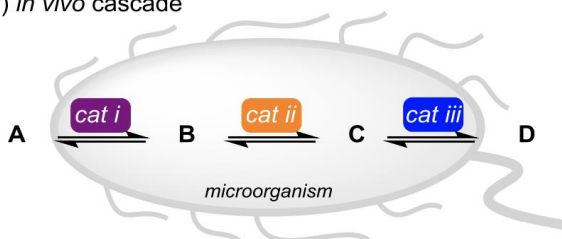
also numerous challenges related to regulatory mechanisms for cell growth and gene expressions. For example, the co-expression of multiple genes in a single organism can lead to metabolic burden of the host resulting in different expression levels of the desired enzymes in the pathway and also affect its optimum growth rate. On the other hand, due to varying kinetic of enzymes, it is often required to determine optimum expression levels of enzymes in the *in vivo* cascade, which can be challenging [118–120]. Furthermore, the presence of numerous endogenous enzymes in the host can lead to the formation of undesired by-products and product decomposition [121].

Commonly, in *in vitro* cascades, genes are overexpressed in one or more hosts, and the enzymes are delivered to the reaction in the form of cell lysates or purified proteins [110]. This design offers flexibility and control over the quantity of biocatalyst(s), temperature and the application of more diverse reagents and solvents, which is often not compatible with living cells. The disadvantage is a required supplementation of expensive cofactors, although a number of recycling strategies are commonly applied [112,117,122]. Some studies demonstrate a hybrid cascade construction, which relies on the combination of both mentioned designs: heterologously expressed enzyme(s) within a single host and overexpressed enzymes in their purified or crude lysate form [123,124].

(i) *in vitro* cascade



(ii) *in vivo* cascade



(iii) hybrid *in vivo/in vitro*

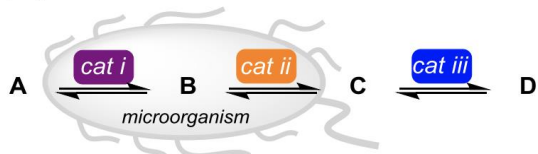


Figure 19. A comparison of the three different biocatalytic cascade designs: (i) *in vitro*, (ii) *in vivo* and (iii) hybrid of cascade reactions. A product D is generated with a starting material A by using selective biocatalysts cat i-iii [123].

The application of biocatalytic cascades in organic synthesis has become increasingly popular, and a number of striking examples have been reported in the literature. This concept has been widely adopted in industry, and a few selected examples are introduced below.

The most recent industrial example of the *in vitro* biocatalytic cascade has been developed by a Merck-Codexis collaboration, leading to the preparation of the investigational HIV drug, islatravir (**76**) (**Figure 20**) [125,126]. The process employed nine enzymes of fungal, bacterial, mammalian and plant origin, of which five were engineered to optimise their properties, and four were additional auxiliary enzymes to regenerate cofactors, displace reaction equilibria and remove inhibitory by-products. The pathway was initiated from a simple achiral building block of ethynylglycerol (**70**), which was oxidised by galactose oxidase (GO). This step also required the action of catalase and horseradish peroxidase to decompose the hydrogen peroxide by-product and regenerate the GO enzyme. The following step involved phosphorylation by ATP dependent pantothenate kinase (PanK), and acetate kinase (Ack) that recycled the ATP cofactor. The third and last step of the cascade was inspired by the bacterial nucleoside salvage pathway, which plays a role in recycling bases and nucleosides formed during degradation of RNA and DNA [127]. This step required a simultaneous action of four enzymes: purine nucleoside phosphorylase (PNP), phosphopentomutase (PPM), deoxyribose-5-phosphate aldolase (DERA) and sucrose phosphorylase (SU), that resulted in the final product (**76**). Eventually, the biocatalytic cascade afforded only a single stereoisomer of islatravir in 51 % overall yield without isolation of intermediates; under mild conditions in a three-step synthesis. Compared to the synthetic methods for that target, the biocatalytic approach required half as many steps; thus, the process is more sustainable and exhibit more efficient atom economy [128,129].

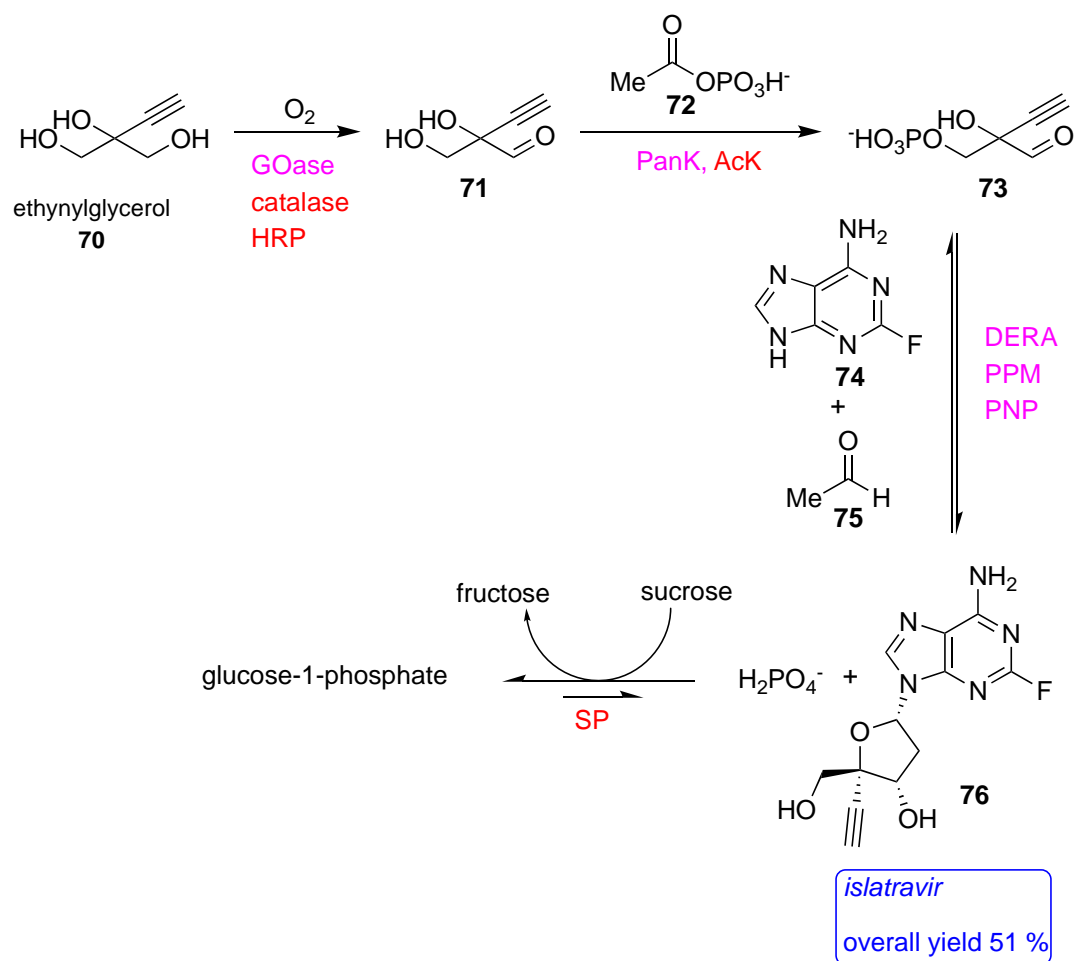


Figure 20. Fully assembled biocatalytic cascade for the total synthesis of islatravir (**76**), which involved nine enzymes: immobilised galactose oxidase (GOase), catalase and horseradish peroxidase (HRP), immobilised pantothenate kinase (PanK), and acetate kinase (AcK), and cell lysates of purine nucleoside phosphorylase (PNP), phosphopentomutase (PPM), deoxyribose-5-phosphate aldolase (DERA) and sucrose phosphorylase (SU). Engineered and auxiliary enzymes are marked in magenta and red respectively.

Another impressive example of an artificial biocatalytic cascade in a one-pot system was used for the preparation of disubstituted piperidines and pyrrolidines, by coupling regioselective monoamination of diketones or keto aldehydes by transaminases with subsequent stereoselective reduction of the generated cyclic imines by imine reductases (**Figure 21**). Initial results demonstrated that the presence of imine reductases in the sequential cascade with transaminases inhibited the transamination reaction. This problem was overcome by allowing complete consumption of the diketone substrate by the transaminase (24 h), before the addition of imine reductase in the same pot [124]. This system applied

the LDH/GDH equilibrium displacement strategy for the transaminase, which will be discussed in detail in section 1.2.1.2.

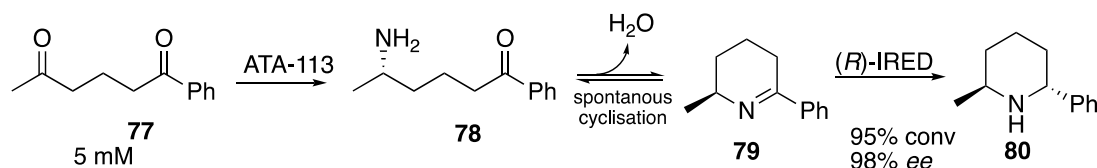


Figure 21. An example of a one pot biocatalytic cascade for the preparation of (2*R*,5*R*) disubstituted piperidine, which recruits transaminase (TA) and (*S*)-selective imine reductase IRED. The reaction condition: keto aldehyde substrate (**77**) (5 mM), ATA-113 (TA) (2.5 mg/mL), L-alanine (250 mM), PLP (1 mM), GDH (1 mg/mL), LDH (0.5 mg/mL), glucose (100 mM), NAD⁺ (1.5 mM), NaPi (100 mM, pH 7), 30 °C, 250 rpm, 24 h followed by addition of wet cells containing IREDs (200 mg/mL) and incubation at at 30 °C, 250 rpm for 24 h [124].

A similar *in vivo* cascade was applied for the synthesis of disubstituted piperidines and pyrrolidines (**Figure 22**). It begins with reduction of a carboxylic acid (**77**) achieved by carboxylic acid reductase (CAR) followed by biocatalytic transamination and imine reduction. In addition, the system required overexpression of 4'-phosphopantetheinyl transferase (Sfp) that is required by CAR enzymes for the posttranslational modifications [130]. Five non-chiral ketoacid substrates were screened and all of them showed the formation of the chiral amine, of which two were subsequently used in the preparative scale biotransformations yielding cyclic amine products from 58-59 %, [123].

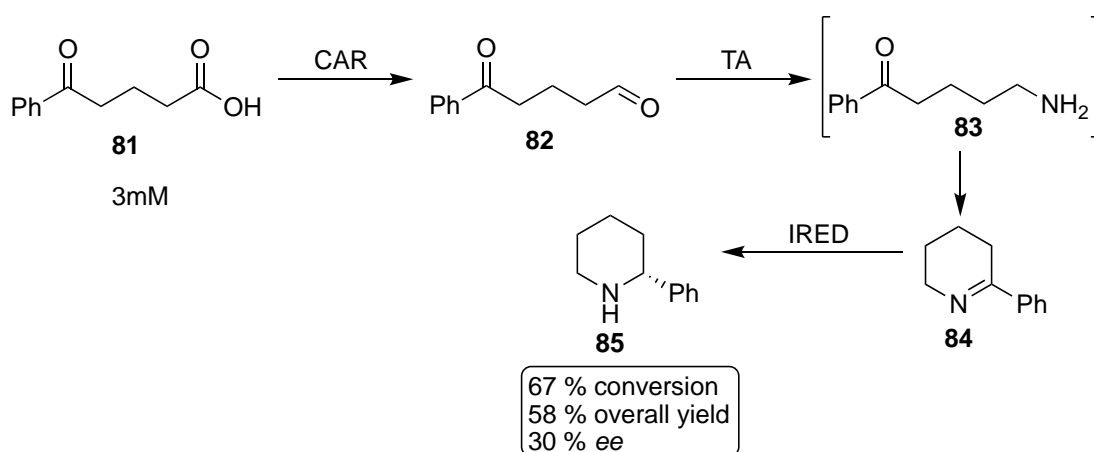


Figure 22. An example of the application of the *in vivo* cascade in the preparative-scale biotransformation for the preparation of disubstituted piperidines starting from carboxylic acid (**81**). The cascade involved co-expressed carboxylic acid reductase (CAR), transaminase (TA) and imine reductase (IRED) in BL21(DE3) [123]. The reaction conditions: keto acid substrate (**81**) (3 mM), glucose (50 mM), D-alanine (250 mM), wet BL21 cells containing three plasmids encoding for CAR, TA and IRED (40 mg/mL) NaPi (500 mM, pH 7), 30 °C, 24 h [123].

Another example of the *in vivo* cascade exploited a combination of carboxylic acid reductase or alcohol oxidase (AO) and reductive aminase (RedAm) in the preparation of secondary *N*-alkylated amines on a preparative scale yielding 49-74 % of a final product (**Figure 23**). This system required the application of the ATP and NADPH recycling strategy and employed AMP phosphotransferase (PAP), adenylate kinase (ADK) and glucose dehydrogenase (GDH) [131].

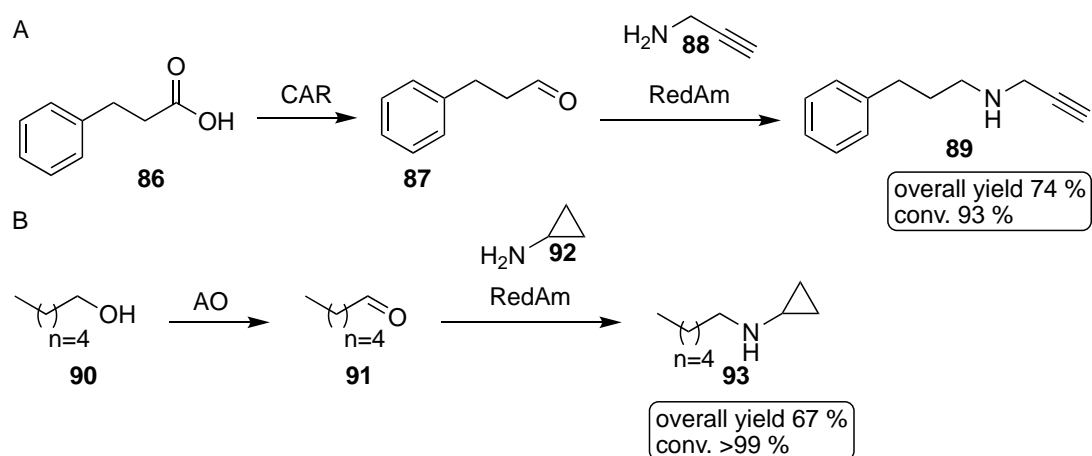


Figure 23. An example of the preparative biotransformation of keto acid (**86**) or alcohol (**90**) by the application of the *in vivo* cascade, which yielded 59 % of the final product. It recruited two sets of enzymes starting from carboxylic acid reductase (CAR) or alcohol oxidase (AO), which was followed by reductive amination with reductive aminase (RedAm) [123]. Reaction conditions of A: acid substrate (**86**) (10 mM), amine substrate (**88**) (20 mM), ATP (0.1 mM), NADP⁺ (0.08 mM), glucose (100 mM), MgCl₂ (100 mM), polyphosphate (4 mg/mL), DMSO (2 mL), RedAm (0.2 mg/mL), CAR (0.25 mg/mL), Adk (0.25 mg/mL), PAP (0.25 mg/mL), CDX-901 GDH (0.1 mg/mL), Tris buffer (100 mM pH 7.5), 30 °C, 250 rpm, 24 h. Reaction conditions of B: alcohol (**90**) (25 mM), amine donor (**92**) (50 mM) NADP⁺ (0.2 mM), glucose (50 mM), RedAm (0.2 mg/mL), lysate formed *E. coli* expressing alcohol oxidase (AcCO₆) (derived from 3 g of wet cells), CDX-901 GDH (0.3 mg/mL), KPi buffer (100 mM pH 7), 30 °C, 250 rpm, 24 h.

Enzymatic cascades have also been successfully used in the deracemization of organic compounds, for example nitrogen heterocycles [132] or tetrahydroisoquinolines [133]. A study of Heath *et al.*, employs a combination of an engineered monoamine oxidase (MAO) 6-HDNO and imine reductases (IREDs) in a one-pot process to deracemize a number of substituted pyrrolidines and piperidines yielding from 45-89 % of the enantiomerically pure product, (**Figure 24**) [132].

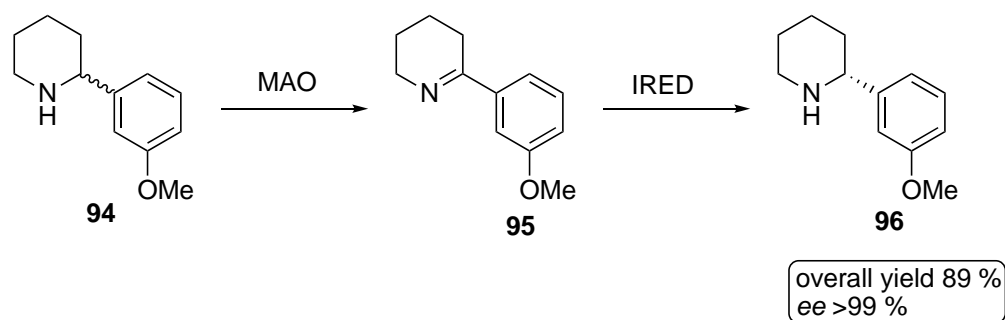


Figure 24. An example of a one-pot deracemization process employing monoamine oxidase (MAO) and imine reductase (IRED) for the preparation of enantiopure heterocycles [132]. The reaction conditions: racemic substrate **94** (5 mM), whole BL21 cells expressing (*R*)-IRED (50 mg wet weight), whole BL21 cells expressing 6-HDNO E350L/E352D variant (50 mg wet weight), KPi (1 M, pH 7.4), 10 mM glucose, 30 °C, 250 rpm, 24 h.

The following sections describe mechanisms and applications in organic synthesis of the enzymes, which were relevant or used in this project, namely transaminases (TAs), alcohol dehydrogenases (ADHs) or alcohol oxidases (AOs), imine reductases (IREDs) and monoamine oxidases (MAOs).

1.2.1 Transaminases

Transaminases (TAs) also known as amine transaminases (ATAs) are PLP dependent enzymes, which catalyse the reversible transfer of an amino group from a suitable amine donor to a carbonyl acceptor: ketone, aldehyde, or ketoacid. In nature, transaminases are ubiquitous across all organisms, and their primary role is the synthesis of α -amino acids from α -keto acids from an amine source or the amino acid decomposition from proteins, which indicates the vital role they play in the nitrogen metabolism, (**Figure 25**) [92].

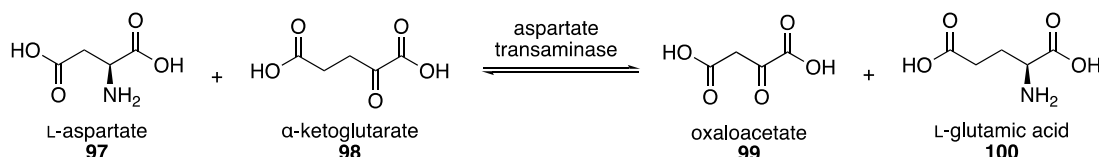


Figure 25. An example of a natural reaction catalysed by aspartate transaminase involving the reversible interchange of L-aspartate and α -ketoglutarate to L-glutamic acid and oxaloacetate [134].

TAs are industrially very important enzymes due to their successful applications for the preparation of various chiral amines [135–140]. Chiral amines are prevalent motifs in small drug molecules (40-45 %) but also other industrially important fine

chemicals and agrochemicals [141]. However, one of the main challenges associated with these enzymes is the reversibility of the reaction, which inspired the development of methods to displace the equilibrium towards product formation [142,143]. The section below discusses the general mechanism of transaminases, strategies for the equilibrium displacement and synthetic applications.

1.2.1.1 Catalytic mechanism of transaminases

Transaminases depend on pyridoxal 5'-phosphate (PLP) (**102**) for activity. The coenzyme acts to shuttle the amine group from a sacrificial amine donor (**101**) to form pyridoxamine 5'-phosphate (PMP) (**108**) (**Figure 26**). The transformation is characterised by a reversible ping-pong bi-bi mechanism, which begins with a conserved lysine residue attacking enzyme-bound PLP (E-PLP) and forming a complex, called the internal aldimine (**103**). In the following step, an amine donor undertakes a nucleophilic attack at the iminium carbon of the internal aldimine, resulting in a geminal diamine intermediate (**104**), which frees the catalytic lysine. This leads to an external aldimine, which is formed *via* a Schiff base between E-PLP and the amine donor. The subsequent deprotonation of the external aldimine yields a quinonoid intermediate (**105**), which is stabilised by resonance. The intermediate collapses, with nitrogen from the pyridine ring donating its lone pair of electrons to form a ketimine (**106**), which is subsequently hydrolysed to form E-PMP (**108**). From now, the enzyme performs the reaction sequence in reverse. The E-PMP reacts with an amine acceptor (ketone **109**) leading to a ketimine (**110**), which undergoes proton abstraction and again, forms a quinonoid intermediate (**111**). The intermediate collapses through re-aromatisation of the pyridine ring, and the enzyme provides a proton to form a chiral external aldimine. In the final step, the external aldimine undergoes nucleophilic attack by the catalytic lysine, followed by elimination to release the desired chiral amine product (**113**), and the internal aldimine ready for another round of catalysis [144].

Transaminases belong to fold I and fold IV of PLP dependent enzymes and catalyse the formation of chiral amines with (*S*)- and (*R*)-selectivity, respectively [145]. They can be further grouped according to the substrate acceptance: α -transaminases (α -

TAs) exclusively accept α -amino and α -keto acids, while ω -transaminases (ω -TAs), also referred as amine transferases (ATAs) accept substrates with distal carboxylate group or no carboxylate group at all and hence these predominantly are used for synthetic applications [146].

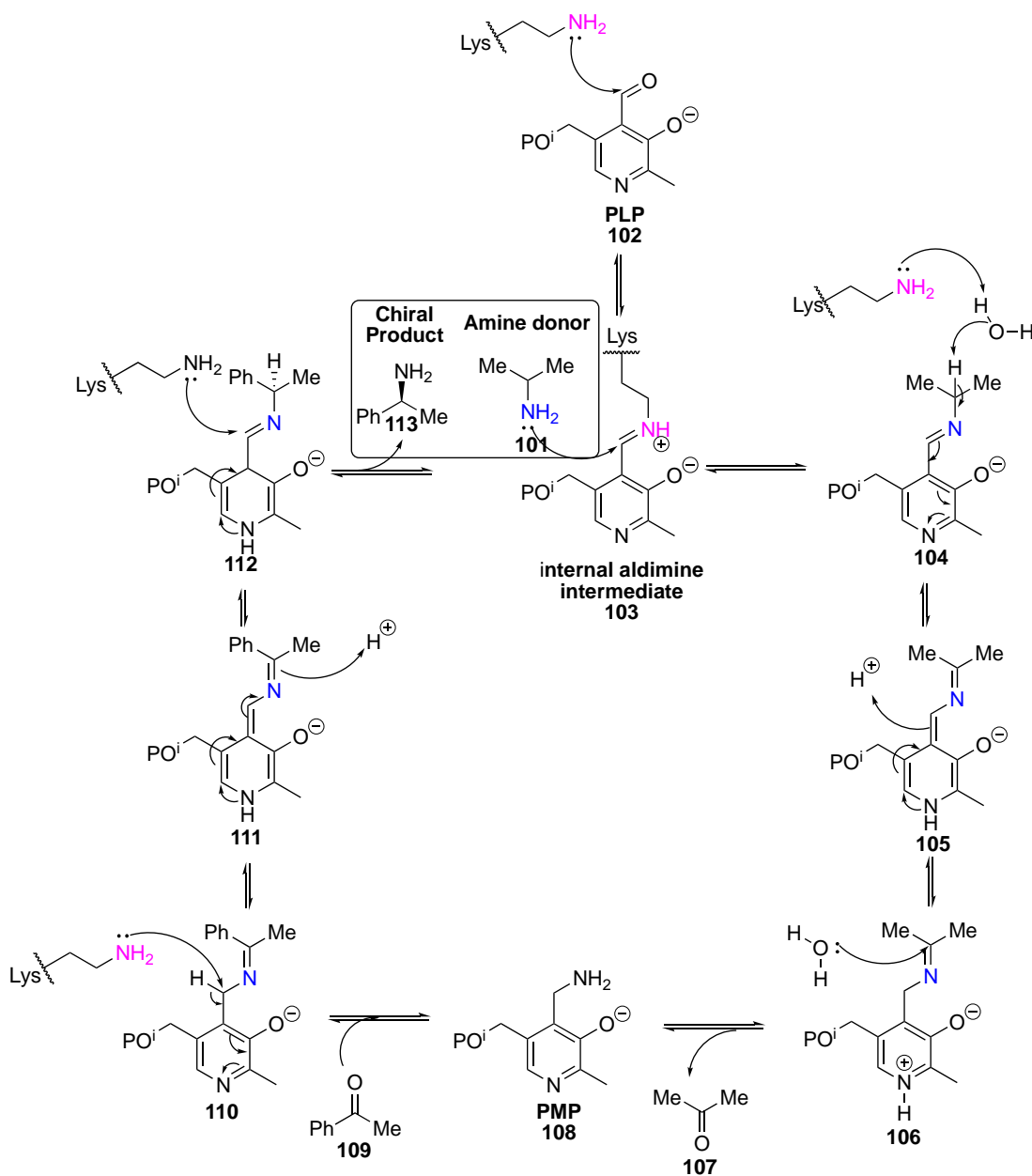


Figure 26. A ping-pong bi-bi catalytic mechanism used by transaminases proceeds *via* the PLP cofactor (**102**) that undergoes a reversible prototropic tautomerisation (**105**) followed by hydrolysis with an amino group to generate pyridoxalamine (PMP) (**108**), which effectively acts as a transport for the amine group and electrons between amine donor and acceptor. Modified from [144].

1.2.1.2 Displacing equilibrium

A significant drawback of the application of TAs in the synthesis is that the reaction equilibrium is often unfavourable. However, a number of methods have been developed to overcome this problem and displace the reaction towards product formation [147,148]. One example is the application of the enzymatic LDH/GDH by-product removal system, (**Figure 27**). This involves utilisation of alanine (**114**) as an amine donor, which is converted to pyruvate (**115**) and further reduced *in situ* by lactate dehydrogenase (LDH) to form lactic acid (**116**). In this strategy, the nicotinamide co-factor required by LDH is regenerated by glucose dehydrogenase (GDH); making use of glucose to recycle NAD(P)^+ back to NADH(P)H forming gluconic acid as a by-product [92,149]. An alternative approach utilises diamines as amine donors, which undergo an intramolecular cyclisation that drives the reaction to completion. An early example of this methodology makes use of *o*-xylylenediamine (**114**), which after transamination forms an amino-aldehyde. This by-product undergoes spontaneous cyclisation to an imine (**116**), which tautomerizes to isoindole (**117**). Isoindole spontaneously polymerises to polyisoindole and precipitates out of solution, forming a dark insoluble polymer [143], (**Figure 28**). The 'smart' amine donor methodology has been further extended to other diamines and successfully applied with a number of TAs [142,150].

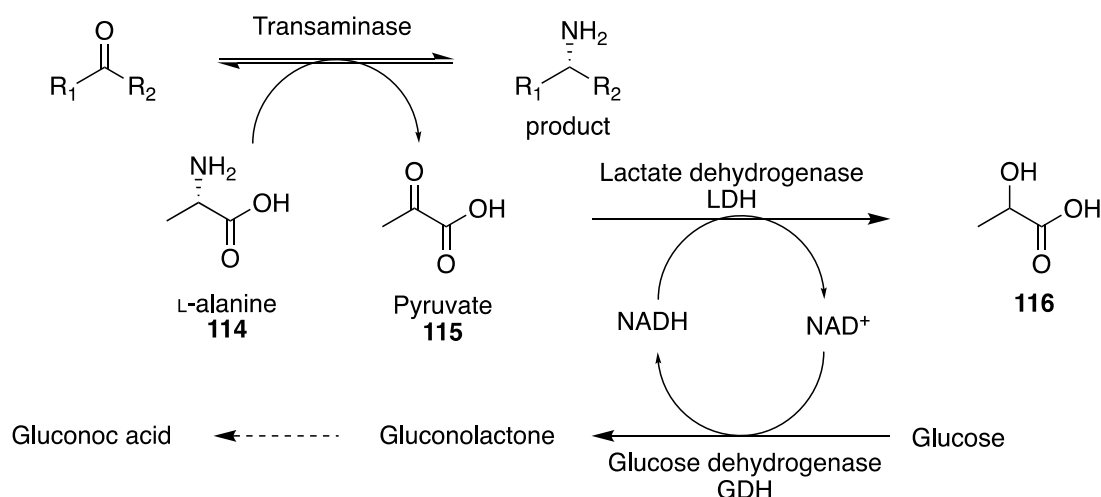


Figure 27. Enzymatic coupled by-product removal system, which uses LDH and GDH to drive the equilibrium of transaminase reactions [92].

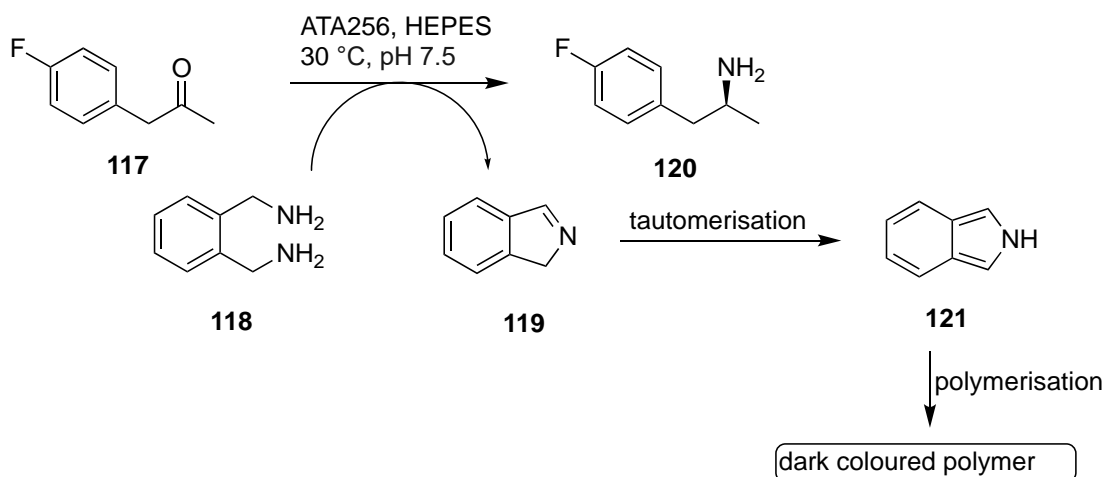


Figure 28. An example of the application of smart amine donor *o*-xylylenediamine (**118**) for the production of chiral amine (**120**). After transamination, the amine donor (**118**) is converted into amino aldehyde, which spontaneously cyclises to form an imine (**119**). The imine product undergoes tautomerization to isoindole (**121**), which polymerises and precipitates out of solution. The reaction conditions: 4-fluorophenylacetone (**117**) (100 mM), *o*-xyl (**118**) (100 mM), ATA256 (1.5 mg/mL), PLP (1 mM), HEPES (100 mM, pH 7.50), 30°C, 200 rpm, 24h. 99 % conversion, >99 % *ee* [143].

1.2.1.3 TA applications in chemical synthesis

Transaminases have been widely applied in asymmetric synthesis for the preparation of enantiopure chiral amines. The wild types have been shown to accept a broad substrate scope including various bulky ketones, bicyclic and small ketones [135,136], and been further engineered to convert bulky-bulky substrates and aliphatic ketones [137,139] (**Figure 29**).

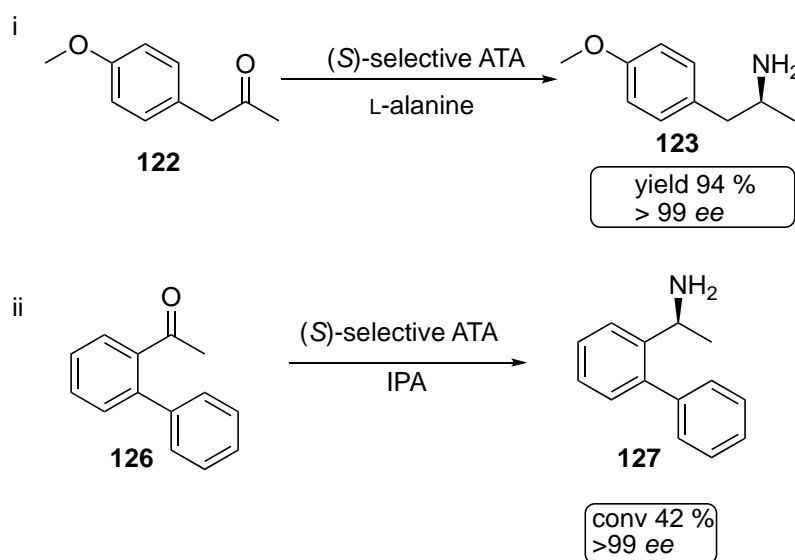


Figure 29. Examples of transformations catalysed by wild type (i) [135] and engineered transaminases (ii) [151].

Transaminases have been employed in the synthesis of natural products and pharmaceutical intermediates [138,140,152,153], (**Figure 30**). One of the most striking industrial examples is the application of a biocatalytic transamination step by Merck for the preparation of the antidiabetic drug Sitagliptin (**128**). The transamination was carried out by an engineered TA and the chiral amine group was installed in the final step of the synthesis, which proceeded with 92 % yield and >99.95 % *ee*. This single biocatalytic transformation contributed to the significant process improvement, providing sitagliptin with a 10-13 % increase in the overall yield, 53 % increase in the productivity and 19 % reduction in total waste [138].

Recently, novel transaminase activity towards linear sugars that predominantly exist in the cyclic form has been reported by our research group [154]. Two wild type TAs, namely 3HMU and HEWT and commercially available ATA-256, transformed seven five-membered aldoses with D- and L-configuration, achieving up to 94 % conversion. The biocatalytic reactions with the commercial TA were further performed on the preparative scale with isopropylamine (IPA) as an amine donor, and the isolated yields ranged from 11-69 % [154]. Later, TA activity towards one ketosugar, D-fructose was found, resulting in the formation of a chiral aminopolyol (**135**) [155], (**Figure 31**).

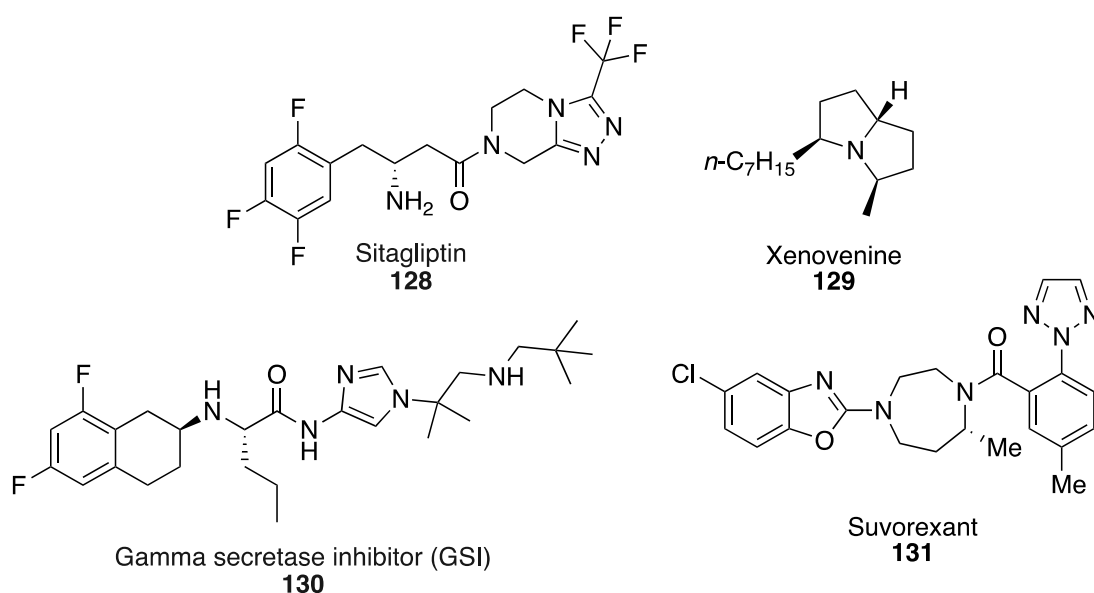


Figure 30. Structures of licensed drugs and natural products that were synthesised using a chemo-enzymatic approach with transaminases. References: **128** [138], **129** [152], **130** [140], **131** [153].

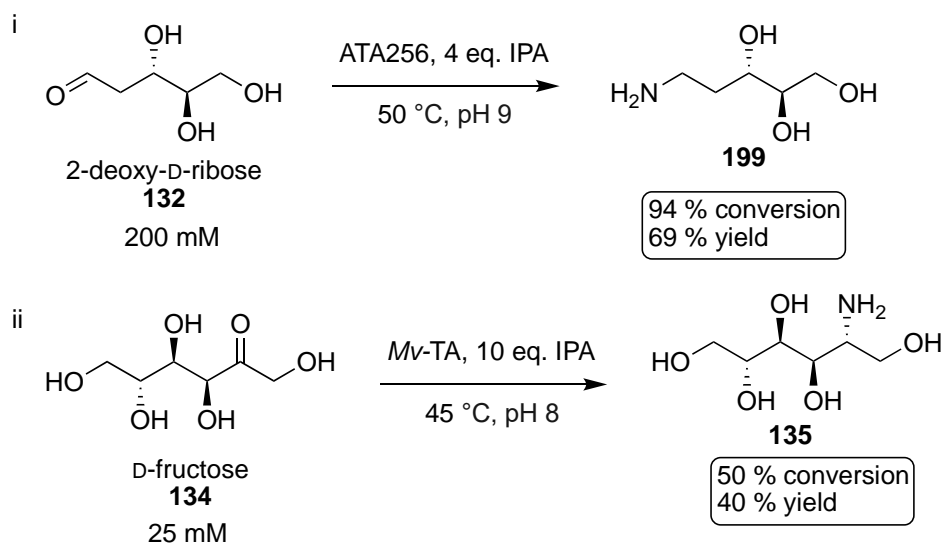


Figure 31. Examples of biocatalytic transformations of simple monosaccharides 2-deoxy-D-ribose (**132**) and D-fructose (**134**) with a commercial transaminase ATA-256 [154] and a wild type transaminase from *Mycobacterium vanbaalenii* (Mv-TA) [155].

1.2.2 Alcohol dehydrogenases and alcohol oxidases

Alcohol dehydrogenases (ADHs) and alcohol oxidases (AOs) are enzymes belonging to the oxidoreductases class, which regioselectively oxidise alcohols to carbonyl, (**Figure 32**). They are widely present in nature and found in bacteria, yeasts, fungi, plants, insects and mammals [156,157]. Both alcohol dehydrogenases and alcohol oxidases proceed *via* dehydrogenation mechanism. Some of them require a suitable cofactor such as nicotinamide adenine dinucleotide (NAD^+ or NADP^+) [158], flavin adenine dinucleotide (FAD) [159] or pyrroloquinoline quinone (PQQ) [160], and others possess a radical copper centre to carry out the oxidation [161].

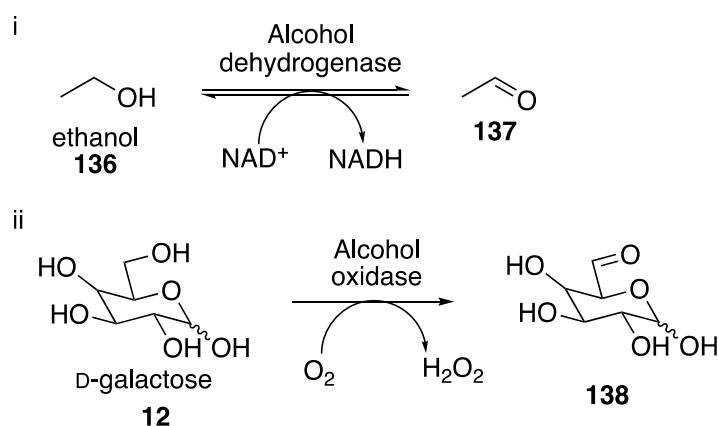


Figure 32. Examples of the natural transformations catalysed by i) liver alcohol dehydrogenase (ADH) [162], and ii) galactose oxidase, which belongs to the group of alcohol oxidases (AO) [163].

Several biocatalytic methods with ADHs and AOs for the oxidation of primary and secondary alcohols have been developed, which offer mild reaction conditions, high selectivity and catalytic efficiency [164–166]. The oxidations are either performed with heterologously expressed and isolated enzymes or as whole-cell biotransformations. The latter one comprises microbiological transformations involving known or unknown enzyme [165–167]. The biocatalytic methods for alcohol oxidation have been extensively studied, and the following section discusses the most relevant enzymes and their applications for the oxidations of (amino)-polyols.

1.2.2.1 Catalytic mechanism and cofactor dependence of ADHs and AOs

The dehydrogenation mechanism employed by AOs and ADHs occurs *via* hydride and proton transfer from the substrate to the cofactor/coenzyme, which requires a subsequent re-oxidation in order to perform a new catalytic cycle. The cofactor regeneration in dehydrogenases proceeds through reduction of another organic substrate, while oxidases use O₂ that is converted to H₂O₂ [167].

The zinc-containing NAD(P)⁺-dependent alcohol dehydrogenases are the most frequently used in organic chemistry. These enzymes catalyse the reversible oxidation of primary or secondary alcohols to aldehydes or ketones (**Figure 33**) [165].

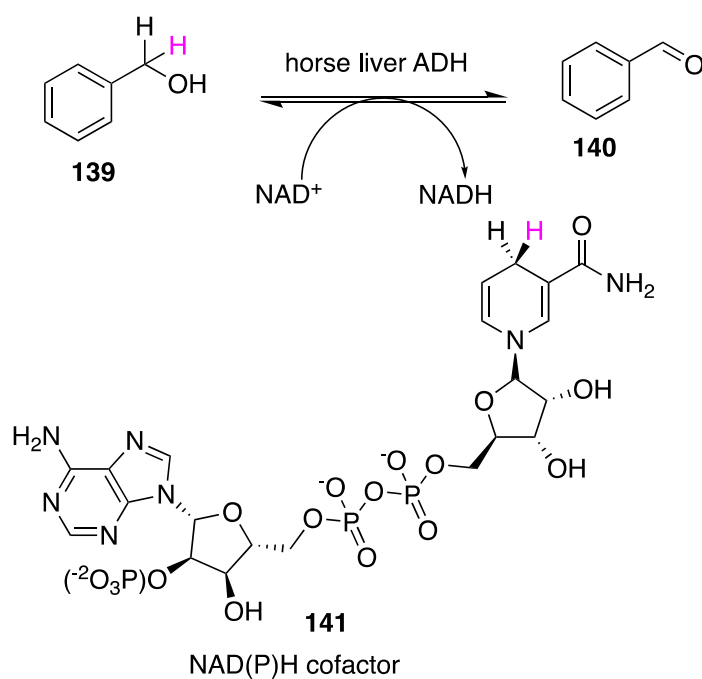


Figure 33. An example of the transformation of benzyl alcohol to benzyl aldehyde by the NAD⁺ dependent horse liver alcohol dehydrogenase (HLADH) [168].

A classic example is an NAD⁺-dependent ADH derived from horse liver (HLADH), which has been extensively studied and applied in chemical synthesis [169–171]. The HLADH features a dimeric structure with two Zn²⁺ ions bound to each subunit but only one is catalytically active and coordinated by two cysteine residues, a histidine and water molecule [158]. The analysis of the HLADH crystal structure suggests that the residues taking part in the proton transfer are His-51 and Ser-48, (**Figure 34**). The catalytic mechanism starts with the binding of NAD⁺, followed by the substrate, which displaces a water molecule coordinated to the zinc ion. The substrate is deprotonated through a proton transfer to the surrounding medium *via* the serine residue, the 2'OH on the NAD⁺ cofactor, and the histidine residue at the enzyme surface, resulting in the formation of the alkoxide intermediate. The hydride is transferred onto the nicotinamide ring of the cofactor, which leads to the final product release and dissociation of NADH [172–174].

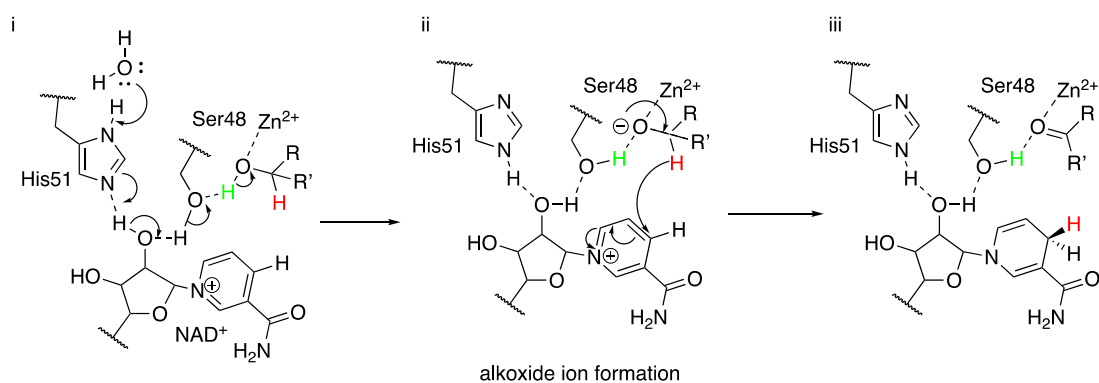


Figure 34. The catalytic action of HLADH begins with binding NAD⁺, followed by the substrate that replaces a water molecule coordinated to Zn²⁺. The hydride transfer is initiated with deprotonation of His51 by bulk water and electron transfer *via* His51, 2'OH of the NAD⁺, and Ser48 (i), which subsequently deprotonates the alcohol substrate. This results in the formation of a zinc alkoxide intermediate (ii), which is followed by the hydride transfer onto the nicotinamide cofactor (iii). In the final step involves the product release and dissociation of NADH (not shown). Adapted from [173].

The high price of nicotinamide cofactors forced chemists to develop efficient methods for their recycling and reusing, in order to make the process economically feasible. One of the most frequently applied method for the NAD(P)^+ regeneration is the coupled enzyme approach, which involves the addition of the second enzyme and sacrificial substrate. One example of such a system is the application of NAD(P)H oxidase enzyme (NoX), which oxidises NAD(P)H to NAD(P)^+ while concomitantly reducing molecular oxygen to water (**Figure 35**) [92,175].

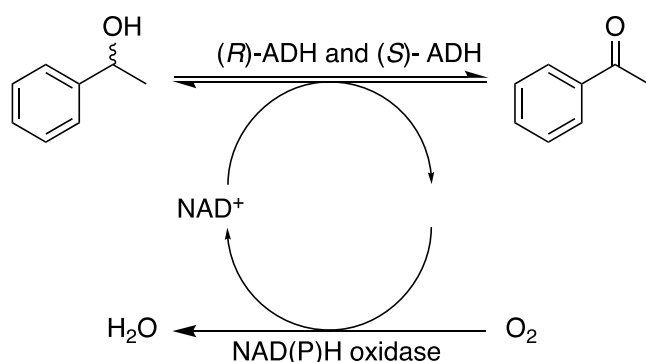


Figure 35. An example of the application of the NAD(P)H oxidase for the NAD(P)^+ cofactor regeneration in the biocatalytic oxidation of racemic 1-phenylethanol (**142**) to acetophenone (**143**) with (R)- and (S)- selective ADHs [175].

Other ADHs utilise PQQ (**145**) and FAD (**144**) cofactors [176] in a similar way to the commonly used AOs that also depend on the flavin cofactor [159], (**Figure 36**). These enzymes catalyse the irreversible oxidation of alcohols, which makes them very attractive for applications in organic synthesis. In the ADHs, the generated electrons are transferred to ubiquinone, cytochrome-c or blue copper proteins, which are found towards the oxidative end of the biological redox scale [177][104], while AOs employ O_2 as electron acceptors [159]. These oxidoreductases achieve dehydrogenation through a hydride transfer mechanism (**Figure 37**) [159,178]. This involves the abstraction of the hydroxyl proton by a strong catalytic base, which in FAD proteins is often a conserved histidine [179] and in the well-studied PQQ-methanol dehydrogenase, is aspartic acid [180]. From the resulting alkoxide, a hydride ion is transferred onto the flavin or quinone moiety respectively affording the aldehyde substrate and reduced cofactors.

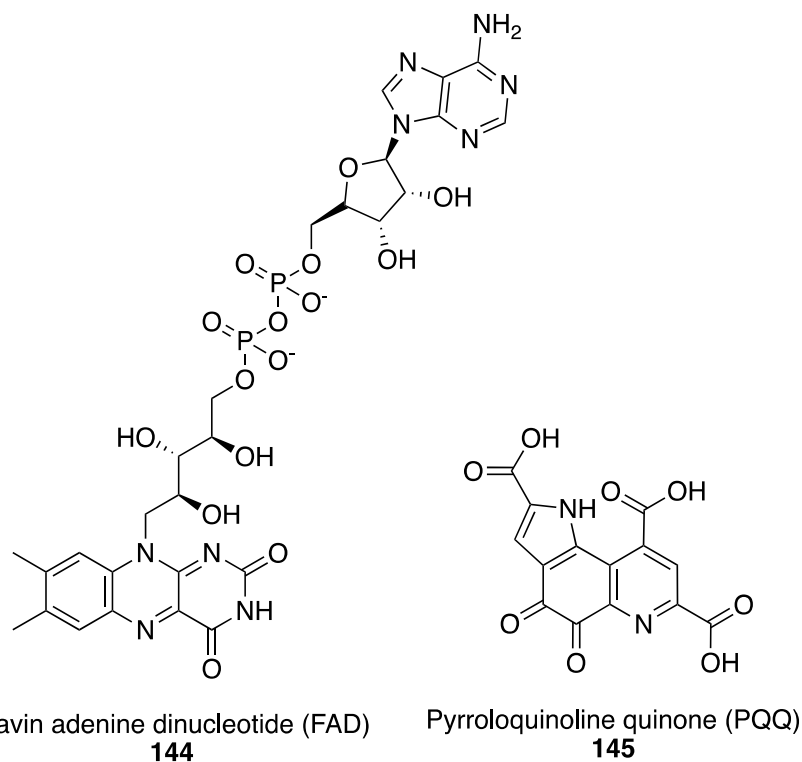


Figure 36. Structure of flavin adenine dinucleotide (FAD) and pyrroloquinoline quinone (PQQ) cofactors, which are prosthetic groups of some alcohol dehydrogenases.

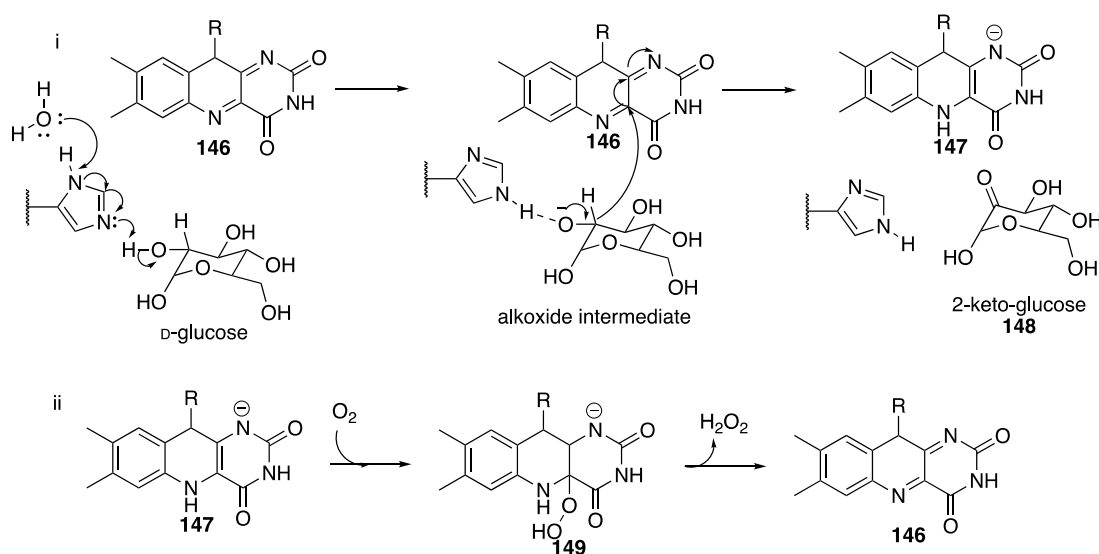


Figure 37. The overall catalytic mechanism of pyranose-2-oxidase is divided into two stages (i) reductive half of reaction (carbohydrate oxidation) and ii) oxidative half of reaction (reoxidation of flavin). The first half of reaction, begins with deprotonation of the catalytic histidine by bulk water. This is followed by the proton abstraction of the C-2-OH bond in the *D*-glucose substrate by the catalytic base histidine and results in the formation of an alkoxide intermediate. The hydride is transferred from the alkoxide onto the flavin moiety (**146**), affording a keto product (**148**) and reduced flavin cofactor (**147**). In the second half of reaction, the reduced flavin (**147**) is reoxidised by reducing O_2 to H_2O_2 [181].

Instead of a FAD cofactor, certain alcohol oxidases contain a transition metal copper atom in their catalytic centre, the most interesting of which is a galactose oxidase (GO). This enzyme catalyses the two-electron oxidation of a large number of primary alcohols to aldehydes [161]. The copper centre in galactose oxidase is coordinated by two histidine imidazoles, one oxygen atom of a cysteine modified tyrosyl radical, an axial tyrosine ligand and a water molecule (Figure 38 A). The unusually stable protein radical is formed from the redox-active side chain of a cross-linked tyrosine residue (Tyr–Cys) [182,183] Reduction of this radical by one electron produces an inactive enzyme. In the first step of the catalytic mechanism, the alcohol substrate binds to the tyrosyl radical Cu active site replacing the water molecule. The axial tyrosinate ligand abstracts a hydroxyl proton from the coordinated alcohol substrate converting it into an alkoxide (B). The next step is the abstraction of the hydrogen atom by the equatorial tyrosyl radical, affording a ketyl intermediate (C), which is reduced to a Cu (I) species and the aldehyde product (D). Finally binding of molecular oxygen results in a regeneration of the active Cu (II) – tyrosyl radical, along with hydrogen peroxide generation (F) [184–186].

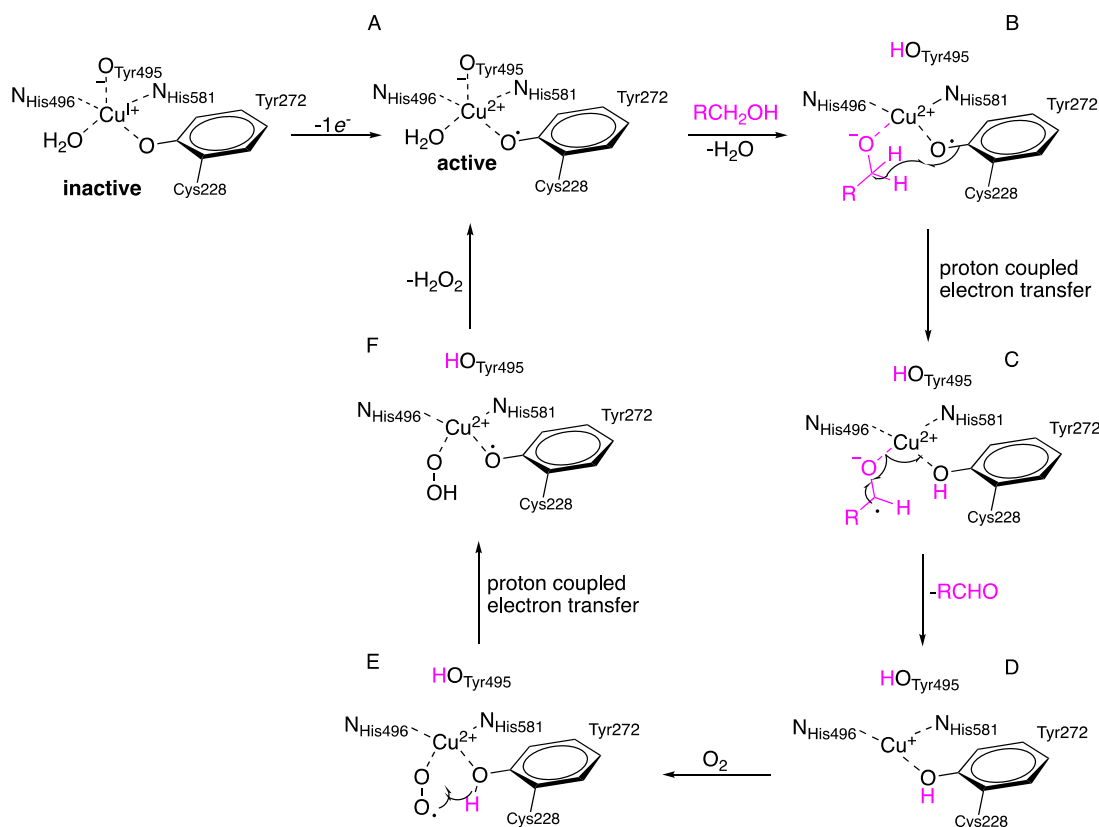


Figure 38. The inactive form of galactose oxidase features a tyrosine ligand covalently linked to a cysteine. Oxidation of Tyr-272 generates a radical, providing the second redox center in the active state of the enzyme. The catalytic mechanism begins with a displacement of the water molecule with a primary alcohol substrate, followed by the hydroxyl proton abstraction by the axial Tyr495. The next step involves the proton abstraction by the equatorial tyrosyl radical (Tyr-272) resulting in the ketyl radical anion species (C), which undergoes a rapid intramolecular electron transfer with reduction of Cu (II) to Cu (I) and a release of aldehyde product (D). Finally binding of molecular oxygen results in a regeneration of the active Cu (II) –tyrosyl radical, along with hydrogen peroxide generation (F). Adapted from [185,186].

1.2.2.2 Biocatalytic oxidations of polyol substrates

The stereo- and regioselectivity displayed by enzymes make their application in organic synthesis highly desirable. In particular, high regioselectivity is useful in the oxidation of carbohydrates, due to the number of potential positions of reactivity. In traditional synthesis, the regioselective oxidation of polyfunctional starting materials requires multiple protection and deprotection steps, making the process long and expensive. In contrast, biocatalysts such as alcohol oxidases and polyol/alcohol dehydrogenases display exclusive regioselectivity, which is exploited in a range of preparative and industrial applications. For example, the oxidation of various primary alcohols of mono-, di- and tri-saccharide substrates such as methyl-

α -D-galactopyranoside, D-galactose, 2-deoxy-D-galactose, lactulose and raffinose to the corresponding aldehydes can be achieved by galactose oxidase reaching close to quantitative conversion [187]. In addition, engineered galactose oxidase variants display activity towards diols, and aliphatic aminoalcohols, including Cbz-protected derivatives, and have been also used for the preparation numerous iminosugars [188], (**Figure 39**). The reactions with GOs on a preparative scale require the simultaneous action of catalyse, which breaks down the toxic hydrogen peroxide by-product to water and oxygen and maintains the enzymatic activity [189].

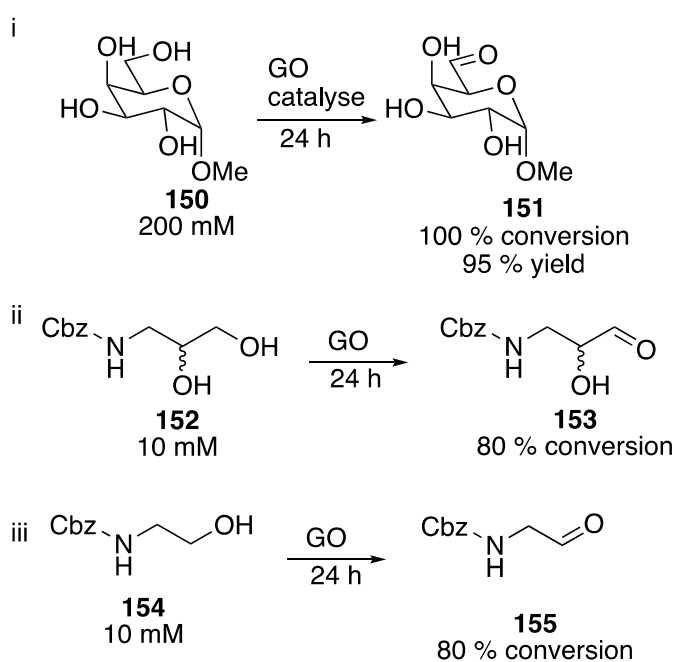


Figure 39. Examples of oxidative transformations with galactose oxidase (GO) of i) methyl α -D-galactopyranoside (**150**) ii), Cbz protected racemic diols B (**152**) and iii) Cbz protected aliphatic aminoalcohols (**154**) [187,189].

Another example of the regioselective oxidation of primary alcohols towards carbohydrate substrates was reported with an engineered NAD-dependent mannitol-1-dehydrogenase (MDH) from *Apium graveolens*. This enzyme naturally converts D-mannitol to D-mannose, and several other polyols including ribitol, D-arabitol, galactitol to their L-sugar counterparts [190,191]. The improved enzymatic variant was further applied on a preparative scale to convert ribitol to L-ribose, (**Figure 40**).

The oxidation of primary alcohols in several aminopolyols was reported by a medium-chain-dehydrogenase from *Bacillus amyloliquefaciens*, which was

heterologously expressed in *E. coli*. However, the products of these transformations were not isolated and hence not characterised [192]. This enzyme is thought to take part in the biosynthesis of mannojirimycin [193].

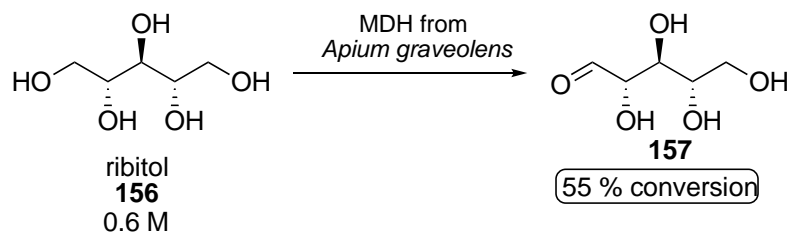


Figure 40. Preparative oxidation of ribitol (**156**) to L-ribose (**157**) catalysed by an engineered mannitol dehydrogenase (MDH) from *A. graveolens* [191].

The PQQ and FAD-containing dehydrogenases play a smaller role in preparative biocatalysis to their nicotinamide-dependent counterparts. However, certain species of acetic acid bacteria, such as *G. oxydans*, which naturally express multiple membrane-bound ADHs have been industrially exploited in the whole-cell oxidation of (amino)-polyols, alcohols and related compounds [19,194,195]. The membrane-bound enzymes regioselectively oxidise secondary alcohols according to the Bertrand- Hudson rule, which says that only polyols displaying *cis*-arrangement of two secondary hydroxyl groups, in the D-configuration undergo oxidation to the corresponding ketones, (**Figure 41**) [196]. The majority of the dehydrogenases that carry out these reactions have not been isolated and characterised [195]. A number of soluble NAD⁺-dependent cytosolic polyol dehydrogenases from *G. oxydans* have been cloned and heterologously expressed, however, they have not been applied in the preparative biocatalysis. These dehydrogenases exhibit activities towards several polyol substrates, for example, D-sorbitol and including those, which do not correspond to the Bernard- Hudson rule like xylitol [197–200].

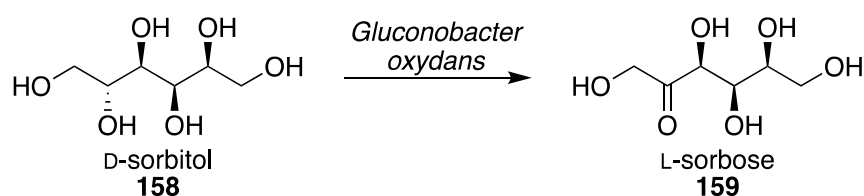


Figure 41. A polyol D-sorbitol displays *cis*-arrangement of two secondary hydroxyl groups, in the D- configuration undergoes oxidation by *Gluconobacter oxydans*. This biotransformation step is a part of the chemo-biocatalytic process for the synthesis of ascorbic acid [201].

The oxidative capability of *G. oxydans* have been exploited in a number of industrial applications, for example the synthesis of ascorbic acid from D-sorbitol (**158**), DNJ (**4**) from D-glucose or dihydroxyacetone (**161**) (DHA) from glycerol (**160**) [19,201,202]. A-membrane bound glycerol dehydrogenase responsible for the oxidation of glycerol in *G. oxydans* was characterised and overexpressed, which resulted in the improved production of DHA by 2.5-fold compared to the wild type, (**Figure 42**). The repeated batch fermentation afforded 96 g/L of DHA over 34 h starting from 100 g/L of glycerol [203].

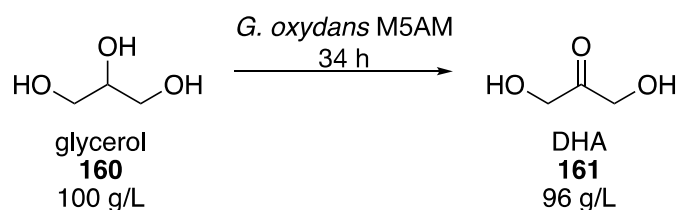


Figure 42. A scale-up DHA production with the mutant of *Gluconobacter oxydans* M5AM with the overexpressed membrane bound glycerol dehydrogenase [203].

The substrate promiscuity and the ability to provide quantitative yields makes the *Gluconobacter* strains very attractive for the pharmaceutical industry, in particular for the already described chemo-enzymatic synthesis of iminosugars from protected aminopolyols derived from D-arabinose, D-galactose and D-glucose [19,106,107].

1.2.3 Imine reductases

Imine reductases belong to the NAD(P)H-dependent oxidoreductases that catalyse the asymmetric reduction of preformed prochiral imines to the corresponding amines [204]. Recently, a new subclass of IREDs, called reductive aminases (RedAms) has been discovered displaying both activities: reductive amination between carbonyl substrates and amine nucleophiles and the reduction of the preformed substrates [205]. In nature, IREDs are involved in a number of biosynthetic pathways, which lead to the production of a variety of metabolites such as folate, siderophores, antibiotics and alkaloids [206–208]. An example is a dihydrofolate reductase (DHFR), whose physiological role is the formation of the 5,6,7,8-tetrahydrofolate cofactor (**163**), (**Figure 43**) [209,210].

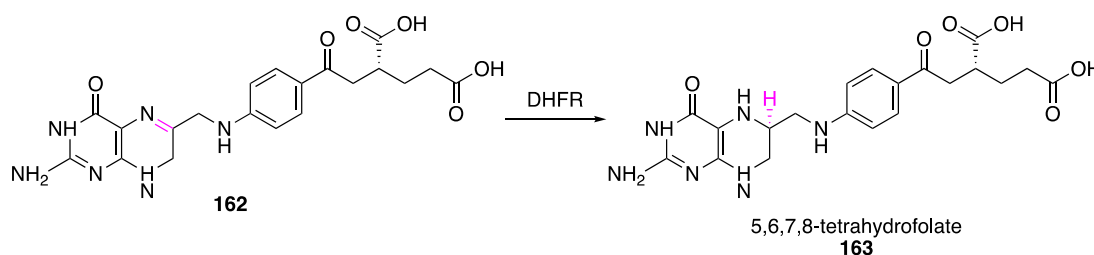


Figure 43. A stereoselective imine bond (coloured in magenta) reduction catalysed by dihydrofolate reductase (DHFR) in the natural transformation that results in the formation of 5,6,7,8-tetrahydrofolate (**163**).

Over the past years, imine reductases have been increasingly applied in organic synthesis for the preparation of chiral amines, showing high activity and enantioselectivity toward a range of cyclic imines and iminium ions [211–213].

1.2.3.1 Catalytic mechanism and cofactor dependence of IREDs

The catalytic mechanism of imine reductases is not yet fully elucidated; nevertheless, it relies on general acid-base catalysis involving the following steps: i) hydride transfer from the NADPH coenzyme to the imine carbon atom ii) proton transfer onto the nitrogen atom of the imino group, (**Figure 44**) [210]. The exact proton donating group is still unknown, but the suggested catalytic residues have been conserved aspartic acid and tyrosine at 187 position in the (*R*)- and (*S*)-

selective IREDs, respectively [214,215]. Following studies demonstrated that mutations of the corresponding aspartic acid residues in different (*R*)-selective IREDs did not result in the inactive enzyme but only decreased the activity, which may suggest that other proton donors are involved [216]. In contrast, a mutation of the tyrosine residue in (*S*)-selective IREDs afforded a completely inactive enzyme [216]. In the fungal reductive aminase from *Aspergillus oryzae*, a tyrosine residue at 177 position is thought to play a role of in either proton donation or product anchoring, and mutations of this residue led to a drastic decrease in activity [205].

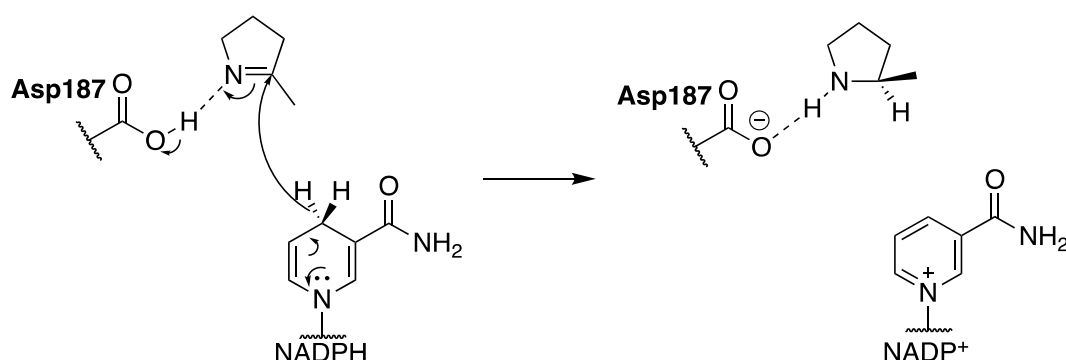


Figure 44. Proposed catalytic mechanism of the (*R*)-selective imine reductase from *Streptomyces kanamyceticus*. This involves: i) hydride transfer from the C-4 of the cofactor nicotinamide ring to the imine carbon atom, and ii) the transfer of a proton onto the nitrogen atom of the imine moiety [214].

Like ADHs, IREDs require cofactor regeneration in order to be applied in organic synthesis, and the most frequently used system involves glucose dehydrogenase (GDH), which recycles the nicotinamide cofactor by oxidising glucose to gluconic acid **Figure 45** [92].

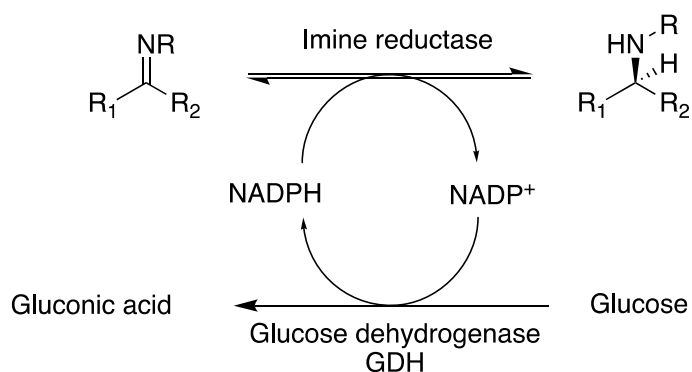


Figure 45. General transformation of the imine reductions using imine reductases, which utilise nicotinamide cofactor. NADP⁺ is converted back to NADPH when glucose dehydrogenase (GDH) oxidises a sacrificial substrate of glucose to gluconolactone, which spontaneously converts to gluconic acid [92].

1.2.3.2 Applications of imine reductases in organic synthesis

The stereoselective reduction of C=N bonds is an important transformation in organic synthesis, providing access to chiral amines; highly desired building blocks of many pharmaceutical compounds. In 2010, the discovery of two IREDs in *Streptomyces* strains that selectively reduce an imine bond in 2-methyl-1-pyrroline **164** (2-MPN) (**Figure 46**), captured the fascination of the catalytic research community, resulting in a number of newly developed applications in synthetic chemistry [204,217]. Imine reductases with (*R*)- and (*S*)- selectivity were shown to reduce a wide range of prochiral cyclic imines and iminium ions including substituted pyrrolidines [204,217] piperidines [215,218,219], azepane [215,219] and isoquinolines [215,220–222]. Acyclic imines were less preferred but also accepted by IREDs, for example, isopropylamine and *N*-methyl-2-pentanaminer [218]. Besides the reduction of cyclic imines, reductive aminases (RedAms) – a subclass of IREDs is particularly attractive for the formation of secondary amines by the ability to perform intermolecular reductive amination from a wide range of ketones [205,223] and chiral aldehydes [224].

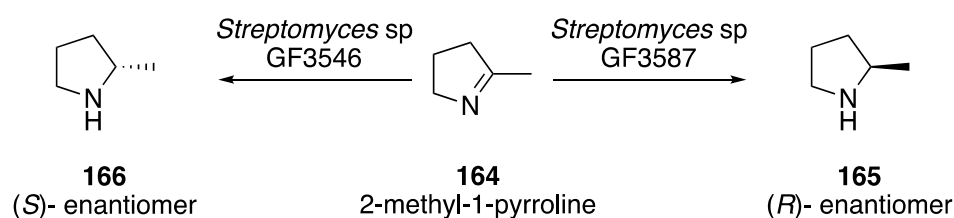


Figure 46. Reduction of 2-methyl pyrroline (2-MPN) (**164**) by the GF3546 and GF3587 *Streptomyces* sp IREDs affording (*S*)- and (*R*)- enantiomers respectively.

Imine reductases were successfully applied in a number of preparative-scale transformations for the synthesis of pharmaceutically important compounds (**Figure 47**, A, B, C and D). For example, a natural product of an alkaloid (*R*)-coniine (example A) was generated at 25 mM affording 90 % yield and 99 % *ee* [219]. Moreover, stereoselective reduction with IREDs of a wide range of aryl substituted cyclic dihydroisoquinolines led to the generation of various tetrahydroisoquinolines (THIQs), which are pharmaceutically important scaffolds (example B and C) [211]. Interestingly, a highly efficient wild type (*S*)-IRED from *Stackebrandtia nassauensis*

reduced 100 mM of 1-methyl dihydroisoquinoline in 4 h with >99 % conversion, 72 % yield and 99 % selectivity (example C). Bulky dihydroisoquinolines were also converted to the corresponding THIQs affording good yields and moderate to excellent enantioselectivities [212]. Moreover, several imine reductases selectively reduced various dibenzazepine imines (example D), which resulted in the corresponding dibenzazepines. The preparative transformations with (*R*)- and (*S*)-selective IRED afforded enantioselective pure 5-methyl-6,7-dihydro-5H-dibenzazepine (**174**) products with 95 % (example D) and 93 % yield respectively [225].

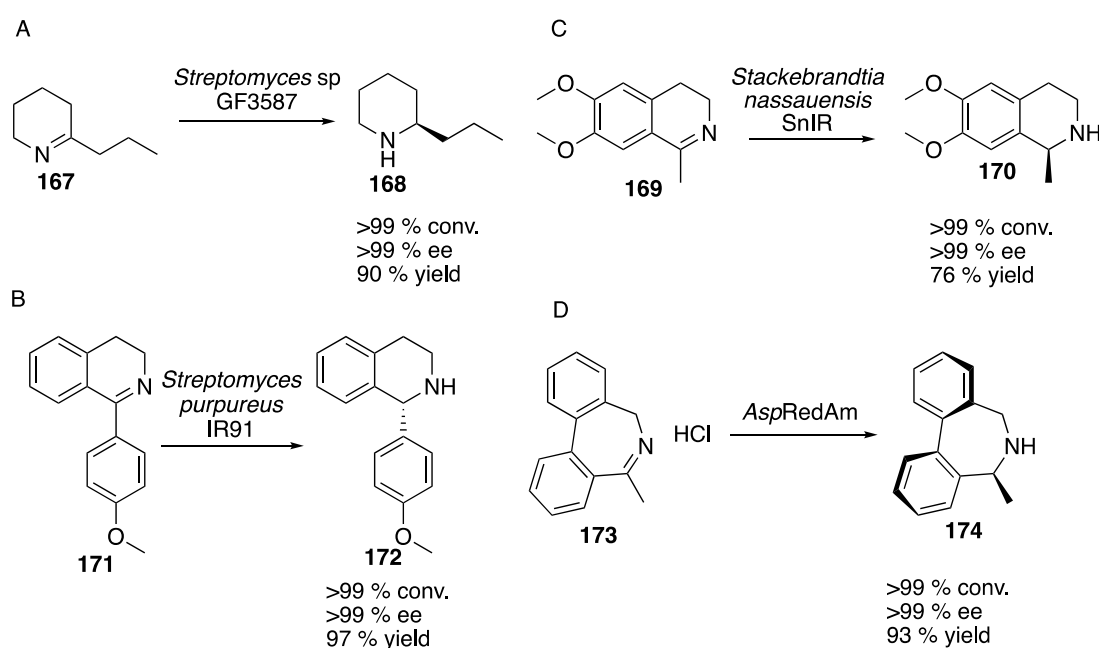


Figure 47. Selected synthesis of pharmaceutically relevant compounds on preparative scale using IREDs. References: A [219], B [211], C [212], D [225].

Imine reductases are regarded as one of the most promising biocatalysts by the pharmaceutical industry. Recently the first industrial application of IREDs was reported by GSK, where an engineered reductive aminase (RedAm) was used for the production of a potential active ingredient for the treatment of leukaemia, GSK2879552 on the kilogram scale [226].

1.2.4 Monoamine oxidases

Monoamine oxidases (MAOs) are oxidoreductive enzymes capable of oxidising amines to imines. In nature, they are commonly found in microorganisms such as bacteria and fungi, and higher organisms like mammals, including humans. Similarly to alcohol oxidases, they use molecular oxygen as a final electron acceptor, which is converted to hydrogen peroxide [227]. Their biological role is inactivation and metabolisation of naturally occurring amines [228]. An example is dopamine degradation catalysed by a human MAO-A to 3,4-dihydroxyphenylacetaldehyde (DOPAL), which occurs with concomitant formation of ammonia and hydrogen peroxide, (**Figure 48**) [229].

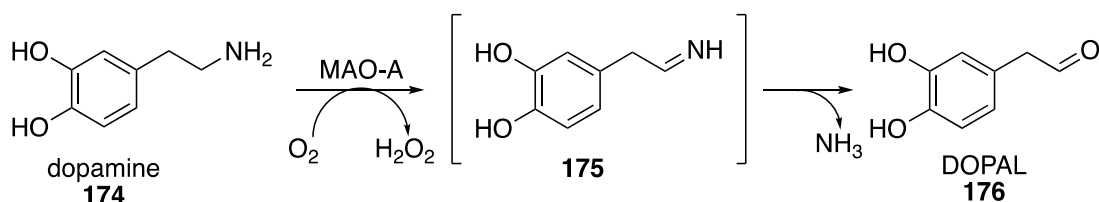


Figure 48. Natural reaction catalysed by human monoamine oxidase A (MAO-A), resulting in the unstable imine intermediate that hydrolyses into 3,4-dihydroxyphenylacetaldehyde (DOPAL **176**) with concomitant formation of ammonia and hydrogen peroxide [229].

Like alcohol oxidases, MAOs are divided into the family of copper containing centres and flavin-dependent [92]. An (*S*)-selective fungal monoamine oxidase from *Aspergillus niger* (MAO-*N*) that belongs to the FAD family have been extensively used in synthetic chemistry, especially in the kinetic resolution of racemic substrates [230] and deracemization of chiral amines [231–233]. Other MAOs that were also applied in organic synthesis are (*S*)-selective cyclohexylamine oxidase (CHAO) from *Brevibacterium oxydans* and (*R*)-selective 6-hydroxy-D-nicotine oxidase (6-HDNO) from *Arthrobacter nicotinovorans* [234,235].

1.2.4.1 Catalytic mechanism of monoamine oxidases

The catalytic action of flavin dependent MAO enzymes is not fully elucidated, and three mechanisms have been proposed: radical, nucleophilic and hydride transfer, of which the last two are most commonly postulated [236,237] (**Figure 49**). The nucleophilic mechanism begins with the amine attack on the flavin cofactor, which

abstracts the proton from the α -carbon of the substrate and results in the imine formation and reduced flavin. The last step is releasing of the imine product and re-oxidation of the flavin cofactor by molecular oxygen, which leads to the hydrogen peroxide by-product [92,236,237].

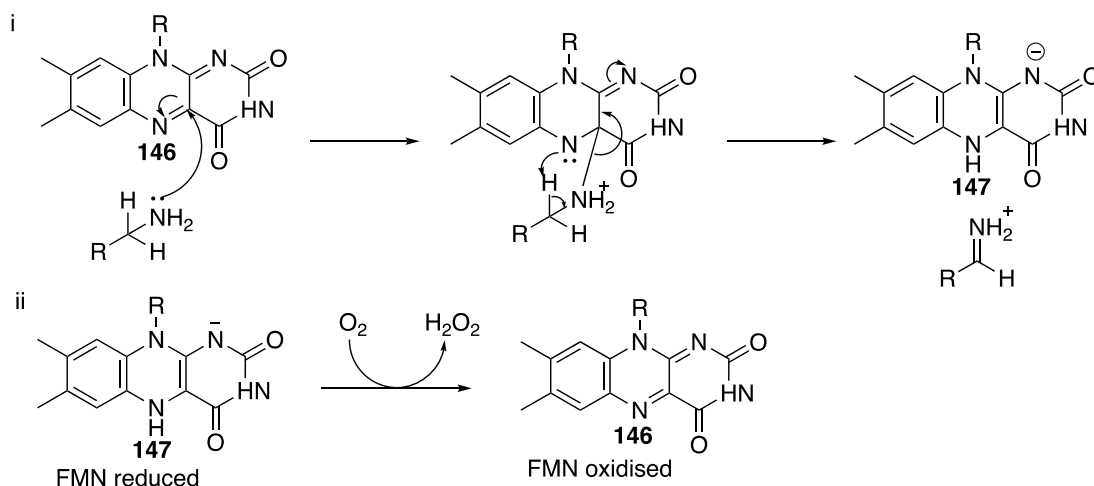


Figure 49. A proposed nucleophilic mechanism for the for the monoamine oxidase catalysing oxidation of amines. It is initiated with the amine attack on the flavin cofactor (**146**). The flavin anion abstracts the proton from the substrate α -carbon that results in the imine formation and reduced flavin. The final step is releasing of the imine product and re-oxidation of the flavin cofactor by molecular oxygen, which leads to a by-product hydrogen peroxide. Modified from [236].

1.2.4.2 Synthetic applications of monoamine oxidases

Monoamine oxidases (MAOs) are remarkably useful tools in organic synthesis, especially for the kinetic resolution of racemic substrates [230] and deracemization of amines, which were carried out by variants of monoamine oxidase from *Aspergillus niger* [238,239]. The deracemisation approach exploits the high (*S*)-selectivity of MAO-*N* enzymes utilising their ability to exclusively accept only one enantiomer, which leads to the imine formation. The addition of the non-selective reducing agent ($BH_3.NH_3$) results in the eventual accumulation of a single (*R*)-enantiomer, **Figure 50** [92].

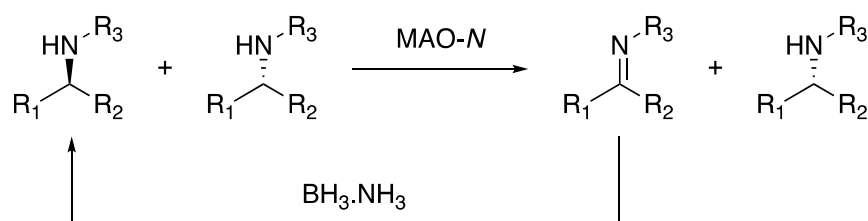


Figure 50. A general process of deracemization carried by MAO-*N*, which involves the addition of the non-selective reducing agent such as $\text{BH}_3\cdot\text{NH}_3$. As MAO-*N* exclusively accepts the (*S*)- enantiomer, it eventually leads to the accumulation of the optically pure single (*R*) enantiomer [92].

Engineered variants (D3, D5, D9 and D11) of the MAO-*N* enzyme from *Aspergillus niger*, generated by the directed evolution approach were shown to oxidise a wide range of primary amines secondary and tertiary amines including bulky amines, (**Figure 51**). Their application in the deracemization process on the preparative scale led to the production of the optically pure chiral amines, including pharmaceutically relevant building blocks [232,238,240,241]. Similarly, to galactose oxidase, the preparative processes with monoamine oxidases require the addition of catalyse to break down the peroxide by-product and maintain the stability of the enzyme.

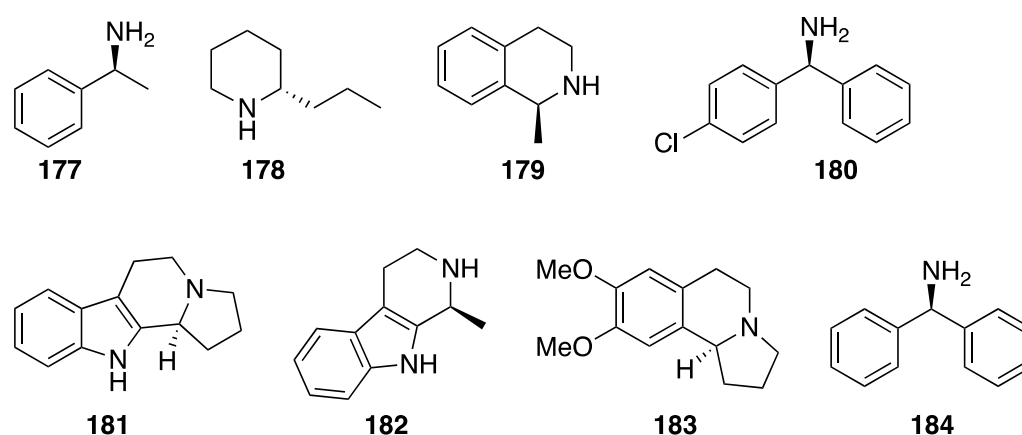


Figure 51. Selected substrates oxidised by the engineered variants of MAO-*N* [238,240,241].

The MAO-*N* catalysis was also applied in the desymmetrisation (introduction of chirality) of a range of symmetrical pyrrolidines [242]. This approach was further utilised on the industrial scale by Merck and Codexis in the improved synthetic route of Boceprevir (drug against Hepatitis C), (**Figure 52**). In this process, MAO-*N* desymmetrised a pyrroline derivative (**185**) resulting in an imine product (**186**). The imine reacted with sodium bisulfite to form the sulfonate intermediate (**187**) that was further reacted to produce Boceprevir (**188**) [92,243].

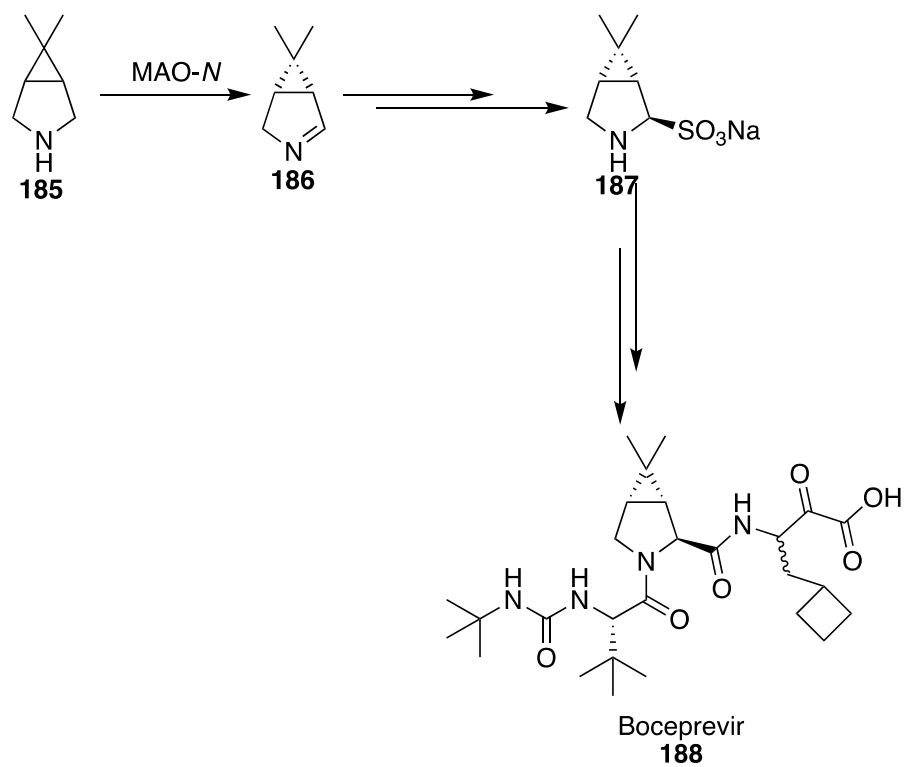


Figure 52. The synthesis of boceprevir with the application of MAO-N that carries on the desymmetrisation of the pyrrolidine substrate [92,243].

2 Aims and Objectives and Key Challenges

The overall aim of this project is to construct an artificial biocatalytic cascade for the synthesis of iminosugars. The following aspects were considered to accurately establish the multiple-step cascade design: i) thermodynamical favourability ($\Delta G_{\text{cascade}} < 0$), ii) high specificity of selected enzymes, iii) application of a possibly minimal number of steps and iv) use of inexpensive and readily available starting materials.

The proposed cascade proceeds through three steps and recruits the following highly specific enzymes: transaminase, alcohol dehydrogenase or alcohol oxidase and imine reductase, transforming a simple monosaccharide substrate in a one-pot system (**Figure 53**). The choice of the oxidative enzyme determines the requirement for the cofactor regeneration system.

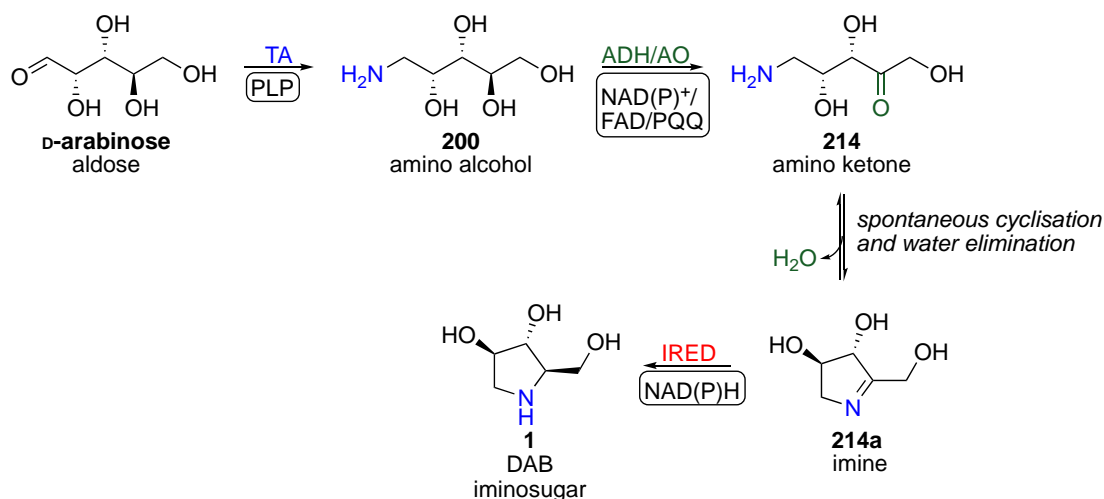


Figure 53. An example of the application of the proposed one-pot biocatalytic cascade for the preparation of iminosugars starting from a simple aldose. It proceeds through three enzymatic steps: transamination of an aldehyde group with TA, regioselective alcohol oxidation of a hydroxyl group with ADH or AO and imine reduction in preformed polyhydroxylated imines with IRED.

The feasibility of the transamination step has been demonstrated by Cairns *et al.*, [154] and Subrizi *et al.*, [155]. Transaminases accept six and five-membered aldoses converting them to amino alcohols, which are intermediates of iminosugars in the proposed cascade. This work investigates the oxidation and reduction step, with a particular focus on the former one. A rational selection of the biocatalyst capable of the regioselective oxidation of a suitable secondary alcohol group in amino alcohol

is of the utmost importance for this project. Ideally, the biocatalyst should exhibit a broad substrate scope towards amino alcohols with L- and D-configuration. The reduction step also is highly critical, enabling access to the enantiopure iminosugar compounds. Thus, a highly selective imine reductase accepting polyhydroxylated substrates is required. Finally, the lack of a chromophore and high polarity of the compounds challenge the purification and reaction monitoring methods, which also need to be addressed.

3 General Biological Methods and Materials

3.1 Materials

Commercially available lyophilised cells of *Gluconobacter oxydans* DSM 2003 and genomic DNA derived from a strain of *Pseudomonas putida* DSM 291 were purchased from DSMZ, Germany. Oligonucleotide primer synthesis and DNA sequencing was performed by Eurofins Genomics. Restriction endonucleases, T4 DNA Ligase were obtained from Thermo Fisher Scientific, and DNA polymerase (Hi-Fi) was purchased from PCR biosystems.

3.2 Sterilisation

Glassware, plasticware and solutions were autoclaved for 30 min at 121°C before use. All microbiological work was done close to a Bunsen burner flame with all surfaces disinfected using methylated spirits.

3.3 Stock solutions

50 mM sodium phosphate buffer, pH 7	Na ₂ HPO ₄ (4.10 g), NaH ₂ PO ₄ (2.53 g) in distilled water (1 L) adjusted to pH 7 with 4 M HCl
100 mM Tris-HCl buffer, pH 8	Tris-HCl (12.11 g) in distilled water (1 L), adjusted to pH 8 with 10 M NaOH
100 mM potassium phosphate, pH 7.7	K ₂ HPO ₄ (14.20 g), KH ₂ PO ₄ (2.51 g) in distilled water (1 L) adjusted with 10 M NaOH to pH 7.7
SDS-PAGE stain	0.25 % w/v Coomassie Brilliant blue, 30 % v/v methanol, 10 % v/v glacial acetic acid
SDS-PAGE de-stain	30 % v/v methanol, 10 % v/v glacial acetic acid

3.4 Microbiological media preparation

LB media for *E. coli* cultures

Luria-Bertani (LB) medium was prepared by dissolving yeast extract (5 g), tryptone (10 g), and sodium chloride (10 g) in distilled water (1 L final volume). The pH of the solution was adjusted to 7.0 and subsequently sterilised by autoclave.

LB agar

LB agar was prepared by dissolving commercially available LB agar formula (8.75 g) to distilled water (250 mL). The solution was autoclaved, allowed to cool to 45 °C and subsequently supplied with 250 µL of the appropriate antibiotic stock (1000x conc.).

Autoinduction media

Autoinduction media was prepared according to a study of Studier 2014 [306]. It consisted of tryptone (20 g), yeast extract (5 g) and NaCl (5 g) in phosphate buffer (30 mM, pH 7.2, 1 L), which was sterilised by autoclaving. The following solutions of 60 % of glycerol (10 mL), 10 % of glucose (5 mL) and 8 % of lactose (25 mL) were sterile filtered and added to the cool solution of the previously autoclaved media and followed by the supplementation with the appropriate antibiotic.

Media for *G. oxydans* cultures

G. oxydans medium was prepared according to the protocol reported by Oikonomakos *et al.* [106], which contained sorbitol (100 g) and yeast extract (10 g) in distilled water (1 L final volume) followed by autoclaving.

***G. oxydans* solid media**

G. oxydans solid media was prepared according to the protocol recommended by DSMZ, which contained glucose (25 g), yeast extract (2.5 g), bacteriological agar (3.75 g) and CaCO₃ (5 g) in distilled water (250 mL) followed by autoclaving.

3.5 Bacteria culturing

Culturing *E. coli*

Working close to a Bunsen burner flame, single colonies were picked from previously streaked LB agar plates and inoculated into 5 mL of liquid LB media supplied with the appropriate antibiotic. The culture was cultivated overnight at 37°C at 200 rpm. The resulting initial culture that was then used to inoculate a larger volume of LB liquid or autoinduction medium supplied with the suitable appropriate antibiotic (1 % of the starting culture) or centrifuged for plasmid purification.

Culturing *G. oxydans*

Working close to a Bunsen burner flame, multiples colonies (<50 were picked from previously streaked *G. oxydans* agar plates and inoculated into 5 mL of *G. oxydans* liquid media (see section 3.4). The culture was cultivated overnight at 30°C at 280 rpm. The resulting initial culture that was then used to inoculate a larger volume of *G. oxydans* in liquid medium (10 % of the starting culture).

3.6 Agarose gel electrophoresis

Agarose gel electrophoresis were performed to analyse PCR products and purify digested DNA. PCR product or digested DNA product (10 µL) was added to 6x DNA gel loading dye (2 µL) (ThermoFisher) and loaded onto agarose gel cast (1 %, w/v) supplied with SYBR™ nucleic acid gel stain (1x conc.). A DNA ladder (1kB, ThermoFisher) was loaded onto the gel for reference. Electrophoresis was performed using Biorad PowerPac Basic Electrophoresis Power Supply in TAE (Tris-Acetic acid-EDTA) buffer at 100 V for 30 mins. Produced agarose gels were visualised on a UV or blue light-transilluminator.

3.7 Cloning of I Pip2CR/Pyr2CR from *Pseudomonas putida*

PCR procedure

The *dpkA* gene encoding for Pip2CR/Pyr2CR from a strain of *Pseudomonas putida* DSM 291 was amplified by PCR using the following primers, which contained *Bam*I (highlighted in green) and *Not*I (highlighted in red) linkers respectively:

Forward: GGATCCATGTCCGCACCTTCCACCAGCAC

Reverse: AAAAA^{GCGGCCGC}AGCGCCAAGCAGCTCTTTCAGGC.

Reagents in the quantities shown below were pipetted into PCR tubes.

Reagent	Quantity
HF Buffer (PCR Biosystems)	10 µL
Primer (FWD) (10 µM)	2 µL
Primer (RVSE) (10 µM)	2 µL
<i>P. putida</i> DNA template (120 ng/µl)	1 µL
HiFi Polymerase (PCR Biosystems)	0.5 µL
DNAase free H ₂ O	34.5 µL

The resulting PCR mixture was placed in a thermal cycler and ran according to the program below.

Initial denaturation	Denaturation	Annealing	Extension	Final extension
98 °C for 30 s	98 °C for 10 s	61 °C for 30 s	72 °C 60 s	72 °C for 2 min
	X 30 cycles			

Digestion of PCR products and plasmid

The PCR product and pET21a(-) plasmid were digested separately using *BamI* and *NotI* specific restriction endonucleases (FastDigest Thermofisher) at 37 °C for 5 min using following quantities:

Reagents:	Quantity
Green buffer (FastDigest)	4 µL
BamI	2 µL
NotI	2 µL
pET21 a(-) (150 ng/µl)	13 µL
<i>dpka</i> PCR product (89 ng/mL)	6 µL
DNAse free water	Filled to 40 µL

Subsequently, the reactions were stopped by subjecting to a heat at 80 °C for 5 min, and the products were gel purified with Thermofisher GeneJET Gel Extraction Kit.

Ligation

The resulting *dpka* insert was subjected to ligation with pET21a(-) using T4 DNA ligase (Thermofisher) with a plasmid to insert ratio of 1:3 for 2 h at room temperature. The following product was immediately transformed into *E. coli* (DH5 α). A correct insert assembly was determined by DNA digestion followed by electrophoresis and by gene sequencing.

3.8 Plasmid isolation

Isolation of plasmid DNA from overnight bacterial cells was performed with the GeneJET Plasmid Miniprep Kit from ThermoFisher. Isolated DNA was examined by agarose gel electrophoresis (see section 3.6).

3.9 Preparation of *E. coli* chemically competent cells

A single colony was picked from a freshly streaked plate of the required strain of *E. coli* cells and inoculated into 5 mL of LB with no antibiotic. This culture was grown overnight at 30 °C and 200 rpm. This overnight culture was used to inoculate a 500 mL volume of LB with no antibiotic and grown until OD₆₀₀ reached 0.4. The grown

cells were aliquoted into 50 mL volume falcon tubes and placed on ice for 30 min. Cells were harvested by centrifugation at 4000 rpm at 4°C, and the resulting cell pellets were resuspended in 5 mL of a sterile ice-cold solution of 100 mM MgCl₂. The suspensions were combined, and the cells were again harvested by centrifugation. The resulting cell pellets were resuspended in 40 mL of a sterile ice-cold solution of 100 mM CaCl₂, and the cells were again harvested by centrifugation. The resulting cell pellets were resuspended in 25 mL of a sterile ice-cold solution containing 85 mM CaCl₂ and 15 % v/v glycerol, followed by centrifugation. The resulting cell pellets were finally resuspended in 1 mL solution containing 85 mM CaCl₂ and 15 % v/v glycerol, aliquoted into 50 µL volume and stored at -80°C.

3.10 Transformation of chemically competent cells

Aliquots of chemically competent *E. coli* cells (DH5α or BL21(DE3), 50 µl) were allowed to thaw on ice for 30 min. Subsequently, plasmid DNA (~120 ng/µL) was added to the cells, which were kept on ice for another 30 min. Then, the cells with plasmid DNA were subjected to heat shock at 42 °C for 1.5 min and placed back on the ice for a minimum 2 min. To the cells, LB medium (500 µL) was added and allowed to grow 37°C for 45 min. In the final step, 100 µL of the culture was resuspended onto an agar plate supplied with the appropriate antibiotic and incubated at 37 °C overnight.

3.11 Heterologous protein expression

IREDs expression

The initial starter culture of transformed *E. coli* BL21 (DE3) with the desired plasmid was prepared as detailed in section 3.5. A starter culture (1 mL) was used to inoculate 100 mL of LB and the culture was incubated at 37 °C, 200 rpm until the measured optical density (OD₆₀₀) reached 0.6 (3-4 hours). Protein expression was induced with the addition of isopropyl β-d-1-thiogalactopyranoside (IPTG) to a final concentration of 0.1 mM. Subsequently, the expression temperature was changed to 25 °C for IREDs from *Streptomyces turgidiscabies*, *Streptosporangium roseum* DSM43021, *Paenibacillus elgii*, *Streptomyces* sp. GF3546. The expression of an IRED

from *Pseudomonas putida* was performed at 20°C, and all were carried out for 16 h. Resulting cells were harvested by centrifugation at 4000 rpm, 4 °C for 20 min. Cell pellets with expressed IREs from *Streptomyces turgidiscabies*, *Streptosporangium roseum* DSM 43021, *Paenibacillus elgii*, and *Streptomyces* sp. GF3546 were resuspended in sodium phosphate buffer (50 mM, pH 7.0) (100 mg per 1 mL) according to the study of Scheller *et al* [216]. Cell pellets with an IRE from *Pseudomonas putida* were resuspended in Tris-HCl (20 mM) pH 7 buffer (100 mg per 1 mL) according to the protocol reported by Muramatsu *et al.*, [267]. To the suspended cells protease inhibitor cocktail (X 1) (Sigma-Aldrich) was added followed by sonication using a QSonica model Q55 sonicator at 40 % amplitude and 15 s intervals for 8 min. Resulting lysed cells were finally centrifuged at 4000 rpm at 4 °C for 45 min to obtain the clarified cell extract, which was aliquoted and stored at - 20 °C for further analysis. For biotransformation reactions the crude extract was used.

MAO-N expression

MAO-N expressions were performed in autoinduction medium. Initial culture of transformed *E. coli* BL21 (DE3) with the desired plasmid was prepared as detailed in section 3.5. The initial culture (1 mL) was added to the autoinduction medium (100 mL), and the expression was carried out for 16 h, 200 rpm and at 25 °C. Resulting cells were harvested by centrifugation at 4000 rpm, 4°C for 20 min. The cell pellets were stored at – 20 °C or sonicated in potassium phosphate, pH 7.7 (100 mM) buffer as stated above to provide crude lysate aliquots. For biotransformation reactions resting cells were used.

3.12 SDS-PAGE

Acrylamide gels were casted using the reagents as shown following:

Reagent	Stacking gel	Resolving gel
H ₂ O	6.1 mL	4.1 mL
Acrylamide (30 %)	1.3 mL	3.3 mL
Tris-HCl (0.5 M, pH 6.8)	2.5 mL	2.5 mL

SDS (10 %)	100 μ L	100 μ L
TEMED	10 μ L	10 μ L
Ammonium persulfate (10 %)	100 μ L	32 μ L

To clarified cell extract (8 μ L) or resuspended in buffer membrane fraction (15 μ L) was added 4x protein loading dye to reach final 1x concertation, and the resulting samples were heated for a minimum of 2 min at 80°C. The entire volume (8 μ L and 20 μ L) of denaturised protein samples were loaded onto the gels and compared against a protein ladder (6 μ L) (PageRuler Broad range, ThermoFisher). Electrophoresis was performed using Biorad PowerPac Basic Electrophoresis Power Supply at 200 V for 55 min, and the resulting gel was stained with Coomassie for 20 mins followed by a 2 h de-staining with SDS de-stain solution (see stock solutions).

4 Chemical synthesis of protected amino alcohols for oxidation with *G. oxydans*

Aims and objectives

The present chapter describes the synthesis of a panel of amino alcohol substrates used to explore the oxidation potential of *G. oxydans* DSM 2003. The synthetically produced substrates will be applied to assess the performance of the biocatalyst and optimise reaction conditions in the following chapter. However, *G. oxydans* accepts only amino alcohols with suitable chemical protection on the amine functionality [19]. This requirement has impacted the final design of the cascade by the introduction of two additional chemical steps: protection and deprotection (Figure 54).

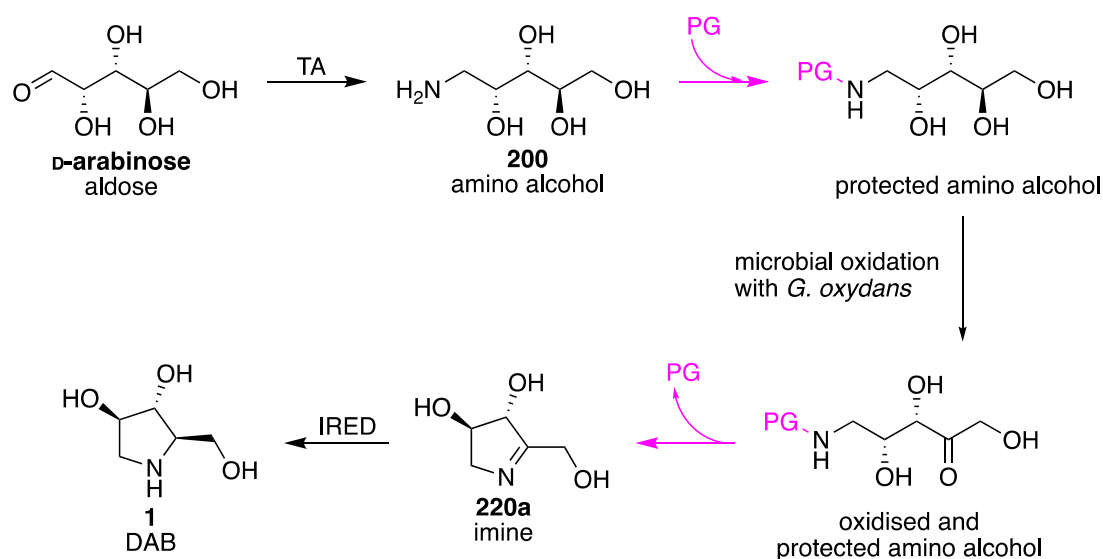


Figure 54. An example of the application of the proposed chemo-biocatalytic cascade for the synthesis of iminosugars, which involves five following steps: transamination with a transaminase (TA), chemical protection of the amine functionality, microbial oxidation with *Gluconobacter oxydans*, removal of the protecting group and finally imine reduction with an imine reductase (IRED).

4.1 Synthesis of protected amino alcohol substrates

Sugar-derived amino alcohols are not commercially available, and therefore these substrates were chemically synthesised and the amine functionality was protected with a suitable group that enables the microbial oxidation. A synthetic route to

generate formyl protected amino alcohols derived from D-arabinose has been previously described and here, the method was modified and optimised to produce several protected amino alcohols [106]. The general scheme outlining the synthesis is depicted in **Figure 55**. The initial step is the reductive amination of a simple aldose, using Raney-Ni and benzylamine (BnNH₂), providing the corresponding benzyl amino alcohol. Cleavage of the benzyl group to afford the amino alcohol product was achieved *via* hydrogenation using Pd/C in water or organic solvent. The final step was the protection of the amine group with benzyl chloroformate (Cbz-Cl) or *N*-(benzyloxycarbonyloxy)succinimide (Cbz-OSu) in the 1,4-dioxane and water mixture, which resulted in the formation of the desired substrates.

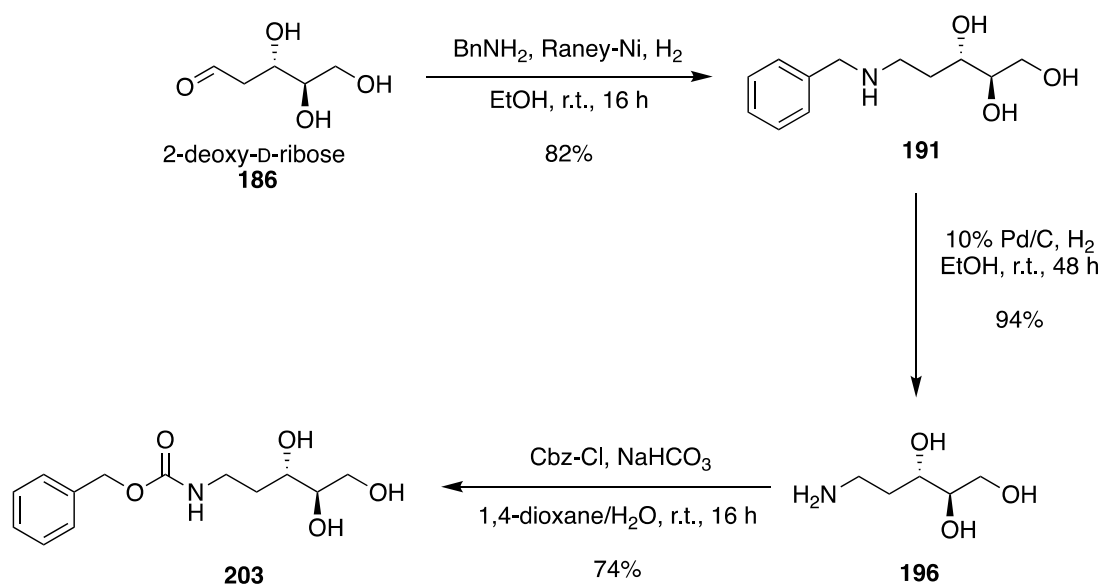


Figure 55. An example of the synthesis of Cbz-protected amino alcohol derived from 2-deoxy-D-ribose, based on the synthetic approach from the study of Oikonomakos *et al.*, 2006 [106].

4.1.1 Benzyl amino alcohols **191-195**: synthesis and biotransformation with *G. oxydans*

The formation of benzyl amino alcohol derivatives *via* reductive amination starting from simple aldopentoses or aldohexoses and benzylamine using Raney-Ni was performed on a preparative scale (16-22 mmol). The hydrogenation reaction was carried out in ethanol at room temperature for 16 h. Although the ¹H NMR analysis of the crude reaction indicated a complete depletion of the starting material and the formation of the desired product (**Figure 56**), the purification process was

problematic. The high polarity of compounds **192**, **193** and **195** (Figure 57) meant very low solubility in organic solvents, meaning purification by flash chromatography would be problematic. These compounds were successfully recrystallised in either ethyl acetate or ethanol; however, this resulted in low yields. The deoxy benzyl amino alcohols **191** and **194** were purified on a silica column in a polar solvent system of 20 % v/v methanol and 80 % v/v acetone, and good yields were achieved.

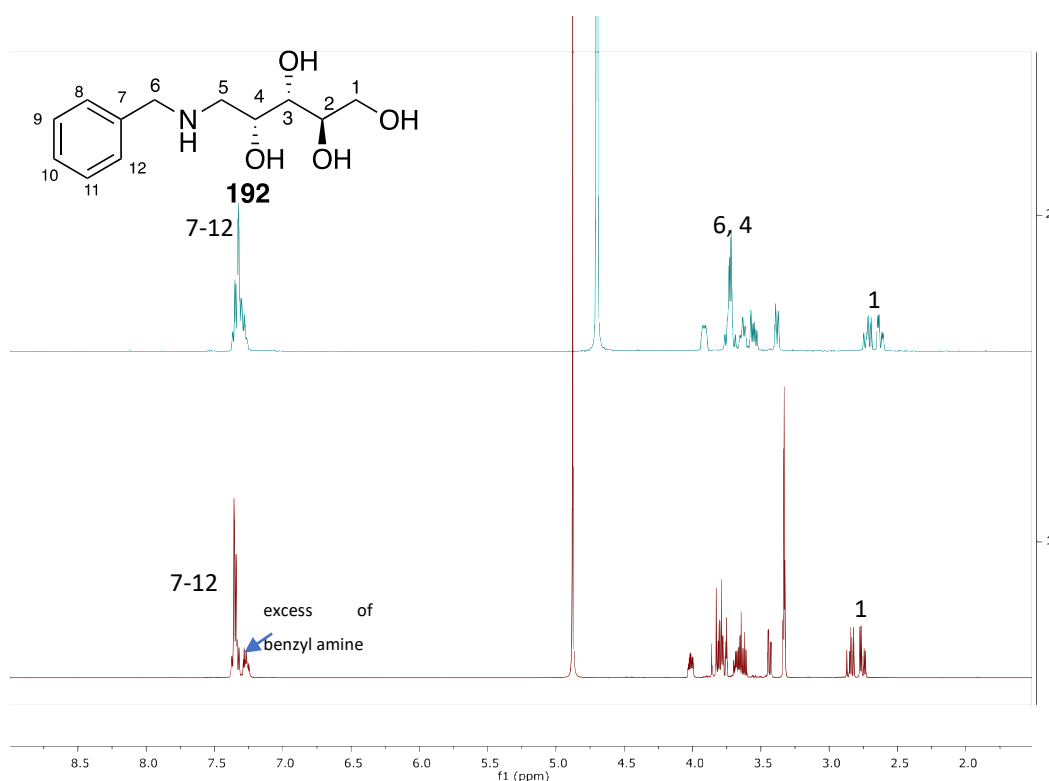


Figure 56. A comparison the ¹H NMR spectra of **192** purified benzyl amino alcohol (blue) derived from D-arabinose to the corresponding crude reaction (burgundy). The crude reaction indicates a complete depletion of the starting material and presence of the product and an excess of benzylamine.

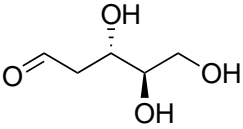
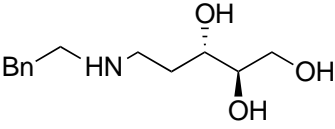
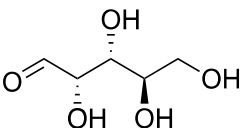
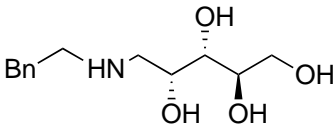
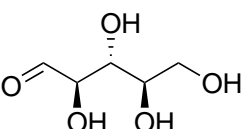
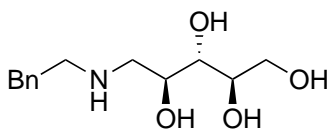
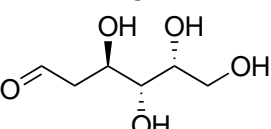
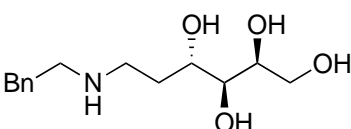
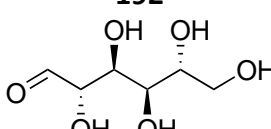
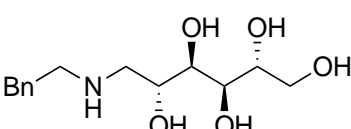
Starting material	Product	Conversion [%]	Yield [%]
 <p>2-deoxy-D-ribose 189</p>	 <p>194</p>	>99	82
 <p>D-arabinose 190</p>	 <p>195</p>	>99	34
 <p>D-ribose 191</p>	 <p>196</p>	>99	34
 <p>2-deoxy-D-galactose 192</p>	 <p>197</p>	>99	54
 <p>D-mannose 193</p>	 <p>198</p>	>99	26

Figure 57. Table of starting materials resulting in the corresponding benzyl amino alcohol products (**194-198**), reaction conversions based on ^1H NMR of the crude mixtures and isolated yields. The products **195**, **196** and **198** were purified *via* recrystallisation in ethyl acetate and **194** and **197** by flash chromatography in 20 % methanol and 80 % acetone.

Literature reports no examples of the benzyl amino alcohol biotransformations with the *G. oxydans* strains, therefore it was logical to test these compounds as well. The biocatalytic reactions with substrates **194-198** showed no product formation based on ^1H NMR analysis, which suggests that this protecting group was not tolerated by the organism.

4.1.2 Formation of amino alcohols 199-205

Reductive cleavage of the benzyl group of the purified **194-198** using a 10 % Pd/C catalyst and with molecular hydrogen afforded the desired amino alcohols **196-202** in 68-90 % yield. The volatile toluene by-product of this reaction was easily evaporated under reduced pressure, leaving the pure products. However, poor recovery of the benzyl amino alcohols affected the overall yield of amino alcohols. The quantitative conversion achieved in the reductive amination step allowed telescoping of the benzyl amino alcohol step, which significantly improved the yield. The direct hydrogenation of the crude reaction mixtures and the excess of benzylamine afforded pure products and the volatile by-products of toluene and ammonia, respectively (**Figure 58**). Thus, further amino alcohol substrates synthesised here were generated using this strategy (**Figure 59**).

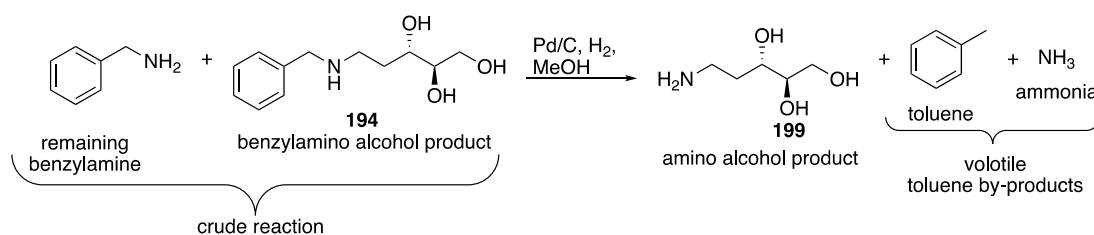


Figure 58. An example of the hydrogenation with a Pd/C catalyst of a crude reaction mixture derived from the quantitative reductive amination of 2-deoxy-D-ribose reaction, which results in a pure amino alcohol product (**199**) and volatile by-products: toluene and ammonia.

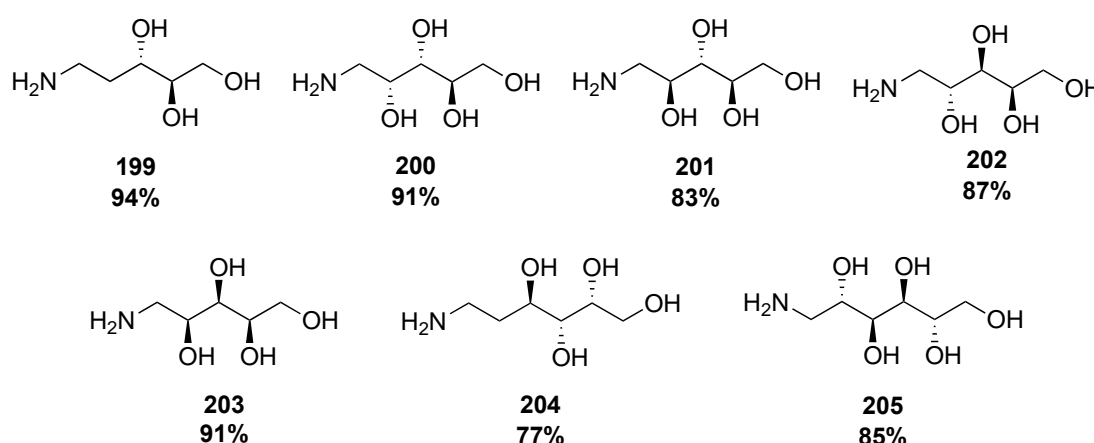


Figure 59. A full list of the synthesised amino alcohols **199-205** including the isolation yield that were obtained with a telescoping the benzyl amino alcohol intermediates.

The hydrogenation reactions also required optimisation. Studies of Oikonomakos *et al.*, 2006 and Sethi *et al.*, 2014 [3] performed hydrogenation of benzyl groups in benzyl amino alcohols that involved temperatures above 50°C using a pressurised system. In order to avoid these rather extreme conditions, the reactions were carried out at room temperature and atmospheric pressure, and the progress was monitored over 24 h and 48 h using ¹H NMR. After 24 h, the conversion reached approximately 60 % and after 48 h, resulting in complete deprotection. In order to further improve the yield, the solvent system was also optimised, as it was observed in this study that it affects the benzyl deprotection efficiency. Water, ethanol and methanol were tested in the reactions, and benzyl amino alcohols derived from five-membered ring sugars **194**, **195**, **196** and a six membered from 2-deoxy-D-galactose **197** underwent a successful deprotection in all organic solvents, contrary to what was observed in water. On the other hand, deprotection of the benzyl group of **198** was more efficient in water, which is likely due to its low solubility in methanol and ethanol.

4.1.3 Derivatisation of the amine group with a suitable protecting group in amino alcohols **206-212**

Gluconobacter oxydans is reportedly unable to oxidise unprotected amino alcohols, therefore a selection of suitable protecting groups for the amine was explored. The perfect protecting group should fulfil the following conditions:

1. retain full microbial oxidation activity
2. maintain stability under biotransformation conditions
3. undergo cleavage easily
4. facilitate the purification process
5. ideally, bear a chromophore to enable analysis on UV/Vis HPLC
6. preferentially, yield volatile or easily removable by-products

A protecting group that does not affect the microbial oxidation was the most critical aspect to consider. Several studies showed that *G. oxydans* DSM 2003 readily accepts amino alcohols protected with formyl and Cbz groups [19,105–107]. A study of Sethi *et al.*, demonstrates that formyl protection of a D-galactose derived amino

alcohol can be successfully carried out at 60 °C under reflux in methanol for 2 h, yielding 95 % of a pure recrystallised product [107]. Similarly, a high yield was obtained (82 %) when the reaction was performed at 20 °C to protect a D-arabinose derived amino alcohol [106]. Hence, these conditions were applied to protect compound **199**; however, based on the ¹H NMR analysis, the conversion reached only 60 %. The final compound could not be purified by silica gel column chromatography due to its high polarity, and recrystallisation resulted in a poor yield (20 %). In order to improve the yield, the reaction time was increased to 24-48 h and different solvents were tested, including tetrahydrofuran, ethanol and water. However, no improvements in conversion were observed.

Other protecting groups that were considered include *tert*-butyl carbamates (Boc), fluorenylmethoxycarbonyl (Fmoc) and benzyloxycarbonyl (Cbz). While literature does not report any examples of the biotransformations of the Boc and Fmoc protected substrates with *Gluconobacter oxydans*, the study of Kinast *et al.*, demonstrates that the Cbz protecting group is well-tolerated by the organism. The protecting group is also easily removed, and volatile by-products are generated [105]. Additionally, the Cbz-derivatives are more amenable to analysis by HPLC, fitted with a UV/Vis detector and this was expected to greatly simplify the analysis.

4.1.3.1 Cbz protection of amino alcohols

The benzyloxycarbonyl group (Cbz) is commonly used in organic synthesis for amine protection, particularly in peptides and amino acid, [244–247] but also small organic molecules [248–250] including amino alcohols [18,251,252]. The Cbz group is installed *via* *N*-(benzyloxycarbonyloxy)succinimide (Cbz-OSu) or benzyl chloroformate (Cbz-Cl), and a base is often required to drive the reaction forward. A study of Espelt *et al.*, employed Cbz-OSu to protect short-chain polar amino alcohols with 82-90 % yield, which were extracted to the organic solvent [18]. A more polar and larger amino alcohol — D-glucamine was protected using Cbz-Cl, and the product was recrystallised, affording the desired compound in 91 % yield [252]. These methods were adopted, optimised and applied to the reaction with of **199-205**, which led to the formation of seven Cbz- protected amino alcohols (**Figure 60**).

The generated amino alcohols differ in chain length, the position, number of hydroxyl groups and in stereochemistry, which has the potential to affect the protection. The initial experiments demonstrated significant variations in the reaction efficiency under the same conditions (Figure 61). Moreover, the products greatly differed in solubility in organic and aqueous solvents, which challenged the purification step. Consequently, both the protection reaction and purification required optimisation of each amino alcohol. The reaction conditions of Cbz protection involved the addition of Cbz-Cl or Cbz-OSu, with the base at room temperature in 1,4-dioxane-water (4:1) for 16 h. In an effort to optimise the reaction conditions, two bases were evaluated: NaHCO₃ and triethylamine (Et₃N). The final products were purified using silica gel column chromatography or *via* recrystallisation.

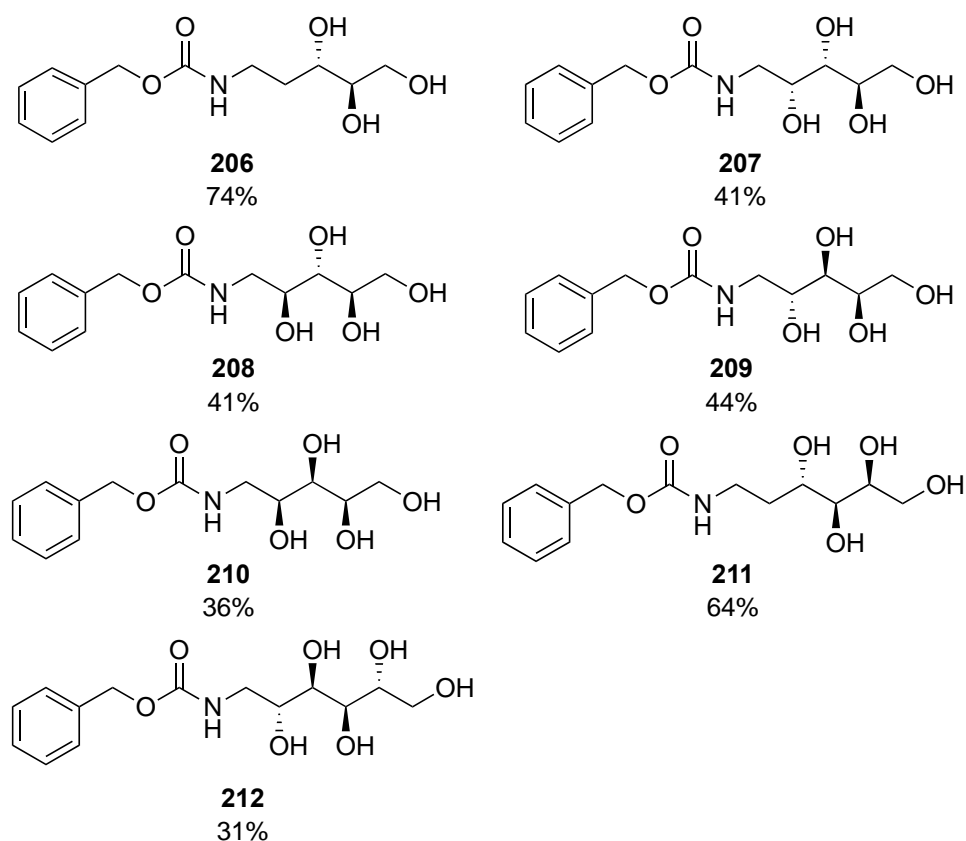


Figure 60. A full list of the Cbz protected amino alcohols (**206-212**) with the highest achieved yields.

The best protection efficiency was achieved with the least polar amino alcohol **199** using Method 1 (**Figure 61**), which yielded 74 % of the protected product **206**. Compound **208** was soluble in methanol and semi-soluble in ethyl acetate and

acetone; however, it could not be successfully recrystallised in these solvents, which may have been due to the presence of oily and viscous by-products. It was purified on a silica column with an 8:1 ratio of acetone – methanol solvent mixture giving 41 % of a pure product. However, employing such a polar solvent system caused a co-elution of the amino alcohol starting material with the final product in the later fractions, which contributed to the overall yield loss. Interestingly, compound **207**, which is a stereoisomer of compound **205**, demonstrated very low solubility in organic solvents, which enabled recrystallisation in ethyl acetate to yield 58 % of a pure product. A patent by Kawahara Kazuo and others demonstrates Cbz protection of D-glucamine [252], which is a stereoisomer of compound **212**. The reaction is performed in a mixture of tetrahydrofuran and water, with Cbz-Cl and K₂CO₃ at 0 °C, yielding 91 % of a pure recrystallised product. The application of the same conditions to protect **205** resulted only in 22 % of the final product. The reaction was also tested in 1,4-dioxane – water (4:1) and methanol, with NaHCO₃ and Et₃N bases, in ambient and 0 °C temperature, with Cbz-Cl and Cbz-OSu. The highest protection efficiency was achieved in water – dioxane, Cbz-Cl and inorganic salt at room temperature. The product could not be successfully recrystallised, and instead, was purified in a 20 % v/v methanol 80 % v/v dichloromethane solvent system. Similarly, for compound **208**, the polar solvent caused a co-elution of the product and starting material contributing to the low yield.

Product	Method 1	Method 2	Method 3	Method 4
206	74 %	22 %	Coeluted	16 %
207	15 %	N/A	N/A	58 %
208	41 %	N/A	Coeluted	N/A
212	31 %	16 %	Coeluted	19 %

Figure 61. Optimisation of the Cbz protecting reactions by testing four different methods, which involved the addition of NaHCO₃ or Et₃N base and purification *via* silica column or recrystallisation. Method 1: NaHCO₃ and silica column, Method 2: NaHCO₃ and recrystallisation, Method 3: Et₃N and silica column, Method 4: Et₃N and silica recrystallisation. The compounds: **206**, **208** and **212** were protected with Cbz-Cl, and compound **207** with Cbz-OSu. Compounds marked N/A were not tested with the corresponding methods.

4.2 Conclusions

This chapter presented the successful chemical synthesis of Cbz – protected amino alcohols, which were used for the optimisation of the biocatalytic step with *G. oxydans* DSM 2003 in the following chapters of this thesis.

The synthetic route involved three steps: catalytic reductive amination with Raney Ni, catalytic hydrogenation with Pd/C and amine protection with a Cbz-group. Each chemical transformation and purification required optimisation. The first two synthetic steps were highly efficient and performed on a gram scale. Telescoping of the intermediate benzyl amino alcohols products allowed a significant yield improvement of amino alcohols, which ranged from 77-94 %.

A Cbz-group was selected for the amine protection because it does not affect the enzymatic activity, produces few easily removable by-products and bears a chromophore, which allows rapid analysis of the biocatalytic reactions using HPLC fitted with a UV detector. However, the Cbz-protection was the least efficient step and the optimisation improved yields only marginally, resulting in 31-74 % of pure protected amino alcohol products. Except for methanol, the Cbz-protected amino alcohols were insoluble even in the most polar organic solvents, which resulted in insufficient product recovery from the silica column. The most suitable method for the purification of these highly polar compounds was reverse phase chromatography, which employs aqueous solvents for the mobile phase.

In general, this synthetic route allowed for the successful generation of seven Cbz-protected amino alcohols with good to moderate yields.

4.3 Experimental

Material and methods

General: NMR spectra were recorded on a Bruker AV 400 NMR spectrometer (^1H at 400 MHz, and ^{13}C at 100 MHz). The chemical shifts were recorded in ppm with the residual CHCl_3 signal referenced to 7.26 ppm and 77.00 ppm for ^1H and ^{13}C respectively. Coupling constants (J) are reported in Hz, are corrected and refer to

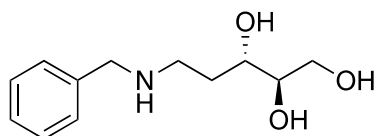
the observed peak multiplicities. Thin layer chromatography was performed on Alfa Aesar silica gel 60 F254 plates. Flash column chromatography was performed on silica gel (60 Å, 230-400 mesh). Mass spectrometry was performed on a Bruker MicroTOF II spectrometer using Electron Spray Ionisation (ESI).

Materials: Commercially available reagents, purchased from Sigma Aldrich or Acros organics, were used throughout without further purification.

General procedure for the synthesis of benzyl- amino alcohols

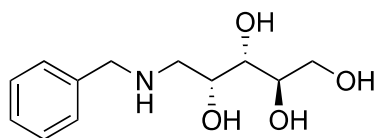
To the corresponding sugar (16-22 mmol) dissolved in 95 % of EtOH (20 mL) benzylamine (1.5 eq.) and Raney-Ni (0.02 g per 1 mmol) were added. The reaction mixture was hydrogenated for 24 h at room temperature using a balloon filled with hydrogen. The resulting compounds were purified either *via* recrystallisation or on a silica gel.

(2*R*,3*S*)-5-(benzylamino)pentane-1,2,3-triol (194)



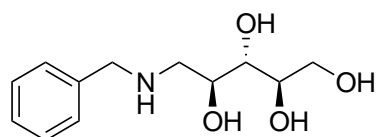
Prepared from 2-deoxy-D-ribose. Colourless oil (4.133 g, 82 %); purified using silica gel column chromatography in acetone and DCM with a 2:8 ratio. ^1H NMR (400 MHz, D_2O) δ 7.50 – 7.25 (m, 5H), 3.76 – 3.68 (m, 3H), 3.67 – 3.59 (m, 1H), 3.60 – 3.51 (m, 2H), 2.80 – 2.70 (m, 1H), 2.70 – 2.60 (m, 1H), 1.85 – 1.71 (m, 1H), 1.69 – 1.55 (m, 1H). ^{13}C NMR (101 MHz, D_2O) δ 139.0, 128.7, 128.6, 127.4, 74.5, 70.5, 62.5, 52.3, 44.9, 31.3. LC-MS(EI) m/z : calculated $\text{C}_{12}\text{H}_{19}\text{NO}_3^+$ $[\text{M}+\text{H}]^+$: 226.1438; found 226.1438.

(2R,3S,4R)-5-(benzylamino)pentane-1,2,3,4-tetraol (195)



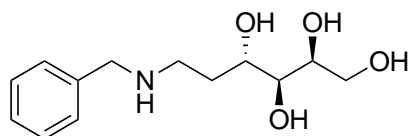
Prepared from D-arabinose. White crystals (1.640 g, 34 %); recrystallised in EtOH. ^1H NMR (400 MHz, D_2O) δ 7.50 – 7.32 (m, 5H), 4.07 – 3.96 (m, 1H), 3.86 – 3.78 (m, 3H), 3.77 – 3.68 (m, 1H), 3.69 – 3.60 (m, 1H), 3.54 – 3.41 (m, 1H), 2.89 – 2.76 (m, 1H), 2.71 (dd, $J = 12.7, 4.2$ Hz, 1H). ^{13}C NMR (101 MHz, D_2O) δ 139.0, 128.7, 128.6, 127.4, 72.0, 71.0, 68.5, 62.9, 52.3, 50.7 LC-MS(EI) m/z : calculated $\text{C}_{12}\text{H}_{19}\text{NO}_4^+$ $[\text{M}+\text{Na}]^+$: 264.1206; found 264.1202. The compound has been previously reported in the literature and characterised in DMSO [106].

(2R,3S,4S)-5-(benzylamino) pentane-1,2,3,4-tetraol (196)



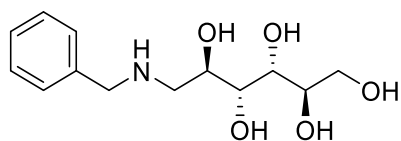
Prepared from D-ribose. White crystals (1.640 g, 34 %) recrystallised in EtOH. ^1H NMR (400 MHz, D_2O) δ 7.46 – 7.08 (m, 5H), 3.86 – 3.78 (m, 1H), 3.77 – 3.60 (m, 4H), 3.60 – 3.50 (m, 2H), 2.81 – 2.71 (m, 1H), 2.65 – 2.55 (m, 1H). ^{13}C NMR (101 MHz, D_2O) δ 139.0, 128.7, 128.6, 127.4, 73.7, 71.8, 70.1, 62.5, 52.3, 49.3. LC-MS(EI) m/z : calculated $\text{C}_{12}\text{H}_{19}\text{NO}_4^+$ $[\text{M}+\text{Na}]^+$: calculated 264.1206; found 264.1207

(2S,3S,4S)-6-(benzylamino) hexane-1,2,3,4-tetraol (197)



Prepared from 2-deoxy-D-galactose. Colourless oil (2.517 g, 54 %) purified using silica gel column chromatography in acetone and MeOH with a 2:8 ratio. ^1H NMR (400 MHz, D_2O) δ 7.36 – 7.19 (m, 5H), 3.85 – 3.73 (m, 1H), 3.66 – 3.48 (m, 5H), 3.36 – 3.27 (m, 1H), 2.75 – 2.53 (m, 2H), 1.87 – 1.71 (m, 1H), 1.63 – 1.44 (m, 1H). ^{13}C NMR (101 MHz, D_2O) δ 138.9, 128.7, 128.6, 127.4, 73.3, 70.4, 69.6, 63.0, 52.3, 44.8, 31.8. LC-MS(EI) m/z : calculated $\text{C}_{13}\text{H}_{22}\text{NO}_4^+$ $[\text{M}+\text{Na}]^+$: 278.1360; found 278.1363.

(2R,3R,4R,5R)-6-(benzylamino) hexane-1,2,3,4,5-pentaol (198)

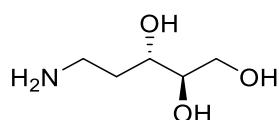


Prepared from D-mannose. White crystals (1.175 g, 26 %) recrystallised in EtOH. ^1H NMR (400 MHz, D_2O) δ 7.40 – 7.24 (m, 5H), 3.82 – 3.52 (m, 8H), 2.87 (dd, $J = 12.6, 3.9$ Hz, 1H), 2.60 (dd, $J = 12.6, 8.3$ Hz, 1H). ^{13}C NMR (101 MHz, D_2O) δ 139.0, 128.7, 128.6, 127.4, 71.4, 70.8, 69.4, 69.3, 63.2, 52.4, 50.7. LC-MS(EI) m/z : calculated $\text{C}_{13}\text{H}_{21}\text{NO}_5^+$ $[\text{M}+\text{H}]^+$: 272.1490; found 272.1492.

General procedure for the removal of benzyl group

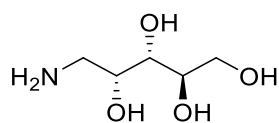
To the crude or purified benzyl amino alcohol dissolved in 95 % of EtOH, with the exception of **195** dissolved in water, 10 % Pd/C (0.05 g/mmol) was added and hydrogenated for 48 h at room temperature. The eluent was filtered and concentrated under reduced pressure to provide the corresponding amino alcohol. No purification was carried out. Yields below were achieved *via* the hydrogenation of the crude benzyl amino alcohol reactions.

(2R,3S)-5-aminopentane-1,2,3-triol (199)



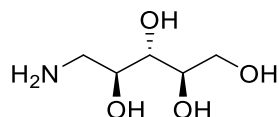
Colourless oil (2.843 g, 94 %); ^1H NMR (400 MHz, D_2O) δ 3.72 – 3.41 (m, 4H), 2.78 – 2.56 (m, 2H), 1.75 – 1.59 (m, 1H), 1.57 – 1.40 (m, 1H). ^{13}C NMR (101 MHz, D_2O) δ 74.6, 70.0, 62.4, 37.4, 34.0. LC-MS(EI) m/z : calculated $\text{C}_5\text{H}_{13}\text{NO}_3^+$ $[\text{M}+\text{H}]^+$: calculated 136.0929; found 136.0931. The result is consistent with a literature example, with slight variations in ^1H NMR and ^{13}C NMR shift [253].

(2R,3S,4R)-5-aminopentane-1,2,3,4-tetraol (200)



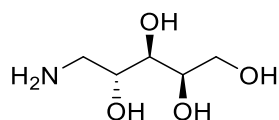
Light brown oil (2.750 g, 91 %); ^1H NMR (400 MHz, D_2O) δ 3.87 – 3.79 (m, 2H), 3.79 – 3.70 (m, 1H), 3.71 – 3.62 (m, 1H), 3.52 (dd, $J = 8.3, 2.1$ Hz, 1H), 2.84 – 2.69 (m, 2H). ^{13}C NMR (101 MHz, D_2O) δ 70.0, 69.6, 69.6, 61.6, 42.0. LC-MS(EI) m/z : calculated $\text{C}_5\text{H}_{14}\text{NO}_4^+$ $[\text{M}+\text{H}]^+$: calculated 166.1074; found 166.1077. The result is consistent with a literature example, with slight variations in coupling and ^1H NMR and ^{13}C NMR shift [253].

(2R,3S,4S)-5-aminopentane-1,2,3,4-tetraol (201)



Light brown oil (2.504 g, 83 %); ^1H NMR (400 MHz, D_2O) δ 3.74 – 3.64 (m, 3H), 3.59 – 3.51 (m, 2H), 2.83 (dd, $J = 13.5, 3.2$ Hz, 1H), 2.64 (dd, $J = 13.4, 8.4$ Hz, 1H). ^{13}C NMR (101 MHz, D_2O) δ 73.1, 72.0, 72.0, 62.4, 42.1. LC-MS(EI) m/z : calculated $\text{C}_5\text{H}_{14}\text{NO}_4^+$ $[\text{M}+\text{Na}]^+$: calculated 174.0737; found 174.0741. The result is consistent with a literature example, with slight variations in coupling and ^1H NMR and ^{13}C NMR shift [253].

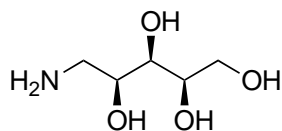
(2R,3R,4R)-5-aminopentane-1,2,3,4-tetraol (202)



Colourless oil (2.633 g, 87 %); ^1H NMR (400 MHz, D_2O) δ 3.88 – 3.79 (m, 1H), 3.64 – 3.53 (m, 3H), 3.42 (dd, $J = 8.1, 2.2$ Hz, 1H), 2.86 (dd, $J = 13.5, 3.4$ Hz, 1H), 2.61 (dd, $J = 13.5, 7.9$ Hz, 1H). ^{13}C NMR (101 MHz, D_2O) δ 71.8, 71.0, 70.2, 62.9, 43.1. LC-MS(EI) m/z : calculated $\text{C}_5\text{H}_{14}\text{NO}_4^+$ $[\text{M}+\text{H}]^+$: 152.0917; found 152.0923. The result is

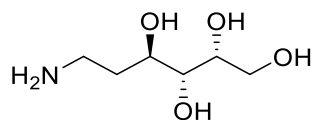
consistent with a literature example, with slight variations in coupling and ^1H NMR and ^{13}C NMR shift [254].

(2R,3R,4S)-5-aminopentane-1,2,3,4-tetraol (203)



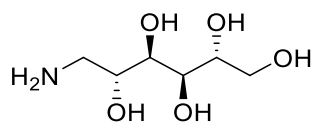
Light yellow oil (2.887 g, 91 %); ^1H NMR (400 MHz, D_2O) δ 3.85 – 3.76 (m, 1H), 3.65 – 3.53 (m, 3H), 3.45 – 3.38 (m, 1H), 2.92 (dd, J = 13.4, 3.3 Hz, 1H), 2.70 – 2.61 (m, 1H). ^{13}C NMR (101 MHz, D_2O) δ 71.8, 70.6, 70.2, 62.9, 43.0. LC-MS(EI) m/z : calculated $\text{C}_6\text{H}_{15}\text{NO}_5^+$ $[\text{M}+\text{Na}]^+$: calculated 174.0737; found 174.0742. The result is consistent with a literature example, with slight variations in coupling and ^1H NMR and ^{13}C NMR shift [253].

(2R,3R,4R)-6-aminoheptane-1,2,3,4-tetraol (204)



Colourless oil (2.324 g, 77 %); ^1H NMR (400 MHz, D_2O) δ 3.87 – 3.77 (m, 1H), 3.72 – 3.62 (m, 1H), 3.62 – 3.50 (m, 2H), 3.36 (dd, J = 7.6, 2.6 Hz, 1H), 2.90 – 2.66 (m, 2H), 1.89 – 1.74 (m, 1H), 1.64 – 1.46 (m, 1H). ^{13}C NMR (101 MHz, D_2O) δ 73.3, 70.4, 69.0, 63.0, 37.3, 33.7. LC-MS(EI) m/z : calculated $\text{C}_6\text{H}_{15}\text{NO}_5^+$ $[\text{M}+\text{H}]^+$: 166.1074; found 166.1080.

(2R,3R,4R,5R)-6-aminoheptane-1,2,3,4,5-pentaol (205)



Light brown oil (2.564 g, 85 %); ^1H NMR (400 MHz, D_2O) δ 3.76 (dd, J = 11.7, 2.4 Hz, 1H), 3.71 – 3.60 (m, 4H), 3.57 (dd, J = 11.7, 5.9 Hz, 1H), 2.95 (dd, J = 13.8, 2.6 Hz, 1H), 2.71 – 2.61 (m, 1H). ^{13}C NMR (101 MHz, D_2O) δ 70.8, 70.6, 70.6, 69.2, 63.2, 43.3. LC-MS(EI) m/z : calculated $\text{C}_6\text{H}_{15}\text{NO}_5^+$ $[\text{M}+\text{Na}]^+$: 204.0842; found 204.0843. The result is

consistent with a literature example, with slight variations in ^1H NMR and ^{13}C NMR shift [255].

Cbz protection of amino alcohols

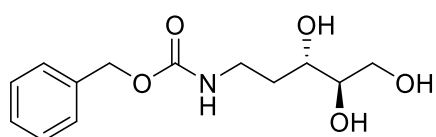
Procedure with benzylchloroformate (Cbz-Cl)

Benzylchloroformate (1.5 eq.) was added dropwise to a solution of amino alcohol (**199**, **201-205**) (11 mmol) and NaHCO_3 (1.5 eq.) in a 1,4-dioxane – water system (4:1, 15 mL). The reaction mixture was stirred at room temperature for 16 h. The crude mixture was concentrated under reduced pressure and purified on a flash silica chromatography column.

Procedure with *N*-(benzyloxycarbonyloxy)succinimide (Cbz-OSu)

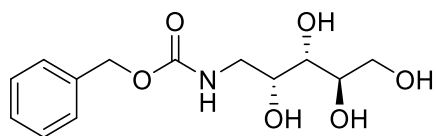
Cbz-OSu (2 eq.) was added a solution of the amino alcohol (**200**) (11 mmol) (**196-202**) and Et_3N (2 eq.) in a dioxane– water system (4:1, 15 mL). The reaction mixture was stirred at room temperature for 16 h. The crude mixture was concentrated under reduced pressure, and the solids were recrystallised in ethyl acetate and washed in cold water.

benzyl ((3*S*,4*R*)-3,4,5-trihydroxypentyl) carbamate (206**)**



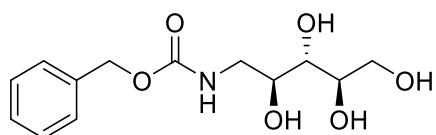
Compound prepared from **199** according to the reaction procedure with Cbz-Cl to give white crystals (2.211 g, 74 %) purified on silica column with 20% MeOH and 80% acetone. ^1H NMR (400 MHz, D_2O) δ 7.43 – 7.22 (m, 5H), 5.03 (s, 2H), 3.63 (d, J = 10.0 Hz, 1H), 3.58 – 3.41 (m, 3H), 3.30 – 3.08 (m, 2H), 1.84 – 1.63 (m, 1H), 1.59 – 1.38 (m, 1H). ^{13}C NMR (101 MHz, D_2O) δ 158.4, 136.5, 128.8, 128.3, 127.6, 74.6, 69.3, 66.8, 62.4, 37.3, 31.7. LC-MS(EI) m/z : calculated $\text{C}_{13}\text{H}_{19}\text{NO}_5^+$ $[\text{M}+\text{Na}]^+$: calculated 292.1155; found 292.1159.

benzyl ((2*R*,3*S*,4*R*)-2,3,4,5-tetrahydroxypropyl) carbamate (207)



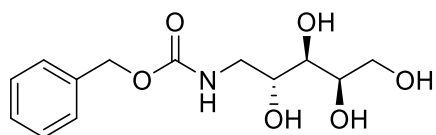
Compound prepared from **200** according to the reaction procedure with Cbz-OSu to give white crystals (1.380 g, 44 %) recrystallised in EtOAc and washed in cold water. ^1H NMR (400 MHz, MeOD) δ 7.44 – 7.24 (m, 5H), 5.08 (s, 2H), 3.98 – 3.87 (m, 1H), 3.79 (dd, $J = 10.9, 3.4$ Hz, 1H), 3.72 – 3.65 (m, 1H), 3.61 (dd, $J = 10.9, 5.8$ Hz, 1H), 3.41 (dd, $J = 8.2, 1.6$ Hz, 1H), 3.30 – 3.20 (m, 2H). ^{13}C NMR (101 MHz, MeOD) δ 157.9, 137.0, 128.0, 127.6, 127.4, 71.4, 71.1, 68.9, 66.1, 63.7, 43.6. LC-MS(EI) m/z : calculated $\text{C}_{13}\text{H}_{19}\text{NO}_6^+$ $[\text{M}+\text{Na}]^+$: 308.1115; found 308.1119.

benzyl ((2*S*,3*S*,4*R*)-2,3,4,5-tetrahydroxypropyl) carbamate (208)



Compound prepared from **201** according to the reaction procedure with Cbz-Cl to give white crystals (1.287 g, 41 %) purified on silica column with 20 % MeOH and 80 % acetone. ^1H NMR (400 MHz, MeOD) δ 7.41 – 7.24 (m, 5H), 5.08 (s, 2H), 3.81 – 3.68 (m, 3H), 3.63 (dd, $J = 10.7, 5.6$ Hz, 1H), 3.52 (t, $J = 6.4$ Hz, 1H), 3.46 (dd, $J = 14.1, 3.4$ Hz, 1H), 3.26 (dd, $J = 14.0, 7.3$ Hz, 1H). ^{13}C NMR (101 MHz, MeOD) δ 158.0, 137.0, 128.0, 127.6, 127.5, 72.9, 72.8, 71.7, 66.2, 63.2, 43.2. LC-MS(EI) m/z : calculated $\text{C}_{13}\text{H}_{19}\text{NO}_6^+$ $[\text{M}+\text{Na}]^+$: calculated 308.1105; found 308.1106.

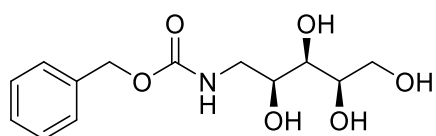
benzyl ((2*R*,3*R*,4*R*)-2,3,4,5-tetrahydroxypropyl) carbamate (209)



Compound prepared from **202** according to the reaction procedure with Cbz-Cl to give white crystals (1.380 g, 44 %) purified on silica column in acetone/MeOH, 8:2. ^1H NMR (400 MHz, D_2O) δ 7.64 – 7.32 (m, 5H), 5.14 (s, 2H), 3.97 – 3.84 (m, 1H), 3.81

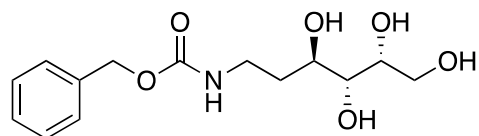
– 3.72 (m, 1H), 3.65 (d, $J = 6.3$ Hz, 2H), 3.55 – 3.47 (m, 2H), 3.25 (dd, $J = 14.4, 7.2$ Hz, 1H). ^{13}C NMR (101 MHz, D_2O) δ 158.7, 136.5, 128.8, 128.4, 127.7, 71.2, 70.2, 69.6, 67.0, 63.0, 43.4. LC-MS(EI) m/z : calculated $\text{C}_{13}\text{H}_{19}\text{NO}_6^+$ $[\text{M}+\text{Na}]^+$: calculated 308.1105; found 308.1100.

benzyl ((2S,3R,4R)-2,3,4,5-tetrahydroxypentyl) carbamate (210)



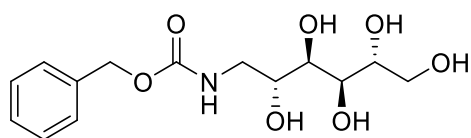
Compound prepared from **203** according to the reaction procedure with Cbz-Cl to give a pale oil (1.123 g, 36 %) purified on silica column in acetone/MeOH, 8:2. ^1H NMR (400 MHz, MeOD) δ 7.45 – 7.23 (m, 5H), 5.08 (s, 2H), 3.83 – 3.71 (m, 2H), 3.68 – 3.56 (m, 2H), 3.55 – 3.50 (m, 1H), 3.35 (dd, $J = 13.8, 5.2$ Hz, 1H), 3.23 (dd, $J = 13.8, 7.3$ Hz, 1H). ^{13}C NMR (101 MHz, MeOD) δ 157.8, 136.9, 128.1, 127.6, 127.4, 72.7, 71.0, 70.8, 66.1, 62.8, 43.5. LC-MS(EI) m/z : calculated $\text{C}_{13}\text{H}_{19}\text{NO}_6^+$ $[\text{M}+\text{H}]^+$: calculated 286.1285; found 286.1293.

benzyl ((3S,4S,5S)-3,4,5,6-tetrahydroxyhexyl) carbamate (211)



Compound prepared from **204** according to the reaction procedure with Cbz-Cl to give white crystals (1.163 g, 64 %) purified on silica column in acetone/MeOH, 8:2. ^1H NMR (400 MHz, D_2O) δ 7.54 – 7.35 (m, 5H), 5.12 (s, 2H), 3.96 – 3.81 (m, 1H), 3.79 – 3.56 (m, 3H), 3.52 – 3.40 (m, 1H), 3.37 – 3.23 (m, 2H), 2.01 – 1.86 (m, 1H), 1.69 – 1.51 (m, 1H). ^{13}C NMR (101 MHz, D_2O) δ 158.4, 136.5, 128.8, 128.3, 127.6, 73.4, 70.5, 68.4, 66.8, 63.0, 37.2, 32.2. LC-MS(EI) m/z : calculated $\text{C}_{14}\text{H}_{21}\text{NO}_6^+$ $[\text{M}+\text{H}]^+$: 300.1442; found 300.1449.

benzyl ((2*R*,3*R*,4*R*,5*R*)-2,3,4,5,6-pentahydroxyhexyl) carbamate (212)



Compound prepared from **205** according to the reaction procedure with Cbz-Cl to give white crystals (1.173 g, 31 %) purified on silica column in DCM/MeOH, 8:2. ¹H NMR (400 MHz, D₂O) δ 7.51 – 7.36 (m, 5H), 5.14 (s, 2H), 3.86 (d, *J* = 11.7, 2.2 Hz, 1H), 3.83 – 3.61 (m, 5H), 3.56 (d, *J* = 14.4 Hz, 1H), 3.26 (dd, *J* = 14.4, 6.9 Hz, 1H). ¹³C NMR (101 MHz, D₂O) δ 158.7, 136.5, 128.8, 128.3, 127.7, 70.8, 70.0, 69.5, 69.1, 67.0, 63.2, 43.7. LC-MS(EI) *m/z*: calculated C₁₄H₂₁NO₆⁺ [M+H]⁺: 316.1391; found 316.1399.

4.4 Disclosure

Purification of benzyl amino alcohols was performed by Dr James Ryan.

5 Biocatalytic oxidations of amino alcohols

Aims and objectives

This chapter aimed to regioselectively oxidise the secondary hydroxyl group in selected amino alcohols, which would lead to desired intermediates of the final iminosugar targets. This transformation corresponds to the second biocatalytic step of the proposed cascade.

Herein, the oxidation was performed with *Gluconobacter oxydans* microorganism. As previously discussed, this biocatalyst accepts only amino alcohols with a suitable chemical protection on the amine functionality. Therefore, this application led to the introduction of two additional chemical steps to the cascade (**Figure 62**).

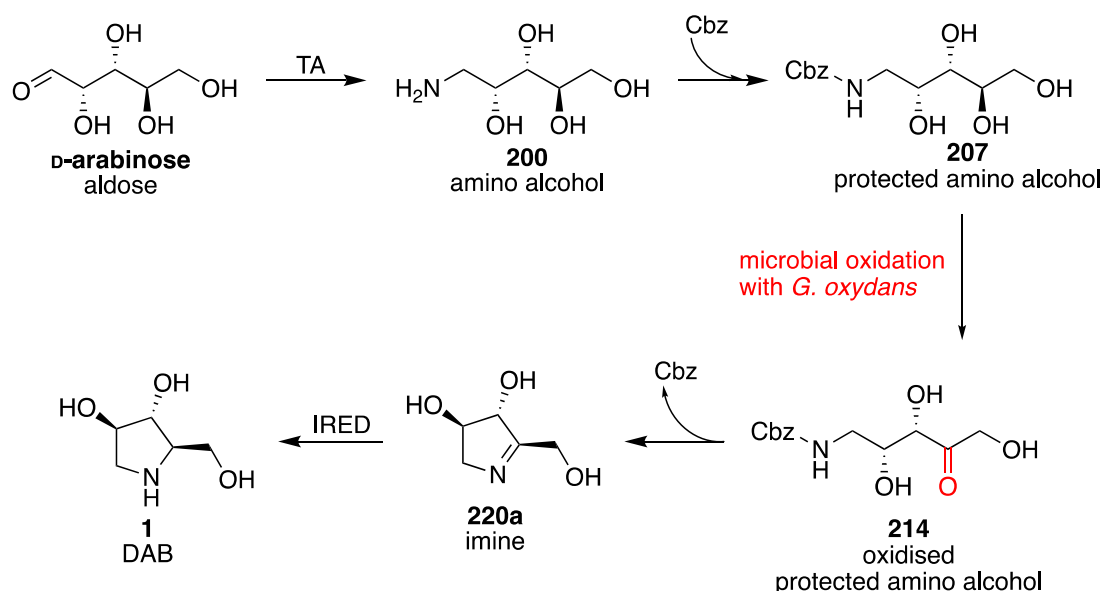


Figure 62. An example of a chemo-enzymatic cascade with the application of *Gluconobacter oxydans* for the oxidation of Cbz protected amino alcohol derived from D-arabinose.

This work presents the results of the regioselective oxidation of Cbz-protected amino alcohols catalysed by resting *G. oxydans* cells. From a number of commercially available *G. oxydans* strains employed for the regioselective oxidation of polyol substrates [256], *G. oxydans* DSM 2003 was selected due to its reported activity towards Cbz-protected amino alcohol, 1-amino-deoxy-D-sorbitol **213** [105]. In addition, the same microorganism oxidised formyl protected amino alcohols derived from D-galactose **214** and D-arabinose **215** [106,107] (**Figure 63**).

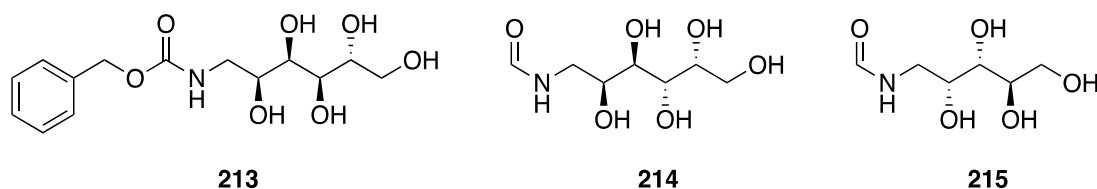


Figure 63. Examples of protected amino alcohol substrates accepted by *Gluconobacter oxydans* DSM 2003, [105–107].

This work aimed to expand the substrate scope of *G. oxydans* DSM 2003 with previously unreported Cbz-protected amino alcohols. This included product isolation, chemical characterisation, reaction optimisation and preparative scale biotransformations.

5.1 Introduction

Strains of *G. oxydans* are industrially very important due to their ability to oxidise a variety of carbohydrates, alcohols and related compounds, including amino alcohols/aminopolyols in a regioselective manner and quantitative yields. These oxidations proceed *via* two independent pathways that recruit PQQ dependent membrane-bound alcohol dehydrogenases, and NAD(P)⁺ dependent cytoplasmic soluble polyol dehydrogenases [195]. The substrate specificity of the membrane-bound enzymes typically follows the Bertrand and Hudson postulate, which states that only polyols displaying *cis*-arrangement of two secondary hydroxyl groups in the D-configuration to the adjacent primary alcohol group are oxidised to the corresponding ketones [195,257]. Soluble dehydrogenases do not appear to be restricted by this rule [256].

G. oxydans has been shown to oxidise amino alcohols only when the amine group is protected [105–107]. Schedel and Kinast describe the occurrence of a minor biooxidation of unprotected D-glucamine; however, the resulting aminoketone suffered from instability. Interestingly, other enzymes such as aldolases or galactose oxidase that transform amino alcohols also require protection of the amine group [18,188]. The isolation of naturally occurring oxidised amino alcohols has not been reported yet, likely due to their instability. It is likely that in nature these fragile intermediates are directly reduced, for example by imine reductases to provide

stable iminosugars, as suggested by Lorraine *et al.*, [307]. Nevertheless, it is unknown why these biocatalysts are unable to tolerate unprotected amino alcohols.

5.2 Evaluation of the regioselective oxidation of amino alcohols

To evaluate the oxidation capability of *G. oxydans* DSM 2003, seven unprotected (**199-205**) and Cbz-protected amino alcohols (**206-212**) (**Figure 64**), were chemically synthesised (*Chapter 4*), of which four exhibited the arrangement of hydroxyls that fit the Bertrand and Hudson rule (unprotected: **199, 200, 201, 205**; protected: **206, 207, 208, 212**). The initial biotransformations were aimed at assessing the substrate specificity and regioselectivity of the oxidation. The reactions with protected and unprotected substrates were performed under the conditions adopted from the study of Schedel and Kinast [105]: 13-15 mM substrate concentration, 100 mg/mL of wet *G. oxydans* resting cells, 30 °C, pH 6.8, 16 h. The conversions were determined from NMR analysis of the crude samples. As expected, the unprotected amino alcohols did not undergo oxidation using the biocatalyst. The biotransformations featuring the protected substrates **206, 207, 208, 211** and **212** resulted in the complete disappearance of the starting material, while **209** and **210** were not converted by the microorganism, (**Figure 65**).

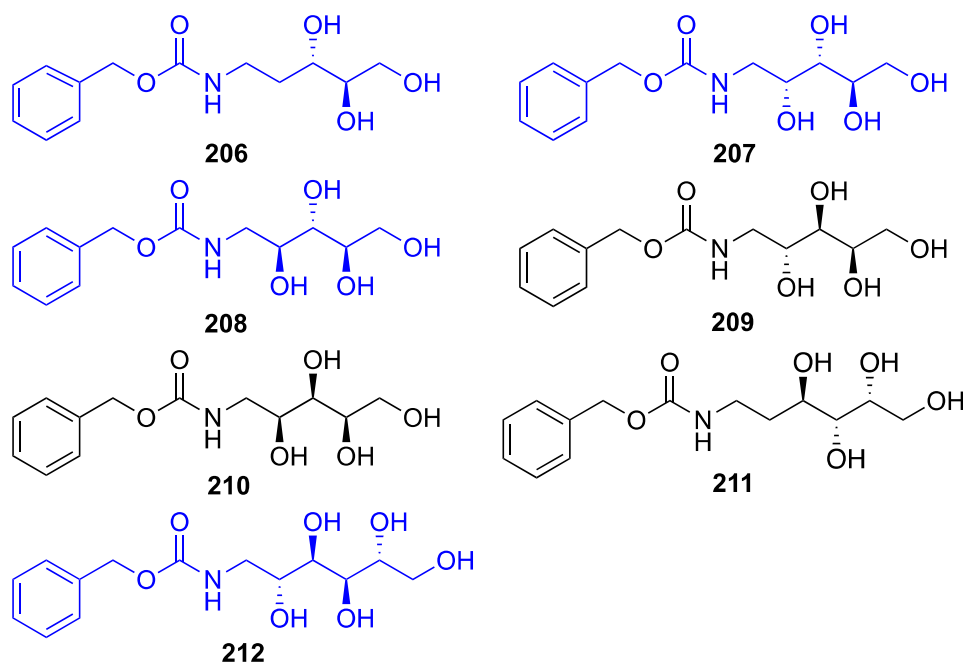


Figure 64. Chemically synthesised Cbz-protected amino alcohols derived from D-aldoses, used for the biotransformations with *G. oxydans* DSM 2003. Protected amino alcohols displaying the hydroxyls arrangement according to the Bertrand and Hudson rule are marked in blue.

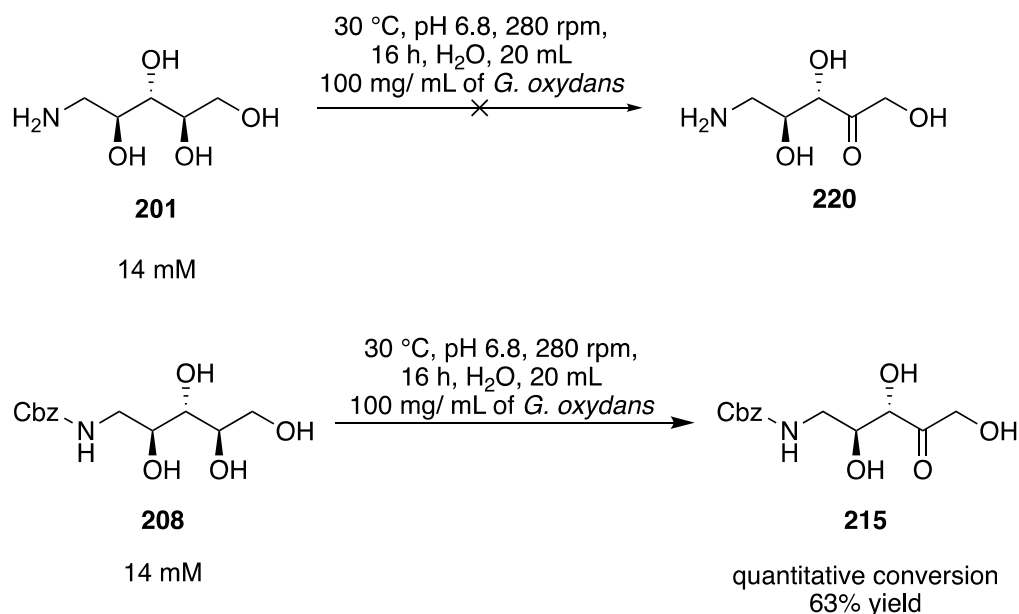


Figure 65. Biotransformations of unprotected (**201**) and Cbz-protected (**208**) amino alcohols with *G. oxydans* DSM 2003. The microorganism did not accept the unprotected substrate, while it oxidised the Cbz-protected amino alcohol in quantitative yield.

The products from five successful biotransformations were purified using silica gel column chromatography, with yields ranging from 15-95 % (**Figure 66**). The structural and stereochemical characterisation was determined by one- and two-dimensional NMR techniques. The NMR analyses of the products **213**, **214**, **215** and **216**, derived from the aminopolyols (**206**, **207**, **208** and **212**) indicated regioselective oxidation of the secondary hydroxyl group adjacent to the primary alcohol group, consistent with the example in **Figure 65**. The oxidation of **206** led to the linear structure **213** that was in equilibrium with its cyclic anomers **213a** in the 1:1 ratio, (**Figure 71**). The biotransformation products derived from **207** and **208** that resulted in compounds **214** and **215** respectively displayed mainly linear structures, (**Figure 72**, **Figure 73**). The relative configuration of their cyclic structures proved to be difficult to assign due to the minor quantities. In general, the linear structures were characterised by a distinctive carbonyl peak around 212 ppm, while the cyclic anomers contained hemiaminal peaks at approximately 90 ppm, which were most evident in molecule **213a**. The product derived from a six-membered substrate **212**

was present in its cyclic structure, *via an* acetal formation (**Figure 67**, **Figure 74**). The distinct acetal carbon peak was shown at around 80 ppm, while no carbonyl peak was present. The relative configuration of the major anomer (**216a**) was determined based on the Nuclear Overhauser Effect Spectroscopy (NOESY), which indicated the interaction between the proton on carbon 3 and protons on carbon 6, (**Figure 67**, **Figure 68**).

Starting material	Concentration [mM]	Yield [%]
206	15	68
207	14	54
208	14	63
211	13	15
212	13	95

Figure 66. Results from the initial biotransformations of Cbz-protected amino alcohols with *G. oxydans*. Reaction conditions: substrate concentrations (13-15 mM), resting cells of *G. oxydans* DSM 2003 (100 mg/mL wet weight), 20 mL H₂O, pH 6.8, 16 h, 280 rpm.

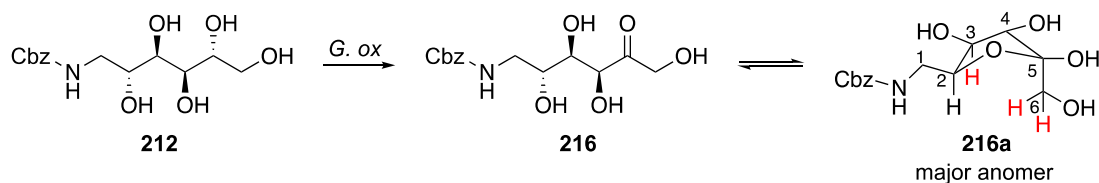


Figure 67. The regioselective oxidation of the hydroxyl group in **212** by *G. oxydans* DSM 2003 resulted in the spontaneous cyclisation *via* acetal formation to the **216a** major anomer.

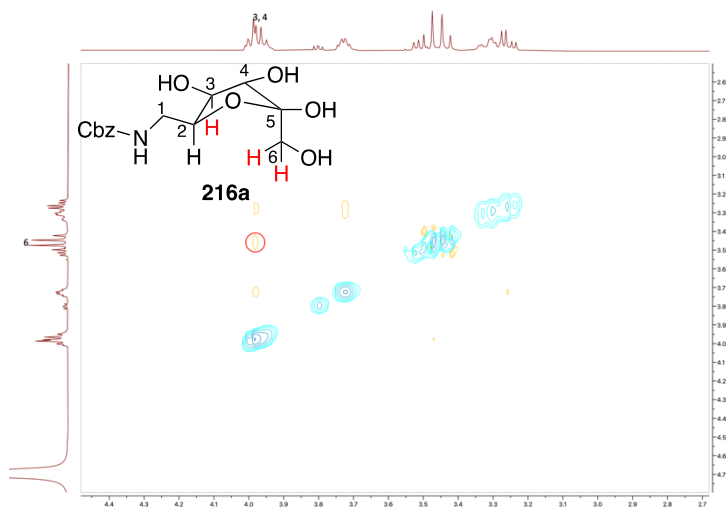


Figure 68. The NOESY analysis that determined the major anomer of the **216a** product is showing an interaction (circled in red) between the protons (highlighted in red) on carbon **3** and carbon **6**.

The oxidation of the six-membered compound **211**, derived from 2-D-deoxy-galactose, underwent complete oxidation; however, the regioselectivity differed when compared to the other products. Here, the oxidation underwent the secondary hydroxyl group on carbon **3** (**Figure 69**). The product was in equilibrium with the linear and cyclic form, which was evident by examining the carbonyl and the acetal carbons in the ^{13}C NMR spectrum. The linear structure constituted the major isomer and was fully assigned (**Figure 75**). However, the product proved to be unstable, and despite the quantitative conversion, only resulted in 15 % isolated yield.

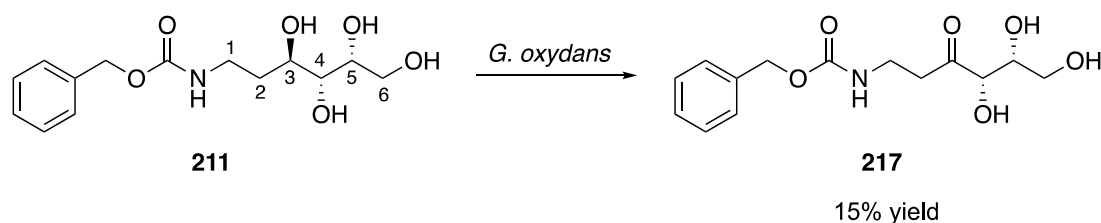


Figure 69. Biotransformation of **211** with *G. oxydans* DSM 2003 resulted in the regioselective oxidation of the secondary hydroxyl group on carbon **3**.

Interestingly, a study by Madhuresh K. Sethi *et al.* [107], reports the oxidation of a formyl protected amino alcohol derived from D-galactose (**218**) with *G. oxydans* DSM 2003 (**Figure 70**). Unlike the 2-D-deoxy-galactose derived amino alcohol, the hydroxyl group that underwent oxidation displayed the *trans*-arrangement with the adjacent hydroxyl group, which is unusual for the oxidation with *G. oxydans* (**Figure**

70). However, the reaction proceeded very slowly; it was carried out for 20 days resulting only in 50 % conversion and 30 % isolated yield.

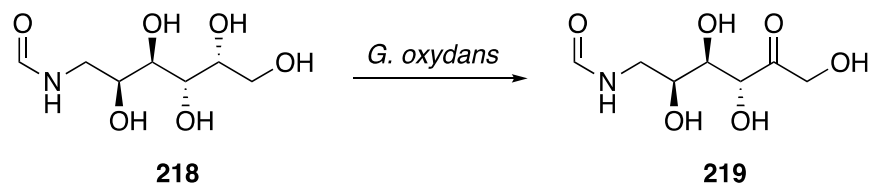


Figure 70. Regioselective oxidation of **218** by *G. oxydans* DSM 2003. The oxidation occurred at the hydroxyl group, which displays a *trans*-arrangement to the adjacent hydroxyl group [107].

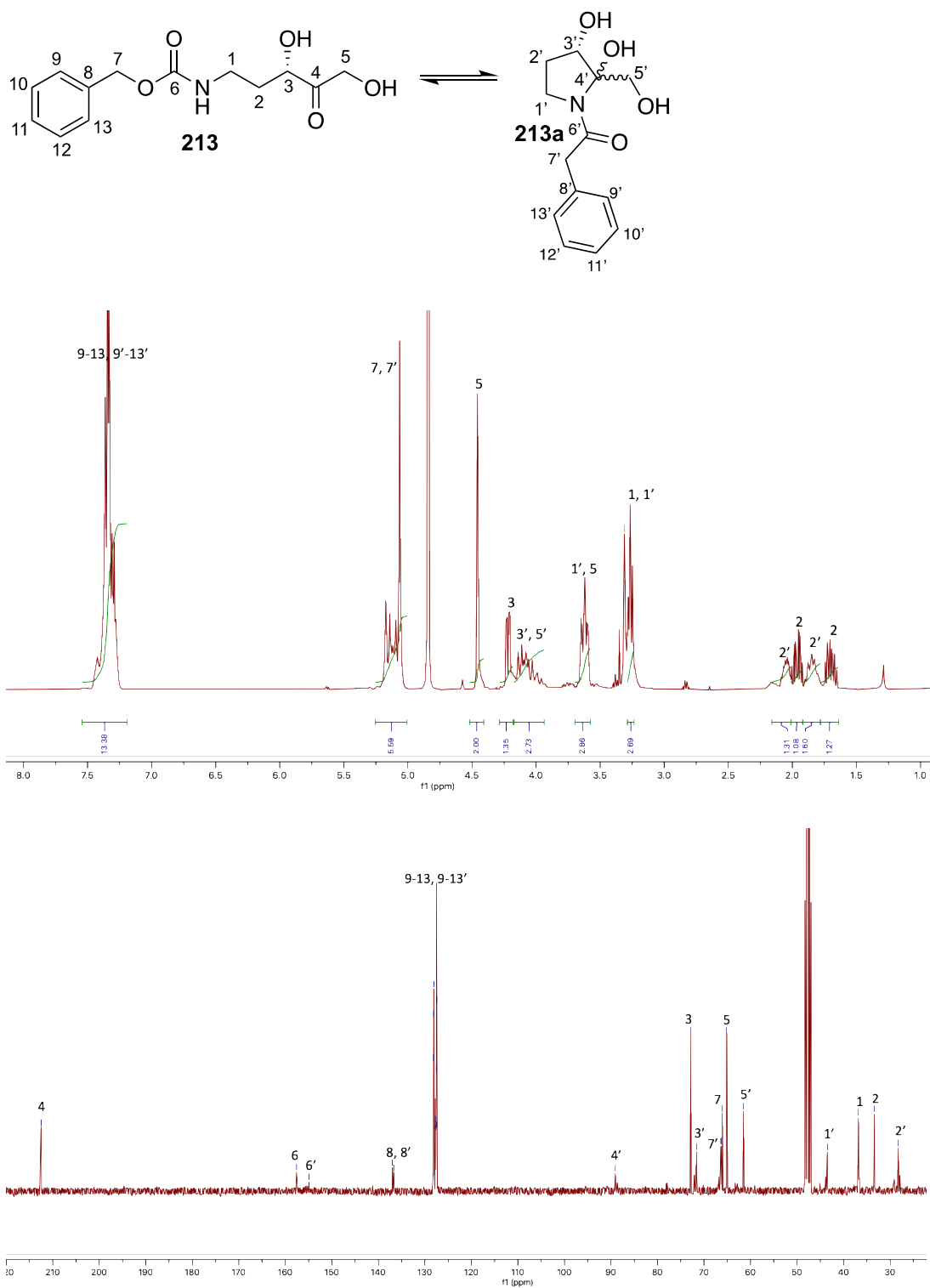


Figure 71. Assigned ^1H NMR and ^{13}C NMR spectra of **213** and **213a** derived from the oxidation of **206**. The distinct carbonyl peak at 212 ppm and hemiacetal peak at 89 ppm indicate the presence of the linear form of **213** and the anomers of the cyclic structure of **213a**. The diastereomeric ratio determined from ^1H NMR spectra was 1:1.

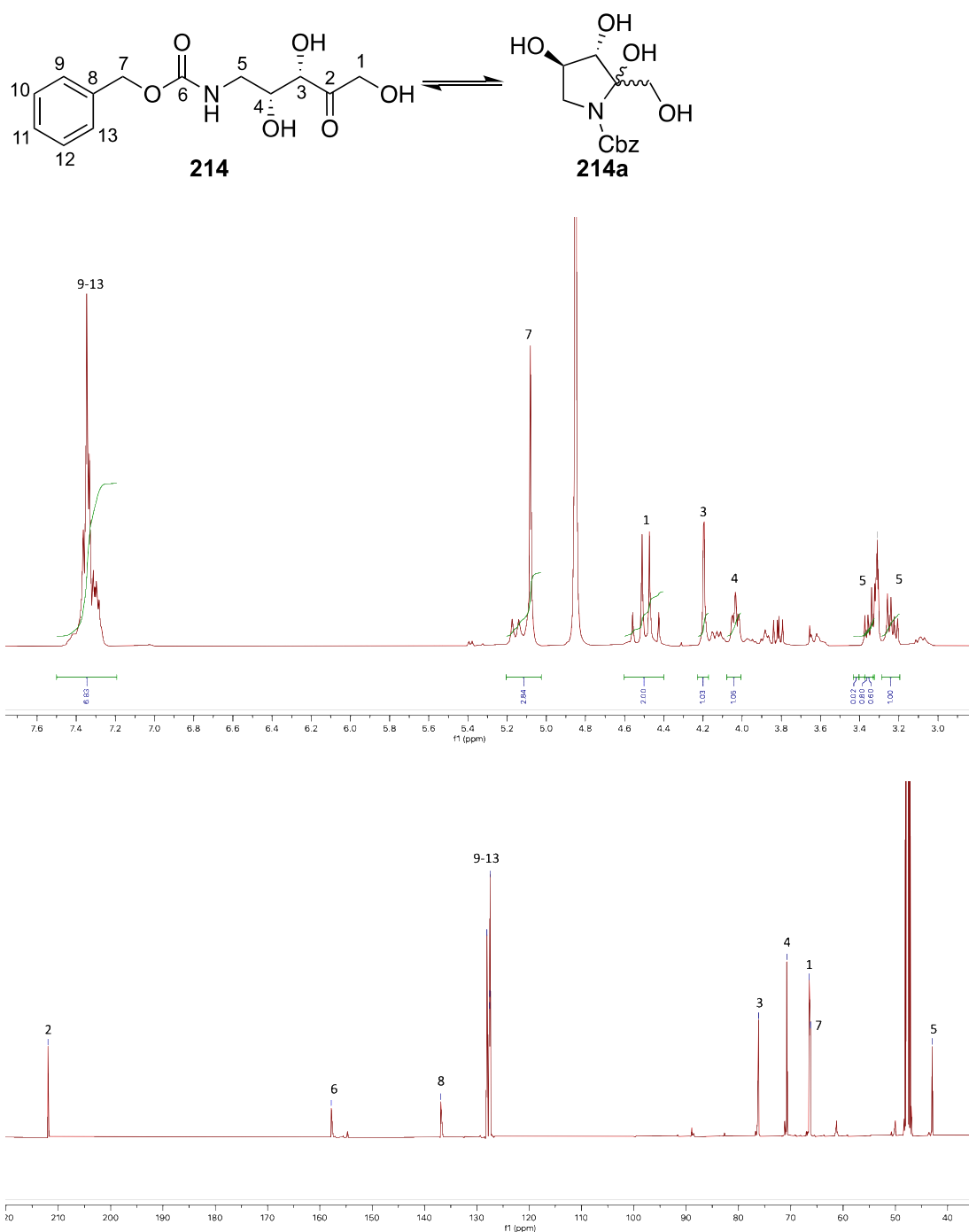


Figure 72. Assigned ^1H NMR and ^{13}C NMR spectra of **214**, derived from the oxidation of **207**. The compound existed predominantly as the linear, with some cyclic forms also present. The linear structure was assigned and characterised by the distinctive carbonyl peak at 212 ppm, and the minor cyclic anomers (**214a**) were indicated by hemiaminal peaks at around 90 ppm.

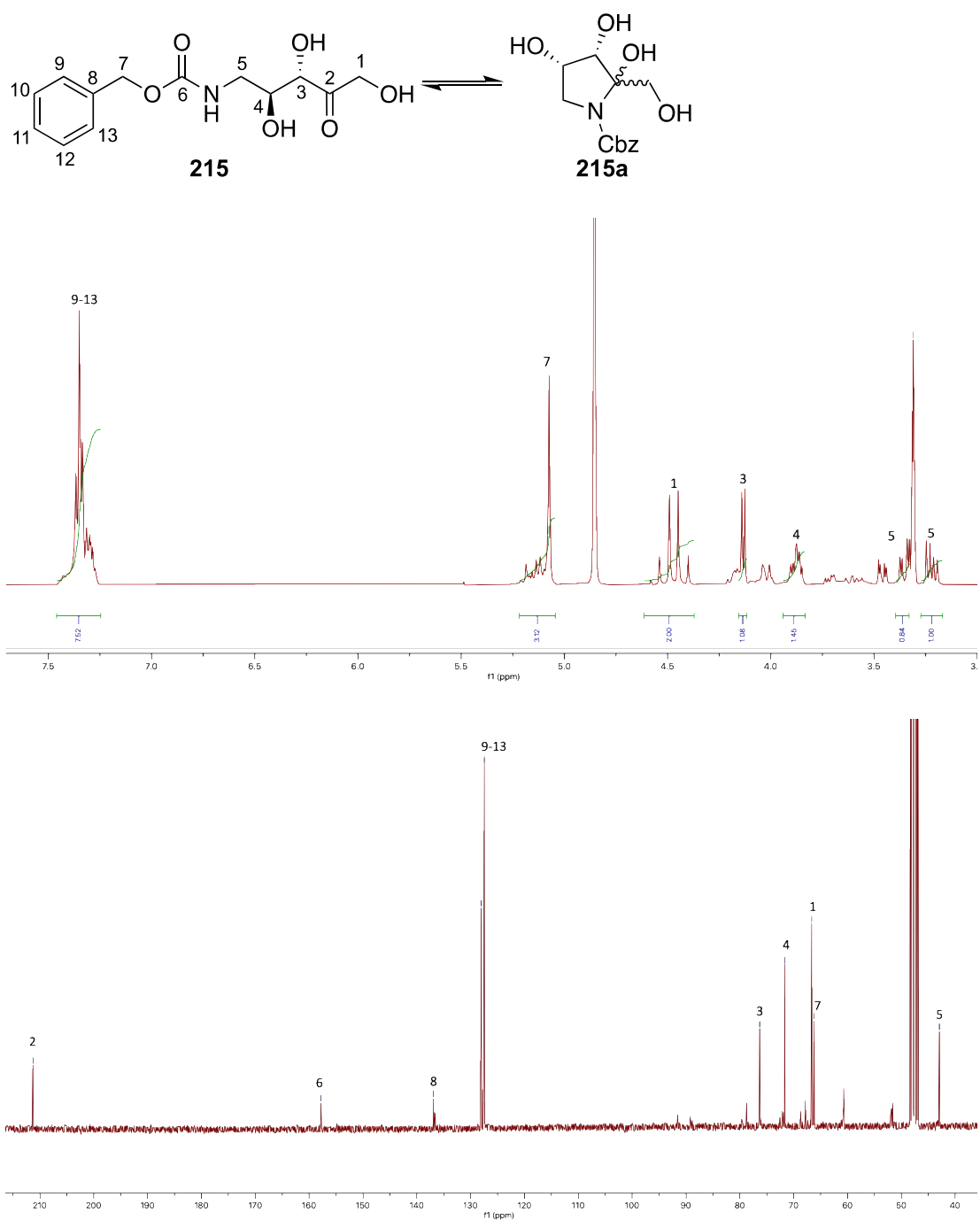


Figure 73. Assigned ^1H NMR and ^{13}C NMR spectra of **215** derived from the oxidation of **208**. The compound existed in equilibrium with the linear and cyclic structure with the former predominating. The linear structure was assigned and characterised by the distinctive carbonyl peak at 212 ppm, and the minor cyclic anomers (**215a**) were indicated by the hemiaminal peaks at around 90 ppm.

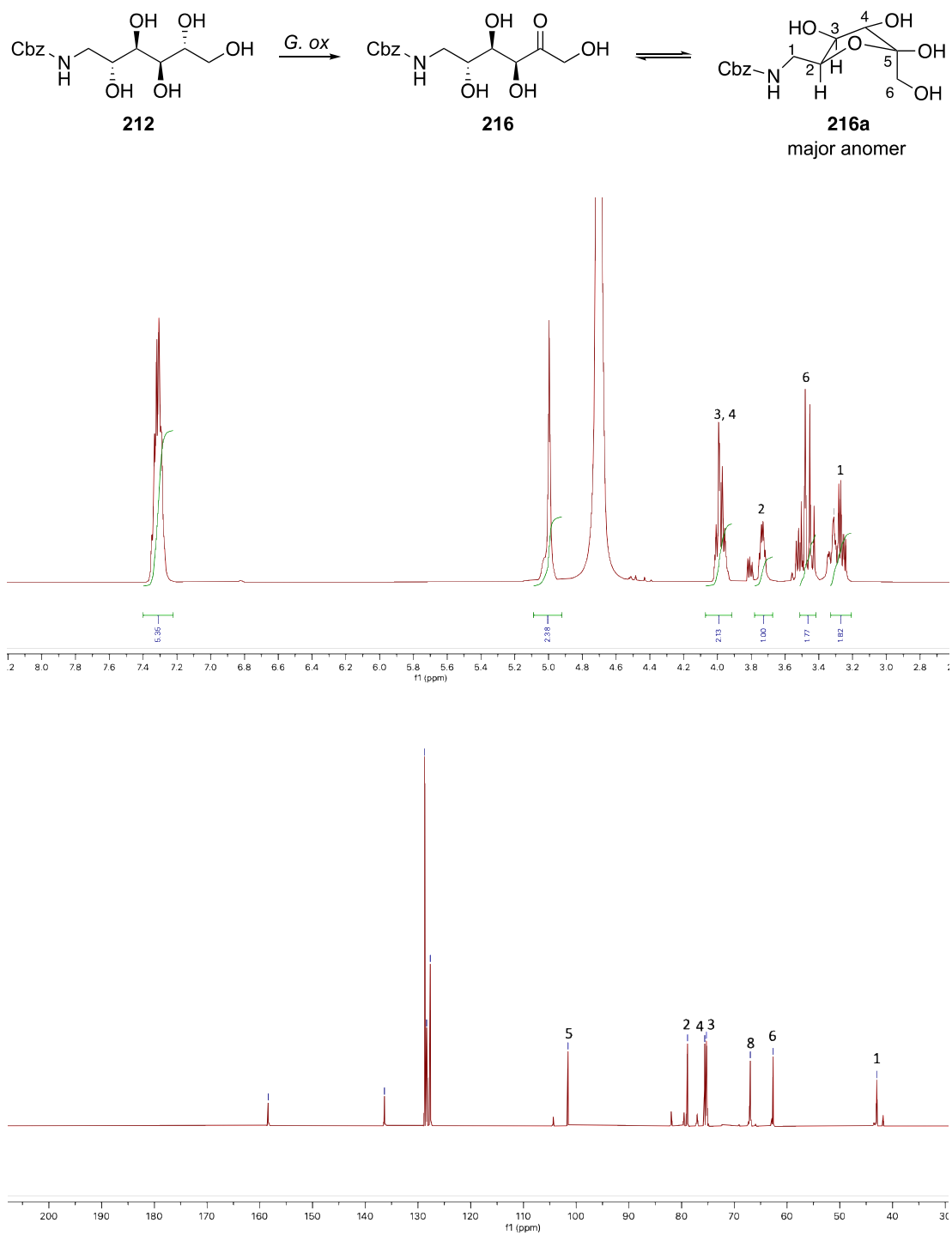


Figure 74. Assigned ¹H NMR and ¹³C NMR spectra of **216a**, which is the major anomer, derived from the oxidation of **212**. The characteristic acetal carbon peak is present at 102 ppm.

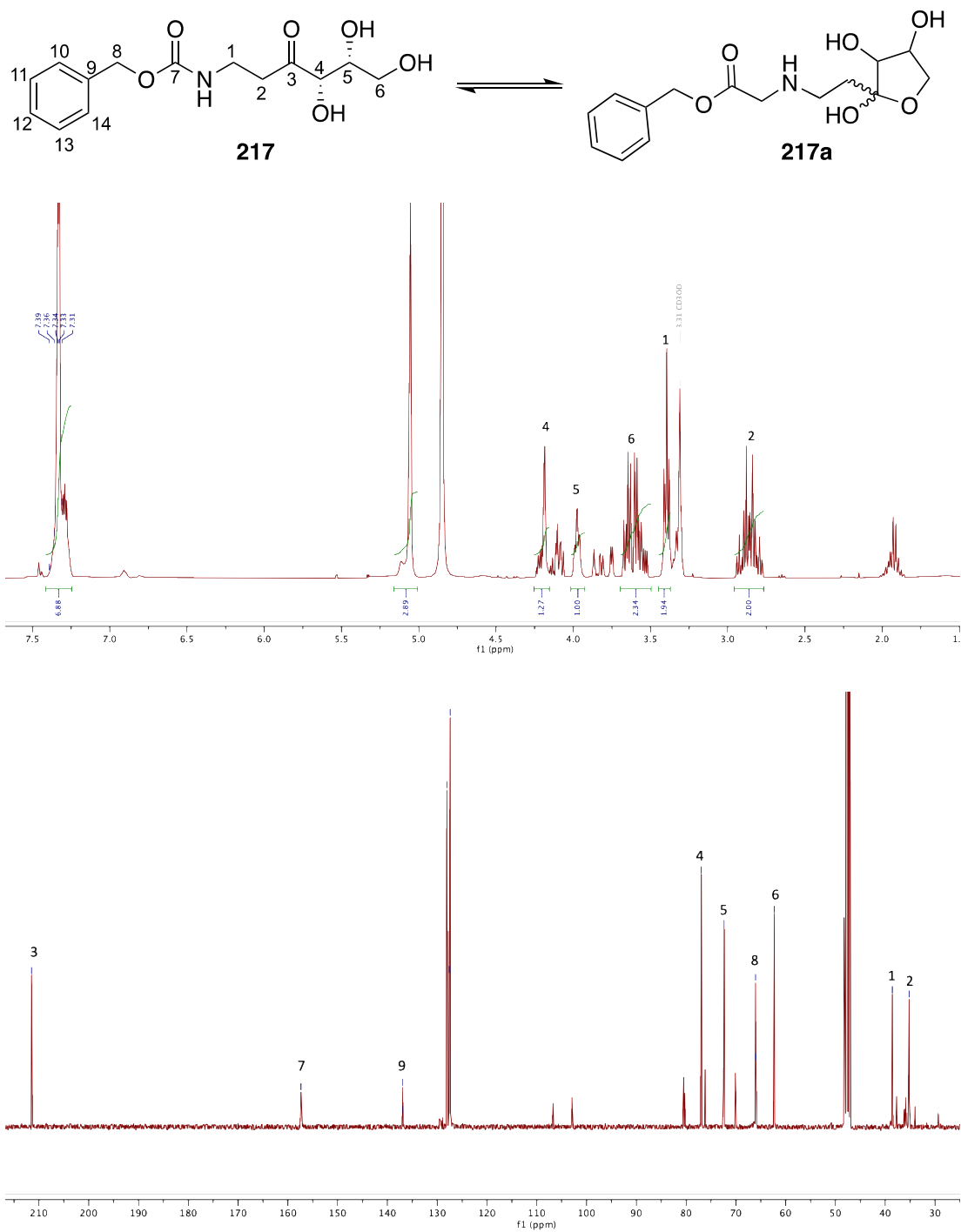


Figure 75. Assigned ¹H NMR and ¹³C NMR spectra of compound **217**, derived from the oxidation of **211**. The product displayed a linear and cyclic form, characterised by the carbonyl and acetal peak respectively. The linear form corresponded to the majority and was fully assigned.

5.3 Reaction optimisation and product quantification

In order to determine the biocatalyst performance and to optimise the conditions for the final preparative-scale transformations, the reactions were carried out on the analytical scale (1 mL), and the product was quantified based on the relative conversion. The products were analysed by HPLC-UV and separated on the HILIC (hydrophilic interaction chromatography) column. Substrates **206**, **207**, **208** and **212** were selected for the optimisation and assessed parameters included a range of temperatures and substrate concentrations. Firstly, the effect of temperature was evaluated. Since unknown enzymes in *G. oxydans* DSM 2003 perform the transformations, it was important to test a range of different temperatures for the individual substrate, as it is likely that more than one enzyme catalyses these reactions. Herein, the reactions were performed with 10 mM substrate at 20 °C, 30 °C, 35 °C and 40 °C.

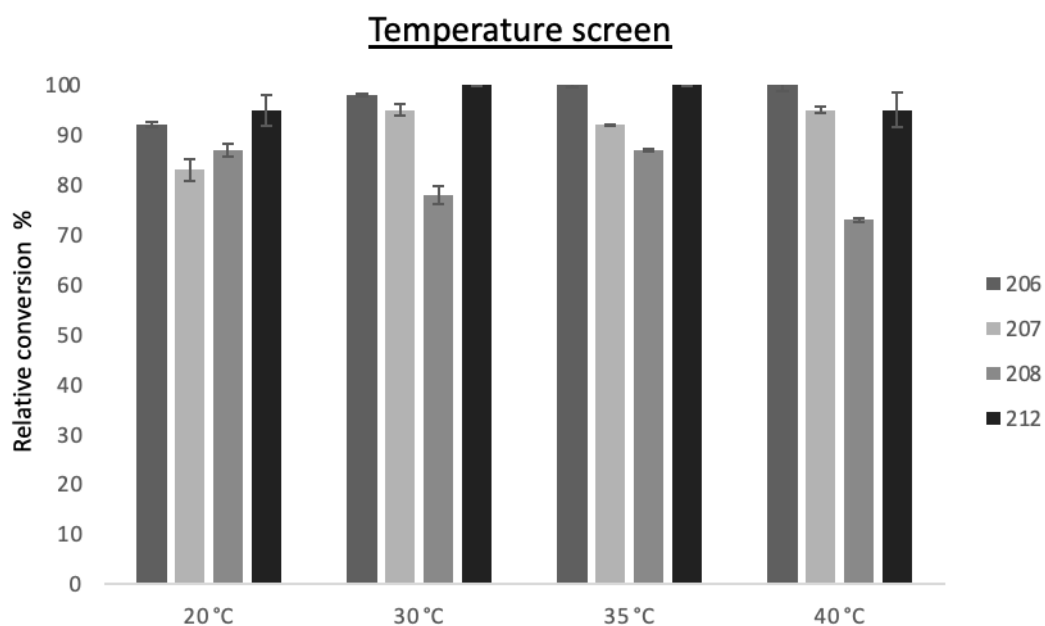


Figure 76. Conversions* of **206**, **207**, **208** and **212** to the corresponding oxidized products. Reaction conditions: 10 mM, 1 mL, water, 100 mg wet resting cells of *G. oxydans* DSM 2003, 16 h, 280 rpm. *Conversions were calculated based on the relative ratio between the product formation and substrate disappearance.

In general, *G. oxydans* maintained high activity in a wide range of temperatures, demonstrating stability even at 40 °C. All tested substrates were successfully

transformed to the corresponding products, ranging from good to quantitative conversions (73-100 %).

In order to optimise the substrate concentration, the analytical scale reactions were tested at 5, 10, 20, 25, 30 and 50 mM in 1 mL volume and with 100 mg wet resting cells of *G. oxydans* DSM 2003. Biotransformations with **206**, **207** and **208** were performed at 35 °C, and with **212** performed at 30 °C. The wild type microbial biocatalyst converted all tested substrates to near quantitative conversion at up to 25 mM concentration. High conversions were also achieved at 30 mM and 50 mM reaching up to 90 % and 77 % respectively.

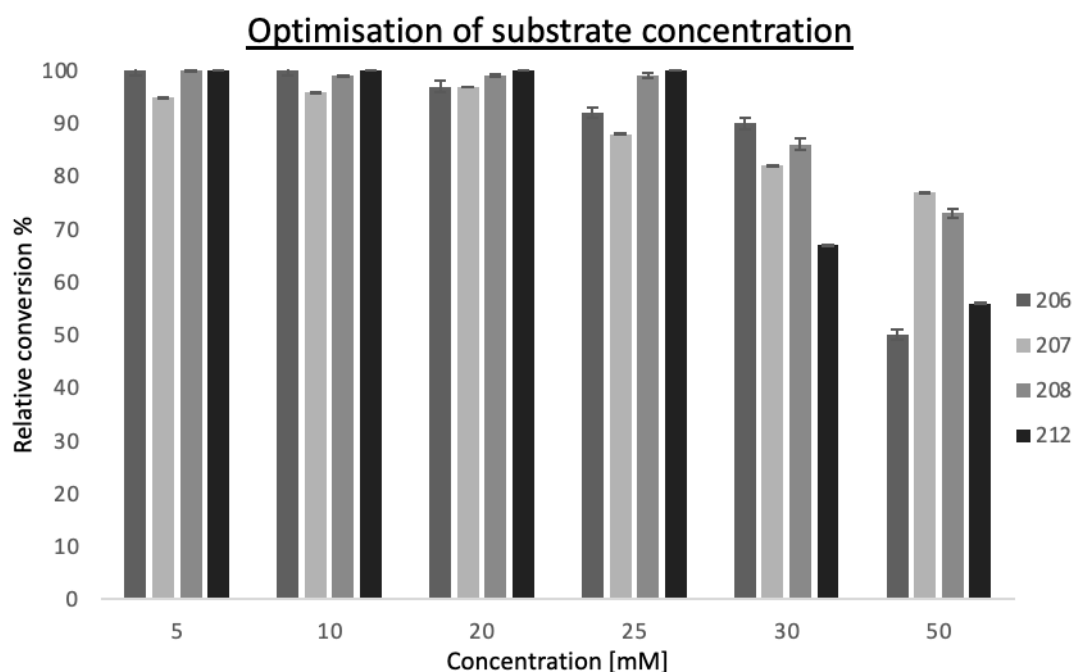


Figure 77. Conversions of **206**, **207**, **208** and **212** to the corresponding oxidised products. The tested substrate concentrations were 5, 10, 20, 25, 30 and 50 mM. Reaction conditions 1 mL, 100 mg wet resting cells of *G. oxydans* DSM 2003, 16 h, 280 rpm. *Conversions were calculated based on the relative ratio between the product formation and substrate disappearance.

5.4 Preparative scale biotransformations

The conditions from the analytical scale biotransformations were applied on the preparative-scale synthesis of **213**, **214**, **215** and **216** (**Figure 78**). The reactions were performed on 20 mL scale employing 20 or 25 mM of the starting material and 2 g of wet resting cells of the biocatalyst. The reaction was performed in water, and the

pH was adjusted to 6.8 according to the conditions reported in the study of Schedel and Kinast 1981 [105]. After 16 h, the pH dropped to 4 but it did not affect the conversion efficiency. Quantitative conversions were achieved with **212** while **206-208** were converted up to 95 % based on the HPLC-UV analyses (see examples in **Figure 79**). Products were purified using silica gel column chromatography in good yields enabling up to 138 mg of the oxidised Cbz-protected aminoalcohol to be isolated.

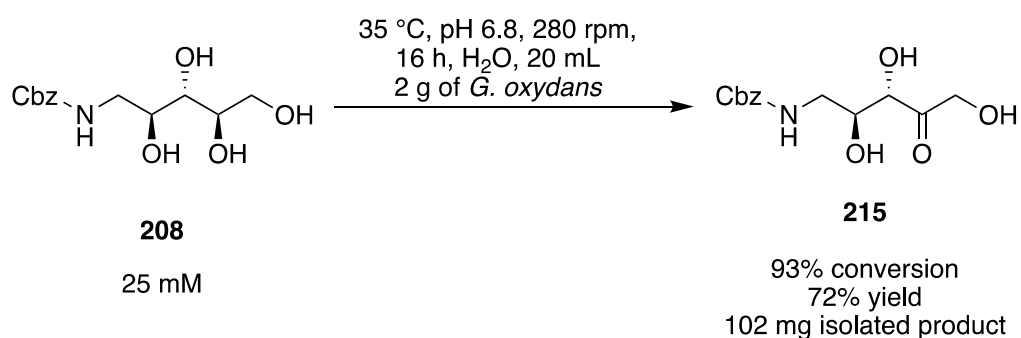


Figure 78. Optimised conditions for the oxidation of **208** with *G. oxydans* DSM 2003.

Substrate	Concentration [mM]	Conversion [%]	Yield [%]	Isolated yield [mg]
206	20	90	65	70
207	20	95	89	101
208	25	93	72	102
212	25	>99	88	138

Figure 79. Biotransformation results from the preparative scale synthesis of **213**, **214**, **215** and **216**. Reaction conditions: volume 20 mL, 20 or 25 mM starting material, H₂O, pH 6.8, 2 g of wet *G. oxydans* DSM 2003, 16 h, 280 rpm, 35°C for **206**, **207** and **208**, 30°C for **212**.

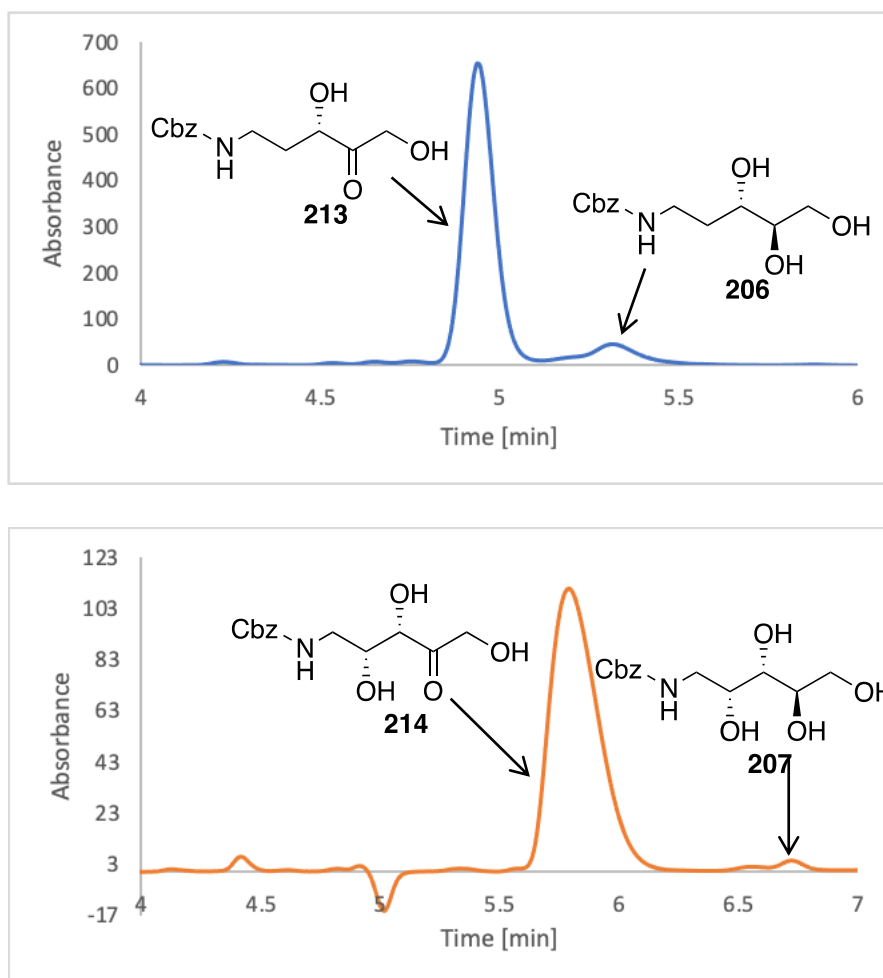


Figure 80. HPLC-UV spectra of the 20 mM preparative biotransformations with **206** and **207**, displaying the relative conversion of the product versus substrate. The product **213** and starting material **206** correspond to the peaks eluting at 4.94 and 5.34 min., respectively, while the product **214** and the substrate **207** eluted at 5.81 and 6.75 min., respectively.

However, it was observed that the biotransformations of the five-membered substrates **206**, **207** and **208** carried out in the range of 20-30 °C resulted in the product disappearance after 16 h giving approximately 40-53 % yield while demonstrating nearly quantitative conversions (**Figure 81**). Also, prolonged biotransformations (>48 h) led to almost a complete disappearance of the product. Interestingly, the optimum growth of *G. oxydans* occurs between 25-30 °C, while temperatures above 37 °C inhibit the growth. Therefore, the observed product disappearance may be due to the residual metabolism of the resting *G. oxydans* DSM 2003 cells that potentially consume the oxidised products. Bacterial growth and metabolism can be controlled by changing temperature, pH or applying osmotic stress [258,259]. This study used the approach to elevate the temperature to

suppress activity of the undesired indigenous enzymes. The biotransformations performed at 35 °C significantly improved the isolated yields by 23-36 %, which translated to a higher total yield of the final iminosugar products. Interestingly, no product disappearance was observed with the oxidation of a six-membered substrate **212** and high isolation yields were obtained from reactions performed at 20 °C and 35 °C. However, to further improve the process and achieve higher yields, future experiments should be focused on the time-resolved conversions at the optimum temperatures. This will allow determining a time point when the highest conversion is achieved while the lowest product disappearance is observed.

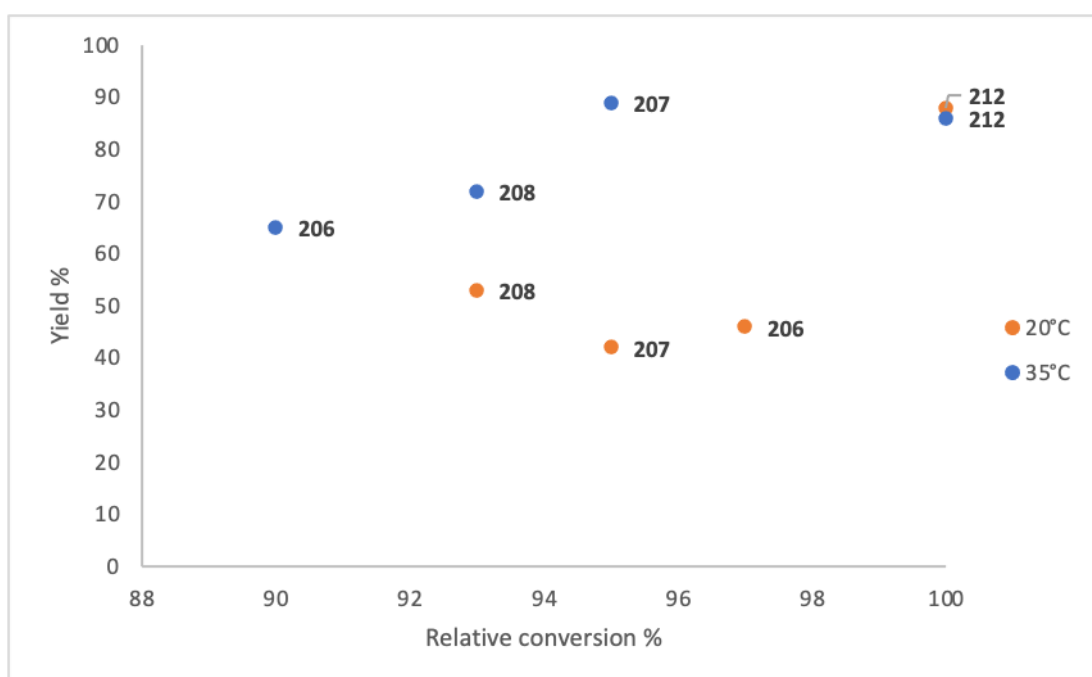
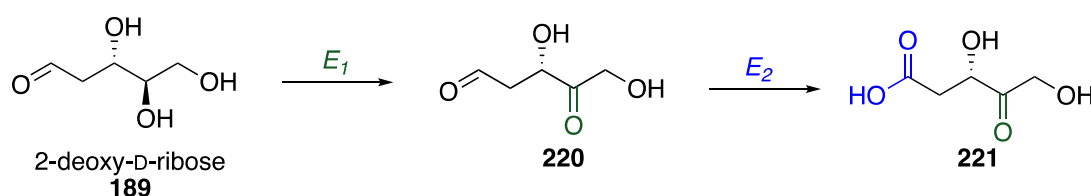


Figure 81. The comparison of the results of the oxidations of substrates **206**, **207**, **208** and **212** performed at 35 °C and 20 °C demonstrating higher isolated yield of the oxidised products derived from the five-membered aldoses at the elevated temperature. High isolation yield was obtained with the biotransformation of **212**, which gave similar results at 20 and 35 °C. Reaction conditions: 20 or 25 mM substrate, 100 mg/mL resting *G. oxydans* cells, 20 mL H₂O, 16 h, 280 rpm, 20 or 35 °C. *Conversions were calculated based on the relative ratio between the product formation and substrate disappearance.

5.5 Regioselective oxidation of simple aldoses with *G. oxydans*

The requirement for chemical protection of amine functionality in amino alcohol substrates prevents the development of the cascade. One way to overcome this challenge would be reversing the biocatalytic steps, and initiate the cascade with oxidation, followed by transamination and reduction. However, studies of Adachi

[260,261] demonstrate that strains of *G. suboxydans* IFO 12528 and *G. oxydans* NBRC 12528 regioselectively oxidise two functionalities in five-membered aldoses including 2-deoxy-D-ribose, D-ribose and D-arabinose resulting in keto and carboxylic acid groups. The studies also indicate that two different enzymes are responsible for these transformations. Both of them have been isolated and purified from the microorganisms; however, no information on their genetic origin is provided (**Figure 82**).



E_1 - D-aldopentose-4-dehydrogenase

E_2 - 4-keto-D-aldopentose-1-dehydrogenase

Figure 82. Oxidation pathway in *G. suboxydans* IFO 12528 and *G. oxydans* NBRC 12528 [260].

Therefore, the strategy of reversing the biocatalytic steps in the cascade is only feasible if the strain of *Gluconobacter oxydans* DSM 2003, which is used in this study, does not perform the oxidation of the aldehyde, and exclusively oxidises the C-4 hydroxyl group. To test that, 2-deoxy-D-ribose (14 mM) was subjected to the semi-preparative scale biotransformation with *G. oxydans* DSM 2003 resting cells (**Figure 83**). Unfortunately, the purification of the product on silica column was unsuccessful due to the highly polar nature of the compound. The mass spectroscopy analysis indicated a formation of **221**, suggesting the occurrence of double oxidation. The NMR analysis of the crude reaction mixture revealed a minor presence of the unreacted starting material, and the oxidised product. The ^{13}C NMR spectrum indicated three-carbon peaks between 174-180 ppm, which corresponds to the chemical shift of carboxylic acid carbonyl group. Interestingly, the expected carbonyl carbon derived from ketone functionality at around 210 ppm was not shown on the spectrum (**Figure 84**). However, in addition to the acetal peaks derived from the starting material, a major acetal peak was present at 90 ppm, most likely deriving from the oxidised product suggesting that it may exist in the cyclic forms (**Figure 85**). Nevertheless, the determination of the exact structure of the product requires comprehensive NMR analysis of its purified form.

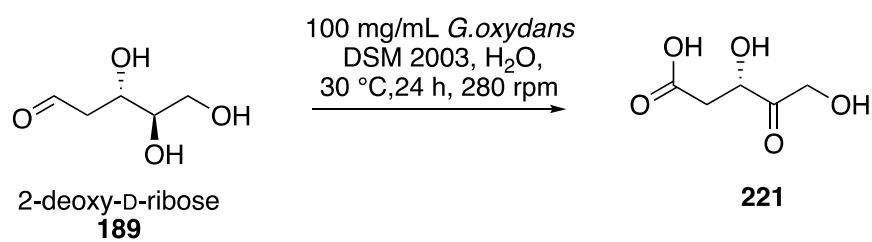


Figure 83. Test biotransformation of 2-deoxy-D-ribose with *G. oxydans* DSM 2003 resting cells.

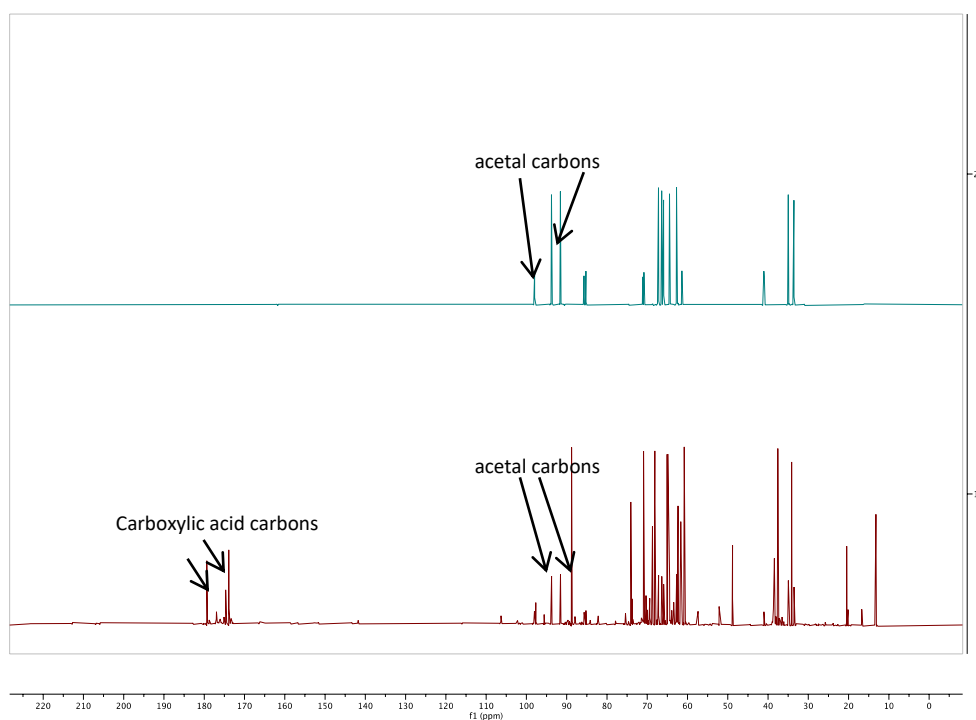


Figure 84. The comparison of the ^{13}C NMR spectra derived from a starting material of 2-deoxy-D-ribose (blue) and the crude biotransformation reaction of 2-deoxy-D-ribose with *G. oxydans* DSM 2003.

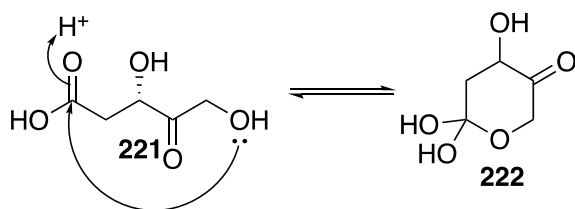


Figure 85. Possible cyclisation of the biotransformation product **221**.

5.6 Summary and conclusions

This chapter presents work that aimed to investigate and expand the substrate scope of *G. oxydans* DSM 2003 towards amino alcohols. This oxidative reaction corresponds to the second biocatalytic step of the proposed cascade for the production of iminosugars (**Figure 62**). The initial experiments revealed that the *G. oxydans* bacterium quantitatively converted five Cbz-protected amino alcohols (**206-208, 211-212**), while it did not tolerate the corresponding unprotected substrates (**199-205**). The requirement for the protection impacted the design of a cascade, and the approach had to be modified to include two additional chemical steps: Cbz protection and deprotection (**Figure 62**).

The initial biotransformations with Cbz-protected amino alcohols aimed at assessing the substrate specificity and regioselectivity of the oxidation led by the *G. oxydans* DSM 2003. Four tested substrates (**206-208, 212**) underwent regioselective oxidation of the secondary hydroxyl group adjacent to the primary hydroxyl (**Figure 71, Figure 72, Figure 73, Figure 74**). Different regioselectivity of oxidation was obtained with compound **211**, which led to the product that was unsuitable for the synthesis of iminosugars with the application of the proposed cascade (**Figure 69**).

The biotransformation reactions were subsequently optimised with substrates **206-208** and **212** to determine the biocatalyst performance at various temperatures and substrate concentrations. The microorganism demonstrated high activity by successfully oxidising all tested substrates in a wide range of temperatures (**Figure 76**). Moreover, close to quantitative conversion was achieved with substrate concentration up to 25 mM (**Figure 77**). High product formation was also achieved with 50 mM substrate concentration, reaching up to 77 %. The optimised conditions were further applied on the preparative-scale transformations carried out at 30 or 35 °C and resulted in high conversions (90-99 %) and yields (65-89 %) (**Figure 79**), enabling up to 138 mg of the oxidised product to be isolated. The results distinctly demonstrate the suitability of this microorganism for the industrial, scalable biocatalytic synthesis of these intermediate products for the preparation of iminosugars.

The possibility of reversing steps in the biocatalytic cascade was tested by subjecting 2-deoxy-D-ribose to *G. oxydans*. While the product of the biotransformation could not be isolated, the crude NMR revealed chemical shift changes when comparing to the starting material. Distinctive peaks corresponding to the carboxylic acid carbonyl group were present and mass spectroscopy analysis indicated a mass of **221**, suggesting that *G. oxydans* DSM 2003 oxidised both an aldehyde and hydroxyl group in 2-deoxy-D-ribose, preventing the application of the proposed strategy.

5.7 Experimental

General methods and materials

For general methods regarding NMR, mass spectrometry analysis and materials, see experimental section 1.4. Analytical HPLC was performed on a Thermo Ultimate 3000 uHPLC system equipped with PDA e λ detector ($\lambda = 210 - 400$ nm). The biotransformations were analysed using an XBridge Amide 3.5 μm 4.6 x 250 mm HILIC column at a flow rate of 0.6 mL/min, and oven temperature 45 °C. The mobile phase was composed of 0.1 % v/v trifluoroacetic acid in H₂O (Solvent A) and 0.1 % v/v trifluoroacetic acid in acetonitrile (Solvent B). The analysis of the chromatograms was conducted using Chromeleon 7 software.

Analytical scale biotransformations of Cbz-protected aminoalcohols

Resting cells of *Gluconobacter oxydans* DSM 2003 (100 mg/mL wet weight) were resuspended in 1 mL of deionised water containing Cbz-protected amino alcohol (5-50 mM). The reaction mixture was incubated at 30 °C (substrate **212**) or 35 °C (for substrate **206**, **207** and **208**), 280 rpm in a shaking incubator. After 16 h, 100 μL of the reaction mixture was added to 900 μL of acetonitrile, and the samples were analysed on HPLC-UV using HILIC column. Isocratic elution methods were used for the separation of compounds (**Figure 86**).

Method	Substrate	Product	Substrate rt [min]	Product rt [min]
80 % B, 20 % A over 10 min	206	213	5.34	4.94
	207	214	5.80	5.30
	208	215	5.93	6.48
85 % B, 20 % A over 10 min	212	216a	5.81	6.75

* rt- retention time

Figure 86. Methods and retention times of the Cbz-protected aminoalcohols and corresponding oxidised products.

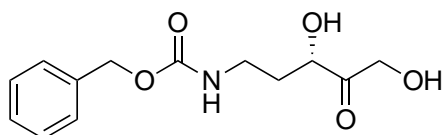
Statistical analysis

All data are presented as a mean \pm standard deviation. Three independent replicas of the analytical scale biotransformation experiments were performed in this study.

Preparative-scale biotransformations of protected aminoalcohols

To a 200 mL baffled flask, deionised water (20 mL) and the Cbz-protected amino alcohol substrate (20 or 25 mM) were added. Resting cells of *Gluconobacter oxydans* DSM 2003 (2 g wet weight) were resuspended, and the pH was adjusted to 6.8 with 10 M NaOH. The biotransformation was incubated at 30 °C (**212**) or 35 °C (**206**, **207**, **208**), 280 rpm in a shaking incubator. After 16 h, the reaction mixture was concentrated under reduced pressure, and the product was purified on the silica column chromatography.

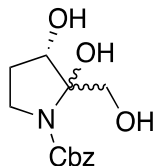
benzyl (S)-(3,5-dihydroxy-4-oxopentyl)carbamate (**213**)



Prepared from **19** (20 mM). Light yellow oil (70 mg, 65 % yield) purified using silica gel column chromatography in MeOH and DCM with a 5:95 ratio. ^1H NMR (400 MHz, MeOD) δ 7.57 – 7.21 (s, 5H), 5.24 – 5.02 (s, 2H), 4.46 (s, 2H), 4.22 (dd, J = 9.0, 3.9 Hz, 1H), 3.29 – 3.23 (m, 2H), 2.00 – 1.92 (m, 1H), 1.77 – 1.64 (m, 1H). ^{13}C NMR (101 MHz,

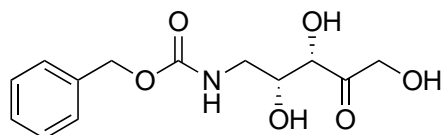
MeOD) δ 212.5, 157.6, 137.0, 127.6, 127.5, 127.4, 72.8, 66.1, 65.1, 36.8, 33.3. LC-MS(EI) m/z: calculated $C_{13}H_{17}NO_5^+$ [M+Na] $^+$: 290.0999; found 290.1005.

benzyl (3S)-2,3-dihydroxy-2-(hydroxymethyl)pyrrolidine-1-carboxylate (213a)



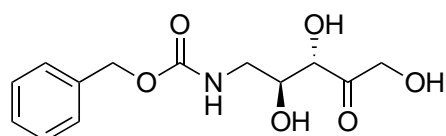
1H NMR (400 MHz, MeOD) δ 7.57 – 7.21 (m, 5H), 5.25 – 5.00 (m, 2H), 4.17 – 3.91 (m, 3H), 3.69 – 3.57 (m, 2H), 2.20 – 2.02 (m, 1H), 1.90 – 1.79 (m, 1H). ^{13}C NMR (101 MHz, MeOD) δ 154.9, 136.7, 128.1, 128.2, 128.1, 89.0, 71.6, 66.4, 61.5, 43.5, 28.3. LC-MS(EI) m/z: calculated $C_{13}H_{17}NO_5^+$ [M+Na] $^+$: 290.0999; found 290.1003.

benzyl ((2R,3S)-2,3,5-trihydroxy-4-oxopentyl)carbamate (214)



Prepared from **20** (20 mM). Light yellow oil (114 mg, 89 % yield) purified using silica gel column chromatography in MeOH and DCM with a 5:95 ratio. 1H NMR (400 MHz, MeOD) δ 7.47 – 7.22 (m, 5H), 5.22 – 5.05 (m, 2H), 4.65 – 4.37 (m, 2H), 4.20 (d, J = 2.1 Hz, 1H), 4.09 – 4.00 (m, 1H), 3.35 (dd, J = 13.8, 6.3 Hz, 1H), 3.23 (dd, J = 13.8, 7.2 Hz, 1H). ^{13}C NMR (101 MHz, MeOD) δ 212, 157.8, 137.0, 127.6, 127.5, 127.5, 76.2, 71.0, 66.5, 66.2, 43.0. LC-MS(EI) m/z: calculated $C_{13}H_{17}NO_6^+$ [M+H] $^+$: 284.1129; found 284.1120.

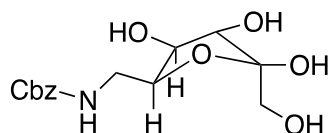
benzyl ((2S,3S)-2,3,5-trihydroxy-4-oxopentyl)carbamate (215)



Prepared from **21** (25 mM). Light brown oil (102 mg, 72 % yield) purified using silica gel column chromatography in acetone and DCM with a 3:7 ratio. 1H NMR (400 MHz, MeOD) δ 7.48 – 7.25 (m, 5H), 5.21 – 5.04 (m, 2H), 4.61 – 4.36 (m, 2H), 4.13 (d, J = 5.5 Hz, 1H), 3.95 – 3.83 (m, 1H), 3.41 – 3.32 (m, 1H), 3.26 – 3.19 (m, 1H). ^{13}C NMR

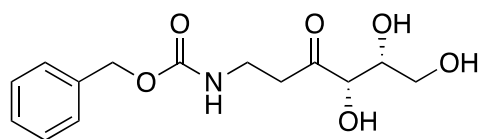
(101 MHz, MeOD) δ 211.0, 157.8, 136.9, 127.6, 127.5, 127.5, 76.3, 71.6, 66.6, 66.2, 42.9. LC-MS(EI) m/z : calculated $C_{13}H_{17}NO_6^+$ $[M+H]^+$: 284.1129; found 284.1125.

benzyl (((2*S*,3*R*,5*S*)-3,4,5-trihydroxy-5-(hydroxymethyl)tetrahydrofuran-2-yl)methyl)carbamate (216a)



Prepared from **25** (25 mM). Light yellow oil (138 mg, 88 % yield) purified using silica gel column chromatography in MeOH and DCM with a 5:95 ratio. 1H NMR (500 MHz, D_2O) δ 7.51 – 7.32 (m, 5H), 5.08 (s, 2H), 4.14 – 4.00 (m, 2H), 3.86 – 3.77 (m, 1H), 3.60 – 3.49 (m, 2H), 3.40 – 3.27 (m, 2H); ^{13}C NMR (101 MHz, D_2O) δ 158.4, 136.4, 128.7, 128.3, 127.7, 101.5, 78.9, 75.7, 75.3, 67.0, 62.7, 43.0. LC-MS(EI) m/z : calculated $C_{14}H_{19}NO_7^+$ $[M+H]^+$: 314.1234; found 314.1240.

benzyl ((4*S*,5*R*)-4,5,6-trihydroxy-3-oxohexyl)carbamate (217)



Prepared from **24** (14 mM). Brown oil (12 mg, 15 % yield) purified using silica gel column chromatography in acetone and DCM with a 2:8 ratio. 1H NMR (400 MHz, MeOD) δ 7.64 – 7.14 (m, 5H), 5.06 (s, 2H), 4.26 – 4.15 (m, 1H), 3.98 (m, 1H), 3.70 – 3.51 (m, 2H), 3.40 (t, $J = 6.7$ Hz, 2H), 2.99 – 2.70 (m, 2H). ^{13}C NMR (101 MHz, MeOD) δ 211.5, 157.4, 137.0, 128.1, 127.6, 127.4, 77.0, 72.3, 66.0, 62.3, 38.6, 35.2. LC-MS(EI) m/z : calculated $C_{14}H_{19}NO_6^+$ $[M+Na]^+$: 320.1110; found 320.1113.

5.8 Disclosure

The multiples assignment and NMR analysis were done in the collaboration with Dr James Ryan.

6 Reduction of oxidised alcohols

Aims and objectives

The application of *G. oxydans* for the regioselective oxidation of the Cbz-protected amino alcohols led to the generation of four compounds intermediates, which existed in equilibrium between linear and cyclic forms. In the final step of the proposed chemo-enzymatic cascade, the cyclic imine species are selectively reduced by an imine reductase, to access the Cbz-protected enantiopure iminosugar products (**Figure 87**).

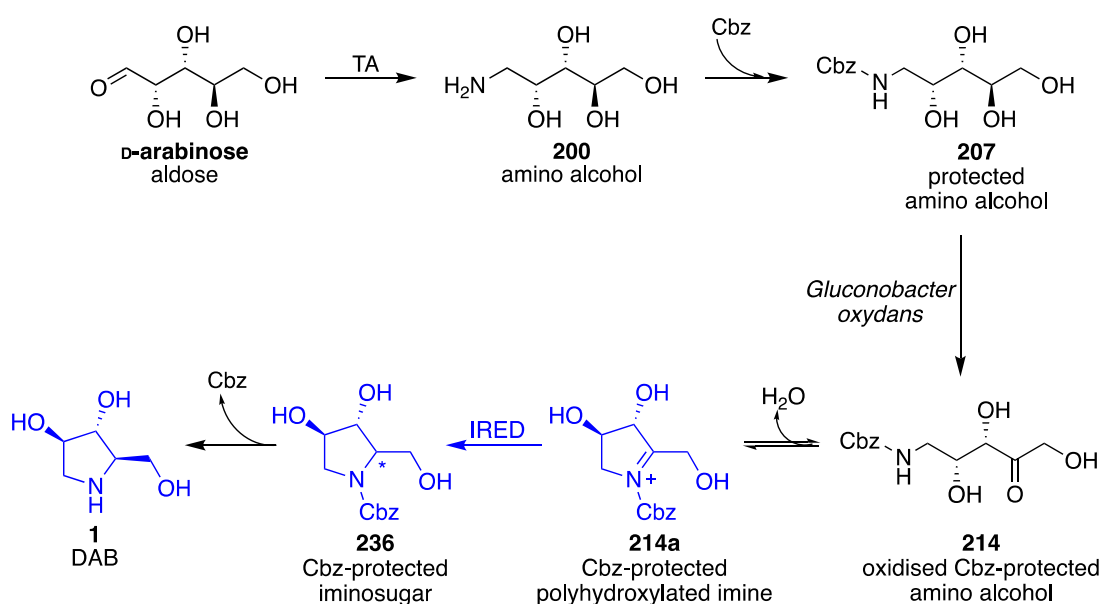


Figure 87. An example of the proposed application of a chemo-enzymatic cascade involving transaminase (TA), *Gluconobacter oxydans*, and imine reductase (IRED) for the synthesis of the enantiopure iminosugars. * chiral centre with undefined stereochemistry.

This chapter explores biocatalytic and chemical approaches for asymmetric imine reduction. A primary objective of this work was to assess the enzymatic activity of selected known IREDs towards the polyhydroxylated imine substrates. A secondary objective dealt with the application of a commonly established chemical method employing a Pd/C catalyst for the reduction of an imine bond. Finally, three variants of monoamine oxidase were evaluated in the deracemisation process of iminosugar compounds.

6.1 Introduction

Imine reduction is one of the key transformations in organic chemistry, as it allows access to chiral amines; highly desired building blocks in the pharmaceutical industry. Both biocatalytic [208,210,262] and chemical methods [263–265] have been extensively used for the cleavage of the C=N bonds.

Common chemical approaches for the synthesis of iminosugars involve the *in-situ* cleavage of nitrogen protecting group and the subsequent reduction of the imine intermediate, which is frequently achieved by hydrogenation with Pd/C [18,86,100,266]. Generally, this process is highly efficient and widely used by industry, due to its applicability on a preparative scale. However, the major drawback of this approach is a poor selectivity of the metal catalyst, which frequently leads to a mixture of enantiomers and distereoisomers.

Among the biocatalytic tools, imine reductases have been increasingly exploited in the asymmetric reduction of small and bulky cyclic and acyclic imines, and successfully applied in the numerous preparative scale transformations. These enzymes have been relatively recently added to the biocatalytic toolbox, but their discoveries and synthetic applications are continuously being expanded. However, the investigation of the IRED substrate scope is significantly hampered by the instability of imine compounds in the aqueous conditions, which tend to hydrolyse to a carbonyl and an amine. Thus, their enzymatic activity has been mostly assessed towards stable cyclic imines featuring the non-polar character (see examples in section 1.2.3.2). A known exception of polar imines reduction by IREDs is performed by the Δ^1 -pyrroline-2-carboxylate reductase/ Δ^1 -piperidine-2-carboxylate reductase (Pyr2CR/Pip2CR), which reduces small cyclic imino acids (**223** and **225**) to L-proline (**224**) and L-pipecolic acid (**226**). However, this enzyme exhibits a very narrow substrate scope [267].

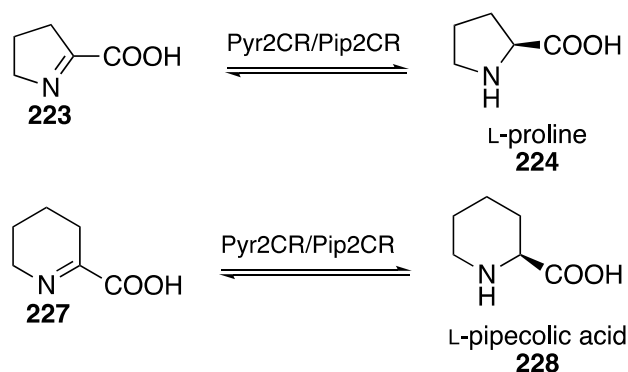


Figure 88. Biosynthetic pathways involving Pyr2C/Pip2CR catalysing selective reduction of small imino acids (**223** and **227**) to L-proline (**224**) and L-pipecolic acid (**228**) [267].

Engineered monoamine oxidase variants from *Aspergillus niger* (MAO-N) have been shown to oxidise a range of amine substrates including aliphatic, small and bulky cyclic amines and their exceptional stereoselectivity was exploited in the deracemisation process of these molecules [232,239,240]. These enzymes exclusively accept the (*S*)-enantiomers, leading to a mixture of enantiopure amine and imine. The imine is reduced *in situ* with a non-selective reducing agent ($\text{BH}_3\cdot\text{NH}_3$) and after a number of cycles of oxidation and reduction, a single enantiomer accumulates.

6.2 IRED enzyme selection

Chapter 5 investigated the regioselective oxidation of the Cbz-protected amino alcohols with *G. oxydans*, which revealed the presence of the linear and cyclic species existing in an equilibrium. However, only cyclic species derived from five-membered amino alcohols could form imines. While the NMR analysis revealed a clear presence of a **213a**, the imine species is expected to be transiently formed by water elimination (**Figure 89**). A six-membered oxidised amino alcohol **216** did not form an imine and cyclised *via* acetal carbon to **216a**.

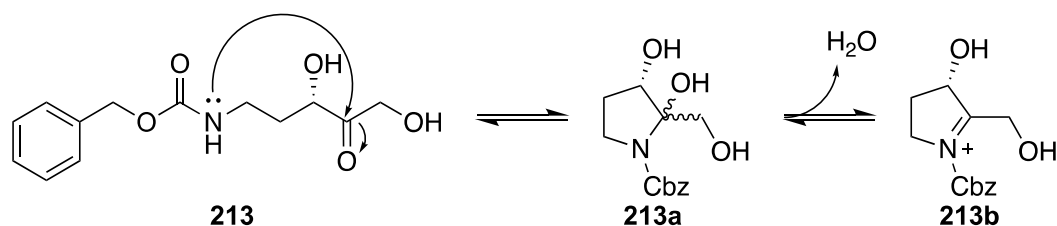


Figure 89 The equilibrium between the linear **213** and cyclic species **213a** derived from the oxidation of **19**. The transient imine intermediate **3b** is formed *via* water elimination.

Imine reductases selectively cleave an imine bond in the preformed imines allowing access optically pure amines. The produced polyhydroxylated imines were proposed to be reduced with known IREDs. However, the primary challenge of this work was the rational selection of a suitable IRED. As previously mentioned, the IRED substrate scope is largely limited to the cyclic imines featuring the non-polar character, while this work required an IRED candidate, which accepts highly polar cyclic imines. Currently, no activity towards similar substrates has been reported.

Imine reductase candidates (1-4, see below) selected for this study have been previously demonstrated to reduce a diverse range of non-polar cyclic imines. Moreover, Pyr2CR/Pip2CR (5, see below) is the only known IRED example acting on the small cyclic polar imines. Hence, the candidates (1-4) were selected to determine whether, in addition to non-polar small cyclic imines, they can also accept small polar imines. An IRED from *Pseudomonas putida* was chosen due to its activity towards polar substrates. Therefore, since IREDs have never been tested towards highly polar substrates, this study aimed at expanding the substrate scope with previously unreported polyhydroxylated imine substrates.

List of the known IRED candidates used in the study:

1. (*R*)-selective from *Streptosporangium roseum* DSM43021 ((*R*)-IRED-Sr)
2. (*R*)-selective from *Streptomyces turgidiscabies* ((*R*)-IRED-St)
3. (*S*)-selective from *Paenibacillus elgii* ((*S*)-IRED-Pe),
4. (*S*)-selective from *Streptomyces* sp GF3546 ((*S*)-St. sp. GF3546)
5. (*S*)-selective from *Pseudomonas putida* ((*S*))- Pyr2CR/Pip2CR)

6.2.1 IREDs cloning, expression and activity test

The constructs of (*R*)-IRED-*Sr*, (*R*)-IRED-*St* and (*S*)-IRED-*Pe* were obtained from Dr Bettina M. Nestl of the University of Stuttgart. A plasmid containing (*S*)-*St. sp. GF3546* gene was received from Professor Nicholas Turner of the University of Manchester. The *dpkA* gene encoding for the (*S*)-Pyr2CR/Pip2CR reductase was amplified from a genome of *Pseudomonas putida* ATCC12633 strain and cloned into the pET-21a vector according to the procedure reported by Muramatsu *et al.*, [267], (see section 3.7). The PCR primers were design based on the reported Pyr/Pip2CR sequence (Uniprot Q5FB93). The cloned *dpkA* construct was sequenced, confirming a correct insert assembly inside the vector. However, the results also revealed a slight variation compared to the published *dpkA* sequence. At the protein level, the sequences differed by 12 amino acids and the identity was 95 %.

The plasmids carrying genes encoding for the IRED enzymes were transformed into *E. coli* BL21(DE3) and protein expression was induced through IPTG addition (see section 3.11). IREDs from *Streptomyces turgidiscabies*, *Streptosporangium roseum* DSM43021, *Paenibacillus elgii* and *Streptomyces sp. GF3546* were expressed according to the protocol established by Scheller *et al.*, [216]. The expressions were carried out at 25 °C for 16 h resulting in soluble enzymes that were approximately 30 kDa in size, as shown on the SDS-PAGE analysis, which was consistent with the results reported in the literature [262,268] (**Figure 90**). The expression of Pyr2Cr/Pip2CR was performed at 20 °C for 16 h. The soluble protein was produced already after 5 h, which is evidenced by a prominent band at around 36 kDa in the SDS-PAGE (**Figure 91**). For the negative controls, the crude cell lysate of BL21 (DE3) containing empty pET21a vector was used.

Subsequently, enzymatic activities of the expressed IREDs were tested against their respective benchmark reported substrates. The (*R*)-IRED-*Sr*, (*R*)-IRED-*St* and (*S*)-IRED-*Pe* and (*S*)-*St. sp. GF3546* enzymes transformed 2-methylpyrroline (**164**) (5 mM) in the analytical scale biotransformations (1 mL), using modified reaction conditions from the study by Scheller *et al.*, [216], (**Figure 92**). The reaction required the application of the NADPH recycling system, which involved the addition of glucose

dehydrogenase and glucose (4 eq.) as a sacrificial substrate to drive the reaction towards the amine formation. The 16 h biotransformation resulted in quantitative conversions and >99 % *ee*, based on the GC analysis (data not shown).

To assess the enzymatic activity of Pyr2CR/Pip2CR required a synthesis of its model substrate of piperidine-2-carboxylic acid (**227**) using a modified method of Lu and Lewin [269]. The enzymatic activity monitored the NADPH consumption, which was indicated by a decrease in absorbance at 340 nm over time. Negative control reactions were performed with a crude lysate of BL21 (DE3) containing empty pET21a vector showed no change in the NADPH oxidation (**Figure 93**).

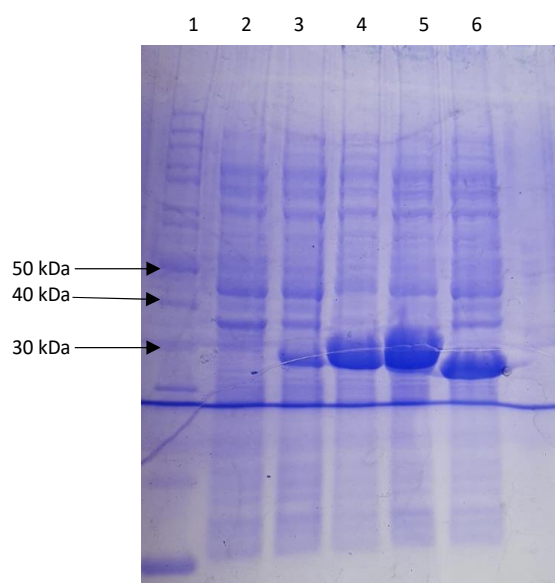


Figure 90. SDS-PAGE showing overexpression of IREDs and an empty vector pET-21a from soluble fraction of clarified cell lysate of IPTG induced BL21 (DE3) after 16 h. **1:** PageRuler Unstained Broad Range Protein Ladder (ThermoFisher); **2:** pET-21a negative control; **3:** (*R*)-IRED-*Sr*, **4:** (*R*)-IRED-*St*, **5:** (*S*)-IRED-*Pe*; **6:** (*S*)-*St*. sp GF3546. The size of the expressed proteins was 30 kDa; in accordance with the literature data [216,268].

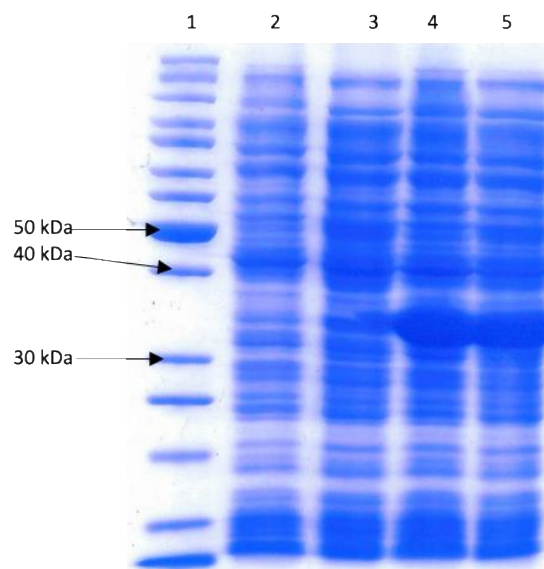


Figure 91. SDS-PAGE showing overexpression of Pip/Pyr2CR and an empty vector pET-21a from soluble fraction of clarified cell lysate of IPTG induced BL21 (DE3) after 5 h and 16 h. **1:** PageRuler Unstained Broad Range Protein Ladder (ThermoFisher); **2 and 3:** pET-21a negative control after 5 h and 16 h; **4 and 5:** Pip2CR/Pyr2CR- after 5 h and 16 h. The size of the expressed proteins was 36 kDa, in the accordance with the literature data [267].

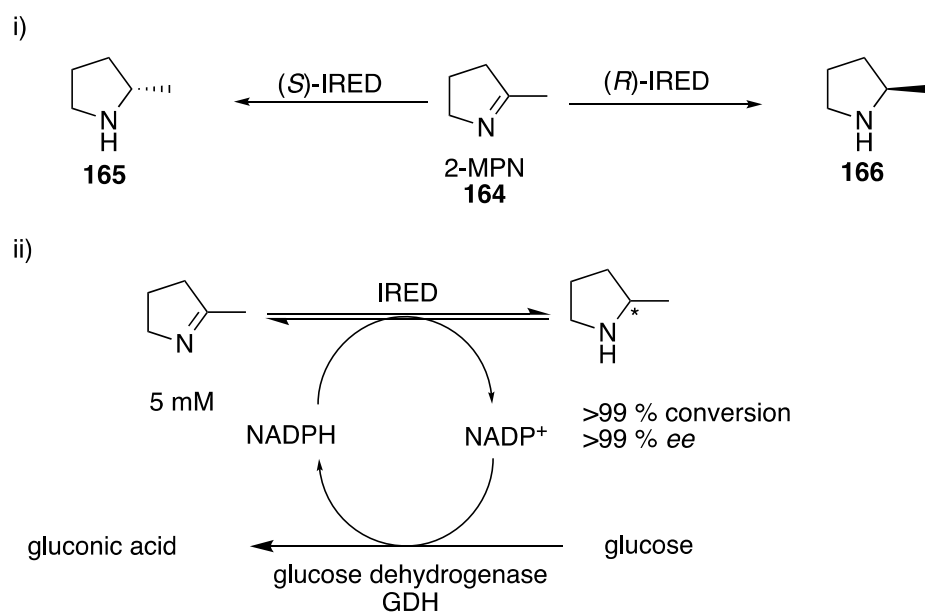


Figure 92. The reduction of a benchmark substrate 2-methyl-pyrroline (2-MPN **164**) with the (*R*)-selective IREDs *Sr*,-*St* and (*S*)- selective IREDs – *Pe*, -*St*. and -*sp* GF3546 to the corresponding chiral amine (**165** or **166**). Reaction conditions: 2-MPN (5 mM), NADPH (2.5 mM), GDH (1 mg/mL), glucose (20 mM), lysate crude cell extract (200 μ l), sodium phosphate buffer (50 mM, pH 7), 200 rpm, 16 h, 25 $^{\circ}$ C.

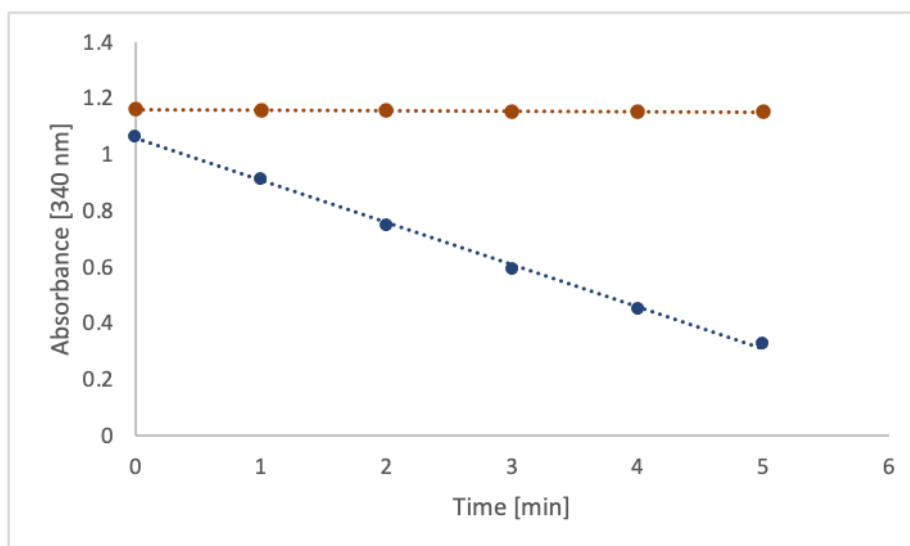
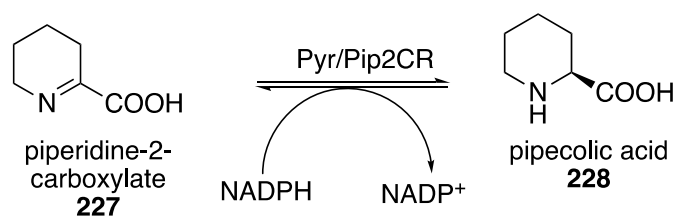


Figure 93. An enzymatic assay monitoring NADPH depletion at 340 nm over time demonstrated an active Pyr/Pip2CR enzyme (blue) in comparison to a negative control BL21 (DE3) (orange) that contained an empty pET-21a vector. Reaction conditions: 2-piperidine-2-carboxylate (**227**) (10 mM), NADPH (150 μ M), lysate crude cell extract (100 μ l), sodium phosphate buffer (50 mM pH 7).

6.3 Biotransformations of cyclic polar imines with IREDs

To evaluate the reduction capability of the IREDs towards polyhydroxylated imines **213b**, and **215b** (**Figure 94**), test biotransformations were run on a semi-preparative-scale (14 mM) in 5 mL volume using modified conditions reported by Scheller et al., [216], (**Figure 95**). Negative control reactions were performed with a crude lysate BL21 (DE3) containing empty plasmid pET21a. Interestingly, these highly polar imines are not well solubilised in water and the addition of 3 % v/v DMSO was necessary to dissolve the substrates in the aqueous buffer. Studies of Nestl. et al, [262] and Mitsukura [268] show that these IREDs maintain high activity with a DMSO co-solvent up to 5 %. The biotransformation products were purified on silica column chromatography and analysed on NMR and targeted mass spectroscopy.

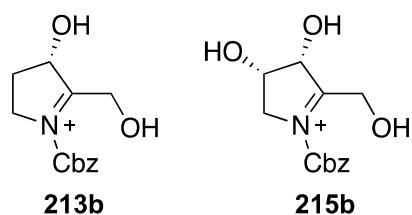


Figure 94. Transient imine intermediates derived from the cyclic species **213a** and **215b**.

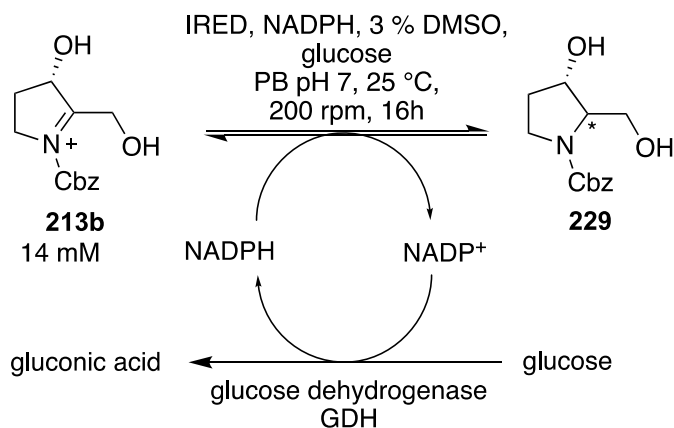


Figure 95. An example of the test biotransformation of **213b** with IRED. Reaction conditions: substrate (14 mM), NADPH (5 mM), glucose (40 mM), GDH (1mg/mL), lysate crude cell extract (500 μ l), 3 % DMSO sodium phosphate buffer (50 mM, pH 7), 200 rpm, 16 h, 25 °C. *Chiral centre with undefined stereochemistry.

Biotransformations with imine reductases of the polyhydroxylated imine substrates were compared to a chemically reduced substrate (reduced with non-selective catalyst of ammonia borane), negative control biotransformation, and starting material. The results showed that five tested imine reductases did not accept either of the polyhydroxylated imine substrates, based on the NMR analysis (**Figure 96**, **Figure 97**). No significant similarities were observed between the ^1H NMR spectra of chemically reduced products and the IRED samples. Similarly, negative controls and IRED biotransformations did not show major differences in the chemical shift. Although, an ^1H NMR spectra of a negative control sample derived from **213b** (turquoise) revealed an unexpected doublet at 4.2 ppm (**Figure 96**), which is absent in the IRED sample and chemically reduced sample. This could be caused by the more prevalent contamination with DMSO indicated by a peak at 2.65 ppm. The presence of DMSO also impacted the ratio of the linear to cyclic species showing significant shift differenced to the starting material. Finally, mass spectroscopy analysis was performed in order to determine a trace amount of product, that

otherwise could not be detected by NMR. The results also confirmed no formation of iminosugars.

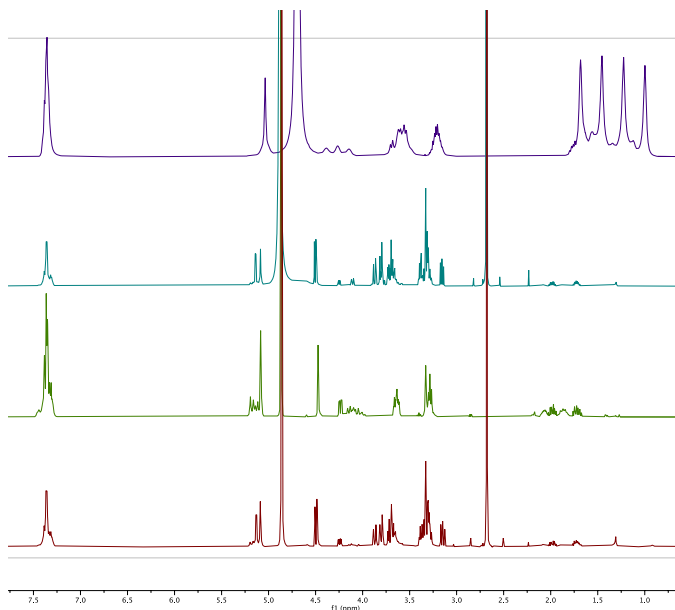


Figure 96. Stacked NMR spectra comparing (*S*)-IRED-Pe biotransformation (burgundy) to chemically reduced **213b** (purple), negative control of BL21 containing empty vector (turquoise) and a starting material (green). The biotransformation samples (turquoise and burgundy) were contaminated with DMSO (2.65 ppm). The crude form of chemically reduced sample was contaminated with $\text{NH}_3\cdot\text{BH}_3$ indicated by the peaks from 1.84-0.88 ppm.

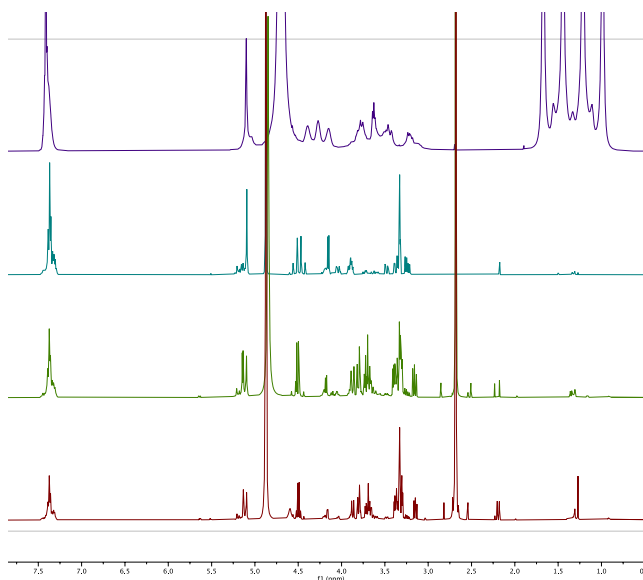


Figure 97. Stacked NMR spectra comparing (*S*)-IRED-Pyr/Pip2CR biotransformation (burgundy) to chemically reduced **215b** (purple), a starting material (turquoise) and negative control of BL21 containing empty vector (green). The biotransformation samples (green and burgundy) were contaminated with DMSO (2.65 ppm). The crude form of chemically reduced sample was contaminated with $\text{NH}_3\cdot\text{BH}_3$ indicated by the peaks from 1.82-0.87 ppm.

Several studies investigating the structure of imine reductases revealed a presence of the highly hydrophobic binding pocket [214,221]. Therefore, it was not surprising that these enzymes did not tolerate the highly polar substrates. Moreover, the role of the hydrophobic active site is to stabilize the formation of imines, which tend to be labile in an aqueous environment. While non-cyclic imines most often undergo hydrolysis in water, cyclic imines remain stable [92,315]. Interestingly, some studies suggest the existence of IREDs, which selectively reduce polar imines and generate iminosugars [192,193]. Therefore, in principle, it is possible to use IREDs, which exhibit more hydrophilic character in the active site, to reduce cyclic polar imine substrates. Thus, future studies should be focused on the discovery and engineering of such IREDs, displaying a completely new substrate preference. These enzymes could be sought in organisms such as *Saccharomyces cerevisiae* or *Gluconobacter oxydans*, which inhabit sugar rich environments. IREDs are relatively newly discovered enzymes, not commonly engineered. However, recently, GSK has reported a >38,000-fold improvement of an IRED variant, which was produced with a directed evolution approach and further applied on the industrial scale [226].

6.4 Chemical reduction of polyhydroxylated cyclic imines

Numerous chemical methods for imine reduction exist, and these typically include the application of reducing agents such as sodium cyanoborohydride, sodium triacetoxyborohydride or ammonia borane; hydrogenation with a metal catalyst [270,271,272] and hydrosilylation with Lewis acid or base catalyst [273]. While these methods can be very stereoselective on their own, they often require the use of chiral auxiliaries [274,264] or ligands [265,275] to achieve the asymmetric reduction. A study of Espelt *et al.*, [18] performed a simultaneous imine reduction and Cbz group deprotection in a range of polyhydroxylated imines with hydrogenation on Pd/C in the preparation of iminosugars. However, the achieved stereoselectivity varied among the products, and was dictated by the stereochemistry of the starting material.

The current study also employed Pd/C catalyst in a hydrogenation process to reduce four oxidised Cbz-protected amino alcohol derivatives (**213-215**, **216**), which led to

the formation of pure iminosugar products in high yields ranging from 87-93 % (**Figure 98**). The structural and stereochemical characterisation was determined by one- and two-dimensional NMR techniques. A selective reduction was achieved with substrate **214** and **216**, yielding single diastereoisomers, **1** and **232**, respectively. Iminosugar **1** known as DAB is a natural product, which has been isolated from a variety of plants [276–278] while the six-membered iminosugar **232** is a distereoisomer of DNJ, which was extracted form a bark of *Angylocalyx pynaertii* [279].

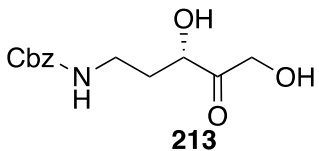
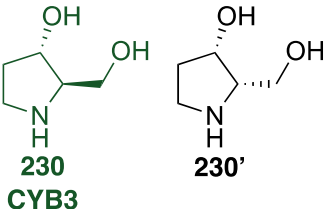
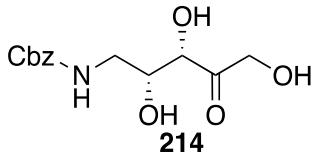
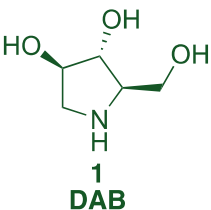
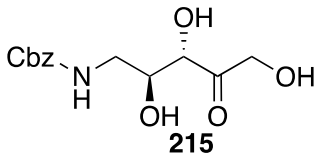
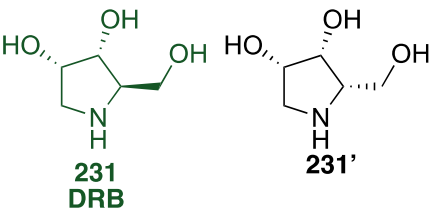
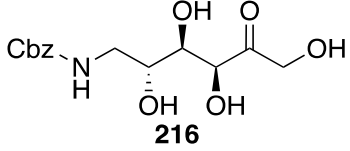
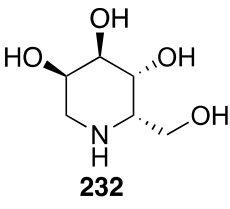
Linear substrate for deprotection and reduction	Iminosugar	Ratio	Reported inhibition
 <p>213</p>	 <p>230 CYB3</p> <p>230'</p>	1:1	<p>230- isomaltase [280].</p> <p>230'- no effect towards α-glucosidase, α-mannosidase and fucosidase [281].</p>
 <p>214</p>	 <p>1 DAB</p>	Single	<p>1- glycogen phosphorylase [282], isomaltase [283], sucrase [284]</p>
 <p>215</p>	 <p>231 DRB</p> <p>231'</p>	1:2	<p>231- α-mannosidase [285], intestinal sucrase [283], lactase [286]</p> <p>231'- rhamnosidase, α-glucosidase, fucosidase [287]</p>
 <p>216</p>	 <p>232</p>	Single	<p>232- α-D-fucosidase [288]</p>

Figure 98. Structures of isolated iminosugar products derived from the corresponding amino alcohol derivatives, and their reported inhibitory properties towards carbohydrate-processing enzymes. Natural products are coloured in green.

Poor selectivity was obtained with the chemical reduction of **213** and **215**, yielding a mixture of diastereoisomers, with an enantiomeric ratio ranging from 50-67 %. The resulting iminosugars included natural products- CYB3 (**230**), and DRB (**231**), which have been isolated from plants *Castanospermum australe* [289] and *Morus alba* [290], respectively. Structures of all the produced iminosugars and their inhibitory properties towards numerous glycosidases have been previously reported in literature (**Figure 98**). The relative configuration of all iminosugar products was confirmed by NOESY NMR analysis. For example, the mixture of diastereoisomers **230** and **230'** revealed an explicit coupling between H-3' and H-4' in the *cis*-stereoisomer **230'**, indicating an interaction across space between those protons, while no interaction was present between protons H-3 and H-4 in the *trans*-stereoisomer **230** (**Figure 99**).

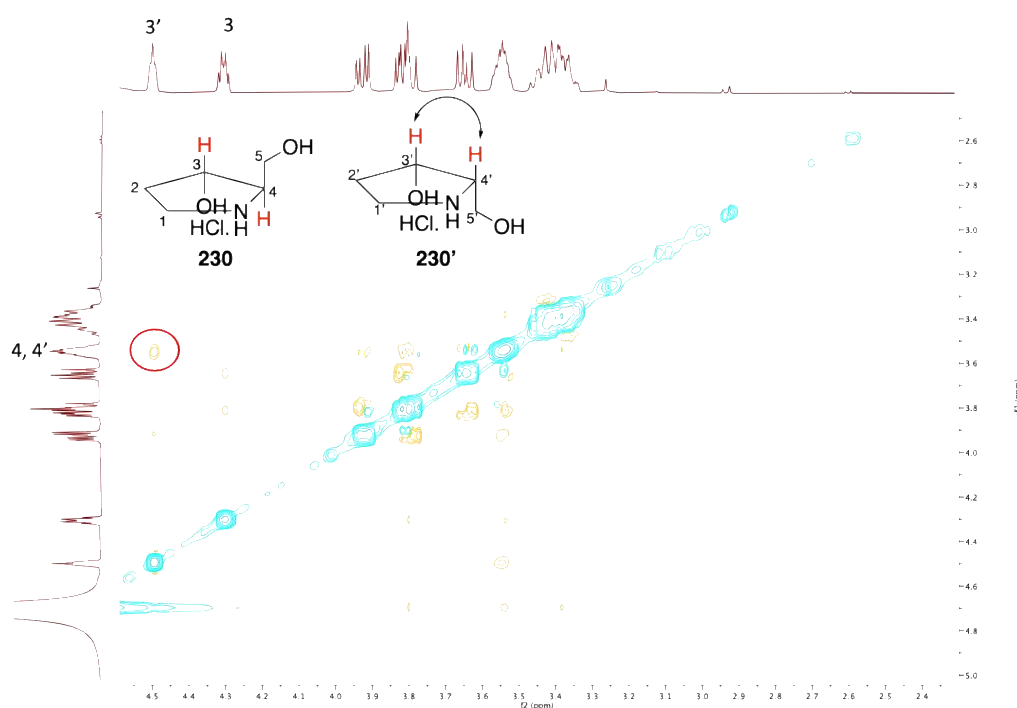


Figure 99. An example of the NOESY analysis for determination of stereochemistry of 9 and 9' iminosugar products mixture. A clear interaction between 3' and 4' indicates the **230'** anomer (circled in red), revealing *cis* configuration, while a *trans*-conformer **230** showed no coupling between the protons 3 and 9.

The study of the Espelt *et al.* [18] specifies the requirements of the configuration of polyhydroxylated pyrrolidine imines, which allows stereoselective hydrogenation with Pd/C. The work suggests that the hydrogenation occurs from the face opposite to the C-2 hydroxyl group, and the configuration on the C-2 carbon strictly controls

the stereoselectivity of the reaction, regardless of the other ring substituents (**Figure 100**). However, the study does not rationalise these postulations.

Nonetheless, the above claims are not consistent with the findings of this study, which indicates that the stereoselective reduction may be dictated by the relative configuration of the hydroxyl groups on both carbons C-2 and C-3, and that a chirality on the C-3 carbon is also assisting in achieving stereoselectivity (**Figure 101**). Specifically, the reduction of **213b**, which displays only one chiral centre on the C-2 carbon, led to a racemic mixture. On the other hand, the polyhydroxylated imines **215b** and **214b** are diastereoisomers differing by the relative configuration of the hydroxyl groups. The non-selective reduction was observed with a *cis*-isomer **215b**, while its *trans* equivalent **214b** resulted in the optically pure iminosugar product. Nevertheless, the factors controlling the stereoselectivity of the reduction of polyhydroxylated imines still remain unclear and require more examples and in-depth investigation.

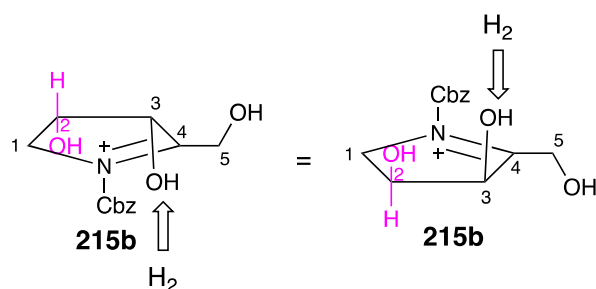


Figure 100. A representation of diastereoselectivity of the imine reduction with hydrogenation on Pd/C based on the study of Espelt *et al*, [18]. The study indicates that the hydrogenation of five-membered polyhydroxylated imines is occurring from the face opposite to the C-2 hydroxyl group and the stereoselectivity of the reaction is controlled by the stereochemistry on the C-2 carbon regardless the other ring substituents.

Imine substrate and rel. conf of hydroxyls	Diastereomeric ratio	Product and diastereomeric ratio
<p>213b</p>	1:1	<p>230 230'</p>
<p><i>cis</i></p> <p>215b</p>	1:2	<p>231 231'</p>
<p><i>trans</i></p> <p>214b</p>	single	<p>1</p>

Figure 101. A table comparing a relative configuration of the hydroxyl groups on carbon 2 and 3 in the polyhydroxylated pyrrolidine imines, which subjected to hydrogenation with Pd/C resulted in the iminosugar products displaying different diastereomeric ratio.

6.5 Biotransformations of iminosugars with monoamine oxidises

Engineered variants D5, D9 and D11 (a number indicates a number of mutations to a wild type) of monoamine oxidases from *Aspergillus niger* (MAO-N) have been successfully used for the deracemisation of numerous amine compounds; however, their activity has not been reported towards iminosugars. In this study, the potential of the MAO-N engineered enzymes was evaluated for the deracemisation of iminosugars. Thus, the variants D5, D9 and D11 were tested in the analytical transformations to selectively oxidise an amine of the (*S*)- enantiomers (**230'** and **231'**) in the optically impure mixture of **230**, **230'** and **231**, **231'**.

Engineered MAO-N D5, D9 and D11 variants were obtained from Professor Nicholas Turner of the University of Manchester. The plasmids were transformed into *E. coli* BL21(DE3) and protein expression was induced with autoinduction media (see section 3.11) according to the protocol described by Ghislieri *et al.*, [232]. Expressions performed at 37 °C resulted mostly in insoluble protein fractions, and

minor soluble protein was present in all MAO-*N* variants (**Figure 103**). A temperature decrease to 25 °C improved the production of a D5 soluble protein, D11 displayed a minor expression, while D9 was not present in either of the fractions. Expressions at 20 °C resulted only in the insoluble production of a D5 variant (not shown). The poor protein expression could be caused by the usage of the inappropriate expression strain of *E. coli* BL21 (DE3), while the optimum strain for MAO-*N* enzymes is reported to be *E. coli* C43(DE3) [227].

Besides, lowering temperature and changing host strain, as was already mentioned, a number of other strategies exist, which could have been used to promote soluble protein expression in the cytoplasm. These include modification of cultivation media, application of molecular chaperones, and a weaker promoter. The medium composition and the fermentation variables, such as pH, induction time, inducer concentration, and addition of cofactors (for example, magnesium or calcium), are essential for preventing protein aggregation. These conditions can be optimised to improve the yield and quality of soluble protein production [308-309]. The co-overexpression of molecular chaperones has been shown to prevent the formation of inclusion bodies [310-311]. These small proteins transiently bind their hydrophobic domains in partially folded polypeptides, shielding them from each other and the solvent [312]. Finally, the application of an expression vector containing a weak promoter, for example, *trc* instead of the T7 promoter, can significantly improve protein solubility [313].

Enzymatic activities of the expressed MAO-*N* variants were tested with a model substrate of (*S*)-methylbenzylamine ((*S*)-MBA), [232]. The amine oxidation in (*S*)-MBA results in the formation of the unstable primary imine, which hydrolyses to ammonia and acetophenone (**Figure 102**).

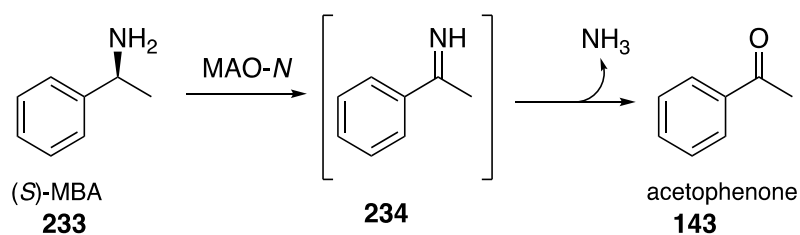


Figure 102. Amine oxidation of (*S*)-MBA (**233**) with a wild type of MAO-*N* results in the unstable imine intermediate (**234**), which decomposes to ammonia and acetophenone. Reaction conditions: (*S*)-MBA (10 mM), whole cells containing MAO-*N* variant (100 mg/mL wet weight), potassium phosphate buffer (1 M), 24 h, 37°C, 280 rpm.

Analytical biotransformations (1 mL) containing (*S*)-MBA and whole cells of MAO-*N* variants expressed at 25 °C and 37 °C were performed using slightly modified conditions reported by Ghislieri *et al.*, [239]. After 16 h of biotransformation, the conversions reached up to 40 %, based on the relative conversion analysed by GC (**Figure 104**). Enzymes expressed at 25 °C performed better to those expressed at 37 °C, which was likely due to the higher amount of the active enzyme in the soluble fraction. Finally, the MAO-*N* variants were tested for the amine oxidation of an (*S*)-enantiomer in the optically impure mixtures of **230**, **230'** and **231**, **231'**. The results were analysed using mass spectroscopy, which indicated no product formation in all tested biotransformations. Based on the performed experiments, which utilized only partly soluble enzymes, it is hard to conclude whether the MAO enzymes exhibit any activity towards iminosugars, and these should be repeated with the fully active and soluble MAO-*N* variants.

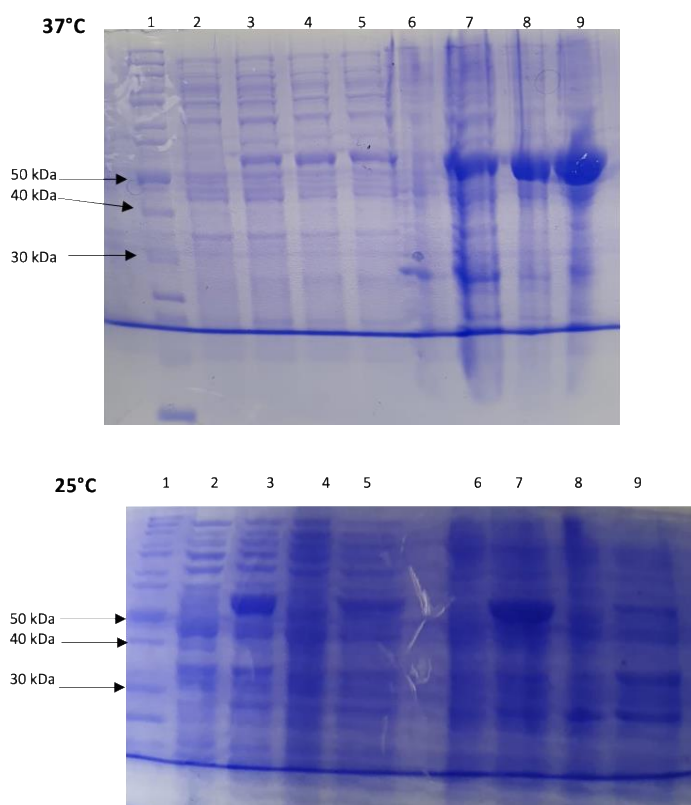


Figure 103. SDS-page comparing overexpression at 37 °C and 25 °C, of the MAO-*N* engineered variants namely D5, D9 and D11 and an empty vector pET21a from soluble fraction of clarified cell lysate and insoluble fraction of a plasma membrane of induced BL21 (DE3) cells with autoinduction media, after 24 h. Expression at 37 °C: **1:** PageRuler Unstained Broad Range Protein Ladder (ThermoFisher); **soluble fractions are 2:** pET21a negative control; **3:** D5; **4:** D9; **5:** D11; **insoluble fractions are 6:** pET21a negative control; **7:** D5, **8:** D9 and **9:** D11. Expression at 25 °C; **1:** PageRuler Unstained Broad Range Protein Ladder (ThermoFisher), **soluble fractions: 2:** pET-21a negative control; **3:** D5; **4:** D9; **5:** D11, **insoluble fractions are: 6:** pET21a negative control; **7:** D5; **8:** D9 and **9:** D11. The expressed MAO-variants were indicated 55 kDa in size.

MAO- <i>N</i> variant	Conversions [%]	
	25°C	37°C
D5	18	14
D9	n/a	13
D11	40	10

Figure 104. Relative conversion results from the analytical biotransformations of (*S*)-MBA (**233**) with MAO-*N* variants expressed at 25 °C and 37 °C.

6.6 Summary and conclusions

This chapter presented work attempting to selectively reduce polyhydroxylated imines with imine reductases to generate optically pure iminosugars. This reaction corresponds to the third biocatalytic step of the proposed cascade (**Figure 87**). In order to achieve this goal, five known IREDs, namely (*R*)-IRED-*Sr*, (*R*)-IRED-*St* and (*S*)-IRED-*Pe* (*S*)-*St*. sp GF3546 and (*S*)-Pyr2CR/Pip2CR were successfully expressed (**Figure 90 and Figure 91**) and tested with their benchmark reported substrates, including 2-methyl-pyrroline (**164**) and piperidine-2-carboxylic acid (**227**). The subsequent preparative-scale biotransformations revealed that the IREDs did not accept any of the desired polyhydroxylated imines (**213b** and **215b**) (**Figure 96 and Figure 97**).

In the second part of this chapter, four oxidised aminoalcohols (**213**, **214**, **215** and **216**) were chemically reduced by hydrogenation with Pd/C, affording pure iminosugar products with excellent yields (82-93 %). High selectivity was achieved with substrate **214** and **216**, resulting in single diastereoisomers, which included a natural product DAB (**1**) and a DNJ diastereoisomer (**232**). Poor selectivity of the metal catalyst was observed in the reduction of **213** and **215**, yielding mixtures of diastereoisomers with the enantiomeric ratio of 1:1 and 1:2, respectively. The mixtures of iminosugar distereoisomers also included the natural products CYB3 (**230**) and DRB (**231**).

Finally, three engineered variants of monoamine oxidases from *Aspergillus niger* were tested to accept an (*S*)-enantiomer in the optically impure mixtures of **230**, **230'** and **231**, **231'**. The generated imines would then be reduced *in situ* in the deracemisation process of the racemic iminosugar compounds. The expression of MAO-*N* variants, namely D5, D9 and D11 in the suboptimum strain of *E. coli* BL21(DE3) was troublesome at 20 °C, 25 °C and 37 °C, and resulted mostly in the insoluble protein production (**Figure 103**). Minor expressions were observed in the soluble fraction. Biotransformations with a model substrate of (*S*)-MBA resulted in low conversions ranging from 10-40 % (**Figure 104**). Finally, analytical biotransformations with resting cells having a minor soluble protein expression

revealed that the MAO-*N* variants did not accept any of the desired iminosugar substrates. To fully determine the MAO-*N* activity towards iminosugars requires active and soluble enzymes.

6.7 Experimental

General methods and materials

For general methods regarding NMR, mass spectrometry analysis and materials, see experimental section 4.4 in *Chapter 4*.

GC-FID analysis was performed on a Bruker Trace 1310 series GC equipped with an autosampler and a Chirasil Dex CB (25 m x 0.25 mm x 0.25 mm) column. The biotransformation products were separated on the column using the following methods:

Method	Substrate	Product	Substrate rt [min]	Product rt [min]
40 °C hold for 5 min, 10 °C min ⁻¹ to 90 °C, hold for 0.5 min, 0.5 °C min ⁻¹ to 150 °C hold for 0.2 min, 30 °C min ⁻¹ to 200 °C hold for 5 min	2-MPN 164	166 (R)	31.26	4.94
	2-MPN 164	165 (S)	5.80	5.30
40 °C hold for 2 min, 20 °C min ⁻¹ to 150, hold for 5 min, 20 °C min ⁻¹ to 225 °C hold for 8 min	(S)-MBA 233	143	7.35	12.18

Analytical scale biotransformations with IREDs (1 mL)

A solution of 2-MPN (5 mM), NADPH (2.5 mM), glucose (20 mM) in sodium phosphate buffer (50 mM, pH 7) was prepared. To this, a crude lysate of IRED (200 µL) and GDH (1 mg/mL) were added and reactions were incubated at 25 °C, 200 rpm for 16 h. After 24 h, the reactions were basified (pH 12), extracted with EtOAc (750 µL), derivatized with triethylamine (10 µL) and acetic anhydride (10 µL) and analysed by GC-FID.

Semi-preparative scale biotransformations with IREDs (5 mL)

A solution of oxidised Cbz-protected amino alcohols **213a** or **215b** (14 mM), dissolved in DMSO (150 μ L), NADPH (5 mM), glucose (40 mM) was prepared. To this a crude lysate of IRED (500 μ L) and GDH (1 mg/mL) were added. Sodium phosphate buffer (50 mM, pH 7) was added to a final volume of 5 mL and reactions were incubated at 25 °C, 200 rpm for 16 h. After 24 h the reactions were purified using silica gel column chromatography in acetone and DCM with a 3:7 ratio.

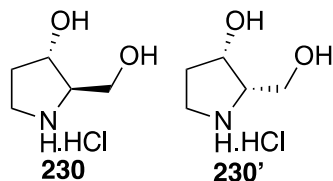
Analytical scale biotransformations with variants of MAO-N (1 mL)

Resting cells of a MAO-N variant, namely D5, D9 and D11 (100 mg/mL wet weight) were resuspended in 1 mL of potassium phosphate buffer (1 M) containing (*S*)-MBA (10 mM) or diastereoisomeric mixture of iminosugars **230**, **230'** or **231**, **231'** (5 mM). The reaction mixture was incubated at 37 °C and 280 rpm in a shaking incubator. After 24 h, the reactions were basified (pH 12), extracted with EtOAc (750 μ L), derivatized with triethylamine (10 μ L) and acetic anhydride (10 μ L) and analysed by GC-FID.

Cbz deprotection and reduction of oxidised aminoalcohols

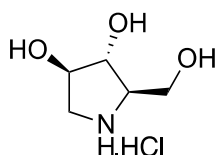
To the corresponding oxidised Cbz protected amino alcohol (0.17-0.40 mmol) dissolved in MeOH (15 mL) was added 10 % Pd/C (0.05 g/mmol). The reaction mixture was hydrogenated for 24 h at room temperature under one atmospheric pressure of hydrogen. The solution was filtered, acidified to pH 2 with aqueous HCl (37 %) and concentrated under reduced pressure to provide the corresponding iminosugar compound as the hydrochloride salt.

(2R,3S)-2-(hydroxymethyl)pyrrolidin-3-ol hydrochloride (230) and (2S,3S)-2-(hydroxymethyl)pyrrolidin-3-ol (230')



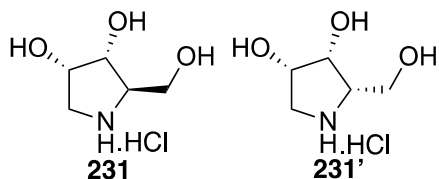
Prepared from **213**. Light brown oil (35 mg, 87 %) with an diastereoisomeric ratio of 1:1. ^1H NMR (500 MHz, D_2O) δ 4.62 – 4.56 (m, 1H), 4.43 – 4.35 (m, 1H), 4.02 (dd, J = 12.2, 4.8 Hz, 1H), 3.95 – 3.86 (m, 2H), 3.74 (dd, J = 12.4, 7.2 Hz, 1H), 3.68 – 3.60 (m, 2H), 3.57 – 3.42 (m, 4H), 2.34 – 2.22 (m, 2H), 2.16 – 2.01 (m, 2H). ^{13}C NMR (126 MHz, D_2O) δ 70.8, 69.7, 67.1, 65.2, 58.3, 57.5, 43.7, 43.1, 32.5, 31.8. LC-MS(EI) m/z : calculated $\text{C}_5\text{H}_{11}\text{NO}_2^+$ $[\text{M}+\text{Na}]^+$: 118.0863; found 118.0864. The result is consistent with the literature examples, and the slight variation is in the coupling, due to the application of a different NMR frequency and the presence of both diastereoisomers in the same sample. References: [291,292].

(2R,3R,4R)-2-(hydroxymethyl)pyrrolidine-3,4-diol hydrochloride (1)



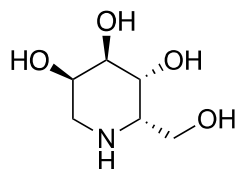
Prepared from **214**. Light yellow oil (59 mg, 89 %). ^1H NMR (500 MHz, D_2O) δ 4.40 – 4.32 (m, 1H), 4.15 – 4.09 (m, 1H), 3.98 (dd, J = 12.2, 4.5 Hz, 1H), 3.90 – 3.80 (m, 1H), 3.69 – 3.62 (m, 1H), 3.62 – 3.56 (m, 1H), 3.39 (dd, J = 12.6, 2.7 Hz, 1H). ^{13}C NMR (126 MHz, D_2O) δ 75.6, 74.2, 66.6, 58.9, 50.0. LC-MS(EI) m/z : calculated $\text{C}_5\text{H}_{11}\text{NO}_3^+$ $[\text{M}+\text{H}]^+$: 134.0812; found 134.0813. The result is consistent with the literature examples, with slight variations in coupling and ^1H NMR shift. References: [106,293].

2*R*,3*R*,4*S*)-2-(hydroxymethyl)pyrrolidine-3,4-diol hydrochloride (231) and (2*S*,3*R*,4*S*)-2-(hydroxymethyl)pyrrolidine-3,4-diol hydrochloride (231')



Prepared from **215**. Light brown oil (52 mg, 87 %). ^1H NMR (500 MHz, D_2O) δ 4.43 (td, $J = 7.3, 4.1$ Hz, 1H), 4.42 – 4.39 (m, 1H), 4.28 (t, $J = 4.2$ Hz, 1H), 4.22 (dd, $J = 8.6, 4.1$ Hz, 1H), 4.02 (d, $J = 4.8$ Hz, 1H), 3.93 – 3.87 (m, 1H), 3.84 (dd, $J = 12.7, 6.0$ Hz, 1H), 3.86 – 3.79 (m, 1H), 3.72 – 3.64 (m, 1H), 3.67 – 3.61 (m, 1H), 3.52 – 3.45 (m, 1H), 3.54 – 3.47 (m, 1H), 3.44 – 3.33 (m, 1H), 3.15 (dd, $J = 12.2, 7.3$ Hz, 1H). ^{13}C NMR (126 MHz, D_2O) δ 71.1, 70.0, 69.8, 69.37, 62.5, 61.7, 58.0, 57.6, 49.6, 47.0. LC-MS(EI) m/z : calculated $\text{C}_5\text{H}_{11}\text{NO}_3^+$ $[\text{M}+\text{H}]^+$: 134.0812; found 134.0809. The result is consistent with the literature examples, with slight variations in coupling and ^1H NMR shift, due to the application of a different NMR frequency and the presence of both diastereoisomers in the same sample. References: [294–296].

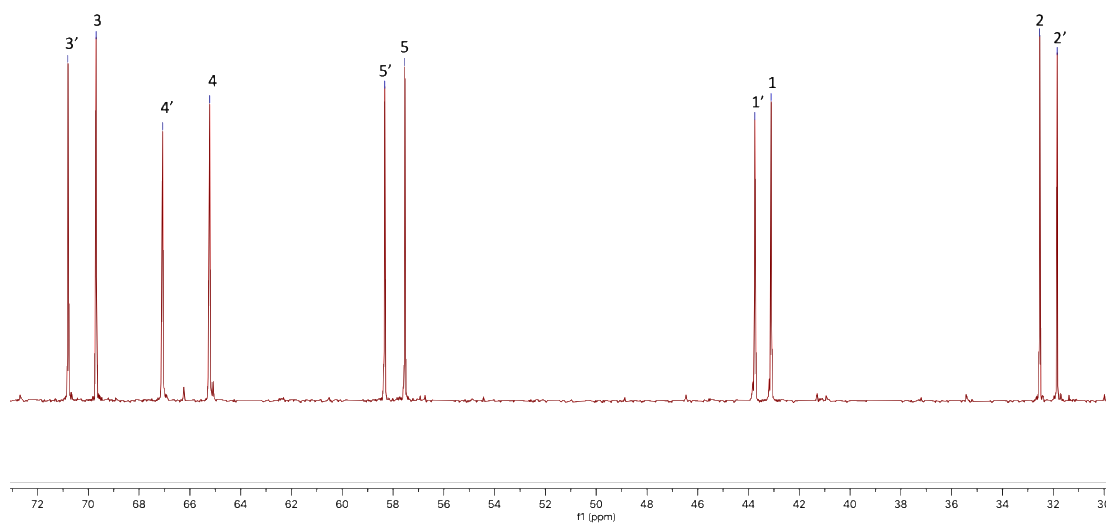
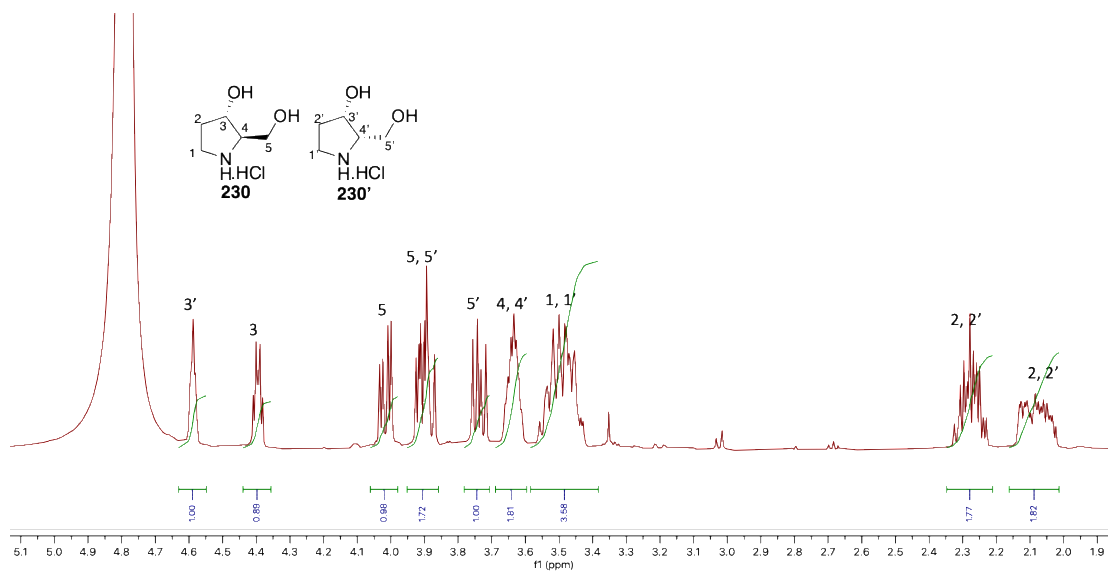
(2*S*,3*R*,4*S*,5*S*)-2-(hydroxymethyl)piperidine-3,4,5-triol hydrochloride (232)



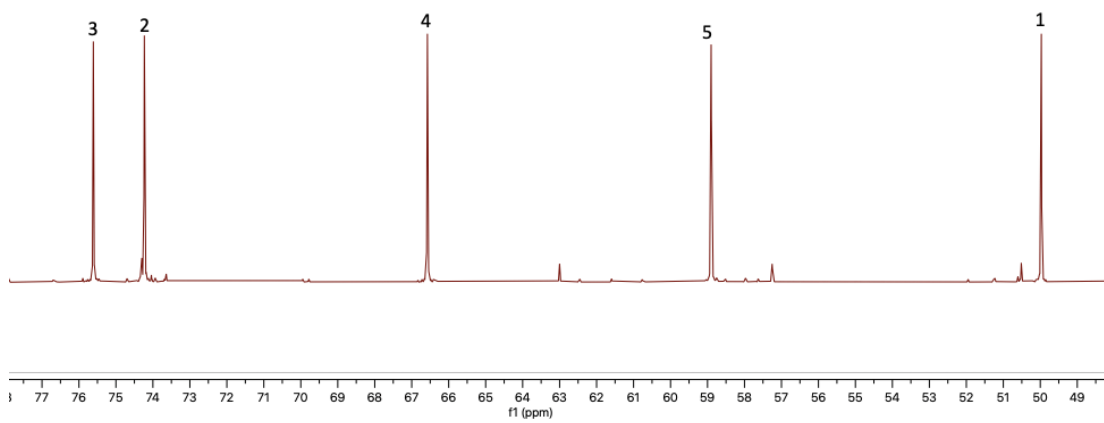
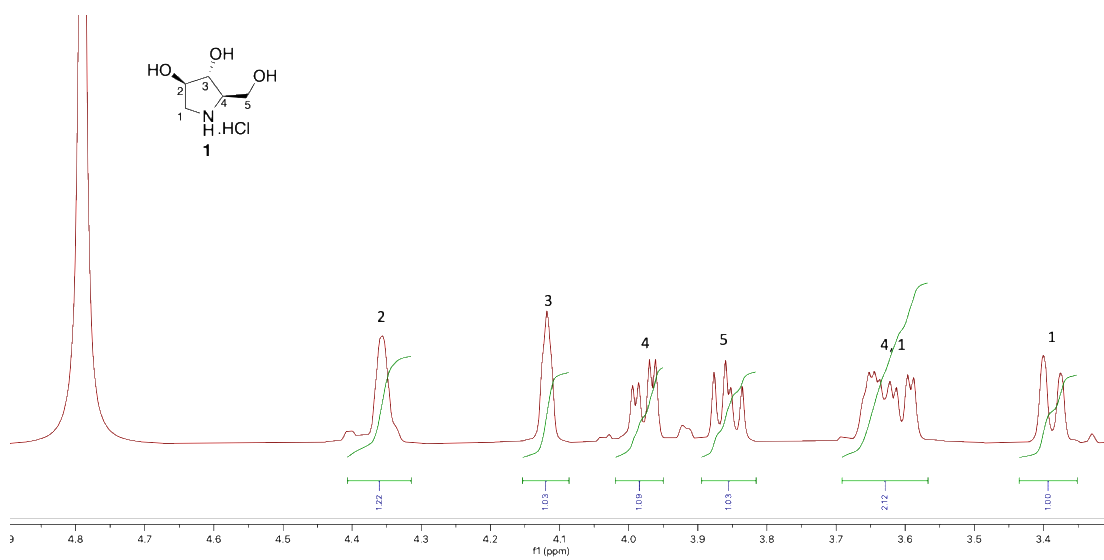
Prepared from **216**. Light yellow oil (74 mg, 93 %). ^1H NMR (400 MHz, D_2O) δ 4.30 – 4.23 (m, 1H), 4.01 (dd, $J = 12.6, 3.3$ Hz, 1H), 3.92 – 3.83 (m, 2H), 3.71 (dd, $J = 9.5, 3.0$ Hz, 1H), 3.44 (dd, $J = 13.6, 3.1$ Hz, 1H), 3.27 (dd, $J = 13.6, 1.5$ Hz, 1H), 3.22 – 3.14 (m, 1H). ^{13}C NMR (101 MHz, D_2O) δ 72.4, 65.8, 65.7, 60.3, 58.1, 47.5. LC-MS(EI) m/z : calculated $\text{C}_6\text{H}_{13}\text{NO}_4^+$ $[\text{M}+\text{H}]^+$: 164.0917; found 264.0928. The result is consistent with a literature example, with the slight variation is in the coupling, due to the application of a different NMR frequency. References: [297].

Assigned NMR spectra of the final products

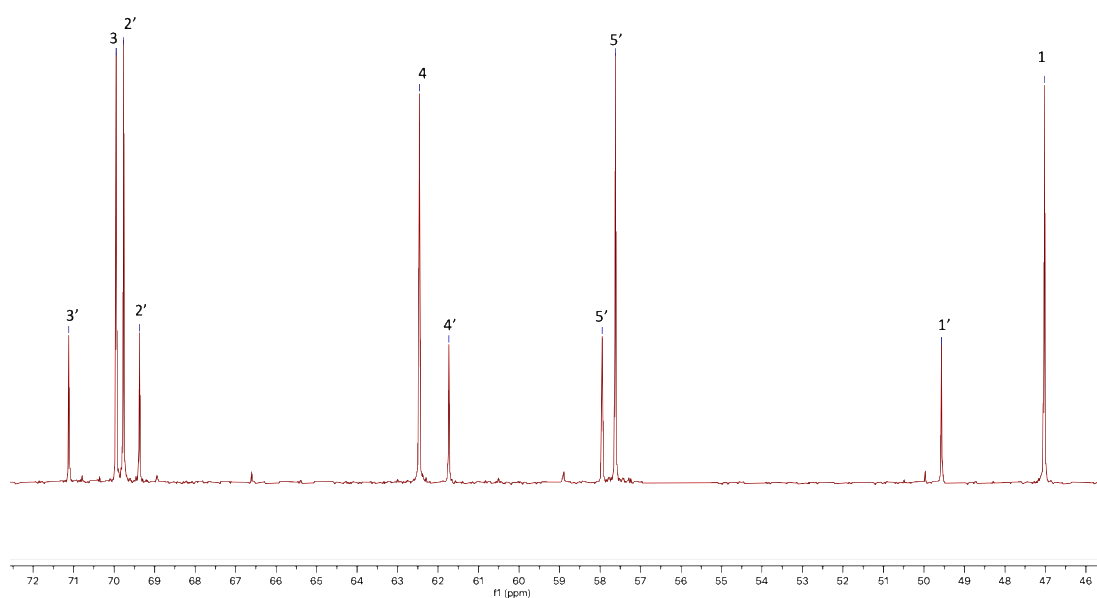
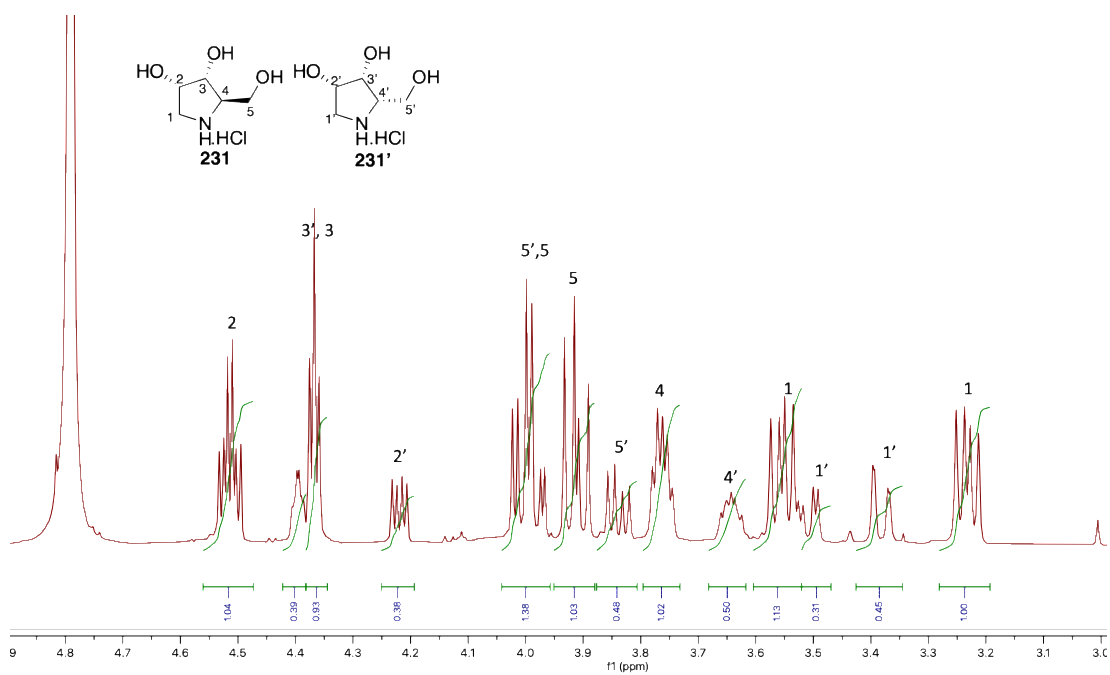
The structural and stereochemical characterisation was determined by one- and two-dimensional NMR techniques.



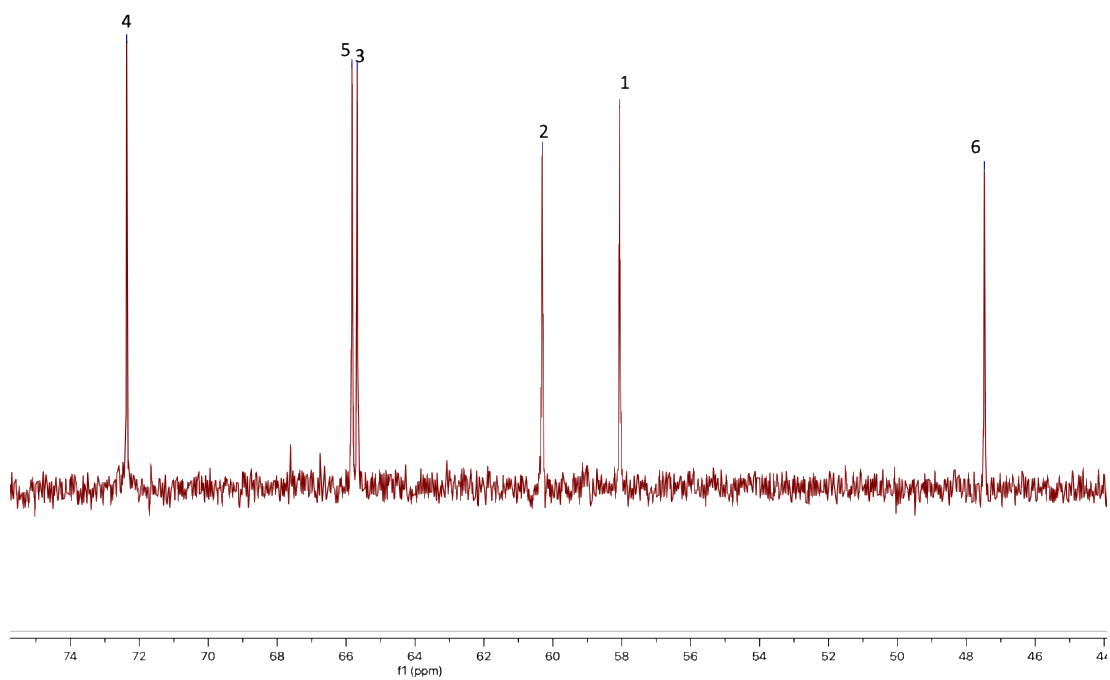
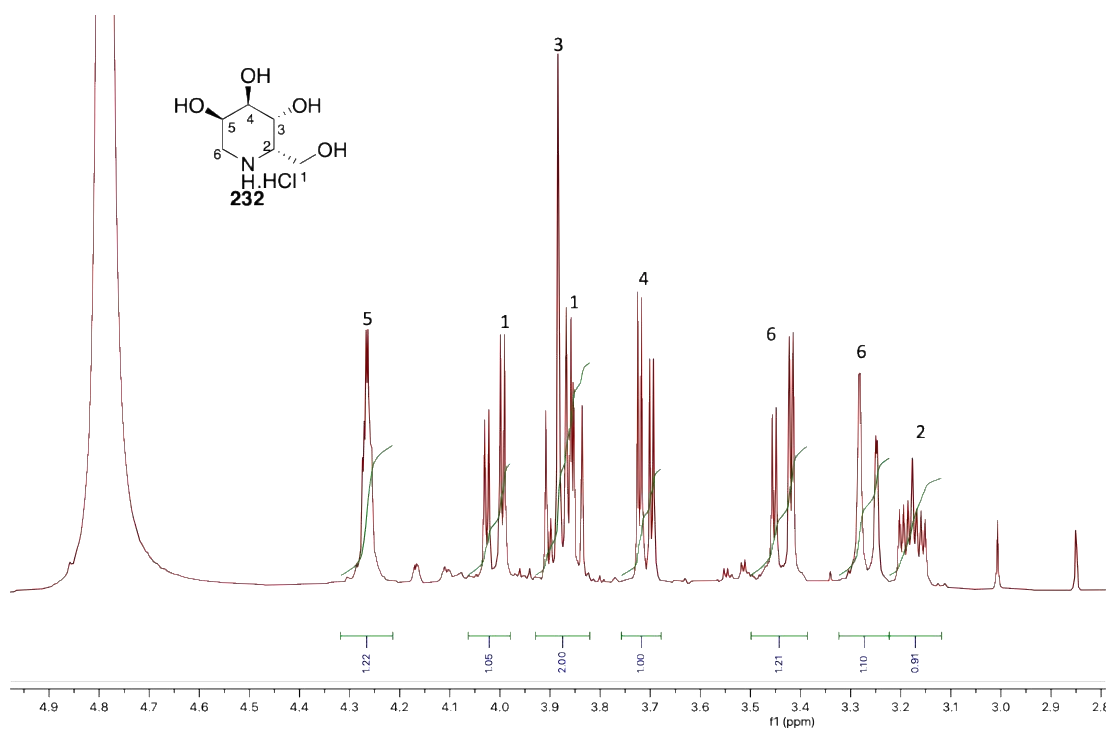
References: [291,292].



References: [106,293].



References: [294–296].

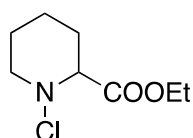


References: [297].

Synthesis of piperidine-2-carboxylate (**227**)

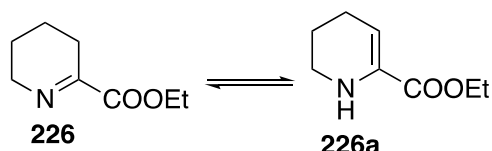
The imine of piperidine-2-carboxylic acid substrate was synthesised according to the protocol from [269] with slight modifications. The synthesis proceeded through three steps: synthesis of ethyl 1-chloropiperidine-2-carboxylate (**225**), followed by the synthesis of ethyl 3,4,5,6-tetrahydropyridine-2-carboxylate (**226**) and finally 3,4,5,6-tetrahydropyridine-2-carboxylic acid (piperidine-2-carboxylate) (**227**).

ethyl-1-chloropiperidine-2-carboxylate (**225**)



To a solution of *N*-chlorosuccinimide (2.04 g, 15.3 mmol) in dry diethyl ether (50 mL) at 0-5 °C under nitrogen atmosphere, avoiding exposure to light, was added ethyl pipercolinate (2.00 g, 12.7 mmol) and the reaction was stirred for 4 h, or until TLC analysis indicated total consumption of the starting material. Petroleum ether (60 mL) was added and the white solids were removed by filtration and washed with petroleum ether (20 mL) four times. The solvents were evaporated and the filtrate was concentrated using vacuum rotary evaporator. A colourless oil (2.49 g, 78 % yield). ¹H NMR (400 MHz, CDCl₃): δ 4.26 (2H, q, *J* = 8.0 Hz), 3.63-3.58 (1H, m), 3.50-3.46 (1H, m), 2.98-2.91 (1H, m), 1.99-1.93 (1H, m), 1.85-1.68 (4H, m), 1.4-1.34 (1H, m), 1.32-1.28 (3H, t, *J* = 8.0 Hz). The result is consistent with a literature example [269].

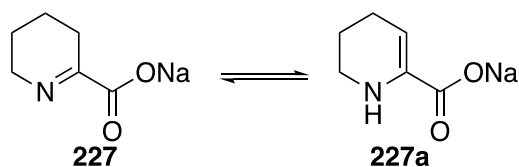
ethyl 3,4,5,6-tetrahydropyridine-2-carboxylate (**226** and **226a**)



To a solution/suspension of ethyl 1-chloropiperidine-2-carboxylate (**225**) (2.49 g, 12 mmol) in dry diethyl ether (60 mL), was added 4.5 mL of 33 % DABCO (1,4-diazabicyclo[2.2.2]octane) (1.45 g, 13 mmols) and stirred overnight under an atmosphere of nitrogen. The white solids were removed by filtration and the

solution was washed with cold 20% aqueous NaHCO₃. The organic phase was concentrated in vacuo to give a mixture of tautomers of ethyl 3,4,5,6-tetrahydropyridine-2-carboxylate and ethyl 1,4,5,6-tetrahydropyridine-2-carboxylate. Colourless oil (1.62 g, 86 % yield) ¹H NMR (400 MHz, CDCl₃), Enamine: 5.69-5.66 (1H, t, *J* = 4 Hz), 4.24-4.18 (2H, q, *J* = 8), 3.19-3.16 (2H, m), 2.21-2.17 (2, m), 1.83-1.77 (2H, m), 1.31-1.28 (3H, t, *J* = 8). The proportion of imine to enamine was 1:12 respectively. The result is consistent with a literature example [269].

sodium 3,4,5,6-tetrahydropyridine-2-carboxylate (piperidine-2-carboxylate) (227 and 227a)



A solution of NaOH (0.258 g, 6.4 mmol) in H₂O (10 mL) was added to ethyl 3,4,5,6-tetrahydropyridine-2-carboxylate (**226**) dissolved in 1,4-dioxane (10 mL). The reaction mixture was stirred overnight and then freeze-dried, which resulted in a pale yellow solid containing enamine **227a** and imine **227** in a 1:2 ratio respectively. Pale yellow solids (1.30 g, 90 % yield); ¹H NMR (400 MHz, D₂O), imine: 5.70-5.68 (1H, t, *J* = 4), 3.06-3.04 (2H, m), 2.17-2.13 (2H, m), 1.79-1.74 (2H, m); enamine: 3.55-3.52 (2H, m), 2.41-2.37 (2H, m), 1.71-1.66 (2H, m), 1.63-1.57 (2H, m). Ratio of enamine to imine was 1:2. The result is consistent with a literature example [269].

6.8 Disclosure

The multiples assignment and NMR analysis was done in a collaboration with Dr James Ryan. The synthesis and NMR assignments of piperidine-2-carboxylate (**227 and 227a**) was performed by Dr James Ryan.

7 Chemo-enzymatic route for the synthesis of iminosugars

Aims and objectives

The final chapter aims to integrate the previously established biocatalytic and chemical reactions in to a four-step chemo-enzymatic route for the preparation of iminosugars, starting from simple aldoses (**Figure 87**). The route exploits the ability of the transaminase to perform direct amination of monosaccharides to amino alcohols [154,155], which are intermediates of the proposed cascade. The second step involves Cbz-protection of the amine functionality, followed by the regioselective oxidation mediated by *G. oxydans*. The final step recruits a chemical metal catalyst Pd/C in a hydrogenation process to simultaneously remove Cbz group and reduce imine intermediates furnishing final iminosugar products. The need for chemical protection prevents the development of a one-pot cascade, as it applies conditions that are incompatible with enzymatic reactions. Thus, each intermediate requires isolation before being applied to the enzymatic or chemical step.

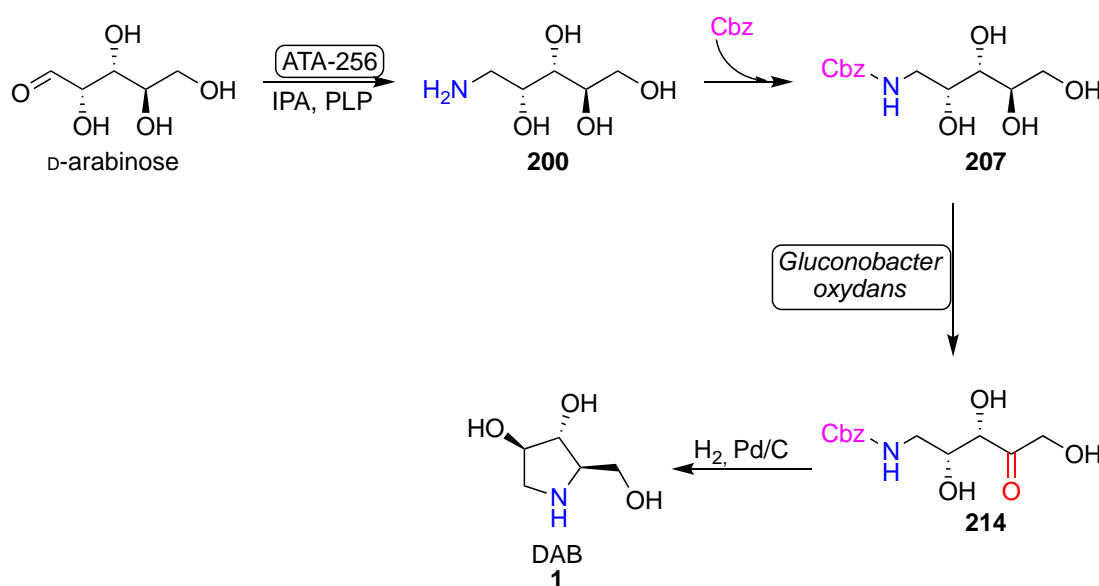


Figure 105. An example of the application of the fully assembled chemo-enzymatic route involving transamination with transaminase (TA), Cbz protection step, microbial oxidation with *G. oxydans*, and reduction with Pd/C and H₂ for the synthesis of iminosugars.

7.1 Step 1 and 2: transamination of aldoses and Cbz-protection

Studies of Cairns *et al.*, [154] and Subrizi *et al.*, [155] demonstrated novel transaminase activity towards sugars that exist predominantly in their cyclic form at equilibrium, but where there is the presence of a sufficient amount of the linear form of the sugar to act as a TA substrate. A number of pentoses and a few hexoses underwent transamination by wild and commercial TAs with a clear preference towards pentoses.

This study exploited the TAs ability to generate amino alcohols, which are intermediates in the synthesis of iminosugars in the proposed cascade. Three simple D-aldoses, which are precursors of the natural iminosugar products were selected, namely 2-deoxy-D-ribose, D-ribose and D-arabinose, and subjected to transamination with a Codexis commercial transaminase ATA-256 (**Figure 106**). Preparative-scale biotransformations were carried out at 50-200 mM of substrate concentration and 4 eq. of amine donor IPA.HCl. Conversions were analysed by ^1H NMR using a method reported by Cairns *et al.*, [154]. To accurately determine the percentage conversion, maleic acid was added to the NMR sample as an internal standard and the product protons H_B were monitored (**Figure 107**). Conversions were achieved up to 86 %, and the purification using ion-exchange resins DOWEX resulted in yields ranging from 34-65 %.

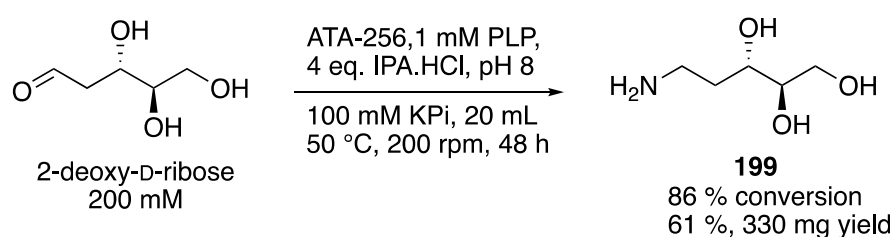


Figure 106. Transamination of 2-deoxy-D-ribose with an ATA-256 commercial transaminase.

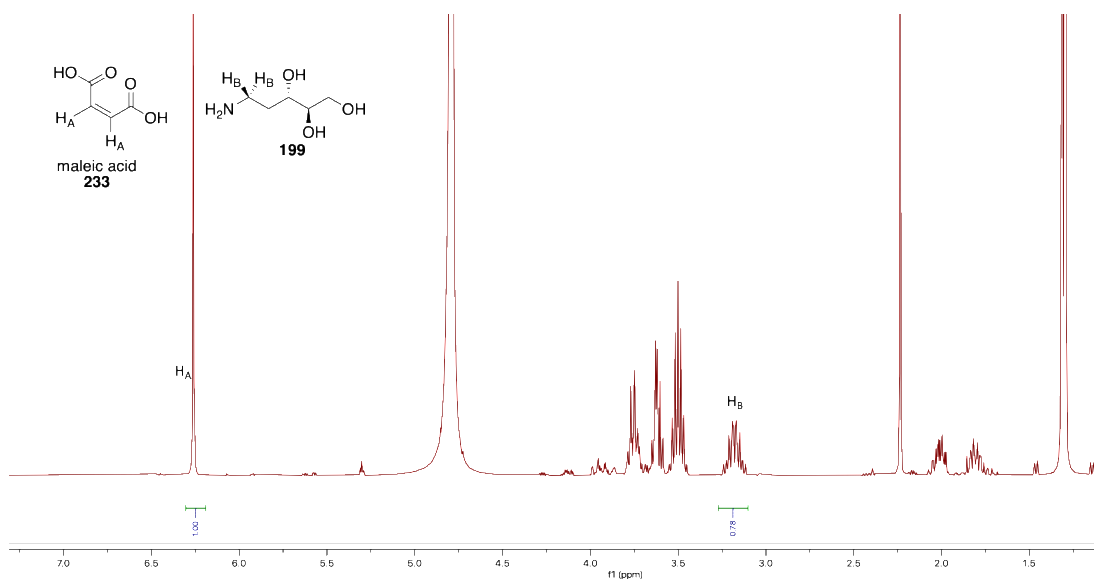


Figure 107. Representative NMR spectra of a biotransformation of 2-deoxy-D-ribose with ATA-256 after 48 h. The reaction is supplied with maleic acid standard and indicates the formation of the amino alcohol product (**199**). Conversion was calculated by comparing the integration of H_A derived from maleic acid to H_B of the amino alcohol. The final conversion rate was calculated by multiplying the H_B integration value by 1.1 (dilution factor).

In the following step, the isolated amino alcohols were protected with a Cbz group using Cbz-Cl or Cbz-OSu (see section 4.3). The products were purified using silica column chromatography or preparative reverse-phase HPLC in moderate to good yields ranging from 30-69 %.

Substrate	Amino alcohol	Conv. ATA-256 [%]	Yield [%]	Isolated [mg]	Cbz-amino alcohol	Yield [%]	Isolated [mg]
2-deoxy-D-ribose	199	86	61	330	206	69	453
D-arabinose	200	62	34	77	207	30	43
D-ribose	201	74	65	146	208	37	102

Figure 108. Results from the conversion and isolation yields derived from transamination reactions and Cbz protection. Biotransformation conditions: starting material (50 or 200 mM), IPA.HCl (4 eq.), PLP (1 mM), phosphate buffer (100 mM, pH 8), 50 °C, 200 rpm, 48 h. Chemical protection: Cbz-Cl (2 eq) or Cbz-OSu (1.5 eq), NaHCO₃ (2 eq) or Et₃N (2 eq), 1,4-dioxane-water (4:1), rm, 24 h.

7.2 Step 3 and 4: microbial oxidation with *G. oxydans* and chemical reduction

The Cbz-protected amino alcohols were microbiologically oxidised by *G. oxydans* DSM 2003 using the optimised conditions established in *Chapter 5*, resulting in excellent conversions (**Figure 109**). The biotransformation products were isolated, and subjected to the deprotection and reduction with 10 % Pd/C, which provided pure iminosugar products in high yields (**Figure 109**). The total yields were calculated revealing low to moderate yields over four steps ranging from 7-37 % (**Figure 110**). It's likely that these can be improved by optimising the purification steps.

Substrate	Conv. <i>G. ox.</i> [%]	Yield [%]	Isolated [mg]	Iminosugar	Yield [%]	Isolated [mg]	Total yield [%]
206	89	63	68	230, 230'	88	42	37
207	97	87	35	1	92	15	7
208	99	65	63	231, 231'	92	30	15

Figure 109. Conversions and isolated yields of the biocatalytic oxidation of **206**, **207** and **208**. Biotransformation conditions: starting material (20 or 25 mM), *G. oxydans* DSM 2003 (100 mg/mL wet weight), H₂O, pH 6.8, 16 h, 280 rpm, 35°C. Chemical reduction conditions: MeOH (5 mL), 10% Pd/C (0.05 g/mmol), H₂, atmospheric pressure, 24 h, r.t.

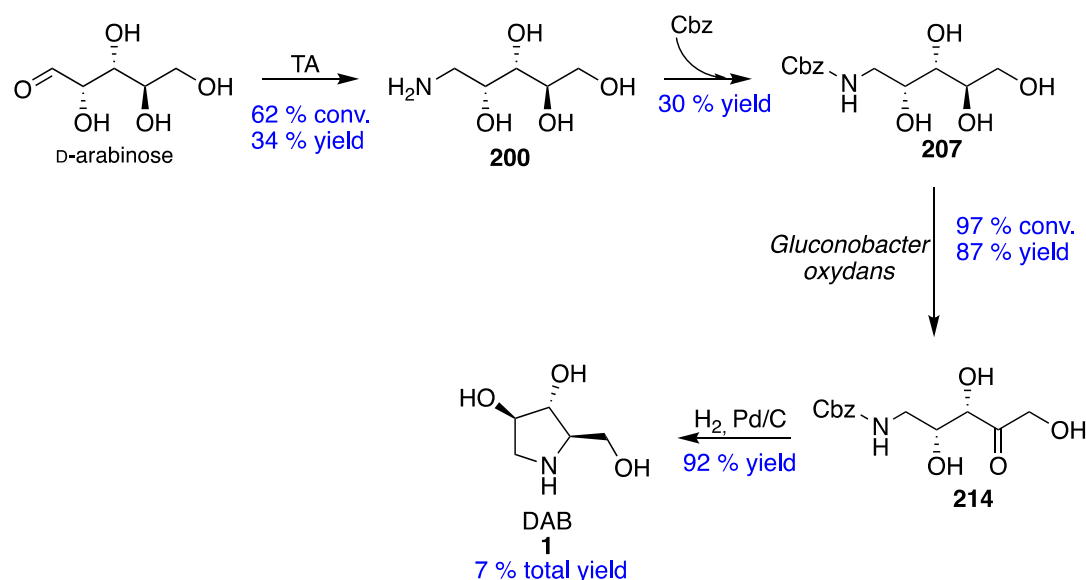


Figure 110. Chemo-enzymatic route involving ATA-256 transaminase and *G. oxydans* DSM 2003 resting cells leading to the synthesis of the DAB (**1**) natural iminosugar.

7.3 Summary and conclusions

This chapter allowed a successful integration of two biocatalytic and two chemical steps in the chemo-enzymatic route for the preparation of three iminosugar products, starting from readily available aldoses. These steps involved transamination carried out by a Codexis commercial transaminase variant of ATA-256, microbial oxidation mediated by *G. oxydans* DSM 2003 and chemical deprotection and reduction using catalytic hydrogenation with 10 % Pd/C. The requirement for the chemical protection of an amine group prevented the development of this process in one-pot.

Three simple D-aldoses were selected, namely 2-deoxy-D-ribose, D-ribose and D-arabinose and subjected to transamination on the preparative scale (50-200 mM). The biotransformation products were isolated up to 65%, followed by the chemical protection with Cbz. The microbial regioselective oxidation was performed using previously optimised conditions (on 20 or 25 mM scale) and resulted in nearly quantitative conversions and high isolation yields (63-87 %). The catalytic hydrogenation with Pd/C furnished the final iminosugar products (diastereomeric mixture of **230** and **230'**; **1** and diastereomeric mixture of **231** and **231'**) achieving 7-37 % of the total yield.

The introduction of just two biocatalytic steps significantly shortened the route in comparison to the traditional synthetic methods, which also exploited simple monosaccharides as starting materials for the same or similar targets [17,298–300]. The application of transaminase eliminated the need for reductive amination, which is usually performed with toxic hydride reagents such as sodium cyanoborohydride or transition metal catalysts. The application of *G. oxydans* granted the regioselectivity and eliminated the need for difficult and complicated multiple protection of hydroxyl groups. Furthermore, this microbial biocatalyst demonstrated high efficiency and robustness by quantitatively converting several Cbz-amino alcohols on relatively high scale considering its wild type origin. Both biocatalysts were applicable for the preparative scale transformations and

demonstrated the potential of this methodology for the scalable synthesis of iminosugars from simple monosaccharides.

7.4 Experimental

General methods and materials

For general methods regarding NMR, mass spectrometry analysis and materials, see experimental section 4.4 in *Chapter 4*. For conditions regarding Cbz-protection and biotransformation with *G. oxydans*, see experimental section 4.4 in *Chapter 4* and 6.7 in *Chapter 6*, respectively.

Preparative reverse-phase purification of 207

Preparative reverse-phase HPLC was performed using a Waters 1525 binary pump HPLC equipped with a dual wavelength UV detector set to 210 nm and 280 nm. Product **207** was purified on a Waters Sunfire 5 μm (C-18) preparative column with 5- μm particle size, 19 x 150 mm, operating at a flow rate of 6 mL min⁻¹ using a mobile phase of 0.1 % v/v trifluoroacetic acid in water (Solvent A) and 0.1 % v/v trifluoroacetic acid in acetonitrile (Solvent B) with 15-60 % gradient. The product eluted at 21 min (43 mg, 30 % yield).

Preparative-scale biotransformations of monosaccharides

To phosphate buffer (20 mL or 30 mL, 100 mM, pH 8) monosaccharide (200 mM or 50 mM) and IPA were added. The pH was adjusted to 8 and commercially available (*S*)-selective ATA-256 (2.5 mg/mL) was resuspended. The biotransformation was incubated at 50 °C, 200 rpm. After 48 h, the reaction mixture was concentrated under reduced pressure followed by the addition of hot methanol (20 mL). The mixture was filtrated and again reduced under reduced pressure. The crude residue was dissolved in water and loaded onto DOWEX 50WX8 ion exchange column and washed with water. The product was eluted with 30 % aq. NH₃ (100 mL) and concentrated under reduced pressure to provide pure amino alcohol product.

General procedure and NMR experiment for monitoring conversions of amino alcohols

After 48 h, a 500 μL of reaction mixture was added to 50 μL of maleic acid (110 mM in D_2O) and monitored by NMR, using a method from Cairns *et al.*, [154]. Water suppressed ^1H NMR spectra were recorded using a zgcppr pulse sequence on a Bruker AV(III)500 instrument fitted with a 5mm autotunable dual $^1\text{H}/^{13}\text{C}$ (DCH) cryoprobe. Data was collected with 64k points with a sweep width of 20 ppm. Experiments were performed with 64 scans using a relaxation delay of 10 seconds and an acquisition time of 3.2 seconds, at 298 K. Manual phase correction around the maleic acid peak was applied, when required. Automated baseline correction, Bernstein polynomial fit "order 3". The integrated peak area of the amino alcohol was compared to the maleic acid peak area, and the product concentration was determined by multiplying the integration value by 1.1 (a dilution factor).

7.5 Disclosure

Preparative biotransformations of monosaccharides with ATA-256 and Cbz-protection was performed by Dr James Ryan.

7.6 Final conclusions and future work

Iminosugars are the most known class of carbohydrate mimetics, which are very attractive drug candidates due to their unique biological and chemical properties. These small organic molecules are reversible inhibitors of numerous carbohydrate processing enzymes associated with various diseases, which were treated with iminosugar based therapeutics [16]. However, the inefficient synthetic routes that are commonly applied for their preparations constitute one of the primary obstacles affecting the commercialisation and development of iminosugar based therapeutics. Typically, those methods involve extensive group manipulations, which lead to long synthetic sequences and low overall yields [2].

This project aimed at simplifying the synthesis of iminosugars by the development of a one-pot enzymatic biocascade, which recruits three selective enzymes, namely transaminase, alcohol oxidase/alcohol dehydrogenase and imine reductase, starting

from readily available aldoses. In particular, this thesis investigates on the biocatalytic oxidation and reduction and describes the finding and contributions made towards the development of the biocascade.

Chapter 5: Biocatalytic oxidations of amino alcohols

This chapter explored the application of *G. oxydans* for the regioselective oxidations of amino alcohols. The microbial biocatalyst accepted five Cbz-protected amino alcohols and did not tolerate their unprotected equivalents. It allowed the generation of the desired intermediates suitable for the synthesis of pyrrolidine and piperidine iminosugars. Nevertheless, the requirement for the amine protection impacted the initial cascade design, which was then modified by the addition of two chemical steps: protection and deprotection. *G. oxydans* proved to be very efficient by performing nearly quantitative conversion of the substrates at high concentrations and was readily applicable on preparative-scale transformations. Moreover, the biocatalyst displayed an excellent activity in a range of temperatures and was not affected by the changing pH.

The inability of *G. oxydans* to accept non-protected amino alcohol substrates is the major bottleneck of the current system, having involved two chemical steps, which prevents the development of the biocascade. However, the requirement for the protected amine functionality is also common among other enzymes acting on amino alcohols, including galactose oxidase and aldolase, but the rationality of this phenomenon is unknown. Other known enzymes that mediate regioselective oxidations of carbohydrates are predominantly limited to the polyol substrates and therefore were not applicable in the proposed cascade.

One way to overcome the problem of chemical protection is reversing the order of the biocatalytic steps; initiating the cascade with the oxidation followed by transamination and reduction. However, this is not a straightforward task, as five-membered aldoses subjected to the transformation with *G. oxydans* lead to the oxidation of two functionalities – the desired C-4 hydroxyl and the aldehyde group [260,261]. Study of Adachi *et al.*, suggests that two different enzymes are responsible for these transformations [260]. Therefore, this strategy to be

successful requires the identification of the gene encoding for the aldehyde oxidase and then reducing its expression by gene silencing or knockdown techniques. Another approach could be genome mining aiming at the discovery of novel enzymes, which are capable of the regioselective oxidation of the C-4 hydroxyl group in aldoses. Ideally, the enzymes accept monosaccharides with D- and L-configuration. These could be explored, in organisms living in sugar-rich environments, for example, *Gluconobacter* or *Saccharomyces* [301,302].

Chapter 6: Reduction of oxidised amino alcohols

The previous study established the formation of the desired intermediates, which cyclise *via* amination carbon forming polyhydroxylated imines. These imines were screened against five-known imine reductases, which did not accept any of the tested substrates. Chemical reduction and deprotection involving catalytic hydrogenation with Pd/C led to the formation of the final iminosugar products. However, the reduction with the metal catalyst was selective only with two substrates derived from D-arabinose and D-mannose. Mixtures of iminosugar diastereoisomers were produced from the intermediates derived from 2-deoxy-D-ribose and D-ribose. The racemic mixtures were attempted to be deracemised with engineered variants of monoamine oxidases from *Aspergillus niger*; however, either of the enzymes accepted these highly polar substrates.

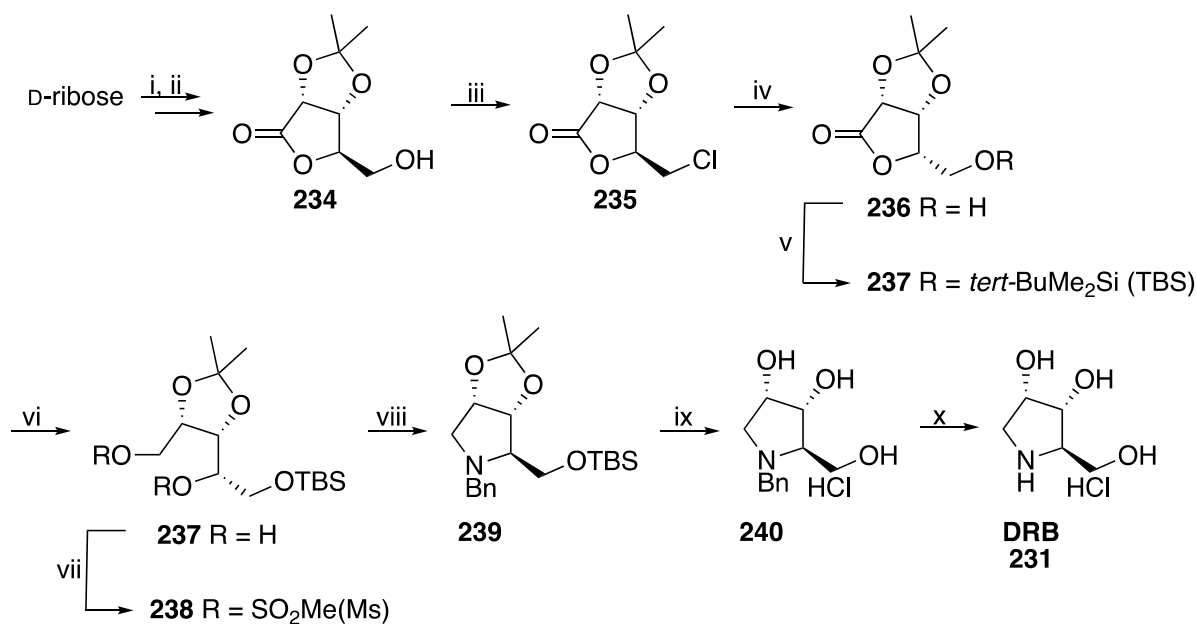
Imine reductases seem like a perfect tool to selectively reduce polyhydroxylated imines and access enantiopure iminosugars. Unfortunately, known IREDs are limited in their substrate scope, largely only accepting stable cyclic imines that feature non-polar character. Structural characterisation of IREDs revealed a presence of hydrophobic active site [214,221], which may not be suitable for binding polar substrates. On the other hand, this project required IREDs accepting highly polar imines. Therefore, future studies should focus on the discovery and engineering of IREDs, displaying a completely new substrate preference. These enzymes could also be possibly sought in organisms inhabiting sugar-rich environments.

Chapter 7: Chemo-enzymatic route for the synthesis of iminosugars

The final chapter integrated the established biocatalytic and chemical steps in the chemo-enzymatic route allowing the preparation of three iminosugar products starting from readily available aldoses. The biocatalytic steps employed a commercial transaminase ATA-256 and *G. oxydans*, while chemical steps involved Cbz-protection and reduction with Pd/C.

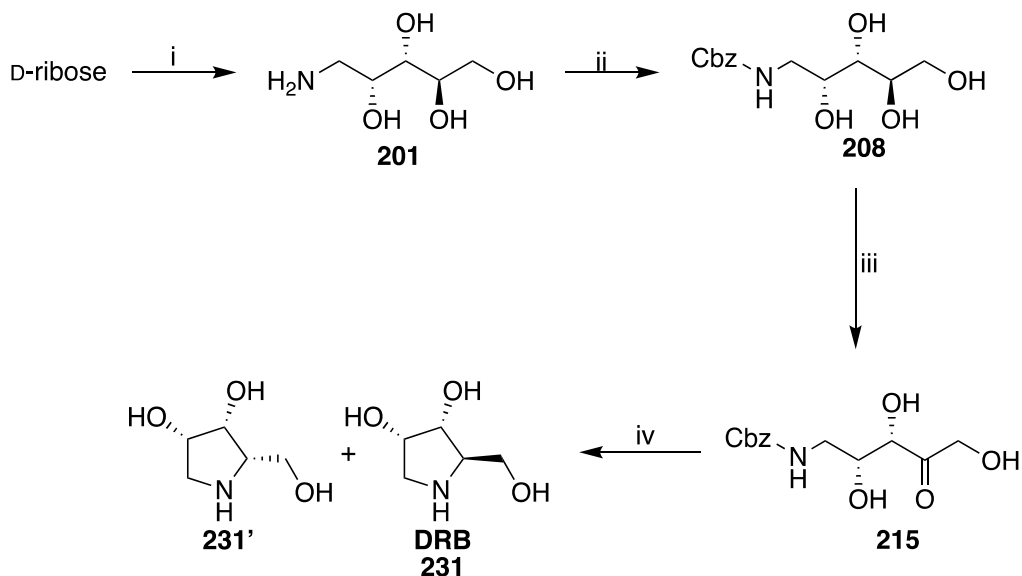
Despite the current state of the project, which does not allow yet for the one-pot cascade application, the implementation of just two biocatalytic steps significantly shortened the route, when comparing to the synthetic sequences used for the same or similar targets from carbohydrate based-starting materials [298–300], (**Figure 111**). The transamination step with ATA-256 eliminated the need to use a toxic reductive amination reagent such as sodium borohydride. The application of *G. oxydans* secured the regioselective oxidation of the desired hydroxyl group. On the other hand, synthetic methods used for the oxidation of polyol substrates usually proceed through complicated chemical protection of multiple hydroxyl groups, such as acetone, TBS, DMP or TrCl, resulting in long and inefficient routes. A direct comparison of the newly developed chemo-enzymatic route with the established synthetic route for the same target and using the same starting material demonstrates that the newly developed method requires more than 50 % fewer steps, and is more environmentally friendly (**Figure 111**).

Synthesis of DRB iminosugar with synthetic method



(i) Br₂, H₂O, K₂CO₃ (ii) acetone, H₂SO₄ (iii) (COCl)₂, DMF, CH₂Cl₂, (iv) KOH, H₂O, then, 3 M HCl, (v) TBSCl, imidazole, CH₂Cl₂ (vi) NaBH₄, MeOH, (vii) MsCl, pyridine, (viii) PhCH₂NH₂ (BnNH₂), toluene, (ix) 1 M HCl, (x) H₂, 10% Pd/C, H₂O

Synthesis of DRB iminosugar with chemo-enzymatic method



(i) ATA-256, 1 mM PLP, 4 eq. IPA.HCl, pH 8 (ii) CbzCl, NaHCO₃, 1,4-dioxane, H₂O (iii) 100 mg/mL of *G. oxydans*, 35 °C, pH 6.8, H₂O (iv) H₂, 10% Pd, MeOH

Figure 111 A comparison of the established synthetic method to the newly developed chemo-enzymatic route for the production of DRB iminosugar starting from D-ribose.

8 Appendix

PIPS Reflective Statement Template

Note to examiners:

This statement is included as an appendix to the thesis in order that the thesis accurately captures the PhD training experienced by the candidate as a BBSRC Doctoral Training Partnership student.

The Professional Internship for PhD Students is a compulsory 3-month placement which must be undertaken by DTP students. It is usually centred on a specific project and must not be related to the PhD project. This reflective statement is designed to capture the skills development which has taken place during the student's placement and the impact on their career plans it has had.

My three-month placement, I spent in a German biotech start-up – TissUse in Berlin. The company develops unique Multi-Organ-Chip (MOC) platforms that mimic the microarchitecture and functions of living human organs, for example, the lung, intestine, kidney, heart, skin, bone marrow and blood-brain barrier. These microdevices offer a potential to replace often wildly inaccurate traditional animal testing in preclinical trials. Moreover, MOC can be applied in drug discovery, vaccine development, stem cells engineering and studying diseases [303].

I was a part of a Business Development team working on several projects in parallel. However, my main objective was to develop a quantitative-qualitative mathematical model to estimate the animal model market size. I became familiar with animal testing procedures in clinical trials, as well as the process of clinical trials. Moreover, I was responsible for writing press releases about recent achievements of the company, which were published in the German newspaper (Firmenpresse). Also, I had the opportunity to communicate the importance of MOC technology to the EU member of parliament. I performed extensive competitive analysis, and I researched new areas of partnerships between TissUse and biotech and tech companies. Last but not least, I participated in the weekly company meetings, which aimed at updating the results of the ongoing projects and discussing future work and upcoming changes.

The placement in TissUse allowed me to explore the business side of science in the biotech company. Importantly, I have learnt about the importance of collaboration between R&D and business development. The business development team deals

with the customers, which includes gathering information about customer needs, their satisfaction from the services, and determining areas of further improvements, while the R&D team works on the technology development and execution. I gained knowledge about the scientific and commercial side of organ-on-a-chip technology, and its massive potential in the application in pharmaceutical industry, diagnostics and clinical trials. Moreover, a fast-paced nature of the start-up required me to learn quickly and be creative when completing tasks.

Without a doubt, the placement in TissUse has changed my view on the possible career paths after graduating from a PhD programme in Biotechnology. I discovered huge potential and need for scientists in the business sector. I have learnt that many skills that I have gained as a researcher are readily transferable into the business, for example, analytical skills, (science) communication, presentation and problem-solving skills. Also, the ability to understand the scientific aspect of the technology makes it much easier to adapt and complete the analytical business tasks. Currently, I am in the process of applying for the management consulting and science consulting positions.

Overall, the PIP placement in TissUse has been incredibly valuable, exposing me to entirely new ways that scientific skills can be applied and opening my eyes to new opportunities for career development.

Bibliography

1. Watson AA, Fleet GWJ, Asano N, Molyneux RJ, Nash RJ: **Polyhydroxylated alkaloids—natural occurrence and therapeutic applications.** *Phytochemistry* 2001, **56**:265–295.
2. Horne G: **Iminosugars: therapeutic applications and synthetic considerations.** In *Carbohydrates as drugs*. Edited by Seeberger PH, Rademacher C. Springer International Publishing; 2014:23–51.
3. Wong CH, Dumas DP, Ichikawa Y, Koseki K, Danishefsky SJ, Weston BW, Lowe JB: **Specificity, inhibition, and synthetic utility of a recombinant human. α -1, 3-fucosyltransferase.** *J Am Chem Soc* 1992, **114**:7321–7322.
4. Compain P, Martin OR: **Design, synthesis and biological evaluation of iminosugar-based glycosyltransferase inhibitors.** *Curr Top Med Chem* 2003, **3**:541–560.
5. Heightman TD, Vasella A, Tsitsanou KE, Zographos SE, Skamnaki VT, Oikonomakos NG: **Cooperative Interactions of the Catalytic Nucleophile and the Catalytic Acid in the Inhibition of β -Glycosidases. Calculations and their validation by comparative kinetic and structural studies of the inhibition of glycogen phosphorylase b.** *Helv Chim Acta* 1998, **81**:853–864.
6. Bols M, Hazell RG, Thomsen IB: **1-Azafagomine: A Hydroxyhexahydropyridazine That Potently Inhibits Enzymatic Glycoside Cleavage.** *Chem Eur J* 1997, **3**:940–947.
7. Somsak L, Nagy V, Hadady Z, Docsa T, Gergely P: **Glucose analog inhibitors of glycogen phosphorylases as potential antidiabetic agents: recent developments.** *Curr Pharm Des* 2003, **9**:1177–1189.
8. Horenstein BA, Zabinski RF, Schramm VL: **A new class of C-nucleoside analogues. 1-(S)-aryl-1, 4-dideoxy-1, 4-imino-D-ribitols, transition state analogue inhibitors of nucleoside hydrolase.** *Tetrahedron Lett* 1993, **34**:7213–7216.

9. Schramm VL, Tyler PC: **Imino-sugar-based nucleosides**. *Curr Top Med Chem* 2003, **3**:525–540.
10. Lee RE, Smith MD, Nash RJ, Griffiths RC, McNeil M, Grewal RK, Yan W, Besra GS, Brennan PJ, Fleet GWJ: **Inhibition of UDP-Gal mutase and mycobacterial galactan biosynthesis by pyrrolidine analogues of galactofuranose**. *Tetrahedron Lett* 1997, **38**:6733–6736.
11. Lee RE, Smith MD, Pickering L, Fleet GWJ: **An approach to combinatorial library generation of galactofuranose mimics as potential inhibitors of mycobacterial cell wall biosynthesis: Synthesis of a peptidomimetic of uridine 5'-diphosphogalactofuranose (UDP-Galf)**. *Tetrahedron Lett* 1999, **40**:8689–8692.
12. Moriyama H, Tsukida T, Inoue Y, Yokota K, Yoshino K, Kondo H, Miura N, Nishimura S-I: **Azasugar-based MMP/ADAM inhibitors as antipsoriatic agents**. *J Med Chem* 2004, **47**:1930–1938.
13. Butters TD: **Gaucher disease**. *Curr Opin Chem Biol* 2007, **11**:412–418.
14. Kohler L, Puertollano R, Raben N: **Pompe disease: from basic science to therapy**. *Neurotherapeutics* 2018, **15**:928–942.
15. Zarate YA, Hopkin RJ: **Fabry's disease**. *Lancet* 2008, **372**:1427–1435.
16. Sorbera, L.A.; Castaner, J; Bayes M: **Miglustat**. *Drugs Futur* 2003, **28**:229.
17. Cipolla L, La Ferla B, Nicotra F: **General methods for iminosugar synthesis**. *Curr Top Med Chem* 2003, **3**:485–511.
18. Espelt L, Parella T, Bujons J, Solans C, Joglar J, Delgado A, Clapés P: **Stereoselective Aldol Additions Catalyzed by Dihydroxyacetone Phosphate-Dependent Aldolases in Emulsion Systems: Preparation and Structural Characterization of Linear and Cyclic Iminopolyols from Aminoaldehydes**. *Chem - A Eur J* 2003, **9**:4887–4899.
19. Schedel M: **Regioselective oxidation of aminosorbitol with Gluconobacter oxydans, key reaction in the industrial 1-deoxynojirimycin synthesis**.

Biotechnology 2000, **8**:295–308.

20. Compain P, Martin OR: *Iminosugars: From synthesis to therapeutic applications*. John Wiley & Sons; 2007.
21. Inouye S, Tsuruoka T, Niida T: **The structure of nojirimycin, a piperidinose sugar antibiotic**. *J Antibiot (Tokyo)* 1966, **19**:288–292.
22. Schmidt DD: **Glucosidase-inhibitoren aus Bazillen**. *Naturwissenschaften* 1979, **66**:584–585.
23. Paulsen H: **Carbohydrates containing nitrogen or sulfur in the “hemiacetal” ring**. *Angew Chemie Int Ed English* 1966, **5**:495–510.
24. Yagi M: **The structure of moranoline, a piperidine alkaloid from Morus species**. *Nippon Nogei Kagaku Kaishi* 1976, **50**:571–572.
25. Nash RJ, Bell EA, Williams JM: **2-Hydroxymethyl-3, 4-dihydropyrrolidine in fruits of *Angylocalyx boutiqueanus***. *Phytochemistry* 1985,
26. Welter A, Jadot J, Dardenne G, Marlier M, Casimir J: **2, 5-Dihydroxymethyl 3, 4-dihydropyrrolidine dans les feuilles de *Derris elliptica***. *Phytochemistry* 1976, **15**:747–749.
27. Colegate SM, Dorling PR, Huxtable CR: **A spectroscopic investigation of swainsonine: an α -mannosidase inhibitor isolated from *Swainsona canescens***. *Aust J Chem* 1979, **32**:2257–2264.
28. Hohenschutz LD, Bell EA, Jewess PJ, Leworthy DP, Pryce RJ, Arnold E, Clardy J: **Castanospermine, a 1, 6, 7, 8-tetrahydroxyoctahydroindolizine alkaloid, from seeds of *Castanospermum australe***. *Phytochemistry* 1981, **20**:811–814.
29. Nash RJ, Fellows LE, Dring J V, Fleet GWJ, Derome AE, Hamor TA, Scofield AM, Watkin DJ: **Isolation from *alexia leiopetala* and x-ray crystal structure of alexine, (1r, 2r, 3r, 7s, 8s)-3-hydroxymethyl-1, 2, 7-trihydropyrrolizidine [(2r, 3r, 4r, 5s, 6s)-2-hydroxymethyl-1-azabicyclo [3.3. 0] octan-3, 4, 6-triol], a unique pyrrolizidine alkaloid**. *Tetrahedron Lett* 1988, **29**:2487–2490.
30. Molyneux RJ, Benson M, Wong RY, Tropea JE, Elbein AD: **Australine, a novel**

- pyrrolizidine alkaloid glucosidase inhibitor from *Castanospermum australe*.**
J Nat Prod 1988, **51**:1198–1206.
31. Haschek WM, Rousseaux CG, Wallig MA, Bolon B, Ochoa R: *Haschek and Rousseaux's handbook of toxicologic pathology*. Academic Press; 2013.
 32. Nash RJ, Rothschild M, Porter EA, Watson AA, Waigh RD, Waterman PG: **Calystegines in *Solanum* and *Datura* species and the death's-head hawk-moth (*Acherontia atropus*).** *Phytochemistry* 1993, **34**:1281–1283.
 33. Koshland Jr DE: **Stereochemistry and the mechanism of enzymatic reactions.** *Biol Rev* 1953, **28**:416–436.
 34. Zechel DL, Withers SG: **Glycosyl Transferase Mechanisms: Anatomy of a Finely Tuned Catalyst .** *Acc Chem Res* 2000, **33**:11–18.
 35. Gloster TM, Turkenburg JP, Potts JR, Henrissat B, Davies GJ: **Divergence of catalytic mechanism within a glycosidase family provides insight into evolution of carbohydrate metabolism by human gut flora.** *Chem Biol* 2008, **15**:1058–1067.
 36. Ardèvol A, Rovira C: **Reaction mechanisms in carbohydrate-active enzymes: glycoside hydrolases and glycosyltransferases. Insights from ab initio quantum mechanics/molecular mechanics dynamic simulations.** *J Am Chem Soc* 2015, **137**:7528–7547.
 37. Zechel DL, Withers SG: **Glycosidase mechanisms: anatomy of a finely tuned catalyst.** *Acc Chem Res* 2000, **33**:11–18.
 38. Gloster TM, Davies GJ: **Glycosidase inhibition: Assessing mimicry of the transition state.** *Org Biomol Chem* 2010, **8**:305–320.
 39. Legler G: **Glycoside hydrolases: mechanistic information from studies with reversible and irreversible inhibitors.** In *Advances in carbohydrate chemistry and biochemistry*. Elsevier; 1990:319–384.
 40. Stütz AE, Paulsen H: *Iminosugars as Glycosidase Inhibitors: Nojirimycin and Beyond*, Wiley, 1999.

41. Jespersen TM, Dong W, Sierks MR, Skrydstrup T, Lundt I, Bols M: **Isofagomine, a potent, new glycosidase inhibitor.** *Angew Chemie Int Ed English* 1994, **33**:1778–1779.
42. Jespersen TM, Bols M, Sierks MR, Skrydstrup T: **Synthesis of isofagomine, a novel glycosidase inhibitor.** *Tetrahedron* 1994, **50**:13449–13460.
43. Andersch J, Bols M: **Efficient synthesis of isofagomine and noeuromycin.** *Chem Eur J* 2001, **7**:3744–3747.
44. Ichikawa Y, Igarashi Y: **An extremely potent inhibitor for β -galactosidase.** *Tetrahedron Lett* 1995, **36**:4585–4586.
45. Ichikawa Y, Igarashi Y, Ichikawa M, Suhara Y: **1-N-Iminosugars: Potent and Selective Inhibitors of β -Glycosidases** *J. Am. Chem. Soc.* 1998, **120**, 3007–3018. *J Am Chem Soc* 1998, **120**:5854.
46. Kim YJ, Ichikawa M, Ichikawa Y: **Highly selective synthesis of 1-N-iminosugars of the D-glucose and-glucuronic acid types.** *J Org Chem* 2000, **65**:2599–2602.
47. Look GC, Fotsch CH, Wong CH: **Enzyme-catalyzed organic synthesis: practical routes to aza sugars and their analogs for use as glycoprocessing inhibitors.** *Acc Chem Res* 1993, **26**:182–190.
48. Zamoner LOB, Aragão-Leoneti V, Carvalho I: **Iminosugars: Effects of Stereochemistry, Ring Size, and N-Substituents on Glucosidase Activities.** *Pharmaceuticals* 2019, **12**:108.
49. Junge B, Matzke M, Stoltefuss J: **Chemistry and structure-activity relationships of glucosidase inhibitors.** In *Oral Antidiabetics*. . Springer; 1996:411–482.
50. Asano N, Ishii S, Kizu H, Ikeda K, Yasuda K, Kato A, Martin OR, Fan J: **In vitro inhibition and intracellular enhancement of lysosomal α -galactosidase A activity in Fabry lymphoblasts by 1-deoxygalactonojirimycin and its derivatives.** *Eur J Biochem* 2000, **267**:4179–4186.

51. Fleet GWJ, Nicholas SJ, Smith PW, Evans S V, Fellows LE, Nash RJ: **Potent competitive inhibition of α -galactosidase and α -glucosidase activity by 1, 4-dideoxy-1, 4-iminopentitols: syntheses of 1, 4-dideoxy-1, 4-imino-d-lyxitol and of both enantiomers of 1, 4-dideoxy-1, 4-iminoarabinitol.** *Tetrahedron Lett* 1985, **26**:3127–3130.
52. Tiwari VK: *Carbohydrates in Drug Discovery and Development: Synthesis and Application*. Elsevier Science Publishing; 2020.
53. Lillelund VH, Jensen HH, Liang X, Bols M: **Recent developments of transition-state analogue glycosidase inhibitors of non-natural product origin.** *Chem Rev* 2002, **102**:515–554.
54. Kato A, Hirokami Y, Kinami K, Tsuji Y, Miyawaki S, Adachi I, Hollinshead J, Nash RJ, Kiappes JL, Zitzmann N: **Isolation and SAR studies of bicyclic iminosugars from *Castanospermum australe* as glycosidase inhibitors.** *Phytochemistry* 2015, **111**:124–131.
55. Hughes AB, Rudge AJ: **Deoxynojirimycin: synthesis and biological activity.** *Nat Prod Rep* 1994, **11**:135–162.
56. Hettkamp H, Legler G, Bause E: **Purification by affinity chromatography of glucosidase I, an endoplasmic reticulum hydrolase involved in the processing of asparagine-linked oligosaccharides.** *Eur J Biochem* 1984, **142**:85–90.
57. Schweden J, Borgmann C, Legler G, Bause E: **Characterization of calf liver glucosidase I and its inhibition by basic sugar analogs.** *Arch Biochem Biophys* 1986, **248**:335–340.
58. Martin OR: **Iminosugars: recent insights into their bioactivity and potential as therapeutic agents.** *Curr Top Med Chem* 2003, **3**:471–591.
59. Alper J: **Searching for medicine's sweet spot.** *Science* 2001; **291**: 2338-2343.
60. Sels J-PJE, Huijberts MSP, Wolffenbuttel BHR: **Miglitol, a new α -glucosidase inhibitor.** *Expert Opin Pharmacother* 1999, **1**:149–156.

61. Hamaguchi J, Nakagawa H, Takahashi M, Kudo T, Kamiyama N, Sun B, Oshima T, Sato Y, Deguchi K, Todo S: **Swainsonine reduces 5-fluorouracil tolerance in the multistage resistance of colorectal cancer cell lines.** *Mol Cancer* 2007, **6**:58.
62. Wrodnigg TM, Steiner AJ, Ueberbacher BJ: **Natural and synthetic iminosugars as carbohydrate processing enzyme inhibitors for cancer therapy.** *Anti-Cancer Agents Med Chem (Formerly Curr Med Chem Agents)* 2008, **8**:77–85.
63. Fleet GWJ, Karpas A, Dwek RA, Fellows LE, Tyms AS, Petursson S, Namgoong SK, Ramsden NG, Smith PW, Son JC: **Inhibition of HIV replication by amino-sugar derivatives.** *FEBS Lett* 1988, **237**:128–132.
64. Fischer PB, Karlsson GB, Butters TD, Dwek RA, Platt FM: **N-butyldeoxynojirimycin-mediated inhibition of human immunodeficiency virus entry correlates with changes in antibody recognition of the V1/V2 region of gp120.** *J Virol* 1996, **70**:7143–7152.
65. Durantel D: **Celgosivir, an α glucosidase I inhibitor for the potential treatment of hepatitis C virus infection.** *Curr Opin Invest Drugs* 2009, **10**:860–870.
66. Radin NS: **Treatment of Gaucher disease with an enzyme inhibitor.** *Glycoconj J* 1996, **13**:153–157.
67. Pineda M, Walterfang M, Patterson MC: **Miglustat in Niemann-Pick disease type C patients: a review.** *Orphanet J Rare Dis* 2018, **13**:140.
68. Horne G, Wilson FX, Tinsley J, Williams DH, Storer R: **Iminosugars past, present and future: medicines for tomorrow.** *Drug Discov Today* 2011, **16**:107–118.
69. Czech MP: **Lipid rafts and insulin action.** *Nature* 2000, **407**:147–148.
70. Ross SA, Gulve EA, Wang M: **Chemistry and biochemistry of type 2 diabetes.** *Chem Rev* 2004, **104**:1255–1282.

71. Braakman I, Van Anken E: **Folding of viral envelope glycoproteins in the endoplasmic reticulum.** *Traffic* 2000, **1**:533–539.
72. Fischer PB, Karlsson GB, Dwek RA, Platt FM: **N-butyldeoxynojirimycin-mediated inhibition of human immunodeficiency virus entry correlates with impaired gp120 shedding and gp41 exposure.** *J Virol* 1996, **70**:7153–7160.
73. Fischer PB, Collin M, Karlsson GB, James W, Butters TD, Davis SJ, Gordon S, Dwek RA, Platt FM: **The alpha-glucosidase inhibitor N-butyldeoxynojirimycin inhibits human immunodeficiency virus entry at the level of post-CD4 binding.** *J Virol* 1995, **69**:5791–5797.
74. Karlsson GB, Butters TD, Dwek RA, Platt FM: **Effects of the imino sugar N-butyldeoxynojirimycin on the N-glycosylation of recombinant gp120.** *J Biol Chem* 1993, **268**:570–576.
75. Cooper GM, Hausman RE: *The cell: a molecular approach.* Sinauer Associates, 2000.
76. Platt FM, d’Azzo A, Davidson BL, Neufeld EF, Tiffit CJ: **Lysosomal storage diseases.** *Nat Rev Dis Prim* 2018, **4**: 27.
77. Fan J-Q: **Iminosugars as active-site-specific chaperones for the treatment of lysosomal storage disorders.** In *Iminosugars From Synthesis to Therapeutic Applications*, Edited by Compain P, Martin OR; John Wiley & Sons; 2007:225-243.
78. Sugawara K, Tajima Y, Kawashima I, Tsukimura T, Saito S, Ohno K, Iwamoto K, Kobayashi T, Itoh K, Sakuraba H: **Molecular interaction of imino sugars with human α -galactosidase: Insight into the mechanism of complex formation and pharmacological chaperone action in Fabry disease.** *Mol Genet Metab* 2009, **96**:233–238.
79. **Fabry disease news.** Clinical trials, <https://fabrydiseasenews.com/galafold-migalastat/>, July 15, 2020.
80. Platt FM, Jeyakumar M, Andersson U, Heare T, Dwek RA, Butters TD:

Substrate reduction therapy in mouse models of the glycosphingolipidoses.

Philos Trans R Soc London Ser B Biol Sci 2003, **358**:947–954.

81. Boglio C, Stahlke S, Thorimbert S, Malacria M: **A Stereoselective Route toward Polyhydroxylated Piperidines. A Total Synthesis of (±)-Deoxymannojirimycin.** *Org Lett* 2005, **7**:4851–4854.
82. Rudge AJ, Collins I, Holmes AB, Baker R: **An enantioselective synthesis of deoxynojirimycin.** *Angew Chemie Int Ed English* 1994, **33**:2320–2322.
83. Olsen JI, Plata GB, Padrón JM, López Ó, Bols M, Fernández-Bolaños JG: **Selenoureido-iminosugars: A new family of multitarget drugs.** *Eur J Med Chem* 2016, **123**:155–160.
84. Dondoni A, Merino P, Perrone D: **Totally chemical synthesis of azasugars via thiazole intermediates. Stereodivergent routes to (-)-nojirimycin, (-)-mannojirimycin and their 3-deoxy derivatives from serine.** *Tetrahedron* 1993, **49**:2939–2956.
85. Ikota N: **Synthesis of (+)-1-deoxynojirimycin from (S)-pyroglutamic acid.** *Heterocycles (Sendai)* 1989, **29**:1469–1472.
86. Behling J, Farid P, Medich JR, Scaros MG, Prunier M, Weier RM, Khanna I: **A Short and Practical Synthesis of 1-Deoxynojirimycin.** *Synth Commun* 1991, **21**:1383–1386.
87. van der Klein PAM, Filemon W, Broxterman HJG, van der Marel GA, van Boom JH: **A cyclic sulfate approach to the synthesis of 1, 4-dideoxy-1, 4-imino derivatives of L-xylitol, L-arabinitol and D-xylitol.** *Synth Commun* 1992, **22**:1763–1771.
88. Zou W, Szarek WA: **A new practical synthesis of (2S, 3R, 4R, 5S)-3, 4-dihydroxy-2, 6-bis (hydroxymethyl) pyrrolidine.** *Carbohydr Res* 1993, **242**:311–314.
89. McCaig AE, Chomier B, Wightman RH: **Hydroxylated piperidines: synthesis of 1, 5-alkylimino-1, 5-dideoxy derivatives of xylitol, D-and L-arabinitol, and**

- ribitol**. *J Carbohydr Chem* 1994, **13**:397–407.
90. Overkleeft HS, van Wiltenburg J, Upendra PK: **An expedient stereoselective synthesis of gluconolactam**. *Tetrahedron Lett* 1993, **34**:2527–2528.
91. Meng Q, Hesse M: **A New Synthesis of (2-S,3-R,4-R)-2-(Hydroxymethyl)pyrrolidine-3,4-diol**. *Helv Chim Acta* 1991, **74**:445–450.
92. Turner NJ, Humphreys L: *Biocatalysis in Organic Synthesis: The Retrosynthesis Approach*. Royal Society of Chemistry; 2018.
93. Sheldon RA, Woodley JM: **Role of biocatalysis in sustainable chemistry**. *Chem Rev* 2018, **118**:801–838.
94. Gijzen HJM, Qiao L, Fitz W, Wong C-H: **Recent advances in the chemoenzymatic synthesis of carbohydrates and carbohydrate mimetics**. *Chem Rev* 1996, **96**:443–474.
95. Silvestri MG, Desantis G, Mitchell M, Wong C: **Asymmetric aldol reactions using aldolases**. *Top Stereochem* 2003, **23**:267–342.
96. Hung RR, Straub JA, Whitesides GM: **. alpha.-Amino aldehyde equivalents as substrates for rabbit muscle aldolase: synthesis of 1, 4-dideoxy-D-arabinitol and 2 (R), 5 (R)-bis (hydroxymethyl)-3 (R), 4 (R)-dihydroxypyrrrolidine**. *J Org Chem* 1991, **56**:3849–3855.
97. Whalen LJ, Wong C-H: **Enzymes in organic synthesis: aldolase-mediated synthesis of iminocyclitols and novel heterocycles**. *Aldrichimica Acta* 2006, **39**:63–71.
98. Romero A, Wong C-H: **Chemo-enzymatic total synthesis of 3-epiaustraline, australine, and 7-epialexine**. *J Org Chem* 2000, **65**:8264–8268.
99. Sugiyama M, Hong Z, Liang PH, Dean SM, Whalen LJ, Greenberg WA, Wong CH: **D-fructose-6-phosphate aldolase-catalyzed one-pot synthesis of iminocyclitols**. *J Am Chem Soc* 2007, **129**:14811–14817.
100. Roldán R, Hernández K, Joglar J, Bujons J, Parella T, Fessner WD, Clapés P: **Aldolase-Catalyzed Asymmetric Synthesis of N-Heterocycles by Addition of**

- Simple Aliphatic Nucleophiles to Aminoaldehydes.** *Adv Synth Catal* 2019, **361**:2673–2687.
101. Liu KKC, Kajimoto T, Chen L, Zhong Z, Ichikawa Y, Wong CH: **Use of dihydroxyacetone phosphate-dependent aldolases in the synthesis of deoxy aza sugars.** *J Org Chem* 1991, **56**:6280–6289.
102. Chen L, Dumas DP, Wong CH: **Deoxyribose 5-phosphate aldolase as a catalyst in asymmetric aldol condensation.** *J Am Chem Soc* 1992, **114**:741–748.
103. Lu F, Xu W, Zhang W: **Polyol dehydrogenases : intermediate role in the bioconversion of rare sugars and alcohols.** *Appl Microbiol Biotechnol* 2019, **103**: 6473-6481.
104. Adachi O, Ano Y, Toyama H, Matsushita K: **Biooxidation with PQQ-and FAD-dependent dehydrogenases.** In *Modern biooxidation: Enzymes, Reactions and Applications*, Edited by Weinheim, Wiley-VCH 2007, 1-41.
105. Kinast G, Schedel M: **A Four-Step Synthesis of 1-Deoxynojirimycin with a Biotransformation as Cardinal Reaction Step.** *Angew Chemie Int Ed English* 1981, **20**:805–806.
106. Oikonomakos NG, Tiraidis C, Leonidas DD, Zographos SE, Kristiansen M, Jessen CU, Nørskov-Lauritsen L, Agius L: **Iminosugars as potential inhibitors of glycogenolysis: structural insights into the molecular basis of glycogen phosphorylase inhibition.** *J Med Chem* 2006, **49**:5687–5701.
107. Sethi MK, Kumar A, Maddur N, Shukla R, Vemula LN: **Gluconobacter mediated synthesis of amino sugars.** *J Mol Catal B Enzym* 2014, **112**:54–58.
108. Bruggink A, Schoevaart R, Kieboom T: **Concepts of nature in organic synthesis: cascade catalysis and multistep conversions in concert.** *Org Process Res Dev* 2003, **7**:622–640.
109. Sheldon RA: **E factors, green chemistry and catalysis: an odyssey.** *Chem Commun* 2008, 3352-3365.

110. Muschiol J, Peters C, Oberleitner N, Mihovilovic MD, Bornscheuer UT, Rudroff F: **Cascade catalysis—strategies and challenges en route to preparative synthetic biology.** *Chem Commun* 2015, **51**:5798–5811.
111. Wandrey C, Fiolitakis E, Wichmann U: **L-Amino acids from a racemic mixture of α -hydroxy acids.** *Ann N Y Acad Sci* 1984, **434**:91–94.
112. Schrittwieser JH, Velikogne S, Hall MM, Kroutil W: **Artificial Biocatalytic Linear Cascades for Preparation of Organic Molecules.** *Chem Rev* 2018, **118**:270–348.
113. Devine PN, Howard RM, Kumar R, Thompson MP, Truppo MD, Turner NJ: **Extending the application of biocatalysis to meet the challenges of drug development.** *Nat Rev Chem* 2018, **2**:409–421.
114. Claaßen C, Gerlach T, Rother D: **Stimulus-Responsive Regulation of Enzyme Activity for One-Step and Multi-Step Syntheses.** *Adv Synth Catal* 2019, **361**:2387–2401.
115. Schofield CJ: **Antibiotics as food for bacteria.** *Nat Microbiol* 2018, **3**:752–753.
116. Bokhove M, Yoshida H, Hensgens CMH, van der Laan JM, Sutherland JD, Dijkstra BW: **Structures of an isopenicillin N converting Ntn-hydrolase reveal different catalytic roles for the active site residues of precursor and mature enzyme.** *Structure* 2010, **18**:301–308.
117. France SP, Hepworth LJ, Turner NJ, Flitsch SL: **Constructing biocatalytic cascades: in vitro and in vivo approaches to de novo multi-enzyme pathways.** *Acs Catal* 2017, **7**:710–724.
118. Glick BR: **Metabolic load and heterologous gene expression.** *Biotechnol Adv* 1995, **13**:247–261.
119. Kuska J, O'Reilly E: **Engineered biosynthetic pathways and biocatalytic cascades for sustainable synthesis.** *Curr Opin Chem Biol* 2020, **58**:146–154.
120. Klumpp S, Zhang Z, Hwa T: **Growth rate-dependent global effects on gene expression in bacteria.** *Cell* 2009, **139**:1366–1375.

121. Kunjapur AM, Tarasova Y, Prather KLJ: **Synthesis and accumulation of aromatic aldehydes in an engineered strain of Escherichia coli.** *J Am Chem Soc* 2014, **136**:11644–11654.
122. Mordhorst S, Andexer JN: **Round, round we go—strategies for enzymatic cofactor regeneration.** *Nat Prod Rep* 2020, **37**:1316–1333.
123. Hepworth LJ, France SP, Hussain S, Both P, Turner NJ, Flitsch SL: **Enzyme cascades in whole cells for the synthesis of chiral cyclic amines.** *ACS Catal* 2017, **7**:2920–2925.
124. France SP, Hussain S, Hill AM, Hepworth LJ, Howard RM, Mulholland KR, Flitsch SL, Turner NJ: **One-pot cascade synthesis of mono- and disubstituted piperidines and pyrrolidines using carboxylic acid reductase (CAR), ω -transaminase (ω -TA), and imine reductase (IREC) biocatalysts.** *ACS Catal* 2016, **6**:3753–3759.
125. Huffman MA, Fryszkowska A, Alvizo O, Borra-Garske M, Campos KR, Devine PN, Duan D, Forstater JH, Grosser ST, Halsey HM: **Design of an in vitro biocatalytic cascade for the manufacture of islatravir.** *Science (80-)* 2019, **366**:1255–1259.
126. O'Reilly E, Ryan J: **Biocatalytic cascades go viral.** *Science* 2019, **366**:1199–1200.
127. Puigserver P: **Signaling Transduction and Metabolomics.** In *Hematology*. . Elsevier; 2018:68–78.
128. McLaughlin M, Kong J, Belyk KM, Chen B, Gibson AW, Keen SP, Lieberman DR, Milczek EM, Moore JC, Murray D: **Enantioselective synthesis of 4'-ethynyl-2-fluoro-2'-deoxyadenosine (EFdA) via enzymatic desymmetrization.** *Org Lett* 2017, **19**:926–929.
129. Kageyama M, Nagasawa T, Yoshida M, Ohrui H, Kuwahara S: **Enantioselective total synthesis of the potent anti-HIV nucleoside EFdA.** *Org Lett* 2011, **13**:5264–5266.

130. Quadri LEN, Weinreb PH, Lei M, Nakano MM, Zuber P, Walsh CT: **Characterization of Sfp, a *Bacillus subtilis* phosphopantetheinyl transferase for peptidyl carrier protein domains in peptide synthetases.** *Biochemistry* 1998, **37**:1585–1595.
131. Ramsden JI, Heath RS, Derrington SR, Montgomery SL, Mangas-Sanchez J, Mulholland KR, Turner NJ: **Biocatalytic N-alkylation of amines using either primary alcohols or carboxylic acids via reductive aminase cascades.** *J Am Chem Soc* 2019, **141**:1201–1206.
132. Heath RS, Pontini M, Hussain S, Turner NJ: **Combined imine reductase and amine oxidase catalyzed deracemization of nitrogen heterocycles.** *ChemCatChem* 2016, **8**:117–120.
133. Ju S, Qian M, Li J, Xu G, Yang L, Wu J: **A biocatalytic redox cascade approach for one-pot deracemization of carboxyl-substituted tetrahydroisoquinolines by stereoinversion.** *Green Chem* 2019, **21**:5579–5585.
134. Antti H, Sellstedt M: **Metabolic effects of an aspartate aminotransferase-inhibitor on two T-cell lines.** *PLoS One* 2018, **13**:e0208025.
135. Nakamichi K, Shibatani T, Yamamoto Y, Sato T: **Asymmetric amination of 4-methoxyphenylacetone and its related compounds with microorganisms.** *Appl Microbiol Biotechnol* 1990, **33**:637–640.
136. Shin J-S, Kim B-G: **Comparison of the ω -transaminases from different microorganisms and application to production of chiral amines.** *Biosci Biotechnol Biochem* 2001, **65**:1782–1788.
137. Pavlidis I V, Weiß MS, Genz M, Spurr P, Hanlon SP, Wirz B, Iding H, Bornscheuer UT: **Identification of (S)-selective transaminases for the asymmetric synthesis of bulky chiral amines.** *Nat Chem* 2016, **8**:1076.
138. Janey JM: **Development of A Sitagliptin Transaminase.** In *Sustainable Catalysis*, Edited by Dunn PJ, Hii KK, Krische MJ, Williams MT, 2013: 75-87.
139. Yun H, Hwang B-Y, Lee J-H, Kim B-G: **Use of enrichment culture for directed**

- evolution of the *Vibrio fluvialis* JS17 ω -transaminase, which is resistant to product inhibition by aliphatic ketones. *Appl Environ Microbiol* 2005, **71**:4220–4224.
140. Burns M, Martinez CA, Vanderplas B, Wisdom R, Yu S, Singer RA: **A chemoenzymatic route to chiral intermediates used in the multikilogram synthesis of a gamma secretase inhibitor.** *Org Process Res Dev* 2017, **21**:871–877.
141. D Patil M, Grogan G, Bommarius A, Yun H: **Recent advances in ω -transaminase-mediated biocatalysis for the enantioselective synthesis of chiral amines.** *Catalysts* 2018, **8**:254.
142. Gomm A, Lewis W, Green AP, O'Reilly E: **A New Generation of Smart Amine Donors for Transaminase-Mediated Biotransformations.** *Chem Eur J* 2016, **22**:12692–12695.
143. Green AP, Turner NJ, O'Reilly E: **Chiral Amine Synthesis Using ω -Transaminases: An Amine Donor that Displaces Equilibria and Enables High-Throughput Screening.** *Angew Chem Int Ed* 2014, **53**:10714-10717.
144. Cassimjee KE, Manta B, Himo F: **A quantum chemical study of the ω -transaminase reaction mechanism.** *Org Biomol Chem* 2015, **13**:8453–8464.
145. Percudani R, Peracchi A: **The B6 database: a tool for the description and classification of vitamin B6-dependent enzymatic activities and of the corresponding protein families.** *BMC Bioinformatics* 2009, **10**:273.
146. Steffen-Munsberg F, Vickers C, Kohls H, Land H, Mallin H, Nobili A, Skalden L, van den Bergh T, Joosten H-J, Berglund P: **Bioinformatic analysis of a PLP-dependent enzyme superfamily suitable for biocatalytic applications.** *Biotechnol Adv* 2015, **33**:566–604.
147. Gomm A, O'Reilly E: **Transaminases for chiral amine synthesis.** *Curr Opin Chem Biol* 2018, **43**:106–112.
148. Adams JP, Brown MJB, Diaz-Rodriguez A, Lloyd RC, Roiban GD: **Biocatalysis: A**

- Pharma Perspective.** *Adv Synth Catal* 2019, **361**:2421–2432.
149. Truppo MD, Rozzell JD, Moore JC, Turner NJ: **Rapid screening and scale-up of transaminase catalysed reactions.** *Org Biomol Chem* 2009, **7**:395–398.
150. Galman JL, Slabu I, Weise NJ, Iglesias C, Parmeggiani F, Lloyd RC, Turner NJ: **Biocatalytic transamination with near-stoichiometric inexpensive amine donors mediated by bifunctional mono- and di-amine transaminases.** *Green Chem* 2017, **19**:361–366.
151. Dourado DFAR, Pohle S, Carvalho ATP, Dheeman DS, Caswell JM, Skvortsov T, Miskelly I, Brown RT, Quinn DJ, Allen CCR: **Rational Design of a (S)-Selective-Transaminase for Asymmetric Synthesis of (1S)-1-(1, 1'-biphenyl-2-yl) ethanamine.** *ACS Catal* 2016, **6**:7749–7759.
152. Payer SE, Schrittwieser JH, Grischek B, Simon RC, Kroutil W: **Regio- and Stereoselective biocatalytic monoamination of a triketone enables asymmetric synthesis of both enantiomers of the pyrrolizidine alkaloid xenovenine employing transaminases.** *Adv Synth Catal* 2016, **358**:444–451.
153. Mangion IK, Sherry BD, Yin J, Fleitz FJ: **Enantioselective synthesis of a dual orexin receptor antagonist.** *Org Lett* 2012, **14**:3458–3461.
154. Cairns R, Gomm A, Ryan J, Clarke T, Kulcinskaja E, Butler K, O'Reilly E, O'Reilly E: **Conversion of Aldoses to Valuable ω -Amino Alcohols Using Amine Transaminase Biocatalysts.** *ACS Catal* 2018, **9**:1220–1223.
155. Subrizi F, Benhamou L, Ward JM, Sheppard TD, Hailes HC: **Aminopolyols from Carbohydrates: Amination of Sugars and Sugar-Derived Tetrahydrofurans with Transaminase.** *Angew Chem Int Ed* 2019, **58**:3854–3858
156. Thompson CE, Freitas LB, Salzano FM: **Molecular evolution and functional divergence of alcohol dehydrogenases in animals, fungi and plants.** *Genet Mol Biol* 2018, **41**:341–354.
157. Goswami P, Chinnadayala SSR, Chakraborty M, Kumar AK, Kakoti A: **An overview on alcohol oxidases and their potential applications.** *Appl*

- Microbiol Biotechnol* 2013, **97**:4259–4275.
158. Plapp B V, Savarimuthu BR, Ferraro DJ, Rubach JK, Brown EN, Ramaswamy S: **Horse liver alcohol dehydrogenase: zinc coordination and catalysis.** *Biochemistry* 2017, **56**:3632–3646.
 159. Romero E, Gadda G: **Alcohol oxidation by flavoenzymes.** *Biomol Concepts* 2014, **5**:299–318.
 160. Oubrie A: **Structure and mechanism of soluble glucose dehydrogenase and other PQQ-dependent enzymes.** *BBA – Proteins and Proteomics* 2003, **1647**:143–151.
 161. Himo F, Eriksson LA, Maseras F, Siegbahn PEM: **Catalytic mechanism of galactose oxidase: A theoretical study.** *J Am Chem Soc* 2000, **122**:8031–8036.
 162. Cederbaum AI: **Alcohol metabolism.** *Clin Liver Dis* 2012, **16**:667–685.
 163. Parikka K, Master E, Tenkanen M: **Oxidation with galactose oxidase: multifunctional enzymatic catalysis.** *J Mol Catal B Enzym* 2015, **120**:47–59.
 164. Hummel W: **New alcohol dehydrogenases for the synthesis of chiral compounds.** In *New enzymes for organic synthesis*. Springer; 1997:145–184.
 165. Kroutil W, Mang H, Edegger K, Faber K: **Biocatalytic oxidation of primary and secondary alcohols.** *Adv Synth Catal* 2004, **346**:125–142.
 166. Romano D, Villa R, Molinari F: **Preparative Biotransformations: Oxidation of Alcohols.** *ChemCatChem* 2012, **4**:739–749.
 167. Molinari F: **Oxidations with isolated and cell-bound dehydrogenases and oxidases.** *Curr Org Chem* 2006, **10**:1247–1263.
 168. Orbegozo T, Lavandera I, Fabian WMF, Mautner B, de Vries JG, Kroutil W: **Biocatalytic oxidation of benzyl alcohol to benzaldehyde via hydrogen transfer.** *Tetrahedron* 2009, **65**:6805–6809.
 169. Lok KP, Jakovac IJ, Jones JB: **Enzymes in organic synthesis. 34. Preparations of enantiomerically pure exo-and endo-bridged bicyclic [2.2. 1] and [2.2. 2]**

- chiral lactones via stereospecific horse liver alcohol dehydrogenase catalyzed oxidations of meso diols. *J Am Chem Soc* 1985, **107**:2521–2526.
170. Lortie R, Villaume I, Legoy MD, Thomas D: **Enzymatic production of long-chain aldehydes in a fixed bed reactor using organic solvents and cofactor regeneration.** *Biotechnol Bioeng* 1989, **33**:229–232.
171. Andersson M, Holmberg H, Adlercreutz P: **Prediction of the remaining activity of horse liver alcohol dehydrogenase after exposure to various organic solvents.** *Biocatal Biotransformation* 1998, **16**:259–273.
172. Hammes-Schiffer S, Benkovic SJ: **Relating protein motion to catalysis.** *Annu Rev Biochem* 2006, **75**:519–541.
173. Moa S, Himo F: **Quantum chemical study of mechanism and stereoselectivity of secondary alcohol dehydrogenase.** *J Inorg Biochem* 2017, **175**:259–266.
174. Kovaleva EG, Plapp B V: **Deprotonation of the Horse Liver Alcohol Dehydrogenase– NAD⁺ Complex Controls Formation of the Ternary Complexes.** *Biochemistry* 2005, **44**:12797–12808.
175. Dias Gomes M, Bommarius BR, Anderson SR, Feske BD, Woodley JM, Bommarius AS: **Bubble Column Enables Higher Reaction Rate for Deracemization of (R, S)-1-Phenylethanol with Coupled Alcohol Dehydrogenase/NADH Oxidase System.** *Adv Synth Catal* 2019, **361**:2574–2581.
176. Matsutani M, Yakushi T: **Pyrroloquinoline quinone-dependent dehydrogenases of acetic acid bacteria.** *Appl Microbiol Biotechnol* 2018, **102**:9531–9540.
177. Jongejan A, Machado SS, Jongejan JA: **The enantioselectivity of quinohaemoprotein alcohol dehydrogenases: mechanistic and structural aspects.** *J Mol Catal B Enzym* 2000, **8**:121–163.
178. Reddy SY, Bruice TC: **Determination of enzyme mechanisms by molecular**

dynamics: Studies on quinoproteins, methanol dehydrogenase, and soluble glucose dehydrogenase. *Protein Sci* 2004, **13**:1965–1978.

179. Wongnate T, Surawatanawong P, Visitsatthawong S, Sucharitakul J, Scrutton NS, Chaiyen P: **Proton-coupled electron transfer and adduct configuration are important for C4a-hydroperoxyflavin formation and stabilization in a flavoenzyme.** *J Am Chem Soc* 2014, **136**:241–253.
180. Zheng Y-J, Xia Z, Chen Z, Mathews FS, Bruice TC: **Catalytic mechanism of quinoprotein methanol dehydrogenase: A theoretical and X-ray crystallographic investigation.** *Proc Natl Acad Sci* 2001, **98**:432–434.
181. Wongnate T, Chaiyen P: **The substrate oxidation mechanism of pyranose 2-oxidase and other related enzymes in the glucose–methanol–choline superfamily.** *FEBS J* 2013, **280**:3009–3027.
182. Whittaker JW: **The radical chemistry of galactose oxidase.** *Arch Biochem Biophys* 2005, **433**:227–239.
183. Petruk AA, Bartesaghi S, Trujillo M, Estrin DA, Murgida D, Kalyanaraman B, Marti MA, Radi R: **Molecular basis of intramolecular electron transfer in proteins during radical-mediated oxidations: Computer simulation studies in model tyrosine–cysteine peptides in solution.** *Arch Biochem Biophys* 2012, **525**:82–91.
184. Zueva E, Walton PH, McGrady JE: **Catalytic alcohol oxidation by an unsymmetrical 5-coordinate copper complex: electronic structure and mechanism.** *Dalt Trans* 2006, 159-167.
185. Ballou DP, Whittaker JW: **Oxygen reactions of the copper oxidases.** *Essays Biochem* 1999, **34**:155–172.
186. Que L, Tolman WB: **Biologically inspired oxidation catalysis.** *Nature* 2008, **455**:333–340.
187. Siebum A, van Wijk A, Schoevaart R, Kieboom T: **Galactose oxidase and alcohol oxidase: Scope and limitations for the enzymatic synthesis of**

- aldehydes.** *J Mol Catal B Enzym* 2006, **41**:141–145.
188. Herter S, McKenna SM, Frazer AR, Leimkühler S, Carnell AJ, Turner NJ: **Galactose oxidase variants for the oxidation of amino alcohols in enzyme cascade synthesis.** *ChemCatChem* 2015, **7**:2313–2317.
189. Borzeix F, Monot F, Vandecasteele J-P: **Bi-enzymatic reaction for alcohol oxidation in organic media: From purified enzymes to cellular systems.** *Enzyme Microb Technol* 1995, **17**:615–622.
190. N Christ T, A Deweese K, D Woodyer R: **Directed evolution toward improved production of L-ribose from ribitol.** *Comb Chem High Throughput Screen* 2010, **13**:302–308.
191. Woodyer RD, Wymer NJ, Racine FM, Khan SN, Saha BC: **Efficient production of L-ribose with a recombinant Escherichia coli biocatalyst.** *Appl Environ Microbiol* 2008, **74**:2967–2975.
192. Wu Y, Arciola J, Horenstein N: **Medium-chain dehydrogenases with new specificity: amino mannitol dehydrogenases on the azasugar biosynthetic pathway.** *Protein Pept Lett* 2014, **21**:10–14.
193. Clark LF, Johnson J V, Horenstein NA: **Identification of a gene cluster that initiates azasugar biosynthesis in Bacillus amyloliquefaciens.** *ChemBioChem* 2011, **12**:2147–2150.
194. Gupta A, Singh VK, Qazi GN, Kumar A: **Gluconobacter oxydans: its biotechnological applications.** *J Mol Microbiol Biotechnol* 2001, **3**:445–56.
195. Deppenmeier U, Hoffmeister M, Prust C: **Biochemistry and biotechnological applications of Gluconobacter strains.** *Appl Microbiol Biotechnol* 2003, **60**:233–242.
196. Kulhánek M: **Microbial dehydrogenations of monosaccharides.** In *Advances in applied microbiology.* . Elsevier; 1989:141–182.
197. Kim T-SS, Patel SKSS, Selvaraj C, Jung W-SS, Pan C-HH, Kang YC, Lee J-KK: **A highly efficient sorbitol dehydrogenase from Gluconobacter oxydans G624**

- and improvement of its stability through immobilization. *Sci Rep* 2016, **6**:1–11.
198. Liu L, Zeng W, Du G, Chen J, Zhou J: **Identification of NAD-dependent xylitol dehydrogenase from *Gluconobacter oxydans* WSH-003.** *ACS omega* 2019, **4**:15074–15080.
199. Cheng H, Li Z, Jiang N, Deng Z: **Cloning, purification and characterization of an NAD-dependent d-arabitol dehydrogenase from acetic acid bacterium, *acetobacter suboxydans*.** *Protein J* 2009, **28**:263–272.
200. Cheng H, Jiang N, Shen A, Feng Y: **Molecular cloning and functional expression of D-arabitol dehydrogenase gene from *Gluconobacter oxydans* in *Escherichia coli*.** *FEMS Microbiol Lett* 2005, **252**:35–42.
201. Pappenberger G, Hohmann H-P: **Industrial production of L-ascorbic acid (vitamin C) and D-isoascorbic acid.** In *Biotechnology of food and feed additives*. . Springer; 2013:143–188.
202. Claret C, Salmon JM, Romieu C, Bories A: **Physiology of *Gluconobacter oxydans* during dihydroxyacetone production from glycerol.** *Appl Microbiol Biotechnol* 1994, **41**:359–365.
203. Li M, Wu J, Liu X, Lin J, Wei D, Chen H: **Enhanced production of dihydroxyacetone from glycerol by overexpression of glycerol dehydrogenase in an alcohol dehydrogenase-deficient mutant of *Gluconobacter oxydans*.** *Bioresour Technol* 2010, **101**:8294–8299.
204. Mitsukura K, Suzuki M, Tada K, Yoshida T, Nagasawa T: **Asymmetric synthesis of chiral cyclic amine from cyclic imine by bacterial whole-cell catalyst of enantioselective imine reductase.** *Org Biomol Chem* 2010, **8**:4533–4535.
205. Aleku GA, France SP, Man H, Mangas-Sanchez J, Montgomery SL, Sharma M, Leipold F, Hussain S, Grogan G, Turner NJ: **A reductive aminase from *Aspergillus oryzae*.** *Nat Chem* 2017, **9**:961.
206. Howell EE: **Searching sequence space: two different approaches to**

- dihydrofolate reductase catalysis.** *ChemBioChem* 2005, **6**:590–600.
207. Finefield JM, Sherman DH, Kreitman M, Williams RM: **Enantiomeric natural products: occurrence and biogenesis.** *Angew Chemie Int Ed* 2012, **51**:4802–4836.
208. Mangas-Sanchez J, France SP, Montgomery SL, Aleku GA, Man H, Sharma M, Ramsden JI, Grogan G, Turner NJ: **Imine reductases (IREDs).** *Curr Opin Chem Biol* 2017, **37**:19–25.
209. Schnell JR, Dyson HJ, Wright PE: **Structure, dynamics, and catalytic function of dihydrofolate reductase.** *Annu Rev Biophys Biomol Struct* 2004, **33**:119–140.
210. Schrittwieser JH, Velikogne S, Kroutil W: **Biocatalytic imine reduction and reductive amination of ketones.** *Adv Synth Catal* 2015, **357**:1655–1685.
211. Zhu J, Tan H, Yang L, Dai Z, Zhu L, Ma H, Deng Z, Tian Z, Qu X: **Enantioselective synthesis of 1-aryl-substituted tetrahydroisoquinolines employing imine reductase.** *ACS Catal* 2017, **7**:7003–7007.
212. Li H, Tian P, Xu J-H, Zheng G-W: **Identification of an imine reductase for asymmetric reduction of bulky dihydroisoquinolines.** *Org Lett* 2017, **19**:3151–3154.
213. Mangas-Sanchez J, Sharma M, Cosgrove SC, Ramsden JI, Marshall JR, Thorpe TW, Palmer RB, Grogan G, Turner NJ: **Asymmetric synthesis of primary amines catalyzed by thermotolerant fungal reductive aminases.** *Chem Sci* 2020, **11**:5052-5057.
214. Rodríguez-Mata M, Frank A, Wells E, Leipold F, Turner NJ, Hart S, Turkenburg JP, Grogan G: **Structure and Activity of NADPH-Dependent Reductase Q1EQE0 from Streptomyces kanamyceticus, which Catalyses the R-Selective Reduction of an Imine Substrate.** *ChemBioChem* 2013, **14**:1372–1379.
215. Wetzl D, Berrera M, Sandon N, Fishlock D, Ebeling M, Müller M, Hanlon S, Wirz B, Iding H: **Expanding the Imine Reductase Toolbox by Exploring the**

- Bacterial Protein-Sequence Space.** *ChemBioChem* 2015, **16**:1749–1756.
216. Scheller PN, Fademrecht S, Hofelzer S, Pleiss J, Leipold F, Turner NJ, Nestl BM, Hauer B: **Enzyme toolbox: novel enantiocomplementary imine reductases.** *ChemBioChem* 2014, **15**:2201–2204.
217. Mitsukura K, Suzuki M, Shinoda S, Kuramoto T, Yoshida T, Nagasawa T: **Purification and characterization of a novel (*R*)-imine reductase from *Streptomyces* sp. GF3587.** *Biosci Biotechnol Biochem* 2011, **75**:1778–1782.
218. Gand M, Müller H, Wardenga R, Höhne M: **Characterization of three novel enzymes with imine reductase activity.** *J Mol Catal B Enzym* 2014, **110**:126–132.
219. Hussain S, Leipold F, Man H, Wells E, France SP, Mulholland KR, Grogan G, Turner NJ: **An (*R*)-imine reductase biocatalyst for the asymmetric reduction of cyclic imines.** *ChemCatChem* 2015, **7**:579–583.
220. Huber T, Schneider L, Präg A, Gerhardt S, Einsle O, Müller M: **Direct Reductive Amination of Ketones: Structure and Activity of *S*-Selective Imine Reductases from *Streptomyces*.** *ChemCatChem* 2014, **6**:2248–2252.
221. Aleku GA, Man H, France SP, Leipold F, Hussain S, Toca-Gonzalez L, Marchington R, Hart S, Turkenburg JP, Grogan G: **Stereoselectivity and structural characterization of an imine reductase (IRE_D) from *Amycolatopsis orientalis*.** *ACS Catal* 2016, **6**:3880–3889.
222. Leipold F, Hussain S, Ghislieri D, Turner NJ: **Asymmetric reduction of cyclic imines catalyzed by a whole-cell biocatalyst containing an (*S*)-imine reductase.** *ChemCatChem* 2013, **5**:3505–3508.
223. Wetzl D, Gand M, Ross A, Müller H, Matzel P, Hanlon SP, Müller M, Wirz B, Höhne M, Iding H: **Asymmetric reductive amination of ketones catalyzed by imine reductases.** *ChemCatChem* 2016, **8**:2023–2026.
224. Matzel P, Wenske S, Merdivan S, Günther S, Höhne M: **Synthesis of β -Chiral Amines by Dynamic Kinetic Resolution of α -Branched Aldehydes Applying**

Imine Reductases. *ChemCatChem* 2019, **11**:4281–4285.

225. France SP, Aleku GA, Sharma M, Mangas-Sanchez J, Howard RM, Steflík J, Kumar R, Adams RW, Slabu I, Crook R: **Biocatalytic routes to enantiomerically enriched dibenz [c, e] azepines.** *Angew Chemie Int Ed* 2017, **56**:15589–15593.
226. Schober M, MacDermaid C, Ollis AA, Chang S, Khan D, Hosford J, Latham J, Ihnken LAF, Brown MJB, Fuerst D: **Chiral synthesis of LSD1 inhibitor GSK2879552 enabled by directed evolution of an imine reductase.** *Nat Catal* 2019, **2**:909–915.
227. Batista VF, Galman JL, Cláudia D, Pinto GA, Silva AMS, Turner NJ, GA Pinto DC, Silva AMS, Turner NJ: **Monoamine oxidase: tunable activity for amine resolution and functionalization.** *ACS Catal* 2018, **8**:11889–11907.
228. Schilling B, Lerch K: **Amine oxidases from *Aspergillus niger*: identification of a novel flavin-dependent enzyme.** *Biochim Biophys Acta (BBA)-General Subj* 1995, **1243**:529–537.
229. Segura-Aguilar J, Paris I, Muñoz P, Ferrari E, Zecca L, Zucca FA: **Protective and toxic roles of dopamine in Parkinson's disease.** *J Neurochem* 2014, **129**:898–915.
230. Eve TSC, Wells A, Turner NJ: **Enantioselective oxidation of O-methyl-N-hydroxylamines using monoamine oxidase N as catalyst.** *Chem Commun* 2007, 530-1531.
231. Batista VF, Galman JL, GA Pinto DC, Silva AMS, Turner NJ: **Monoamine oxidase: tunable activity for amine resolution and functionalization.** *ACS Catal* 2018, **8**:11889–11907.
232. Ghislieri D, Green AP, Pontini M, Willies SC, Rowles I, Frank A, Grogan G, Turner NJ: **Engineering an enantioselective amine oxidase for the synthesis of pharmaceutical building blocks and alkaloid natural products.** *J Am Chem Soc* 2013, **135**:10863–10869.

233. O'Reilly E, Iglesias C, Turner NJ: **Monoamine Oxidase- ω -Transaminase Cascade for the Deracemisation and Dealkylation of Amines.** *ChemCatChem* 2014, **6**:992–995.
234. Li G, Ren J, Iwaki H, Zhang D, Hasegawa Y, Wu Q, Feng J, Lau PCK, Zhu D: **Substrate profiling of cyclohexylamine oxidase and its mutants reveals new biocatalytic potential in deracemization of racemic amines.** *Appl Microbiol Biotechnol* 2014, **98**:1681–1689.
235. Heath RS, Pontini M, Bechi B, Turner NJ: **Development of an R-Selective Amine Oxidase with Broad Substrate Specificity and High Enantioselectivity.** *ChemCatChem* 2014, **6**:996–1002.
236. Gaweska H, Fitzpatrick PF: **Structures and mechanism of the monoamine oxidase family.** *Biomol Concepts* 2011, **2**:365–377.
237. Zapata-Torres G, Fierro A, Barriga-González G, Salgado JC, Celis-Barros C: **Revealing monoamine oxidase B catalytic mechanisms by means of the quantum chemical cluster approach.** *J Chem Inf Model* 2015, **55**:1349–1360.
238. Carr R, Alexeeva M, Dawson MJ, Gotor-Fernández V, Humphrey CE, Turner NJ: **Directed evolution of an amine oxidase for the preparative deracemisation of cyclic secondary amines.** *ChemBioChem* 2005, **6**:637–639.
239. Ghislieri D, Houghton D, Green AP, Willies SC, Turner NJ: **Monoamine oxidase (MAO-N) catalyzed deracemization of tetrahydro- β -carbolines: Substrate dependent switch in enantioselectivity.** *Acc Catal* 2013, **3**:2869–2872.
240. Carr R, Alexeeva M, Enright A, Eve TSC, Dawson MJ, Turner NJ: **Directed evolution of an amine oxidase possessing both broad substrate specificity and high enantioselectivity.** *Angew Chemie Int Ed* 2003, **42**:4807–4810.
241. Dunsmore CJ, Carr R, Fleming T, Turner NJ: **A chemo-enzymatic route to enantiomerically pure cyclic tertiary amines.** *J Am Chem Soc* 2006, **128**:2224–2225.

242. Köhler V, Bailey KR, Znabet A, Raftery J, Helliwell M, Turner NJ: **Enantioselective biocatalytic oxidative desymmetrization of substituted pyrrolidines.** *Angew Chemie Int Ed* 2010, **49**:2182–2184.
243. Znabet A, Polak MM, Janssen E, de Kanter FJJ, Turner NJ, Orru RVA, Ruijter E: **A highly efficient synthesis of telaprevir by strategic use of biocatalysis and multicomponent reactions.** *Chem Commun* 2010, **46**:7918–7920.
244. Yamada T, Okumura K, Yonezawa Y, Shin C: **Useful synthesis of the main dehydrohexapeptide segment of a macrocyclic antibiotic, berninamycin B.** *Chem Lett* 2001, **30**:102–103.
245. Dola VR, Soni A, Agarwal P, Ahmad H, Raju KSR, Rashid M, Wahajuddin M, Srivastava K, Haq W, Dwivedi AK: **Synthesis and evaluation of chirally defined side chain variants of 7-chloro-4-aminoquinoline to overcome drug resistance in malaria chemotherapy.** *Antimicrob Agents Chemother* 2017, **61**:e01152-16.
246. Yasobu N, Kitajima M, Kogure N, Shishido Y, Matsuzaki T, Nagaoka M, Takayama H: **Design, synthesis, and antitumor activity of 4-halocolchicines and their pro-drugs activated by cathepsin B.** *ACS Med Chem Lett* 2011, **2**:348–352.
247. Thétiot-Laurent S, Bouillère F, Baltaze J-P, Brisset F, Feytens D, Kouklovsky C, Miclet E, Alezra V: **Original β , γ -diamino acid as an inducer of a γ -turn mimic in short peptides.** *Org Biomol Chem* 2012, **10**:9660–9663.
248. Tavares FX, Deaton DN, Miller AB, Miller LR, Wright LL: **Ketoheterocycle-based inhibitors of cathepsin K: a novel entry into the synthesis of peptidic ketoheterocycles.** *Bioorg Med Chem Lett* 2005, **15**:3891–3895.
249. Schmuck C, Rehm T, Geiger L, Schäfer M: **Synthesis and Self-Association Properties of Flexible Guanidiniocarbonylpyrrole– Carboxylate Zwitterions in DMSO: Intra-versus Intermolecular Ion Pairing.** *J Org Chem* 2007, **72**:6162–6170.
250. Perron V, Abbott S, Moreau N, Lee D, Penney C, Zacharie B: **A method for the**

- selective protection of aromatic amines in the presence of aliphatic amines.** *Synthesis (Stuttg)* 2009, **2009**:283–289.
251. Geall AJ, Blagbrough IS: **Homologation of polyamines in the rapid synthesis of lipospermine conjugates and related lipoplexes.** *Tetrahedron* 2000, **56**:2449–2460.
252. Kawahara K, Uchiyama H, Kimura J, Miyajima K: *Drug Delivery Systems*, EP0636363A2, filled in 1994, issued in 1995 by European Patent Office (EPO).
253. Braganza CD, Shibata K, Fujiwara A, Motozono C, Sonoda K-H, Yamasaki S, Stocker BL, Timmer MSM: **The effect of MR1 ligand glyco-analogues on mucosal-associated invariant T (MAIT) cell activation.** *Org Biomol Chem* 2019, **17**:8992–9000.
254. Bouchez V, Stasik I, Beaupère D: **Efficient syntheses of 1-bromodeoxy-, 1-azidodeoxy-and 1-aminodeoxypentitols from unprotected d-pentono-1, 4-lactones.** *Carbohydr Res* 1999, **323**:213–217.
255. Chaveriat L, Stasik I, Demailly G, Beaupère D: **The direct synthesis of 6-amino-6-deoxyaldonic acids as monomers for the preparation of polyhydroxylated nylon 6.** *Tetrahedron: Asymmetry* 2006, **17**:1349–1354.
256. De Muynck C, Pereira CSSS, Naessens M, Parmentier S, Soetaert W, Vandamme EJ: **The genus *Gluconobacter oxydans*: Comprehensive overview of biochemistry and biotechnological applications.** *Crit Rev Biotechnol* 2007, **27**:147–171.
257. Hann RM, Tilden EB, Hudson CS: **The Oxidation of Sugar Alcohols by *Acetobacter suboxydans*1.** *J Am Chem Soc* 1938, **60**:1201–1203.
258. Price PB, Sowers T: **Temperature dependence of metabolic rates for microbial growth, maintenance, and survival.** *Proc Natl Acad Sci* 2004, **101**:4631–4636.
259. Csonka LN: **Physiological and genetic responses of bacteria to osmotic stress.** *Microbiol Mol Biol Rev* 1989, **53**:121–147.

260. Adachi O, Hours RA, Shinagawa E, Akakabe Y, Yakushi T, Matsushita K: **Pentose Oxidation by Acetic Acid Bacteria Led to a Finding of Membrane-Bound Purine Nucleosidase.** *Biosci Biotechnol Biochem* 2013, **77**:1131–1133.
261. Adachi O, Hours RA, Shinagawa E, Akakabe Y, Yakushi T, Matsushita K: **Enzymatic synthesis of 4-pentulosonate (4-keto-D-pentionate) from D-aldopentose and D-pentionate by two different pathways using membrane enzymes of acetic acid bacteria.** *Biosci Biotechnol Biochem* 2011, **75**:2418–2420.
262. Scheller PN, Nestl BM: **The biochemical characterization of three imine-reducing enzymes from *Streptosporangium roseum* DSM43021, *Streptomyces turgidiscabies* and *Paenibacillus elgii*.** *Appl Microbiol Biotechnol* 2016, **100**:10509–10520.
263. Wills M: **Imino transfer hydrogenation reductions.** In *Hydrogen Transfer Reactions*. Springer; 2016:69–104.
264. Guizzetti S, Benaglia M, Rossi S: **Highly stereoselective metal-free catalytic reduction of imines: An easy entry to enantiomerically pure amines and natural and unnatural α -amino esters.** *Org Lett* 2009, **11**:2928–2931.
265. Nolin KA, Ahn RW, Toste FD: **Enantioselective reduction of imines catalyzed by a Rhenium (V)–Oxo complex.** *J Am Chem Soc* 2005, **127**:12462–12463.
266. Clemente F, Matassini C, Cardona F: **The Reductive Amination Routes to the Synthesis of Piperidine Iminosugars.** *European J Org Chem* 2020,
267. Muramatsu H, Mihara H, Kakutani R, Yasuda M, Ueda M, Kurihara T, Esaki N: **The putative malate/lactate dehydrogenase from *Pseudomonas putida* is an NADPH-dependent Δ^1 -piperideine-2-carboxylate/ Δ^1 -pyrroline-2-carboxylate reductase involved in the catabolism of d-lysine and d-proline.** *J Biol Chem* 2005, **280**:5329–5335.
268. Mitsukura K, Kuramoto T, Yoshida T, Kimoto N, Yamamoto H, Nagasawa T: **A NADPH-dependent (S)-imine reductase (SIR) from *Streptomyces* sp. GF3546 for asymmetric synthesis of optically active amines: purification,**

- characterization, gene cloning, and expression. *Appl Microbiol Biotechnol* 2013, **97**:8079–8086.
269. Lu S-P, Lewin AH: **Enamine/imine tautomerism in α , β -unsaturated- α -amino acids.** *Tetrahedron* 1998, **54**:15097–15104.
270. Becalski AG, Cullen WR, Fryzuk MD, James BR, Kang GJ, Rettig SJ: **Catalytic asymmetric hydrogenation of imines. Use of rhodium (I)/phosphine complexes and characterization of rhodium (I)/imine complexes.** *Inorg Chem* 1991, **30**:5002–5008.
271. Lévy K, Tóth KD, Kárpáti T, Hegedűs L: **Heterogeneous Catalytic Hydrogenation of 3-Phenylpropionitrile over Palladium on Carbon.** *ACS omega* 2020, **5**:5487–5497.
272. Dorta R, Broggini D, Kissner R, Togni A: **Iridium–Imine and–Amine Complexes Relevant to the (S)-Metolachlor Process: Structures, Exchange Kinetics, and C–H Activation by Iridium Causing Racemization.** *Chem Eur J* 2004, **10**:4546–4555.
273. Riant O: **Hydrosilylation of imines.** *Acid Catal Mod Org Synth* 2008,
274. Burke AJ, Benaglia M, Porta R, Fernandes S, Brenna D: **Stereoselective Metal-Free Reduction of Chiral Imines in Batch and Flow Mode: A Convenient Strategy for the Synthesis of Chiral Active Pharmaceutical Ingredients.** 2016,
275. Chen Q-A, Ye Z-S, Duan Y, Zhou Y-G: **Homogeneous palladium-catalyzed asymmetric hydrogenation.** *Chem Soc Rev* 2013, **42**:497–511.
276. Jones DWC, Nash RJ, Bell EA, Williams JM: **Identification of the 2-hydroxymethyl-3, 4-dihydropyrrolidine (or 1, 4-dideoxy-1, 4-iminopentitol) from angylocalyx boutiqueanus and from arachniodes standishii as the (2R, 3R, 4S)-isomer by the synthesis of its enantiomer.** *Tetrahedron Lett* 1985, **26**:3125–3126.
277. Furukawa J, Okuda S, Saito K, Hatanaka S-I: **3, 4-Dihydroxy-2-hydroxymethylpyrrolidine from Arachniodes standishii.** *Phytochemistry* 1985, **24**:593–594.

278. Watson AA, Nash RJ, Wormald MR, Harvey DJ, Dealler S, Lees E, Asano N, Kizu H, Kato A, Griffiths RC: **Glycosidase-inhibiting pyrrolidine alkaloids from *Hyacinthoides non-scripta***. *Phytochemistry* 1997, **46**:255–259.
279. Asano N, Yasuda K, Kizu H, Kato A, Fan J, Nash RJ, Fleet GWJ, Molyneux RJ: **Novel α -L-fucosidase inhibitors from the bark of *Angylocalyx pynaertii* (Leguminosae)**. *Eur J Biochem* 2001, **268**:35–41.
280. Scofield AM, Fellows LE, Nash RJ, Fleet GWJ: **Inhibition of mammalian digestive disaccharidases by polyhydroxy alkaloids**. *Life Sci* 1986, **39**:645–650.
281. Stocker BL, Jongkees SAK, Win-Mason AL, Dangerfield EM, Withers SG, Timmer MSM: **The ‘mirror-image’ postulate as a guide to the selection and evaluation of pyrrolidines as α -l-fucosidase inhibitors**. *Carbohydr Res* 2013, **367**:29–32.
282. Andersen B, Rassov A, Westergaard N, Lundgren K: **Inhibition of glycogenolysis in primary rat hepatocytes by 1, 4-dideoxy-1, 4-imino-D-arabinitol**. *Biochem J* 1999, **342**:545–550.
283. Yasuda K, Kizu H, Yamashita T, Kameda Y, Kato A, Nash RJ, Fleet GWJ, Molyneux RJ, Asano N: **New sugar-mimic alkaloids from the pods of *Angylocalyx pynaertii***. *J Nat Prod* 2002, **65**:198–202.
284. Muraoka O, Ying S, Yoshikai K, Matsuura Y, Yamada E, Minematsu T, Tanabe G, Matsuda H, Yoshikawa M: **Synthesis of a nitrogen analogue of salacinol and its α -glucosidase inhibitory activity**. *Chem Pharm Bull* 2001, **49**:1503–1505.
285. Popowycz F, Gerber-Lemaire S, Demange R, Rodriguez-García E, Asenjo ATC, Robina I, Vogel P: **Derivatives of (2R, 3R, 4S)-2-aminomethylpyrrolidine-3, 4-diol are selective α -mannosidase inhibitors**. *Bioorg Med Chem Lett* 2001, **11**:2489–2493.
286. Asano N, Oseki K, Kizu H, Matsui K: **Nitrogen-in-the-ring pyranoses and furanoses: structural basis of inhibition of mammalian glycosidases**. *J Med*

Chem 1994, **37**:3701–3706.

287. Mercer TB, Jenkinson SF, Bartholomew B, Nash RJ, Miyauchi S, Kato A, Fleet GWJ: **Looking glass inhibitors: both enantiomeric N-benzyl derivatives of 1, 4-dideoxy-1, 4-imino-D-lyxitol [a potent competitive inhibitor of α -D-galactosidase] and of 1, 4-dideoxy-1, 4-imino-L-lyxitol [a weak competitive inhibitor of α -D-galactosidase] inhibit naringinase, an α -L-rhamnosidase competitively.** *Tetrahedron: Asymmetry* 2009, **20**:2368–2373.
288. Kato A, Kato N, Kano E, Adachi I, Ikeda K, Yu L, Okamoto T, Banba Y, Ouchi H, Takahata H: **Biological properties of D-and L-1-deoxyazasugars.** *J Med Chem* 2005, **48**:2036–2044.
289. Nash RJ, Bell EA, Fleet GWJ, Jones RH, Williams JM: **The identification of a hydroxylated pyrrolidine derivative from *Castanospermum australe*.** *J Chem Soc Chem Commun* 1985,
290. Asano N, Oseki K, Tomioka E, Kizu H, Matsui K: **N-containing sugars from *Morus alba* and their glycosidase inhibitory activities.** *Carbohydr Res* 1994, **259**:243–255.
291. Merino P, Delso I, Tejero T, Cardona F, Marradi M, Faggi E, Parmeggiani C, Goti A: **Nucleophilic Additions to Cyclic Nitrones en Route to Iminocyclitols—Total Syntheses of DMDP, 6-deoxy-DMDP, DAB-1, CYB-3, Nectrisine, and Radicamine B.** *European J Org Chem* 2008, **2008**:2929–2947.
292. Dangerfield EM, Plunkett CH, Stocker BL, Timmer MSM: **Protecting-Group-Free Synthesis of 2-Deoxy-Aza-Sugars.** *Molecules* 2009, **14**:5298–5307.
293. Kim IS, Zee OP, Jung YH: **Regioselective and Diastereoselective Amination of Polybenzyl Ethers Using Chlorosulfonyl Isocyanate: Total Syntheses of 1, 4-Dideoxy-1, 4-Imino-d-Arabinitol and (–)-Lentiginosine.** *Org Lett* 2006, **8**:4101–4104.
294. Goeminne A, McNaughton M, Bal G, Surpateanu G, Van Der Veken P, De Prol S, Versées W, Steyaert J, Haemers A, Augustyns K: **Synthesis and biochemical evaluation of guanidino-alkyl-ribitol derivatives as nucleoside hydrolase**

- inhibitors.** *Eur J Med Chem* 2008, **43**:315–326.
295. Goeminne A, Berg M, McNaughton M, Bal G, Surpateanu G, Van der Veken P, De Prol S, Versées W, Steyaert J, Haemers A: **N-Arylmethyl substituted iminoribitol derivatives as inhibitors of a purine specific nucleoside hydrolase.** *Bioorg Med Chem* 2008, **16**:6752–6763.
296. Fan A, Chuah GK, Jaenicke S: **A novel and environmental friendly synthetic route for hydroxypyrrolidines using zeolites.** *Carbohydr Res* 2019, **472**:103–114.
297. Ganesan M, Ramesh NG: **A new and short synthesis of naturally occurring 1-deoxy-l-gulonojirimycin from tri-O-benzyl-d-glucal.** *Tetrahedron Lett* 2010, **51**:5574–5576.
298. Bouillon ME, Pyne SG: **Diastereoselective concise syntheses of the polyhydroxylated alkaloids DMDP and DAB.** *Tetrahedron Lett* 2014, **55**:475–478.
299. Chirke SS, Rajender A, Rao BV: **A divergent approach for the synthesis of some polyhydroxy pyrrolidines and piperidines from ribosylamine.** *Tetrahedron* 2014, **70**:103–109.
300. Wang G-N, Yang L, Zhang L-H, Ye X-S: **A Versatile Approach to N-Alkylated 1, 4-Dideoxy-1, 4-imino-d-arabinitols and 1, 4-Dideoxy-1, 4-imino-l-xylitols.** *J Org Chem* 2011, **76**:2001–2009.
301. Gupta A, Singh VK, Qazi GN, Kumar A: **Gluconobacter oxydans: its biotechnological applications.** *J Mol Microbiol Biotechnol* 2001, **3**:445–456.
302. Lievens B, Hallsworth JE, Pozo MI, Belgacem Z Ben, Stevenson A, Willems KA, Jacquemyn H: **Microbiology of sugar-rich environments: diversity, ecology and system constraints.** *Environ Microbiol* 2015, **17**:278–298.
303. Wu Q, Liu J, Wang X, Feng L, Wu J, Zhu X, Wen W, Gong X: **Organ-on-a-chip: recent breakthroughs and future prospects.** *Biomed Eng Online* 2020, **19**:9.
- 304 S. V. Evans, A. M. R. Gatehouse, L. E. Fellows, Entomol: **Castanospermine,**

- Swainsonine and Related Polyhydroxy Alkaloids: Structure, Distribution and Biological Activity.** *Exp. App.* 1985, **37**: 257-261.
- 305 Nash RJ, Kato A, Chu-Yi Yu³, Fleet GWJ: **Iminosugars as therapeutic agents: recent advances and promising trends.** *Fut Med Chem* 2011, **3**:1513-1521.
- 306 Studier FW: **Stable expression clones and auto-induction for protein production in E. coli,** *Methods Mol Biol* 2014; **1091**:17-32
- 307 Lorraine CF, Johnson JV , Horenstein NA: **Identification of a Gene Cluster that Initiates Azasugar Biosynthesis in Bacillus amyloliquefaciens,** *ChemBioChem* 2011, **12**:2147– 2150
- 308 Bushmarina NA, Blanchet CE, Vernier G, Forge V: **Cofactor effects on the protein folding reaction: Acceleration of α -lactalbumin refolding by metal ions.** *Protein Sci* 2006, **15**:659–671.
- 309 Sørensen HP, Mortensen KK: **Soluble expression of recombinant proteins in the cytoplasm of Escherichia coli.** *Microb Cell Fact* 2005, **4**:1–8.
- 310 Kyratsous CA, Silverstein SJ, DeLong CR, Panagiotidis CA: **Chaperone-fusion expression plasmid vectors for improved solubility of recombinant proteins in Escherichia coli.** *Gene* 2009, **440**:9–15.
- 311 Ikura K, Kokubu T, Natsuka S, Ichikawa A, Adachi M, Nishihara K, Yanagi H, Utsumi S: **Co-overexpression of folding modulators improves the solubility of the recombinant guinea pig liver transglutaminase expressed in Escherichia coli.** *Prep Biochem Biotechnol* 2002, **32**:189–205.
- 312 Baneyx F, Palumbo JL: **Improving heterologous protein folding via molecular chaperone and foldase co-expression.** In *E. coli Gene Expression Protocols*. . Springer; 2003:171–197.
- 313 Samuelson JC: **Recent developments in difficult protein expression: a guide to E. coli strains, promoters, and relevant host mutations.** *Heterologous Gene Expr E coli* 2011.
- 314 Oba M, Kawaji S, Kushima H, Sano T, Nishiyama K: **Convenient Synthesis of 1,**

4-Dideoxy-1, 4-imino-D-ribitol from D-Ribose. *J Chem* 2013, 2013

315 Patiil MD, Grogan G, Bommarius A, Yun H: **Oxidoreductase-catalyzed synthesis of chiral amines. *ACS Catal* 2018, 8:10985–11015**